VISUAL EVOKED MAGNETIC RESPONSES (VEMR) TO FLASH AND PATTERN REVERSAL STIMULATION

A Thesis submitted for the Degree of Doctor of Philosophy

by Antoinette Slaven

THE UNIVERSITY OF ASTON IN BIRMINGHAM

SEPTEMBER 1992

University of Aston in Birmingham

Visual evoked magnetic responses (VEMR) to flash and pattern reversal stimulation

Antoinette Slaven

Ph.D. 1992

The problems of using a single channel magnetometer (BTi, Model 601) in an unshielded clinical environment to measure visual evoked magnetic responses (VEMR) were studied. VEMR to flash and pattern reversal stimuli were measured in 100 normal subjects. Two components, the P100M to pattern reversal and P2M to flash, were measured successfully in the majority of subjects. The mean latencies of these components in different decades of life were more variable than the visual evoked potentials (VEP) that have been recorded to these stimuli. The latency of the P100M appeared to increase significantly after about 55 years of age whereas little change occurred for the flash P2M. The effects of blur, check size, stimulus size and luminance intensity on the latency and amplitude of the VEMR were studied. Blurring a small (32') check significantly increased latency whereas blurring a large (70') check had little effect on latency. Increasing check size significantly reduced latency of the P100M but had little effect on amplitude. Increasing the field size decreases the latency and increases the amplitude of the P100M. Within a normal subject, most of the temporal variability of the P100M appeared to be associated with run to run variation rather than between recording sessions on the same day or between days. Reproducibility of the P100M was improved to a degree by employing a magnetically shielded room. Increasing flash intensity decreases the latency and increases the amplitude of the P2M component. The magnitude of the effects of varying stimulus parameters on the VEMR were frequently greater than is normally seen in the VEP. The topography of the P100M and P2M varied over the scalp in normal subjects. Full field responses to a large check could be explained as approximately the sum of the half field responses and were consistent with the cruciform model of the visual cortex. Preliminary source localisation data suggested a shallower source in the visual cortex for the flash P2M compared with the P100M. The data suggest that suitable protocols could be devised to obtain normative data of sufficient quality to use the VEMR to flash and pattern clinically.

Key words:- Neuromagnetism, Visual evoked magnetic responses, pattern reversal, flash, normative data

FOR MY GRANDMA

ACKNOWLEDGEMENTS

I would like to express my sincere thanks to the following people :

Dr. Richard Armstrong for his valued supervision, support and encouragement throughout this thesis and for his statistical advice. Thanks also for the many hours spent as a subject and for all the coffee.

Christopher Degg for his support and friendship, time spent under the magnetometer and of course - the beer.

Thanks to Dr. S. Swithenby of the Open University for source localisations carried out on the 42 point mapping data (Figure 5.16).

Many thanks to Cath Nesfield for allowing me to use the half field pattern reversal maps shown in Figure 5.9a, and for her friendship.

To Philip Gethen, my parents and my grandma for their continued support.

Dr. Maria Dengler-Harles for her encouragement and for the provision of the best accomodation in Birmingham.

I am indebted to the Department of Vision Sciences at Aston University for provision of a departmental studentship.

Finally, many thanks to all those who acted as subjects without whom this work would not have been possible.

LIST OF CONTENTS

CHAPTER 2

THE VISUAL SYSTEM AND VISUAL EVOKED POTENTIALS

CHAPTER 3

VISUALLY EVOKED MAGNETIC RESPONSES TO FLASH AND PATTERN REVERSAL IN 100 NORMAL SUBJECTS

CHAPTER 6

GENERAL CONCLUSIONS, FURTHER WORK AND PROTOCOL RECOMMENDATIONS

LIST OF TABLES

LIST OF FIGURES

CHAPTER 1

INTRODUCTION TO MAGNETOENCEPHALOGRAPHY (MEG)

This thesis is concerned with the problems of applying magnetoencephalography (MEG), the measurement of the brains' minute magnetic fields, to the clinical diagnosis of neurological disease. Over the past 25 years, a number of new non-invasive neuro-imaging techniques have been developed and are now finding their way into clinical use. It is with these techniques, and not just the Electroencephalogram (EEG) to which it is most closely related, that MEG must compete. In the following section the advantages and disadvantages of each technique are discussed. Brain imaging technology can be divided into two categories:- a) those that provide anatomical information and b) those providing information on brain function. In the first category are included Magnetic Resonance Imaging (MRI) and Computed Tomography (CT).

1.1 Anatomical Imaging Techniques

1.11 Magnetic Resonance Imaging (MRI)

MRI depends upon the properties of the hydrogen nucleus or proton (Armstrong and Wastie 1987). Normally within a tissue, the protons are randomly oriented and spin rapidly. When exposed to a strong magnetic field they behave like tiny bar magnets. Application of a radiofrequency magnetic field pulse of appropriate frequency and duration causes the protons to change their alignment, flipping through a preset angle and then rotating in phase with each other. When the pulse is switched off, the protons relax to their original positions. As they realign, they emit a weak radio frequency signal which can be detected by coils placed around the subject. The signal strength can be mapped throughout the tissue and computers used to generate an anatomical image. The time taken for the protons to dephase (T2) and realign (T1) can be altered by varying the frequency and duration of the excitatory magnetic field pulse. These values can themselves provide physiological information. At the field strengths used in medical imaging (0.02 to 2 Tesla) the strongest signal arises from the protons in water and fat molecules.

High resolution and excellent white/grey matter differentiation have allowed MRI to be used successfully for the detection of demyelinating lesions, tumours and both generalised and focal brain atrophy (Armstrong and Wastie 1987). However, the patient is exposed to a high strength magnetic field and the long term effects of this are uncertain. In addition, there may be problems obtaining a successful scan as the

patient is required to remain very still for between four and twelve minutes. Despite this, and the cost, which stands currently at around £2 million, MRI scanners have been installed in a small number of hospitals in the UK and most of the major population centres in the USA.

1.12 Computed Tomography (CT)

By contrast with MRI, Computed Tomography uses conventionally generated X-rays with a gas or crystal based detection system (Armstrong and Wastie 1987). This offers greater sensitivity than photographic film, allowing the visualisation of 2000 density variations as opposed to the 20 of conventional X-rays. The data collected are manipulated by computer to create a final image. Scans are normally taken in the axial plane but slices taken successively can be fed into a computer and used to generate a three dimensional image which can then be sampled in any plane desired. Slice thickness can be varied from 1.5 to 10mm, with thinner slices giving better resolution. In addition to the visual images generated, CT scans can be analysed in terms of an increase or decrease in the overall radiodensity of a given brain section. The brains of normal subjects and those with neuropsychiatric disorders can then be compared statistically.

CT scan resolution is not as high as that for MRI but has been used for the diagnosis of tumours and infarcts, and the detection and study of ventricular dilation and brain atrophy in various dementing disorders (Fazakas 1990). The latest CT scanners now cost almost as much as MRI machines (£1.5 to £2 million) but hospitals and neurological centres consider the technique to be valuable and remain undeterred (Armstrong and Wastie 1987). CT also has problems in addition to that of cost. Firstly the image is derived from the differential absorption of X-rays and so no information can be obtained about radioisodense structures and secondly, the technique is invasive. Although one CT scan requires only the same X-ray dose as one set of plain skull films, radiation dose must be carefully considered when repeated scans are envisaged.

Although structural changes have been noted in many disorders, they do not always correlate well with the neurological deficit. This may be because the structural imaging techniques are not yet sensitive enough to detect the small cell losses which may occur in more subtle neurological disorders. In these cases, the functional imaging techniques, including Positron Emission Tomography (PET), Single Photon Emission Computed Tomography (SPECT), EEG and MEG, may be of value.

1.2 Functional Imaging Techniques

1.21 Positron Emission Tomography (PET)

In Positron Emission Tomography (PET) the patient is injected with a radiolabelled biochemical substrate eg. ^{19}F fluorodeoxyglucose, the fate of which is monitored. In this way the metabolic activity of various brain regions can be visualised, again allowing comparison of normal subjects with those suffering from a neurological disorder. Radioactive decay of the labelling atom releases positrons (positively charged electrons) which travel for a few millimetres before annihilating to produce two photons. These photons pass through the tissue relatively unimpeded because of their high energy and are detected using crystal based detection systems. A computer is used to trace the origin of each photon pair and to construct a map on which the density of radioactivity indicates the level of metabolic activity in each brain region. Providing that labels can be attached to biologically significant molecules, PET has great potential. So far the technique has been used to identify infarcts and the resultant ischaemia, and to separate radiation necrosis from tumour recurrence (Wegener and Alavi 1989) and most excitingly, separating normal or depressed subjects from those with Dementia of the Alzheimer Type (SDAT) (Ferris and Leon 1983). The problems with PET scans are the cost of the equipment (nearly £3 million), the need to be near a cyclotron and the invasive nature of the technique ie. the need to inject the patient with a radioactive marker. In addition, the necessarily low levels of radiation of the marker molecule mean that each scan takes about 10 minutes. The result is a 'smeared' temporal scan and it is not possible to measure ongoing functional activity. Despite this, there has in recent years been significant clinical application (Wegener and Alavi 1989, McGreer et al 1990)

1.22 Single Photon Emission Computed Tomography (SPECT)

SPECT is another functional imaging technique requiring the injection or inhalation of a radioactive tracer molecule. It is less sophisticated than PET and has poorer spatial resolution (Fazakas 1990). Again the product of a radioactive decay is measured, this time using a Gamma camera. This consists of a single large crystal of NaI, coupled to an array of photomultiplier tubes. Light produced as the gamma rays hit the crystalline structure is electronically amplified and then converted to an electrical pulse. These pulses are processed and a computer enhanced image produced. Again isotope uptake density is used as a measure of function. Markers for SPECT include $^{133}Xenon$ for looking at brain perfusion and $^{99}Technetium$ labelled red blood cells for studying blood filled volumes. The patterns of activity for normal and clinically affected subjects can be compared. An advantage of the technique is its relatively low cost and

simplicity. On the minus side is the fairly limited knowledge of the fate of the radio ligands used, the poor spatial resolution and the invasive nature of the technique.

1.23 Electroencephalography (EEG)

EEG is the oldest of the brain imaging techniques and the most closely related to MEG. Electrical activity generated in neurons can be detected by electrodes filled with a conducting gel and attatched to the scalp. The potential difference between pairs of electrodes is measured. The resultant traces are usually analysed subjectively by eye or by automated analysis (Lopes da Silva 1987). The presence or absence of certain frequencies or wave features are noted. Although the EEG has been used in the detection and localisation of tumours, it has been used most sucessfully for the diagnosis of epilepsy, showing few specific signs of other abnormalities (Spehlmann 1981). EEG machines cost around £1000 per channel so typical equipment can cost up to about £16,000, making EEG the cheapest, although probably the least useful of currently available imaging techniques. EEG measures the ongoing activity of the brain but in the early 1960s' a technique was devised which allowed the measurement of stimulus linked responses and thus the study of specific brain areas and systems. For example the visual evoked potential (VEP) is obtained by recording from pairs of appropriately located electrodes ie. an active or recording electrode, usually over the occiput in the case of the VEP, and an inactive or reference electrode, usually on the vertex or at a mid-temporal location. The subject is shown a visual stimulus, either a flashing light, a reversing checkerboard or an appearing and disappearing pattern and the response, the potential difference between the electrode pairs is processed by a signal averager. An individual response to the stimulus is very small and cannot normally be seen in the ongoing EEG. However the response is time locked to the stimulus and so it is possible, through the use of an averaging device, to separate the time locked response from the background noise. The previous uses and problems associated with the interpretation of the VEP are outlined in more detail in Chapter 2.

1.3 Theoretical Advantages of MEG

It is the purpose of the present study to examine the problems inherent in recording visual evoked magnetic fields (VEMR) and in addition to consider whether MEG has any intrinsic advantage over the VEP in clinical diagnosis. A number of theoretical advantages for MEG over EEG have been suggested, although many of the early ideas have had to be modified as further studies have investigated their validity. The main perceived advantages are as follows:-

1. MEG is non-invasive and does not require a reference electrode. Although EEG is not considered a truly invasive procedure there may be situations where it is not desirable to abrade the scalp of the patient (ie. in AIDS, hepatitis or in cases of traumatic head injury). In MEG, no physical preparation of the patient is necessary. Unlike techniques such as CT which uses X-rays, or PET which requires the injection of a radioactive tracer, it is not believed that MEG exposes the patient to a recording hazard. Although MEG is not totally independent of a reference (the gradiometer coils act as an intrinsic reference) it is not plagued by some of the problems of EEG. The EEG is the potential difference between electrodes and the resultant signals may be distorted by the use of an active reference site. One example of this is the use of a frontal reference when recording the flash visual evoked response (Hobley 1988). This is a problem particularly when topographic mapping of the electrical potential over the scalp is carried out. Many approaches have been used to reduce the effect of the reference including the use of balanced non-cephalic (ie. paired reference electrodes, one located on the 7th cervical vertabrae and one on the sternoclavicular notch), linked earlobe and average references (Spehlmann 1985). However, being unreferenced means that the magnetic field is an absolute measure and as such can be used to estimate the number of active brain cells involved in a response (Wikswo 1983).

2. Unlike the EEG the MEG is not smeared by skull or scalp. The early work of Grynszpan and Geselowitz, reported by Melcher and Cohen (1988) used a "dipole in a concentric spheres" model to demonstrate that magnetic fields were not affected by the intervening media of varying conductivities. By contrast, electrical potentials are known to be smeared and attenuated by the skull and scalp (Cooper et al 1965). The result is that the magnetic field topography over the head is approximately 1/3 more focal than its electrical counterpart (Cuffin and Cohen 1979, Cohen and Cuffin 1983, Wood 1985) and this, in theory makes source localisation simpler and more accurate. In addition, under optimal conditions, as a result of the greater spatial resolution afforded by MEG it should be possible to separate sources in the neocortex a few millimetres apart (Hari et al 1988). However, the human brain is not spherical and nonspherical changes in conductivity may influence magnetic signals and affect source localisation (Huang et al 1990).

3. EEG reflects the activity of both radial and tangential orientated sources whilst MEG reflects only the tangential ones (Williamson and Kaufman 1981). Therefore, used together, MEG and EEG should provide additional and complementary information regarding a current source in the brain. For example, Wood (1985) proposed two hypotheses to explain the dipolar potential pattern of an early component

of the somatosensory evoked response to median nerve stimulation. This pattern could be the result of a) a single tangential source located probably in area 3b of the sensorimotor cortex or b) two radial sources with current flow in opposite directions located in the crowns of the post-central gyrus. If a) were true then a dipolar pattern whose maxima were at 90° to those of the electrical topographic pattern would be expected magnetically whilst in case b) the two radial sources would be expected to produce no magnetic field outside the head. Taken separately neither EEG nor MEG would have been conclusive but when considered together there was a strong suggestion that the dipolar electrical potential map resulted from the activation of a single tangential source and not two radial dipoles.

Another consequence of the fact that MEG may sense more selective sources than EEG, may be an increased sensitivity to particular brain pathology. As a result of convolutions in the surface of the brain, cells in the fissures and sulci tend to be oriented tangentially with respect to the scalp, whilst those on the crests of the gyri tend to have a radial orientation. If a disease were to selectively affect the cells in the fissures rather than the gyri then the MEG may be more sensitive to these changes than the EEG eg. the selective development of pathological changes in sulci compared with gyri in Alzheimers' disease (Mann 1985, Armstrong et al 1989).

4. MEG signals attenuate more rapidly with distance from the source than EEG signals (Wikswo 1983). This implies that the MEG is more sensitive to cell losses in the brain than EEG as it reflects only a part of the signal seen in EEG and is less likely to be masked by other activity. The MEG reflects activity only under the area of its detection coil and to a depth approximately equivalent to its baseline length (Hari et al 1988) (ie. the distance between the pick-up and compensation coils - see Section 1.84). This usually means that MEG signals originate from a cylinder of tissue whose depth is no more than 3-5cm from the scalp surface. On the other hand the EEG reflects a much wider region of activity and includes the influences of deeper, subcortical structures. An exception to this is the magnetic recording of epileptic foci. These usually originate from sub-cortical areas but are of such a strength, that despite the rapid fall off of field with distance, they still produce detectable fields outside the head (Barth et al 1982, Barth et al 1984).

Hence, the particular clinical advantage of the MEG may be in the less smeared signal and consequently increased sensitivity to pathological changes in the brain.

1.4 Origins of the Brains Magnetic Field

To appreciate the potential of MEG clinically it is necessary to understand how a nerve cell generates a magnetic field. In its' simplest form a single neuron comprises an axon, a cell body or soma and a system of dendrites. The immediate environment of the neuron contains sodium (Na^+) and potassium (K^+) ions amongst others (eg. Cl^-, HCO^{3-}, Ca^{2+}). The neuronal membrane is selectively permeable to these ions by virtue of an energy dependent pump and open / closable pores (Hodgkin 1958, Hodgkin and Horowicz 1959). In the resting state there is potential across the membrane of around -70mV intracellularly (with respect to an extracellular point of zero potential). This is generated by the action of the Na^+/K^+ pump which pumps Na^+ ions out of the cell and K^+ ions in. This process alone would not create a potential difference but in addition, pores are open which allow K^+ but not Na^+ ions to diffuse across the cell membrane and down along their concentration gradient. This selective permeability results in a transmembrane potential difference.

When a neuron receives an excitatory stimulus via its dendrite system or soma there is a transient increase in the concentration of Na^+ locally which results in a reversal of transmembrane potential (to around +40mV) as the Na^+ ions diffuse into the cell. The graded potential is then propagated along the neuron as a consequence of a local circuit of current flow which increases Na^+ permeability in adjacent "inactive" areas of membrane. Thus a cycle of activity is initiated with increased permeability to Na^+ resulting in depolarisation and consequently circuits of current flow which in turn leads to increased Na^+ permeability. This current flowing towards the cell body is called the depolarisation front and is closely followed by a repolarisation front, a regeneration of the resting potential mediated by an increase in permeability to K^+ ions (Wikswo 1983). Hence, associated with the propagating action potential are an extracellular, an intracellular and a transmembrane current (Figure 1.1).

According to the Biot-Savart law the magnetic field strength is proportional to the current density (Tripp 1983). Hence it is thought to be unlikely that the magnetic field detectable outside the head is due to the extracellular or volume currents because, as a consequence of widespread backflow, there is a relatively low current density on the outside of the cell membrane. However, when a number of closely packed neurons are considered rather than a single cell it is possible that there may be some contribution to the magnetic field by the volume currents but this is difficult to calculate because of the complexity of the extracellular medium (Okada 1982).

The extracellular volume current is spread through membranes, skull and scalp creating secondary magnetic sources at the boundaries of different conductivity (Tripp

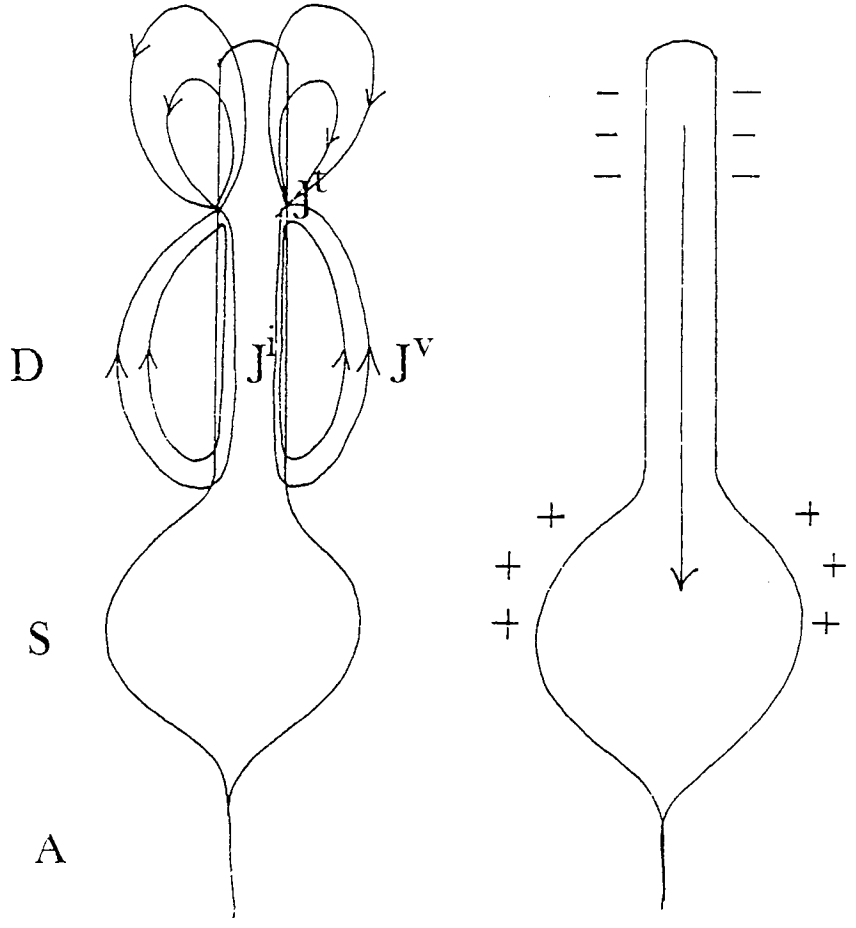

Figure 1.1 : A schematic diagram of a nerve cell membrane showing depolarisation and repolarisation fronts and the associated currents. A=Axon, S=Soma, D=Dendrite, J^i=intracellular current, J^t=transmembrane current, J^v= extracellular volume current.

1983). Currents are detected when electrical recordings are made from the scalp but are thought to contribute little to magnetic recordings when the detector is placed normal to the scalp (Okada 1983, Melcher and Cohen 1988). The transmembrane current is established as a result of electrical variation along the membrane and the ion gradient across it. It is also thought to make a negligible contribution to the externally observable field because of its radial symmetry and thinness (Plonsey 1981). Thus the brains' magnetic field is thought to originate from the high density intracellular current (Wikswo 1983, Wikswo and Roth 1989) and hence MEG may sense the current flow in neurons directly.

In addition, neuronal activity comprises action and graded potentials. It is believed that the field detected outside the head arises not from the action potential but from the dendritic graded potential (Okada 1983). These graded potentials are thought to be initiated by post synaptic membrane permeability changes which are subthreshold for action potential initiation. They are thought to propagate along the neuron by a similar process to that for the action potential. The first reason why graded rather than action potentials are considered the likely source of the external magnetic field is that it is unlikely that the action potential initiation and propagation would occur synchronously in a large population of neurons. It is estimated that at least 10,000 neurons may need to fire to elicit an event related magnetic field (Kaufman and Williamson 1986). Any asynchronicity could result in the cancellation of the field created by the depolarisation front of one neuron by the repolarisation front of another. As the graded potential is an order of magnitude slower, it is considered less susceptible to this form of mutual cancellation. Secondly, the action potential with its close depolarisation and repolarisation fronts can be modelled as a current quadropole for which the field falls off as the inverse cube of the distance from the source ($1/d^3$) whilst the graded potential can be considered as a current dipole with its field falling off at a rate of the inverse square of the distance from the source ($1/d^2$) (Wikswo 1983). Thus, at a location relatively far from the source it is likely that the field from the graded potential predominates (Tripp 1981, Kaufman and Williamson 1986).

1.5 Neuron Morphology

There is a wide range of morphological cell types present in the neocortex of the human brain (Parnavelas and McDonald 1983). However, many neurons can be approximated to two simple models (Figure 1.2). The pyramidal cell type (Figure 1.2a) has an axon and a dendrite oriented axially. This type of cell has an "open field configuration" (Okada 1983) which means that when a number of closely packed cells fire, the field from each individual cell may summate with that of its neighbours. By

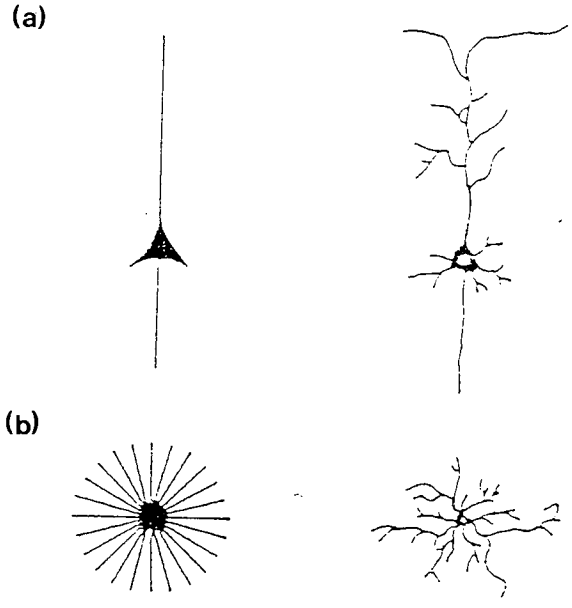

Figure 1.2 : Cortical neurons may be approximated to two types a) a pyramidal type cell - open field configuration b) a stellate type cell - closed field configuration.

contrast, the stellate type cell (Figure 1.2b) has a soma with radially oriented dendrites. When a current flows in the dendrites of this type of cell there is a tendency for the resultant fields to cancel each other out. This is known as the "closed field configuration". It is thought likely therefore that the field observed outside the head originates from the long dendrites of the pyramidal type cells rather than from the stellate cells. There may, however, be intermediate types which also contribute to the magnetic field to some extent, although in a mixed population, the simple pyramidal type should predominate.

1.6 The Columnar Organisation of the Visual Cortex

This study describes magnetic signals elicited by visual stimuli from the visual cortex in the occipital lobe of the human brain. The visual cortex is around 2 mm thick and can be divided into 6 main layers on the basis of cell type, connections and fibre distribution. Layer 1 is closest to the brains surface and layer 6 furthest from it.

Axons from cells in the Lateral Geniculate Nucleus (LGN) pass via the optic tracts and optic radiation to synapse in layer 4 of the cortex (Figure 1.3). Magno- and parvocellular layers of the LGN send axons which synapse on the dendritic trees of small ganglion cells in layers 4Cα and 4A/4Cß respectively. As these granule cells are more stellate with a closed type of configuration, it is unlikely that they would generate an externally observable magnetic field. Axons project from layer 4Cß to layers 2 and 3, and possibly 5, where synaptic connections are made on the dendritic trees of the large pyramidal cells. A Golgi stained preparation (Figure 1.4) shows the long apical dendrites of these pyramidal cells running parallel to each other and perpendicular to the brain surface. It is more likely that the graded potentials in these long apical dendrites result in the externally observable field.

However, little consideration is made of the many collateral connections in the cortex which spread signals laterally as well as vertically. It must also be noted that inputs on a particular nerve cell may be excitatory or inhibitory and that whether a cell responds with the generation of an action potential will be determined by the sum of its' excitatory/inhibitory input. It is sufficient to say that input from the LGN arrives in layer 4, the cells in which make contact with pyramidal cells in layers 2 and 3. The apical dendrites of these pyramidal cells are believed, because of their configuration and columnar organisation, to be the source of the externally observable magnetic field. Layers 2, 3 and 4B send outputs to other areas of the cortex whilst layers 5 and 6 send axons to superior colliculus and LGN respectively.

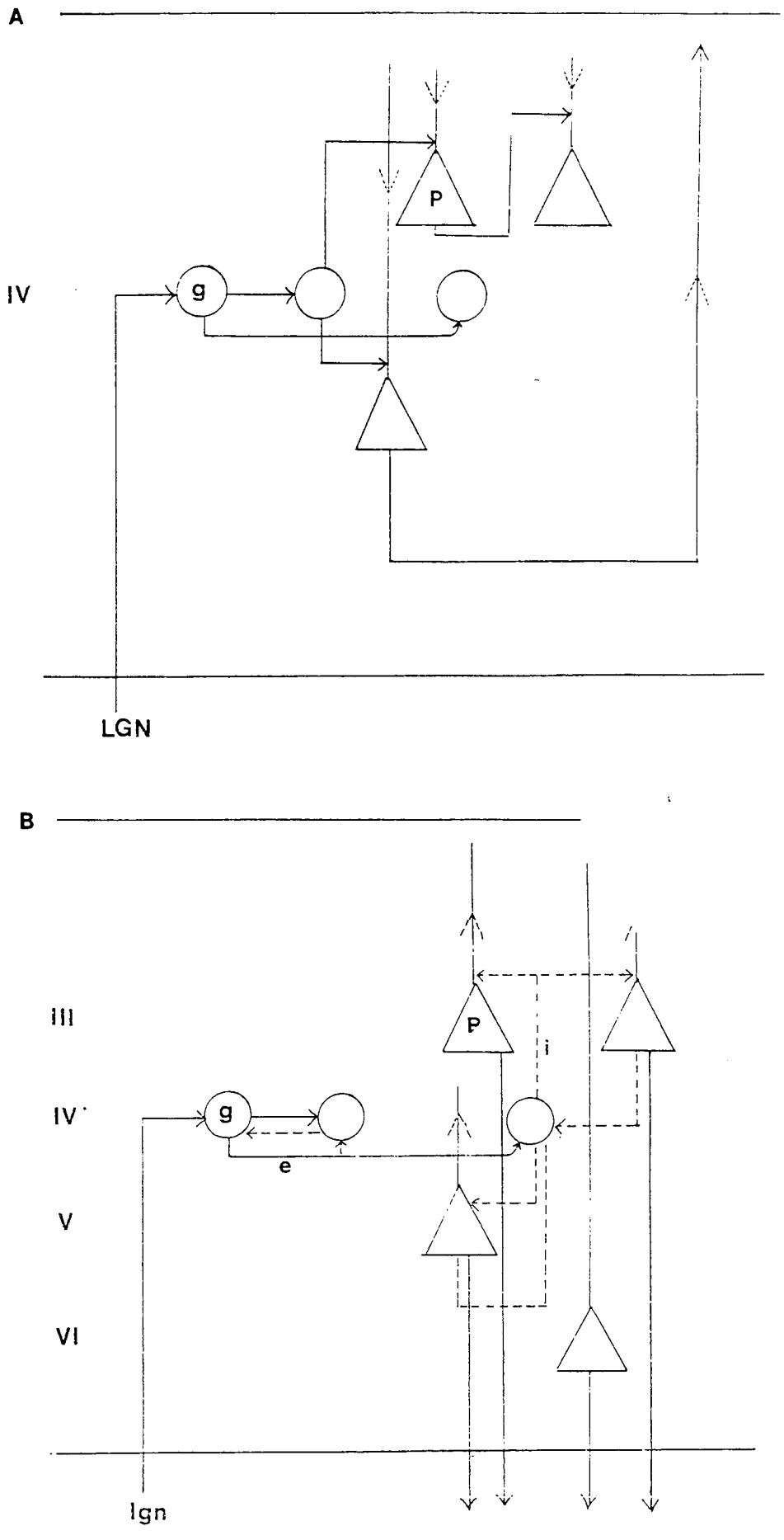

Figure 1.3 : a) main connections made by axons from the Lateral geniculate body (LGN) to the striate cortex (Brodmanns Area 17, Layer IV) and b) the output from the striate cortex to other brain regions; g=granule cell, P=Pyramidal cell, e=excitatory circuit, i=inhibitory circuit.

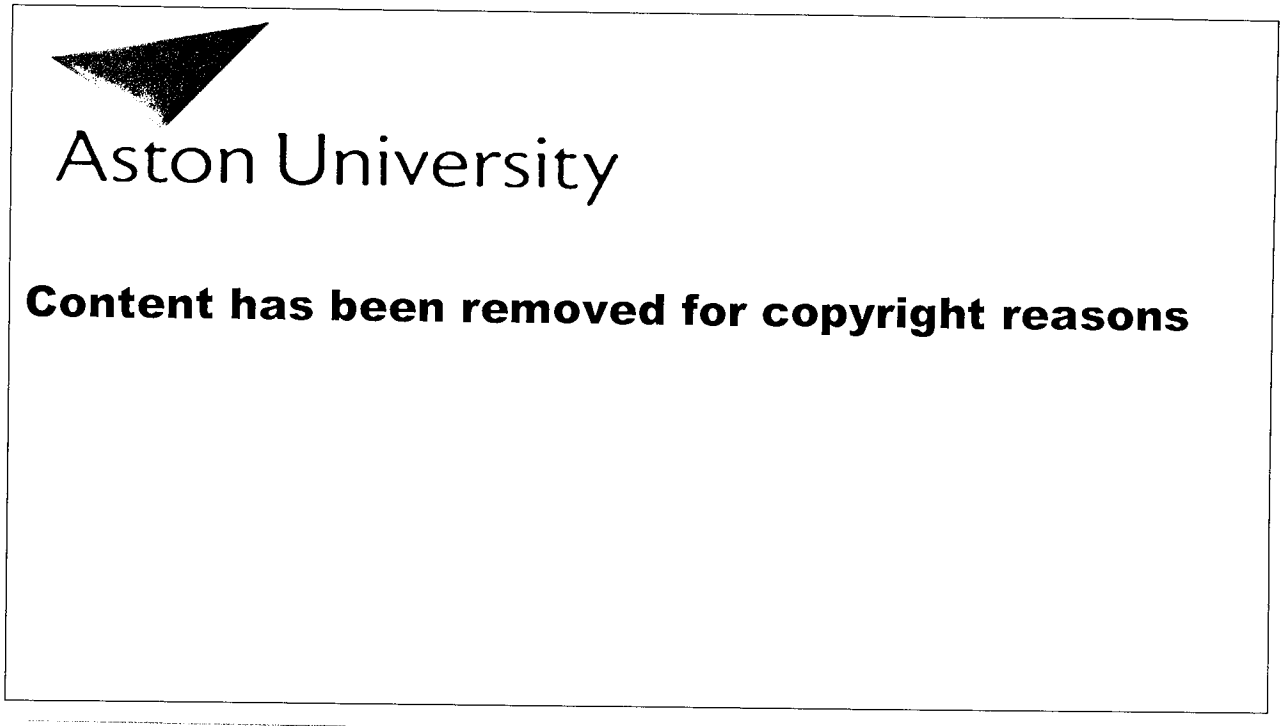

Figure 1.4 : A Golgi stained preparation of the upper layers of the visual cortex illustrating the long apical dendrites of the pyramidal cells in layers 2 and 3 of the visual cortex (Brodmans Area 17); (From Hubel, Eye, Brain and Vision 1988).

1.7 Radial versus Tangential Sources

Cells in the cortex are arranged in columns oriented perpendicular to the brains surface, and are believed to have similar fundamental characteristics (Hubel 1988). In man the cortex comprises fissures (sulci) and ridges (gyri). As a result of these infoldings, cells which are oriented normal to the surface of the brain become more tangentially oriented with respect to the surface of the head when located in the sulci or fissures (Okada 1983). It is likely that cells in the gyri remain more normal to the surface of the head (Figure 1.5).

To understand the effect this infolding may have on the externally observable magnetic field it is necessary to consider Flemings Left Hand rule (See Tripp 1983). This states that a current carrying source generates a magnetic field at 90^{o} to the direction of current flow. Thus when the current is flowing into the paper, the field is rotated clockwise. It is generally believed that neurons located in the gyri and oriented radial to the scalp do not generate an external magnetic field because in a symmetrical volume conductor eg. a sphere, the fields of radially oriented sources cancel (Tripp 1983).

These ideas are based upon theoretical work using a concentric spheres model of the head (Meijs et al 1987). However the head and its compartments deviate significantly from the spherical model. Melcher and Cohen (1988) using dipoles implanted in the heads of rabbits demonstrated that as a result of a) non spherical shape and b) non uniform conductivity and radially oriented sources may not generate a zero field externally but instead a field suppressed by a factor of 4-6 compared to that of a tangential source in the same location. The problems and limitations of using a concentric spheres model of the head will be discussed in a later chapter (Chapter 5).

1.8 Measurement of the Brains' Magnetic Field

1.81 Basic Magnetometer Design

There are two fundamental requirements of a system that is to be used to measure biomagnetic fields. It must be sensitive enough to detect the minute fields produced by the body and yet able to distinguish and reject possibly larger fields produced by more distant sources or noise. Table 1.1 shows the relative strengths of magnetic fields produced by various biological systems and in a range of environments. The brains' magnetic field at 10^{1} to 10^{3} fT is around a millionth of the strength of the earths' magnetic field.

In 1963 Baule and McFee used a 2 million turn coil and low noise amplifiers to record an adult magnetocardiogram (MCG) in an unshielded environment. However, in

Figure 1.5 : Idealised cross section of the scalp, skull and brain showing that neurons in the cortex although perpendicular to the brains surface may be i) radially oriented, ii) tangentially oriented or iii) may show both radial and tangential components (Okada 1983).

order to record the magnetoencephalogram (MEG) magnetic shielding and an averaging technique were necessary (Cohen 1968). An important step forward came with the introduction of SQUID (Superconducting Quantum Interference Device) based magnetometers (Cohen et al 1970, Zimmerman et al 1970). At first, these were used in shielded environments until the implementation by Opfer et al (1974) of an idea first proposed by Zimmerman et al (1971) of using gradiometrically configured detection coils ie. the use of compensating coils to reject uniform fields and uniform field gradients. This development brought the possibility of recording brain activity in an unshielded clinical environment.

Table 1.1: Relative magnetic field strengths in various locations and from biological sources.

Source	**Field Strength**
Earths magnetic field	10^{10} fT
Urban site	10^{8} fT
Magnetised lung contaminant	10^{6} fT
Adult magnetocardiogram (MCG)	10^{4} fT
Foetal magnetocardiogram	10^{3} fT
Magnetoencephalogram (MEG)	10^{3} fT
Evoked fields (ie. VEF, AEF, SEF)	10^{1} to 10^{2} fT
Magnetoretinogram	10^{2} fT
Intrinsic SQUID noise	10fT

The single channel SQUID based magnetometer in use today comprises a gradiometrically configured detection and input coil, a cryogenic vessel (Dewar), a SQUID and its associated electronics.

1.82 SQUID Based Magnetometers

SQUID based magnetometers are essentially very sensitive current to voltage converters. When a changing magnetic field is present at the detection coil, a current is induced in it. This current, flowing through the input coil, impresses a field upon the SQUID. The response of the SQUID to this field is monitored by electronic circuitry which sends out to a connected recording device a voltage equivalent to that created in the detection coil by the presented field. The following paragraphs describe in more detail the individual components of the magnetometer, their design and functioning.

1.83 Cryogenic Vessel (Dewar)

Figure 1.6 shows the structure of a typical single channel biomagnetometer. The dewar is a well insulated storage vessel used to hold the liquid helium necessary to maintain the SQUID and other superconducting components at the 4K required for their operation. Most dewars used in biomagnetism are composed of an epoxy/fibreglass composite which gives both thinness and strength. The helium reservoir is suspended by a tube from the top plate of the dewar and has a capacity of between 5 and 15 litres (Crum 1985). The bottom of the helium reservoir usually narrows to form a tail section where the pick-up coils are located. In most commercially available machines, the distance between the lowest pick up coil and the outer surface of the dewar tail is about 10-13mm (12mm in the machines used in this study). The distance between the lowest pick-up coil and the outside is kept to a minimum because of the rapid fall off of the magnetic field with distance from its source in the head. However, it is not practical to have a spacing of less than 7mm when the dewar is cold because if the vessel was warmed up, the differential thermal expansion would force the inner tail through the outer dewar (Crum 1985).

1.84 Noise, Detection Coils, Gradiometers and Noise Rejection

Noise can generally be attributed to one of three sources; intrinsic system noise, environmental and subject noise. Most of the intrinsic system noise is thermal in origin and is evenly distributed across the frequency spectrum. Except at absolute zero all systems contain thermal energy which causes the basic elements of the system - electrons, nuclei, atoms and molecules - to rotate and vibrate. In for example, the wire of an induction coil, this thermal energy results in variations in the local concentrations of conducting electrons which translate into voltage fluctuations (Zimmerman 1983). This thermal noise (also called Nyquist, Johnson or white noise) sets a lower limit on the induced voltage that can be detected in response to a small

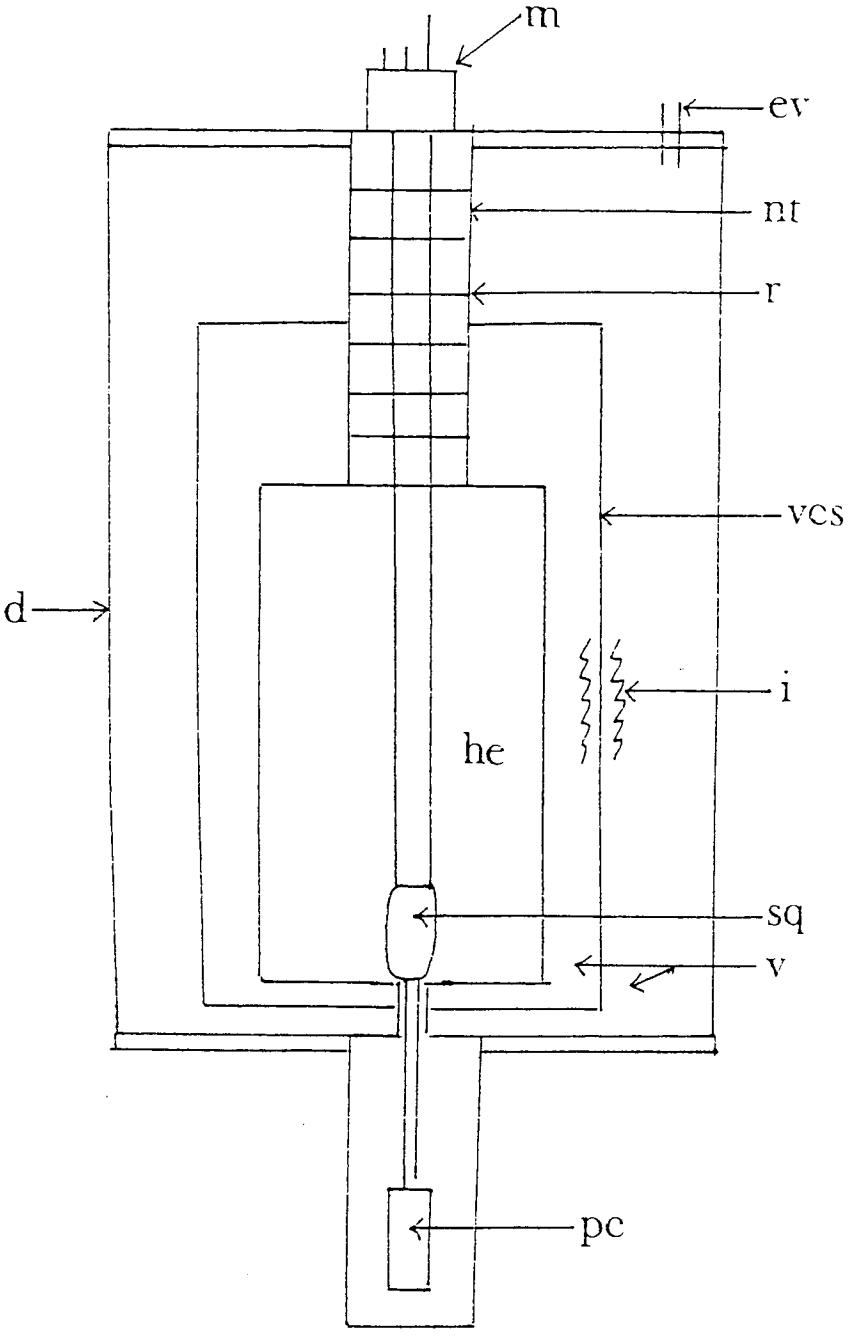

Figure 1.6 : The basic design of the neuromagnetometer. d=Dewar, m=probe, nt=neck tube, r=radiation baffles, vcs=vapour cooled shield, i=superinsulation, sq=SQUID, v=vacuum space, pc=pickup coils, he=liquid helium reservoir, ev=evacuation valve.

change in magnetic field. SQUID based magnetometers have low intrinsic noise because operating at low temperature (ie. 4K) thermal or Nyquist noise is limited. Also present is low frequency noise which increases in amplitude as frequency decreases. This is called 1/f noise and is of unknown origin.

Dewars themselves can contribute to the intrinsic noise of the system in one of three ways:- a) magnetic fields are generated by thermal noise in any conducting materials, particularly, if care is not taken in the superinsulation and vapour-cooled radiation shielding, b) thermal electromotive forces created as a result of large thermal gradients within the dewars produce magnetic fields although these are thought to occur at a frequency below that of interest and are thus rarely a problem (Crum 1985) and c) noise due to Eddy currents induced by ambient magnetic fields.

The strongest magnetic field in any environment is the earths magnetic field (Erne 1983). Solar storms can produce field amplitude fluctuations and any large ferromagnetic objects can appreciably change this field. Any movement of these objects ie. lifts, cars etc. in this field can be detected as low frequency magnetic signals. Movement of the detector with respect to the ambient field, ie. through vibration, can also create spurious signals. In the laboratory, a significant source of environmental noise arises from the power network. This is not only directly detectable by the magnetometer as a 50Hz ac field but may also induce Eddy currents in any nearby large metallic objects such as helium storage dewars, which will result in detectable magnetic fields (Carelli et al 1983).

Subject noise arises from clothing and acessories ie. metal fasteners, belt buckles etc., spectacle frames, hearing aids and watches. In addition, static in hair or clothing may also contribute noise (Cohen 1983). Subject movement under the machine itself creates a magnetic field and will emphasise any field artifacts created by either metal in clothing or acessories.

Of the system noise, only the components due to construction can be reduced ie metal components of the superinsulation are kept to a minimum and care in the design and construction of the radiation shield. Subject noise can be minimised through the avoidance or removal of items containing ferromagnetic metals. Environmental noise can be controlled in a number of ways. One method is through the installation of a magnetically shielded room. This is an expensive solution and therefore not a practical proposition for every facility particularly when the clinical use of MEG has not yet been convincingly demonstrated. In the absence of shielding, large ferromagnetic objects must be kept away from the magnetometer. In addition, signals can be filtered particularly to remove the large 50Hz signal seen in most laboratory environments.

However, the most important form of noise rejection usually takes the form of a gradiometer. Various configurations are available the simplest of which is the vertical axis, first order gradiometer (Figure 1.7). This comprises a detection coil which is placed close to the signal source ie. the head, and a compensating coil wound in the opposite sense, placed parallel to and a fixed distance away (called the baseline) from the detection coil. The result of this configuration is that spatially uniform fields such as those originating from a distant source, produce equal and opposite signals in the two coils which effectively cancel each other out. By varying the baseline the balance between rejection of noise fields and sensitivity to near fields can be adjusted. A second order gradiometer can be created by the serial arrangement of two first order gradiometers. This further improves noise rejection particularly for fields which change linearly, but it is not without the penalty of reduced sensitivity. The more coils there are in a gradiometer the better the noise rejection but the greater the loss of sensitivity. This occurs because as the number of coils increases so too does the length of wire which must share the flux. The inductance of the gradiometer coils can no longer be matched to that of the input coil and so flux transfer becomes less efficient (Erne 1983). A second limitation is a consequence of the method of manufacture. For optimal noise rejection it is important that the effective area of each coil is as close to that of the others as possible. It is also necessary when using second order or higher gradiometers that the baselines of each coil set are closely matched. The matching of the different coils is known as balancing. The manufacturing process produces gradiometer coils which must be improved in match by a factor of ten for the balance to be considered good. In order to achieve the desired balance, superconducting tabs are located close to the coils and these can be used to make their effective areas as identical as possible. The more coils there are, the more difficult it becomes to achieve a good balance. Most single channel systems for use in unshielded environments are second order gradiometers. In addition, some systems have used vertical axis gradiometers with asymmetrical coils. These have particular advantages and are used to address specific problems (Weinberg et al 1984).

Coil diameter and baseline are also important parameters. Although there is no standard coil size, the most frequently used are between 1 and 3cm in diameter with a 4 to 6cm baseline (Williamson and Kaufman 1981, Katila 1989). Larger coil diameters are more sensitive to weak fields since the field is averaged across the total coil area but show poor spatial resolution (Williamson and Kaufman 1981). Conversely smaller coils give better spatial discrimination but show less sensitivity. The baseline is the distance between adjacent coils in a gradiometer and is of importance because as the distance between the pick up coil and the source becomes greater than the baseline, the source has an increasing influence on the upper

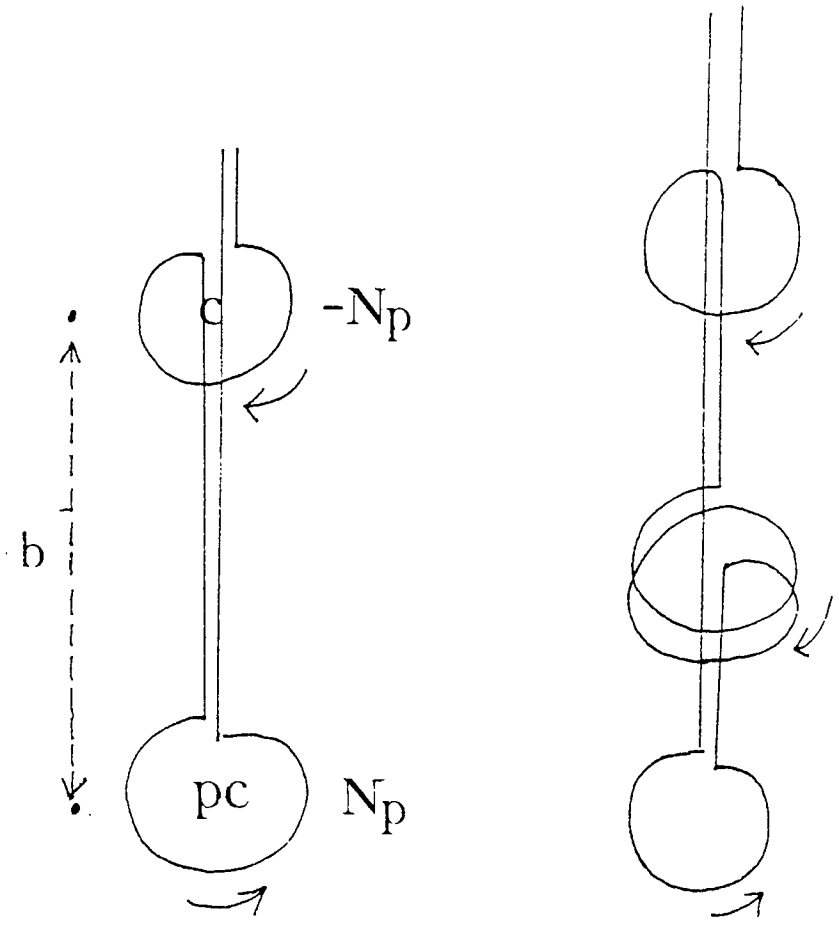

Figure 1.7 : Some vertical axis gradiometer designs a) first order and b) second order gradiometer. (b = baseline, pc = pickup coil, c = compensating coil)

compensating coils which results in signal attenuation (Hari et al 1988). For cortical sources up to a depth of 3cm, baselines of 3-4cm are usual. For deeper sources such as those in the longitudinal fissure of the visual cortex or of subcortical origin baselines of 5 or 6cm are preferable. The magnetometer used in this study has a 2cm coil diameter and a 50.4mm baseline and is hence, suitable for studying MEG signals from the visual cortex.

1.85 Multichannel Systems

Noise rejection using a multichannel systems is a more complex problem. The effectiveness of magnetic shielding and the origin of the system ie. whether commercial or a home made composite, determine whether first or second order gradiometers are used. Since accurate *in situ* balancing is difficult for large multichannel systems, other methods of noise rejection have been used. These have included electronic noise rejection (digital signal processing) and the use of planar gradiometers. The main advantage of planar gradiometers is that they are easy to produce using standard lithographic techniques. These have been shown to compare very favourably with vertical axis gradiometers of similar dimensions in terms of their spatial resolution and their ability to discriminate between multiple sources (Erne and Romani 1985, Carelli and Leoni 1986).

1.86 Superconducting Quantum Interference Devices (SQUIDs)

A simple explanation of how the SQUID works is given by Kaufman and Williamson (1984). A current can be induced in a ring of superconducting material by placing a magnet in its vicinity. When the magnet is removed and the ring cooled in liquid helium to 4K, flux remains trapped in the ring. Shielding currents set up in the surface of the ring prevent any externally applied magnetic field from entering the ring. It is an inherent property of such rings that the trapped flux remains constant (the Meissner effect). The current is carried in the ring by paired electrons known as Cooper pairs and these obey the quantum mechanical laws of motion and exhibit wave like properties. The wavelength is such that the waves do not destructively interfere. The flux is thought to be quantised so that the ring encloses an integer number of flux quanta. The SQUID relies upon the Josephson Effect (Josephson 1962) for its operation and is in essence a very sensitive current to voltage converter. The introduction of one (rf SQUIDs) or two (dc SQUIDS) "weak links" or Josephson junctions into a superconducting ring makes it sensitive to externally applied magnetic fields. These weak links have a number of forms but all behave in the same manner (Duret and Karp 1983, Gallop and Petley 1976). In a two junction dc SQUID a constant current (I) is fed from a source at room temperature to the superconducting

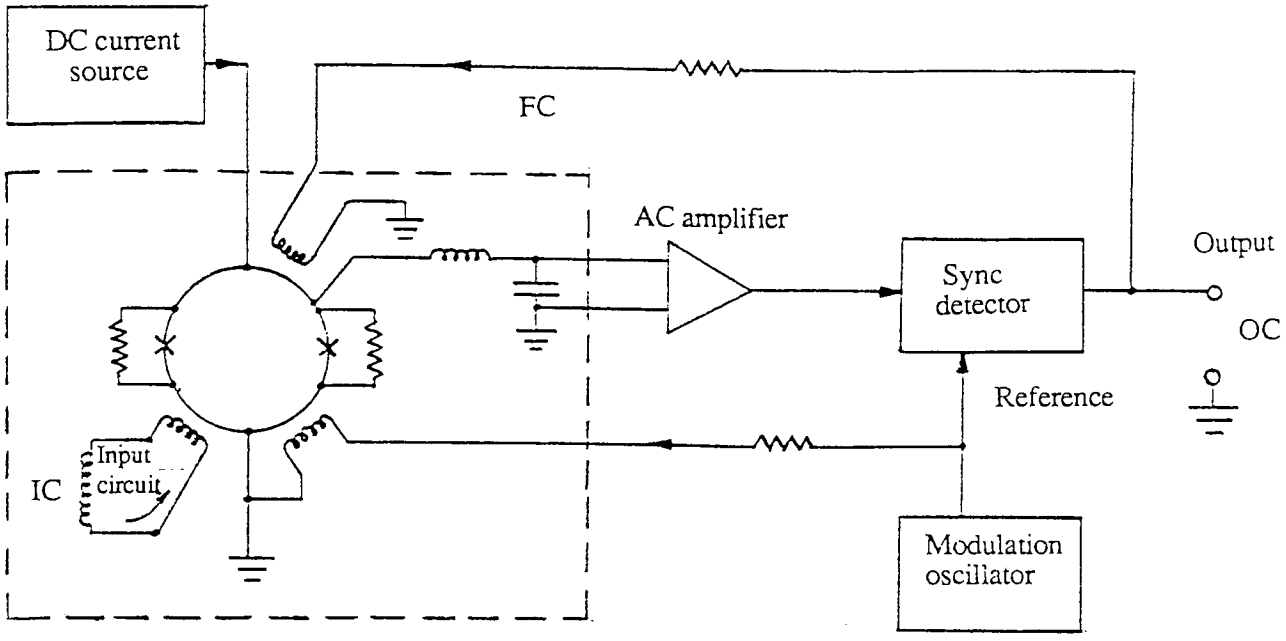

Figure 1.8 : A circuit diagram showing input/output of a SQUID based system. IC = input circuit, FC = feedback current, OC = output current.

ring (Figure 1.8). When a magnetic field is applied to the ring via the input coil (IC) there is an enhancement of net current flow at one junction and a decrease in current at the other. This difference in current flow at the two junctions is detected and a feedback current (FC) is injected back into the ring to return the junctions to equal status. This injected current value is also fed out of the system (OC) after amplification and demodulation, to a connected recording device. The feedback current is linearly related to the current which created the disturbance initially.

CHAPTER 2

THE VISUAL SYSTEM AND VISUAL EVOKED POTENTIALS

2.1 Introduction

Since this thesis is concerned with the measurement of visually evoked magnetic responses (VEMR) from the human brain, the structure and function of those aspects of the visual system and the visual evoked potential (VEP) relevant to neuromagnetic measurements will be briefly described. The following section is limited to a discussion of the general anatomical pathways from the eye to the brain, a consideration of the way in which the visual scene is encoded and the evidence which supports the existence of specific visual information channels. The latter are important in relation to the visual stimuli examined in this study.

Figure 2.1 shows the anatomical arrangement of the visual system from the eye to the cortex. Light enters the eye via the pupil and is brought to focus on the retina by the cornea and the lens. The retina consists of 3 layers of cells, the most posterior of which are the photoreceptor cells. The middle layer comprises the bipolar cells but also contains the cell bodies and processes of laterally oriented cells viz. the amacrines and horizontals. In the most anterior layer are the retinal ganglion cells. Light passes through the more anterior layers before falling onto the photoreceptor cells and initiating a photochemical reaction. The signals produced by the photoreceptors are modulated and processed by the other cells, passing finally to the retinal ganglion cells. Axons from the retinal ganglion cells pass across the surface of the retina, collecting at the optic disc before leaving the eye as the optic nerve. The optic nerve retains the retinotopic organisation, with fibres representing the central visual field travelling in the central slower conducting axons of the nerve (Katz and Rimmer 1989). At the optic chiasm, fibres which originate in the temporal retina of each eye pass to the ipsilateral Lateral Geniculate Nucleus (LGN) whilst those from the nasal retinae decussate and travel on to the contralateral LGN. A small number of fibres follow a non-geniculate pathway, passing instead to the Superior Colliculus, a structure on the dorsal surface of the midbrain. The LGN is made up of 6 distinct layers, two ventral or magnocellular layers and 4 dorsal, parvocellular layers. Fibres from the ipsilateral eye terminate in layers 1, 4 and 6 whilst those from the contralateral eye innervate layers 2, 3 and 5. The LGN acts not only as a relay station but also performs some filtering of the visual signal (Singer 1979). At the LGN, fibres from all six layers combine to form a broad band called the optic tract or radiation which then passes to the primary visual cortex (also called the striate cortex,

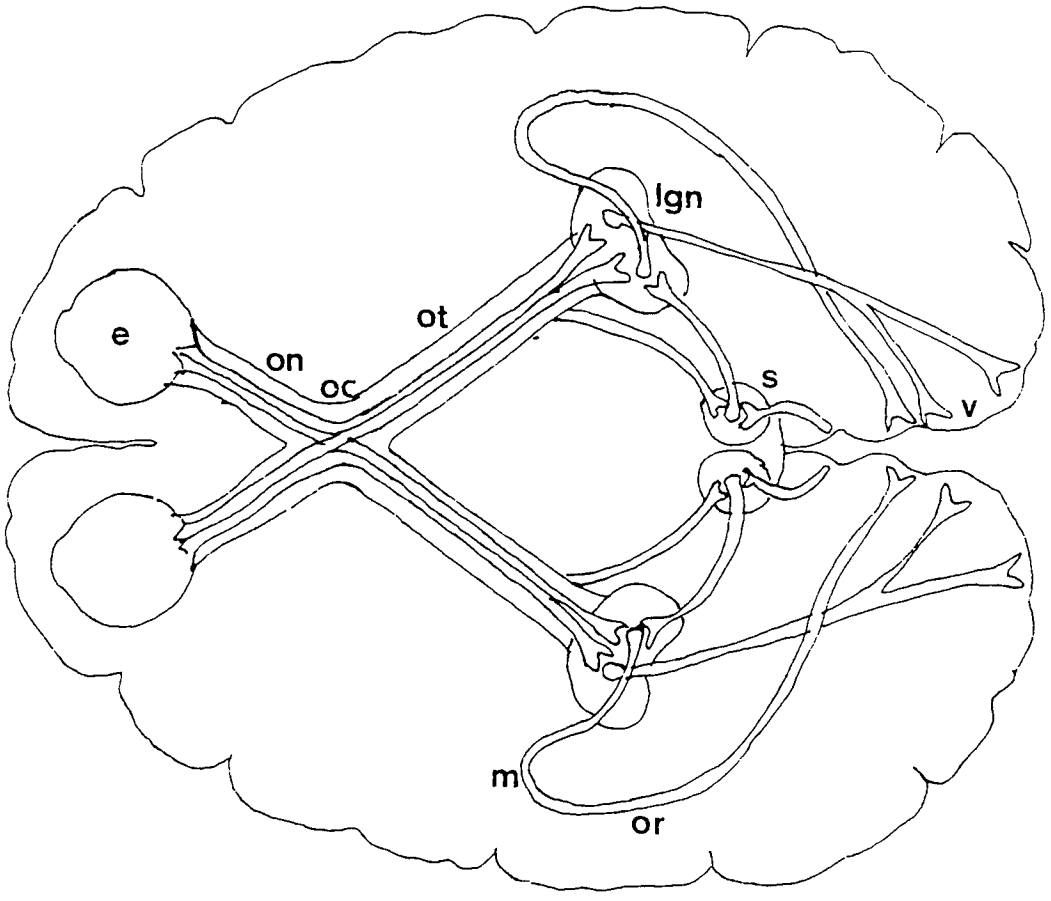

Figure 2.1 : Diagram of the visual system from the eye to the brain (e = eye, on = optic nerve, oc = optic chiasm, ot = optic tract, lgn = lateral geniculate body, s = superior colliculus, m = Meyer's loop, or = optic radiation, v = visual cortex).

Brodmann's area 17 or V1). The retinotopic organisation is retained here with the foveal and central visual field represented at the occipital pole and posterior calcarine fissure while the more peripheral retina is represented more anteriorly. The projection of the retina onto the cortex can be described as a cruciform model (Okada 1983). In this model, the visual field is divided into octants which are represented in an organised manner on the various lips of the calcarine fissure (see Chapter 5).

2.2 Retinal Processing of Visual Information

The idea that there are pathways encoding separate aspects of the visual scene arose from the discovery of functionally distinct classes of retinal ganglion cells and their projection to different brain regions (Rodieck 1979). The first stage of this visual encoding occurs in the retina where there is a considerable convergence of information from the input at the photoreceptor cells to the output of the retinal ganglion cells.

The neural retina (Figure 2.2) comprises three main layers. Most posteriorly lie the photoreceptor cells responsible for the transduction of light into electrical signals. There are two types of photoreceptor cell separable in the first instance in terms of their morphology into rods and cones. They differ also in the photosensitive pigments that they contain and hence, in their response to light and their distribution across the retina. There are approximately 110-125 million rod cells in the retina and they are responsible for vision under dim light (scotopic) conditions when cone cells can no longer function. They contain purple pigments called rhodopsins which absorb light maximally at around 510nm. The density of the rods varies across the retina from zero at the fovea to a maximum of 160,000/mm^2 at an eccentricity of 10^o, decreasing thereafter. The cone cells can be divided into 3 subtypes according to the absorption spectra of the light sensitive pigments they contain. L or red sensitive cones absorb maximally at 560nm, M or green sensitive cones absorb maximally at 530nm and S or blue sensitive cones have an absorption maxima at 420nm. The distribution of each type in the retina varies between species but generally red and green cones are present in a ratio of 1 : 1 while there are slightly fewer blue cones. A regular triangular lattice is formed by the blue cones with the gaps filled randomly by the red and green cones (Kaplan et al 1991). There are around 6.3 to 6.8 million cone cells with a maximal density at the fovea (cf the rod cells) of 147,000/mm^2 decreasing to about 5000/mm^2 at an eccentricity of 10^o (Hubel 1988). The cone cells are believed to be responsible for fine detail and for colour vision.

At present, 7 types of bipolar cell have been identified in the primate retina which differ in the number and type of connections they make (Kaplan et al 1991). The way in which the photoreceptor cells connect with first, the bipolar cells and ultimately, the

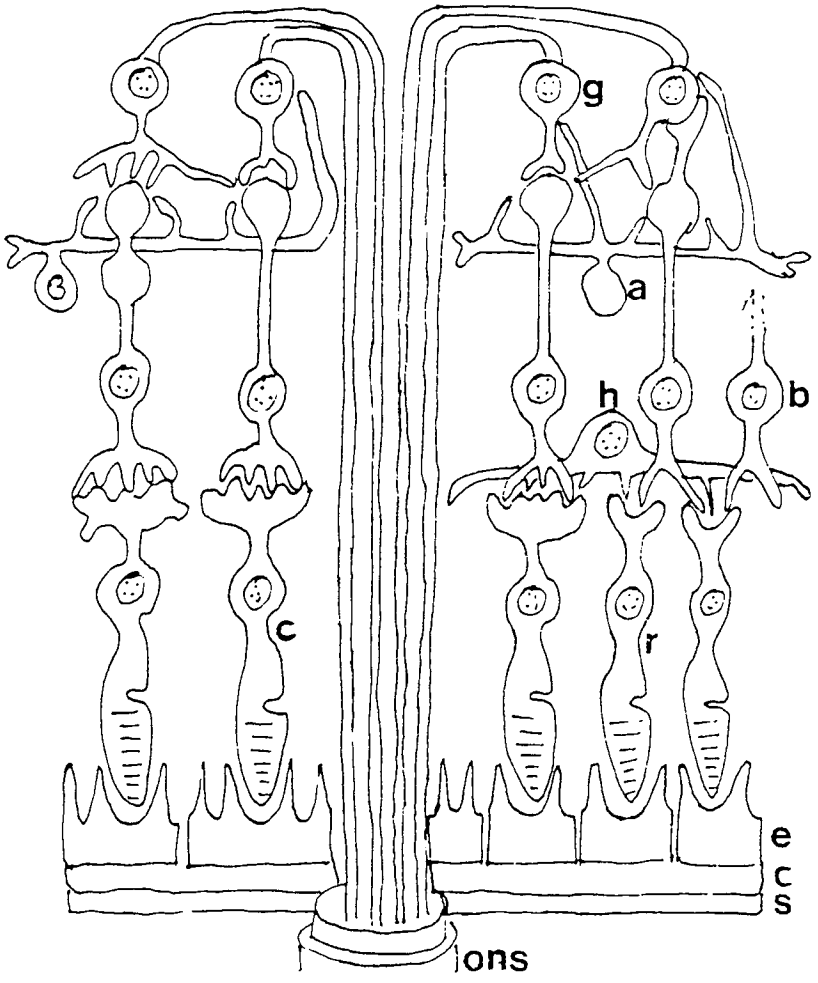

Figure 2.2 : A cross section of the human retina (s = sclera, c = choroid, e = pigment epithelium, r = rod cell, c = cone cell, b = bipolar cell, h = horizontal cell, a = amacrine cell, g = ganglion cell, ons = optic nerve sheath).

retinal ganglion cells differs across the retina. At the fovea a single cone cell connects with a single bipolar cell which in turn connects with one retinal ganglion cell. However, at the periphery more receptors converge on each bipolar and more bipolars are connected to each retinal ganglion cell. There is also a less direct path between the photoreceptors and the retinal ganglion cells - through the lateral connections of the horizontal and amacrine cells.

2.3 Receptive Fields

Retinal ganglion cells have been classified into morphological and functional types. Kuffler (1953) was the first to describe the antagonistic centre surround organisation of retinal ganglion cells. Using the cat, which has fairly large and accessible retinal ganglion cells, he recorded the responses of selected cells to small spots of light shone onto the retina. He discovered that each retinal ganglion cell was connected to an approximately circular area of photoreceptor cells and that the ganglion cell responded in one of two ways to stimulation by a spot of light. He called these ganglion cells on-centre and off-centre according to their behaviour. The area of photoreceptor cells to which stimulation could be applied to provoke a response in a given ganglion cell is known as its receptive field. Kuffler (1953) found that for some retinal ganglion cells, when a light spot was shone on the centre of the receptive field they responded by increasing their firing rate. He also discovered that by shining the light spot onto the peripheral receptive field of the same cell that the rate of firing decreased. The other type of cell he called off-centre for it showed the same centre-periphery antagonism but this time when the centre was stimulated, the firing rate fell. The converse occurred at the periphery.

There are now thought to be 12 distinct types of retinal ganglion cell definable in terms of their receptive field properties. There are nine types of antagonistic centre surround cell (including one colour opponent type) and three show other forms of organisation - one set supressed by the presence of contrast within the receptive field, one responding to movement in a specific direction and one responding to definite edges (Carpenter 1984). The receptive fields of adjacent ganglion cells show considerable overlap and vary in size across the retina. At the fovea receptive fields are smallest, growing larger with greater retinal eccentricity. The increase in receptive field size with eccentricity parallels closely the decrease in visual acuity that has been observed (Kaplan et al 1991).

The existence of these receptive fields has important implications for experimental stimulation of the visual system. In order to stimulate the fovea, where the receptive fields are smallest, the optimum stimulus should be composed of small elements that

do not stimulate the centre and periphery of the receptive fields equally. Neurophysiological studies have indeed demonstrated that the central retina is stimulated more effectively (produces larger cortical response) when small checks or fine gratings are used (Ristanovic and Hadjukovic 1981). The more peripheral retina where receptive fields are larger is optimally stimulated by more coarse, lower spatial frequency stimuli (Ristanovic and Hadjukovic 1981).

Thus, the connection between the photoreceptor cells and the retinal ganglion cells can be described in terms of receptive fields where each ganglion cell connects to a circular array of photoreceptor cells via the bipolars and ganglion cell output is determined by its net input. In addition, the ganglion cells can be described in terms of morphology, physiology and the destination of their axons in the LGN. Early studies were carried out in the cat (for a review see Rodieck 1979) where the ganglion cells could be divided into three types called X,Y and W (Enroth-Cugell and Robson 1966). The X type cell accounted for around 55% of the population and was most densely distributed at and around the fovea. These cells had small cell bodies and small diameter axons. Their conduction velocities were slower and their receptive field size at a given eccentricity were smaller than those of the Y type cell (Kaplan and Shapley 1982). The responses of X type cells to various stimuli were also studied. They show a sustained response to a stepped stimulus, the increased firing rate continuing for the duration of the stimulus. They also showed a linear summation response to a stationary grating and an increase in mean pulse density in response to a drifting grating. Y type cells account for around 25% of the population, tending towards higher densities in the peripheral retina (Shapley et al 1981, Blakemore and Vital-Durand 1981). Y cell bodies and axons are larger than for the X cell and have higher axonal conduction velocities (Kaplan and Shapley 1982). They respond to a stepped light stimulus in a transient manner ie. there is an initial increase in firing rate which then rapidly returns to the baseline. These cells demonstrate a non-linear summation response to a stationary grating and a modulation of pulse density at the drift frequency to a drifting grating. Both X and Y type cells show on and off centre receptive field organisation but X cells tend to be more sensitive to luminance changes while Y cells are more sensitive to edge movement across their receptive field. The characteristics of these cell types can be followed through to the LGN and then to the primary visual cortex (Kaplan et al 1991).

2.4 Parallel Visual Pathways - M and P Cells

The idea of parallel pathways which process different aspects of vision arose initially from the results of psychophysical experiments. This idea was further developed by

the discovery of distinctive retinal ganglion cell types, namely X and Y cells, in the cat. More recently it was realised that analogous cells may exist in the primate retina. These cells, called M and P cells because of their connections in separate, distinctive layers of the LGN, have been studied in detail for 25 years. A considerable amount of information has been collected on their anatomical and physiological properties, their connections in the LGN and visual cortex and on their responses to various stimulus parameters. For a recent detailed review, see Kaplan et al (1991). Overleaf in Table 2.1, the features which best distinguish the two cell types are listed. Two further classes of primate ganglion cell are also thought to occur in the retina and have been called C and E cells. Their characteristics are less well defined but they are known to pass to the superior colliculus and the pre-tectal region rather than the LGN. In addition, M and P cells themselves are not thought to be homogenous but to contain subsets of cells. In particular, M cells have been divided into those with X and those with Y type characteristics (Kaplan et al 1991).

In addition to the morphological differences between M and P cells, M cells having larger cell bodies and more thickly myelinated axons while P cells are smaller with thinner axonal myelination, there are differences in their connections to the LGN. M cells connect with the two ventral, magnocellular layers of the LGN and then onto layer 4C alpha of the primary visual cortex while P cells connect with the four dorsal, parvocellular layers of the nucleus and then layer 4C beta in the cortex. Psychophysical tests have attempted to separate the two systems completely but to date most stimuli are capable only of increasing the activity of one channel with respect to another. As M cells are able to respond to patterns under scotopic conditions whilst P cells may not, this can be used to bias neuronal activity in favour of the M cells. It is argued that high spatial frequency patterns stimulate only the P cells, as M cells do not have the required sampling density. Hence, fine isoluminant red-green gratings have been used in an attempt to preferentially stimulate P cells (Krauskopf et al 1989). The stimuli used in clinical neurophysiology are not usually so subtle. A flash stimulus is considered to have a strong luminance component (although at lower intensities an edge effect is often perceived) and so is felt to preferentially stimulate the M or luminance pathway. A pattern reversal stimulus, produced either by a video screen or via projection onto a screen, is more complex. Small checks with their high spatial frequency are more likely to stimulate the P pathway. However, larger checks with their coarse pattern and possibly less constant luminance, would stimulate the M cell pathway. It is also possible that reversing checks have a motion component as VEP latency is affected by the time taken for the pattern to reverse (Stockard et al 1979). Hence, at the current state of knowledge, it is likely that both large checks and flash stimulate the M cell pathway more than the P cell pathway. In addition, as the spatial

Table 2.1 : Features of the M cell (magnocellular) and P cell (parvocellular) pathways.

FEATURE	M Cells	P Cells
Input	Probably from several cones and diffuse bipolars. Substantial rod component	Probably from 1 cone and few midget bipolars. Rod input significant only in peripheral retina.
Output	To 2 ventral layers of LGN.	To 4 dorsal layers of LGN.
Axons	Larger, thicker myelination.	Mediumsized, thinly myelinated
Dendritic Tree	Rapid increase in diameter with retinal eccentricity.	Constant in central retina, larger in periphery.
Brain Projection	Layer 4Calpha.	Layer 4Cbeta.
Receptive Field Size	Larger.	Smaller.
Conduction Velocity	Higher.	Lower.
Luminance Contrast Gain	8 to ten times higher than for parvocellular	
Linearity of Spatial Summation	75% linear (X type), 25% non-linear (Y type).	All linear.
Response to Light Steps	Phasic (transient).	Tonic (sustained).
Spectral Sensitivity ?	No.	Yes.
Scotopic Pattern Vision	Yes.	No.
Optimal Stimulus Type	Low contrast/luminance.	Fine isoluminant patterns (coloured).
Optimal Stimulus Frequency	20Hz	10Hz
X and Y Characteristics	75% X, Rest Y.	All X type.
Effect of Lesion	Impaired performance in tasks involving movement. No effect on depth perception or stereopsis.	Decrease achromatic contrast sensitivity, visual resolution and chromatic discrimination.
Channel Served	Luminance.	Chromatic channel.
	Coarse pattern perception.	Probably fine detail at high contrast levels.
	Motion detection ?	

frequency of the checks decreases then the P cell pathway may contribute more to the observed responses.

2.5 Processing at the Cortical Level

The primary visual cortex comprises around 200 million neurons (Hubel 1988). Although knowledge of processing is incomplete, more is known about visual processing than of the other sensory systems.

One of the first principles of cortical organisation that was recognised was the existence of ocular dominance columns (Carpenter 1990). Studies using microelectrodes revealed that adjacent columns of cells represented receptive fields of cells in the retina of the left and then the right eye.

Visual processing appears to be divided into a number of stages and is carried out by sets of cells exhibiting behaviour with different levels of complexity. The early stages of cortical processing in area B17 (V1) is carried out by cells which can be divided broadly into simple and complex cells. Although some cells do show the antagonistic centre/surround type of receptive field seen at other levels of the visual system, simple cells have small receptive fields which consist of excitatory and inhibitory strips. A moving bar or edge is a more effective stimulus for these cells than diffuse illumination (Carpenter 1990). These cells are also arranged into columns, each column sharing a preference for stimuli with the same orientation. The preferred orientation of the columns then changes systematically across the cortex.

Like simple cells, complex cells respond best to bars or edges with a preferred orientation but will respond to targets anywhere within their receptive field. A subset of these cells are termed 'hypercomplex' and demonstrate not only orientation preference but also require that the stimulus lies within certain limits of size to be effective.

A further classification of cortical columns has been found in area B17 viz. heavily stained blobs or puffs separated from one another by more lightly stained interblob regions when revealed by cytochrome oxidase (Livingstone and Hubel 1988). Wavelength selective cells were concentrated in the blobs of B17 whereas form selective cells were concentrated in the interblobs

Like B17, B18 (V2) shows a cortical organisation. This takes the form of thick and thin stripes separated by more lightly stained stripes. Wavelength selective cells congregate in the thin stripes while motion sensitive cells are found in the thick stripes. Cells sensitive to form are distributed in both types of stripe. Hence, B17 and B18

appear to act as receiving centres in which different types of visual signal are assembled before relay to more specialised visual areas.

Study of cortical processing in areas B17 and B18 suggest that there are four parallel systems concerned with different attributes of vision:- motion, colour and two systems for form (form alone and form with colour). The motion system appears to reside in area V5 located at the posterior end of the middle temporal gyrus (Zeki 1992) while the colour system depends on area V4. Of the two systems concerned with form, form alone appears to depend on V3 and form with colour on area V4 (Zeki 1992).

2.6 The Visual Evoked Potential (VEP)

The VEP has been useful in the clinical diagnosis of a number of neurological and psychiatric conditions. It is possible that because of the greater sensitivity of the MEG, the VEMR may complement the VEP in clinical diagnosis. The first visual evoked responses used clinically were recorded in response to unstructured flashes of white light (Adrian and Mathews 1934). Subsequently, Halliday et al (1972) using both patterned stimuli and strobe flash, demonstrated an improved sensitivity of pattern over flash in detecting lesions of the visual pathway. A black and white reversing checkerboard was used, centrally fixated and with the response recorded from a single mid-occipital electrode. Despite the emergence of other visual stimuli which include pattern onset-offset, bar gratings, flashed pattern and coloured checks, the reversing (or shifting) checkerboard remains a popular stimulus for clinical use. The stimulus is easy to generate and more importantly the waveform produced by pattern reversal stimulation has been shown to be more consistent in terms of morphology and component latency than that produced by most other stimuli. There are a number of components identifiable in the first 200ms of the response but the major surface positive component occuring at around 100ms (P100) has been shown to be the most consistent and stable and is considered a fairly sensitive indicator of abnormality (Spehlmann 1985). By contrast, flash stimulation tends to be used as an adjunct to pattern reversal. Exceptions to this are in the monitoring of surgery on or around the optic nerve where the information may be used to help preserve the integrity of the nerve (Wright et al 1973), in orbital trauma or dense cataract in order to establish whether or not the pathway between the retina and cortex is intact and finally in the unco-operative patient. As a consequence, most of the following discussion relates to the clinical use of the pattern reversal VEP.

There are a number of problems associated with the interpretation of the VEP. Firstly, there is some variation in the VEP in terms of latency, amplitude and morphology from person to person. This may be due to anatomical differences in the visual cortex

particularly in the extent of foveal/macular representation at the occipital pole, in the angle of the calcarine fissure to the scalp and between hemispheres (Brindley 1972, Stensaas et al 1974). Stimulus parameters can also affect variability. Since the P100 latency variation is small, particularly between eyes in a subject, it is the most useful indicator of abnormality. However a problem arises when comparing the normal P100 with the large surface positive component of the abnormal VEP or in the 6% of normals in whom more than one peak is evident (Shahrohki et al 1978, Blumhardt et al 1982). It is possible that non analagous components are being compared. The P100 may be a complex response from different regions of the visual cortex and hence, a lesion may suppress some aspects of the response and accentuate other components. To overcome this problem, topographic mapping has been necessary in most cases to elucidate these responses (see Chapter 5).

By contrast with latency, amplitude may show a wide normal variability and so is less useful as a diagnostic indicator of abnormality (Snyder et al 1981). Again, interocular difference is the best indicator of pathology but a reduction of more than 50% is necessary for the response to be considered abnormal on amplitude grounds alone (Spehlmann 1985).

Abnormalities of waveform morphology can also occur (Spehlmann 1985) and are usually seen as a broadening or birfurcation of the P100 peak, but are not believed to be characteristic of a specific pathology. An exception to this is the W type (PNP) response which correlates well with the presence of a central scotoma due to damage to the central conducting fibres (Spehlmann 1985).

A number of different strategies have been adopted in order to improve the use of the VEP in clinical diagnosis. The most successful has been the use of monocular and full/half field stimulation (Rowe 1982). Prechiasmal lesions can be detected by recording monocularly the full field response at a mid-occipital electrode (Oz). If the lesion is unilateral then the abnormal response will be seen after stimulation of the affected eye. If the temporal or nasal retina only is affected, then half field stimulation will be necessary to localise the lesion, although any reduction in amplitude or increase in latency should be seen in the full field response.

Post-chiasmal lesions are more difficult to localise using the VEP (Blumhardt 1987). It is necessary to stimulate the left and right half fields separately and record from the lateral locations O_1 or O_3 and O_2 or O_4 rather than on the midline. Unfortunately, as a consequence of anatomical variability, asymmetric responses occur in normals and so, with no knowledge of the pre-morbid response, abnormalities are not readily discerned. Apparent delays may be a consequence of misidentification of the

components of the more complex waveforms resulting from half field stimulation and may be secondary to waveform distortions. Often rather large field defects must be present before the VEP is affected and these are better detected by methods such as perimetry. Furthermore, with the advances seen in CAT and MRI there is probably little role for the VEP in locating circumscribed lesions like tumours along the posterior visual pathway.

The VEP has been used in the diagnosis of a range of conditions including Freidreichs Ataxia (Carroll et al 1980), Parkinsons Disease (Bodis-Wollner et al 1987), Ischaemic Optic Atrophy (Wilson 1978, Harding et al 1980) and Toxic Optic Neuropathy (Kriss et al 1982). Two conditions in which the VEP is of particular diagnostic use in our laboratories and for which theoretically neuromagnetic measurements may offer further information or some advantage, are Optic Neuritis and Alzheimer's Disease.

2.61 Acute Optic Neuritis and Multiple Sclerosis

The detection of areas of demyelination in acute optic neuritis (ON) and multiple sclerosis (MS) has been a major application of the VEP (Blumhardt 1987, Harding and Wright 1986). Acute ON is characterised by sudden, severe and unilateral loss of vision. Often there is pain upon eye movement, a pale, oedematous disc and signs of an afferent pupillary defect ie. a failure of the pupil to constrict when a light is shone into the adjacent, unaffected eye. This condition occurs primarily in the 20-40 year age group and the most common symptom, useful in diagnosis, is that of spontaneous recovery. Initially, when visual acuity (VA) may be reduced to perception of light only, it may be possible to record only the flash VEP, the latency of which may fall outside of normal limits (Harding and Wright 1986). However as VA reaches 6/60 or better it is usually possible to obtain a response to pattern stimulation, although in at least 90% of affected eyes, it will be abnormal. The most common defect is a delay in the P100 (Asselman et al 1975, Cant et al 1978, Shahrohki et al 1978, Harding and Wright 1986), usually of the order of 10-30msec (Cant et al 1978), although abnormalities of amplitude (Shahrokhi et al 1978), morphology (Hoeppner and Lolas 1978, Jones and Blum 1985) and duration (Collins et al 1978, Shahrokhi et al 1978) have also been reported. Interocular latency difference is more effective than absolute latency in detecting abnormalities since there is less variation of latency between eyes than between subjects. Abnormal wave morphology has also been reported. Of particular note is the occurence of a W shaped wave (Hoeppner and Lolas 1978, Jones and Blume 1985). This is thought to be associated with central fibre damage as a central scotoma is a defect commonly seen in optic nerve lesions. Although there are

reports of increased P100 duration, probably as a result of desynchronisation, this is usually accompanied by a delay in latency (Collins et al 1978, Shahrokhi et al 1978). Despite an early reduction in P100 latency (thought to be a consequence of subsiding oedema), in around 95% of subjects it remains abnormally delayed (Halliday et al 1973, Diener and Scheibler 1980).

As the VEP gives a good indication of episodes of past demyelination, it is useful in the confirmation of Multiple Sclerosis (MS), for which at least two separate lesions are necessary for diagnosis (Hallpike 1983).

Hence, in acute unilateral optic neuritis there is a significant delay in pattern reversal P100 latency whereas the flash P2 latency usually falls within normal limits. It is thought that it is the smaller diameter, central fibres of the optic nerve that are particularly affected by demyelination in ON. Peripheral fibres are thought to be less affected in most patients although in a proportion of patients parafoveal, peripheral and arcuate defects can occur (Novak et al 1988). Thus it is possible that the magnetic response would be less affected than the VEP in ON since the most affected cell population, that serving the fovea, is represented on the occipital pole. Here the cells may be oriented more radially to the surface of the head and thus may not contribute significantly to the magnetic response. However, the combined use of the VEP and VEMR could aid the separation of ON, in which the central fibres are most affected, from vascular or neoplastic lesions which tend to affect more peripheral nerve fibres (Beck and Smith 1988). One of the objectives of the following work is to attempt to establish normative values for the magnetic pattern reversal and flash response and the interocular latency difference to facilitate the possible future study of unilateral optic neuritis and other retinal/optic nerve abnormalities.

2.62 Alzheimer's Disease

That the VEP may be a useful aid to the diagnosis of Alzheimer's Disease (AD) was first suggested by Visser et al (1976) who found that the major positive component of the flash VEP (P2) was delayed in sufferers of the disease. This was confirmed by Harding et al (1981) who noted that co-existing with the abnormal flash P2 was a normal response (P100) to pattern reversal. That the latency of the flash P2 reflects the severity of the dementia ie. the more demented the patient the greater the P2 delay has been reported by a number of authors (Cosi et al 1982, Orwin et al 1986, Philpot et al 1990).

Probably the commonest cause of dementia, AD, is thought to account for 50-60% of cases whose onset is in the fifth decade of life, rising to 90% of cases occuring in the

seventh or eighth decade of life. Onset of the disease is often insidious with early symptoms of short term memory loss often masked by the retained intellectual ability and personality of the patient. As the disease progresses, there is an increasingly marked cognitive deficit involving language and speech, visuospatial perception and reasoning. The patient becomes unable to wash, clothe or feed themselves, becomes incapable of social interaction and emotionally labile. Eventually mutism, incontinence and occasionally epilepsy ensue and the patient may appear withdrawn and inaccessible. The differential diagnosis of AD is important as many forms of dementia, eg. normal pressure hydrocephalus or as a consequence of metabolic disorder, may be treatable. Clinical diagnosis is difficult, with psychological tests and physical tests such as the EEG being either non-selective or unreliable. A definitive diagnosis is only possible at post-mortem which is of little use to the patient. There are a number of hypotheses as to why the flash response is selectively affected in Alzheimer's disease. Although exact localisation of these components has not been made, it is thought that the pattern reversal P100 component may originate in area 17 (primary visual cortex) and that the flash P2 component arises in area 18 or 19 (the association cortex) (Harding and Wright 1986, Ducati et al 1988, Armstrong et al 1989). It is believed that the information contained in the pattern reversal stimulus is relayed to the primary visual cortex via the LGN, by small diameter fibres and that the luminance information contained in the flash stimulus travels to the cortex via a non-geniculate pathway through larger diameter fibres (Harding and Wright 1986). In addition, post-mortem studies of Alzheimer brains have revealed that the pathological changes characteristic of the disease occur more prominantly in the fissures as opposed to the crests of the gyri (Armstrong et al 1989). It is also thought that the larger diameter fibres subserving the flash response show more atrophy than the smaller fibres (Katz and Rimmer 1989). As magnetic signals arise from the tangentially oriented cells of the fissures it would be expected that MEG would be more sensitive to this pathology than the electrical recordings which arise from both the fissures and the gyri (tangential and radial sources). It is also of interest that the plaques and neuro-fibrillary tangles characteristic of Alzheimer's disease occur in association with the dendrites of the pyramidal cells in layers II and III of the cortex where the currents which produce the magnetic field are thought to arise (Armstrong et al 1990). Hence, it may be possible, because of the increased sensitivity of the magnetic recording, to detect the disease at an earlier stage than at present.

2.7 Previous Studies Of The VEMR

Although there is a large literature on the VEP there have been relatively few magnetic studies of the visual system compared with the auditory (Hoke et al 1989, Pantev et al

change in magnetic field. SQUID based magnetometers have low intrinsic noise because operating at low temperature (ie. 4K) thermal or Nyquist noise is limited. Also present is low frequency noise which increases in amplitude as frequency decreases. This is called 1/f noise and is of unknown origin.

Dewars themselves can contribute to the intrinsic noise of the system in one of three ways:- a) magnetic fields are generated by thermal noise in any conducting materials, particularly, if care is not taken in the superinsulation and vapour-cooled radiation shielding, b) thermal electromotive forces created as a result of large thermal gradients within the dewars produce magnetic fields although these are thought to occur at a frequency below that of interest and are thus rarely a problem (Crum 1985) and c) noise due to Eddy currents induced by ambient magnetic fields.

The strongest magnetic field in any environment is the earths magnetic field (Erne 1983). Solar storms can produce field amplitude fluctuations and any large ferromagnetic objects can appreciably change this field. Any movement of these objects ie. lifts, cars etc. in this field can be detected as low frequency magnetic signals. Movement of the detector with respect to the ambient field, ie. through vibration, can also create spurious signals. In the laboratory, a significant source of environmental noise arises from the power network. This is not only directly detectable by the magnetometer as a 50Hz ac field but may also induce Eddy currents in any nearby large metallic objects such as helium storage dewars, which will result in detectable magnetic fields (Carelli et al 1983).

Subject noise arises from clothing and acessories ie. metal fasteners, belt buckles etc., spectacle frames, hearing aids and watches. In addition, static in hair or clothing may also contribute noise (Cohen 1983). Subject movement under the machine itself creates a magnetic field and will emphasise any field artifacts created by either metal in clothing or accessories.

Of the system noise, only the components due to construction can be reduced ie. metal components of the superinsulation are kept to a minimum and care in the design and construction of the radiation shield. Subject noise can be minimised through the avoidance or removal of items containing ferromagnetic metals. Environmental noise can be controlled in a number of ways. One method is through the installation of a magnetically shielded room. This is an expensive solution and therefore not a practical proposition for every facility particularly when the clinical use of MEG has not yet been convincingly demonstrated. In the absence of shielding, large ferromagnetic objects must be kept away from the magnetometer. In addition, signals can be filtered particularly to remove the large 50Hz signal seen in most laboratory environments.

interpreted as indicating tuning of the visual system with high spatial frequency tuning allowing analysis of the details of slowly moving stimuli and the low frequency tuning facilitating analysis of the gross features of rapidly moving stimuli. Okada et al (1982) and Williamson et al (1978) also reported that stimuli of increasing spatial frequency took longer to code as indicated by the longer response latency of the higher frequency stimuli.

Early studies of luminance used simple flash stimuli (Teyler et al 1975) and revealed that increasing the intensity of the flash resulted in an increase in amplitude but no systematic change in latency. This result was not in agreement with corresponding data for the VEP which suggests that increasing flash intensity leads to a decrease in the latency of the P2 component (Cobb and Dawson 1960, Tepas and Armington 1962, Vaughan et al 1966, Leuders et al 1980, Hobley 1988). In addition, Okada (1982) reported the effect of mean luminance using a contrast modulated 1cpd sinusoidal bar grating. Previous work on the VEP had suggested that the amplitude of the response remained constant with decreasing luminance although the latency decreased (Van der Tweel et al 1979). Okada (1982) argued that this result could be attributable to a change in the depth or orientation of the source. A subsequent topographical study at three luminance levels (0.5, 5 and 50 cd/m^2) revealed that the field topography does change with luminance suggesting a shift in source orientation. Hence, although it would appear that increased luminance results in increase amplitude of the response this could be due either to a change in the orientation of the source or the number of active neurons.

The effects of contrast on the VEMR may be similar to those of the VEP (Okada 1982). A linear amplitude response was observed for low to moderate levels of contrast, with saturation occurring at higher contrast.

In summary, studies of the VEMR to data have been carried out using stimuli which are more suited to investigation of the fundamental properties of the visual system than to clinical investigation. The results that have been obtained appear to agree with data for the VEP and are consistent with the known anatomy and physiology of the visual system. However, there is clearly a need for fundamental studies of stimulus parameters particularly using clinically relevant stimuli such as pattern reversal and flash.

2.8 Previous Clinical Uses Of Neuromagnetism

The studies of the VEMR presented in this thesis are intended to provide a basis for future clinical application of MEG. Until recently the clinical use of MEG had been

limited almost exclusively to the localisation of epileptic foci as a pre-requisite to surgery in cases of intractable focal epilepsy (Barth et al 1982, Barth et al 1984, Balish and Sato 1989). MEG may provide a better means of localising foci than most alternative techniques. In particular MRI and CT depend upon the presence of a physical lesion. By contrast, EEG may be less sensitive and Electrocorticography (ECoG) is an invasive procedure. However, despite evidence that MEG is at least as accurate as these other techniques it is still at an experimental stage (Sabers et al 1989). Perceived problems of the MEG are :-

a) Epileptogenic foci tend to be located deeper in the brain (Rose et al 1987) and current head models provide their poorest localisations for deep sources. In addition, the single dipolar source may not be an adequate model for epileptic foci .

b) It is difficult to record from a subject during a seizure and so most laboratories record interictal activity. This has two problems; the infrequency of interictal events in some patients and that the epileptogenic focus may not be the same as the source creating interictal spike activity.

c) In addition, the technique may only be useful in the very small number of patients who have focal epilepsy which is unresponsive to drug therapy. However, despite this, there is much hope for the technique which offers epileptic focus localisation of the same sensitivity as ECoG but with less risk and discomfort to the patient.

More recently other clinical applications of MEG have appeared. Hoke et al (1989) found that the waveform of the auditory evoked response in tinnitus sufferers is distinctly different from that in the normal subject. In tinnitus the M200, a magnetic component occurring at around 200 ms, is poorly developed or missing whilst the M100 (occurring at around 100 ms) is significantly augmented. An important characteristic was the ratio of the two components. In subjects below 50 years of age the amplitude ratio in normal hearing subjects (M200/M100) was above 0.5 whilst in the tinnitus sufferer it was below 0.5, thus providing a clear distinction between tinnitus and non-tinnitus sufferers. In the over 50s the normal amplitude ratio falls and so the normal and tinnitus values begin to overlap. As a continuation of this work, Pantev et al (1989) followed the occurrence and remission of tinnitus in a young soldier exposed to heavy gunfire. It was noted that as remission progressed so the M200/M100 ratio returned to normal. This supported their earlier work and lead to the suggestion that this technique may be useful in the objective diagnosis of tinnitus and monitoring of therapy. The same group have also initiated studies of evoked and spontaneous auditory responses in deaf human subjects with cochlear prostheses (Hoke et al 1989).

A limited amount of work has been carried out by Ribary et al (1989) on the auditory steady state response in various psychiatric conditions and by Barkley et al (1990) on spreading cortical depression in migraine. Preliminary studies in patients with Alzheimer's Disease (AD) show that there are reductions in signal amplitude and changes in response dynamics that are not seen in normal age matched controls. However, the specificity of these changes to AD is not yet established and much work remains to be done. In addition, work by Okada et al (1988) using isolated turtle cerebellum demonstrated slow magnetic waves produced by electrical stimulation, a phenomena which was difficult to observe in the surface EEG. They suggested that it may be possible to detect spreading cortical depression in humans. Barkley et al (1990) carried out such a study on migraine sufferers both during and between attacks. They concluded that there were "long duration biphasic field shifts and suppression of ongoing background activity" in migraine patients and that magnetometry may play a useful role in diagnosis and possibly treatment monitoring. It is clear that in the twenty years since the first neuromagnetic signals were recorded that progress towards the ultimate aim of clinical utilisation of the magnetometer has been slow. In addition, there have been few attempts to address the specific problems of recording MEG signals from normal populations and patients.

2.9 Aims And Objectives

Although possible clinical applications of the VEMR can be identified, considerable fundamental work is necessary to establish its clinical value. Flash and pattern reversal stimuli were chosen for detailed study because of the established clinical use of the corresponding VEP. The first aim was to define appropriate magnetic waveforms to each stimulus and to identify components of the waveform which may show some consistency both within and between subjects. Questions which must be asked include : do these components have a distinct morphology, are they distinguishable in all subjects, how variable are they, do they have definable latency/amplitude characteristics and how many repeat recordings are necessary to obtain a good estimate of latency or amplitude ? As the VEP to flash and pattern reversal stimuli is affected by age it is also necessary to establish whether this is true for the VEMR. The ultimate aim of these investigations would be the establishment of normative data of suitable quality for clinical use.

However, particular problems are posed by the use of a single channel system in an unshielded environment. With most of the visual work in MEG to date having been carried out on experienced subjects, we need to investigate the feasibility of recording from an unknown subject or patient. This leads to a consideration of protocol; how

should we approach recording ? We need to know what sources of noise are likely to be associated with subjects and how it will affect the ease with which we can obtain waveforms containing the desired component(s). Another problem is that of recording location. It is impractical to map the magnetic field topography in each subject and so a protocol needs to be devised to minimise the time taken to find an acceptable recording location in the majority of patients. One approach to this problem is to define the field topography in a population of subjects and to see if there are any areas of the scalp which are more likely than others to give a reliable, identifiable response. This information can then be integrated into the recording protocol.

The VEP is known to be very sensitive to variation in stimulus parameters. Field size, check size, luminance, contrast, the degree of reversal and defocus can affect the latency and/or amplitude of the pattern VEP while the intensity can affect the flash response. All need to be systematically investigated before the VEMR can be used clinically. The studies presented in this thesis will concentrate on three aspects :

1. The problems inherent in recording from naive subjects in an unshielded environment and the establishment of a normative data base (Chapter 3).

2. The effect of varying stimulus parameters on the VEMR and the implications that this has for clinical use (Chapter 4).

3. A topographic study of the distribution of the VEMR over the occipital scalp in order to identify a) recording positions for use in single point work and b) the source of magnetic signals in the visual cortex (Chapter 5).

CHAPTER 3

VISUAL EVOKED MAGNETIC RESPONSES TO FLASH AND PATTERN REVERSAL IN 100 NORMAL SUBJECTS

3.1 INTRODUCTION

To date, most magnetic studies have been carried out on a limited number of experienced laboratory personnel (Maclin et al 1983, Pantev et al 1989, Okada et al 1983). However, if MEG is to be of use clinically then the problems of recording from untrained or inexperienced subjects must be addressed. The aim of this study was a) to assess the problems of recording from a large number of untrained subjects in an unshielded environment and b) as a pre-requisite to a possible clinical application of the technique, to establish preliminary normative data across the age span. With little information available on the recording of the VEMR to flash and pattern reversal stimuli in the literature (eg. Teyler et al 1975, Janday et al 1987) we used a simple protocol determined in part by previous electrical findings in our laboratory (Harding and Wright 1986) and from the results of preliminary magnetic measurements of the VEMR. In previous magnetic studies, flashed pattern (Richer et al 1983, Lewis et al 1984), pattern onset- offset (Kouijzer et al 1985, Stok 1986) and contrast reversal sine and square wave gratings (Okada 1982, Maclin et al 1983, Schmidt and Blum 1984) have been used as stimuli. There has been less published work using using plain flash stimulation (Teyler et al 1975, Zimmerman et al 1978) and little carried out using checkerboard pattern reversal (Janday et al 1987) which is the most important of the stimuli used clinically (see Chapter 2). By using stimuli presented at various eccentricities this work has helped to illustrate the retinotopic organisation of the visual cortex (Maclin et al 1982, Schmidt and Blum 1984, Janday et al 1987) and provided evidence that visual information such as luminance, spatial and temporal frequencies may be transmitted by separate channels (Okada 1982). The effect of increasing flash intensity on the latency of the visual evoked magnetic response has also been studied and found to be non-linear (Teyler et al 1975, Zimmerman et al 1978).

This preliminary study is divided into two parts. The first section describes the VEMR obtained to large checks and flash from 100 subjects ranging in age from 16 to 86 years. The second section describes the monocular responses to a small check pattern reversal stimulus in an attempt to determine the interocular latency variation.

3.2 MATERIALS AND METHODS

3.21 Flash and Pattern Reversal Study

3.22 Subjects.

One hundred normal subjects aged between 16 and 86 years participated in the study. All subjects were without ophthalmological problems and had visual acuities of at least 6/6. The majority of subjects were either staff or students from within the University. The older subjects, those over 60 years of age, were from a social club for retired engineers and their spouses. Many of this group attend the department regularly to act as subjects for undergraduate refraction classes and some had previously participated in other experiments within the Neurophysiology Unit. All subjects were interviewed and carefully instructed as to the protocol to relax them prior to recording. We found this to be very important in obtaining successful recordings. This and all subsequent studies described in this thesis were approved by the University Ethical Committee.

3.23 Magnetometer

The recordings were made using a single channel dc SQUID second order gradiometer (BTi Model 601) described in Chapter 1. The pick-up coil, diameter 2cm, was located 12mm from the outer surface of the dewar tail. The white noise level of the system was16.6fT/$\sqrt{}$Hz and the baseline ie. the distance between the pick up coil and the first compensating coil was 50.4mm.

3.24 Stimulus parameters

For clinical use, VEP normative data have been established for a variety of check sizes. For example, small checks may be more useful than large in the detection of optic neuritis (Wright et al 1987). However a large check (70') was chosen for this initial survey as preliminary magnetic studies revealed that larger checks produced more consistent signals of higher amplitude than smaller checks. Stimuli can be presented by TV or back projection. Experiments with both systems were carried out and the back projection system (Drasdo 1976) chosen for the lower noise it generated in the recording laboratory. The checkerboard subtended a 14 x16^{o} field, mean screen luminance was 1050 cd/m^2 and the contrast was maintained at 0.76. A 2/sec. reversal rate was used. The flash stimulus was produced using a Grass PS22 stroboscope set at Intensity 8 (luminance 3939cd/m^2). Flashes were delivered at 1/sec. Both stimuli were viewed binocularly. Some magnetic artifact was produced by the strobe which appears on evoked waveforms within the first 50ms.

3.25 Recording Position

Some simple models of the sources of the VEMR would suggest that lateral locations would be more successful for recording visual evoked responses (Okada 1982). However, preliminary studies based on recording the VEMR at nine positions over the scalp revealed that an area of scalp 6-9cm above the inion on the midline and extending 1-2cm to the left of the midline was a good location for recording in the majority of subjects. Hence, we commenced recording on a new subject at a midline position. However, for those producing a poor response on the midline, it was our experience that moving to a position 1-2cm to the left of the midline usually resulted in the recording of an acceptable signal.

3.26 Signal Processing

Signals were recorded at a magnetometer sensitivity of x1000 and filtered between 0.1 and 30Hz (24dB/octave roll-off). We were restricted in our choice of filter settings both by those available in the SQUID contol unit and by the noise of our unshielded environment. It was necessary to use a narrow bandwidth in order to achieve a workable signal to noise ratio. Between 64-128 responses were averaged using a Datalab DL4000 signal processor. Two averaged series of responses were obtained from each subject to each stimulus. Note that run to run variation and longer term temporal variation of the VEMR will be investigated in Chapter 4.

3.27 Recording Protocol

Subjects were seated comfortably under the magnetometer with the Dewar tail located approximately normal to the scalp at a position 6-9cm above the inion on, or 1-2cm to the left, of the midline. Subjects were asked to fixate the centre of the screen or flash gun and to count reversals/flashes to ensure fixation and attention (Shahrohki et al 1978, Leuders et al 1980, Regan 1977). Subjects were also carefully observed during the recording to ensure attention to the stimulus. Recording was continued until two consistent responses were obtained to each stimulus. Pattern reversal responses were recorded first, followed by a brief interval and then the flash responses were recorded. They were recorded in this order to ensure that, particularly in older subjects, maximum attention was available for the pattern reversal stimulus. Latency and amplitude of the most consistent components were measured for the traces and converted to magnetic units (femtotesla) using a calibration from millivolts to femtotesla appropriate to the particular magnetometer supplied by BTi.

3.3 INTEROCULAR LATENCY VARIATION

3.31 Subjects

Twenty-six normal subjects participated in the study (see above).

3.32 Stimulus Parameters

As small checks have previously proved more useful when detecting some lesions of the visual pathway it was decided to use smaller checks (34') for this study (very small checks ie. 8' to 22' gave poor magnetic responses in preliminary experiments). A circular field subtending 14^{o} was used. Mean screen luminance was $1050cd/m^2$, contrast 0.76 and the reversal rate 2/sec. The stimulus was viewed monocularly, this being achieved by the patching of one eye. A standard eye patch plus cotton wool or cotton wool placed between the eye and spectacles was used. The patched eye was allowed to recover before recording from the other eye.

3.33 Recording Protocol

A similar protocol was used to that for the pattern reversal normative data study except that after the initial recording of two binocular responses (to ensure that a suitable recording position was being used) two monocular responses were recorded. Recording continued alternately with each eye until two consistent responses were obtained for each eye.

3.4 RESULTS

3.41 Flash and Pattern Reversal Study

The study revealed a number of problems inherent in the recording protocol. It was possible to obtain consistent responses from 83 out of the 100 subjects used for each stimulus. In most subjects, consistent waveforms could be obtained in around 4-6 runs. We failed to record waveforms from 17 subjects for a variety of reasons a) 7 mainly elderly subjects were rejected on ophthalmic grounds, their problems including cataracts, nystagmus and reduced visual acuity, b) some subjects could not be recorded because their spectacles created such large magnetic artifacts that recording was not possible, c) 3 subjects were elderly and had signals of a low amplitude and broad morphology which made it difficult to estimate latency, d) 1 subject had a head shape that meant that it was not possible for us to locate the probe normal to the scalp and for the subject to see the stimulator simultaneously and e) the remaining 6 subjects produced no recognisable waveforms after a series of recordings.

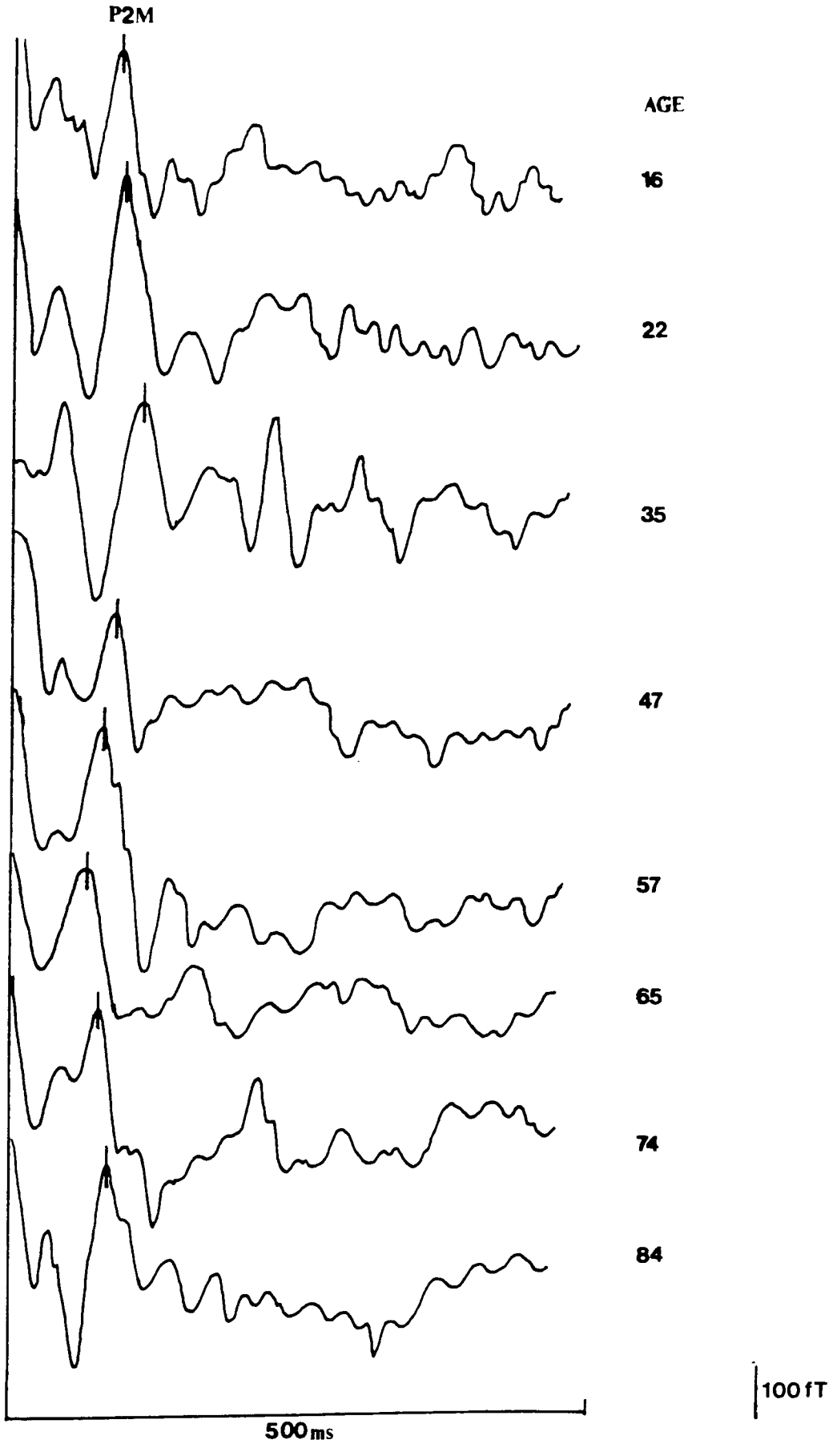

Figure 3.1 : Typical responses to flash stimulation across the age span. The P2M component is evident on each waveform. The early peak is probably a magnetic artifact produced by the strobe.

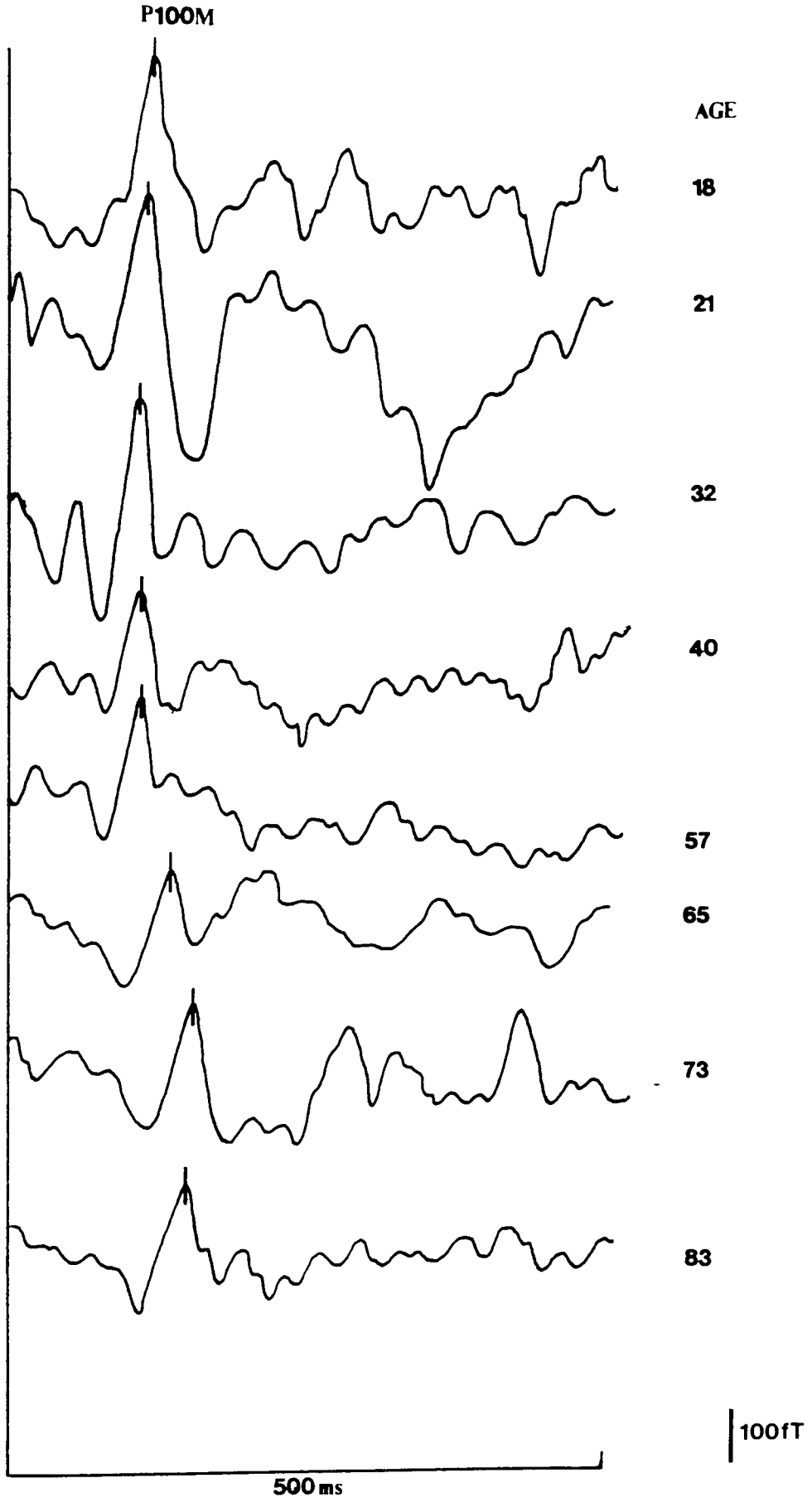

Figure 3.2 : Typical responses to pattern reversal stimulation across the age span. The P100M is evident on each waveform.

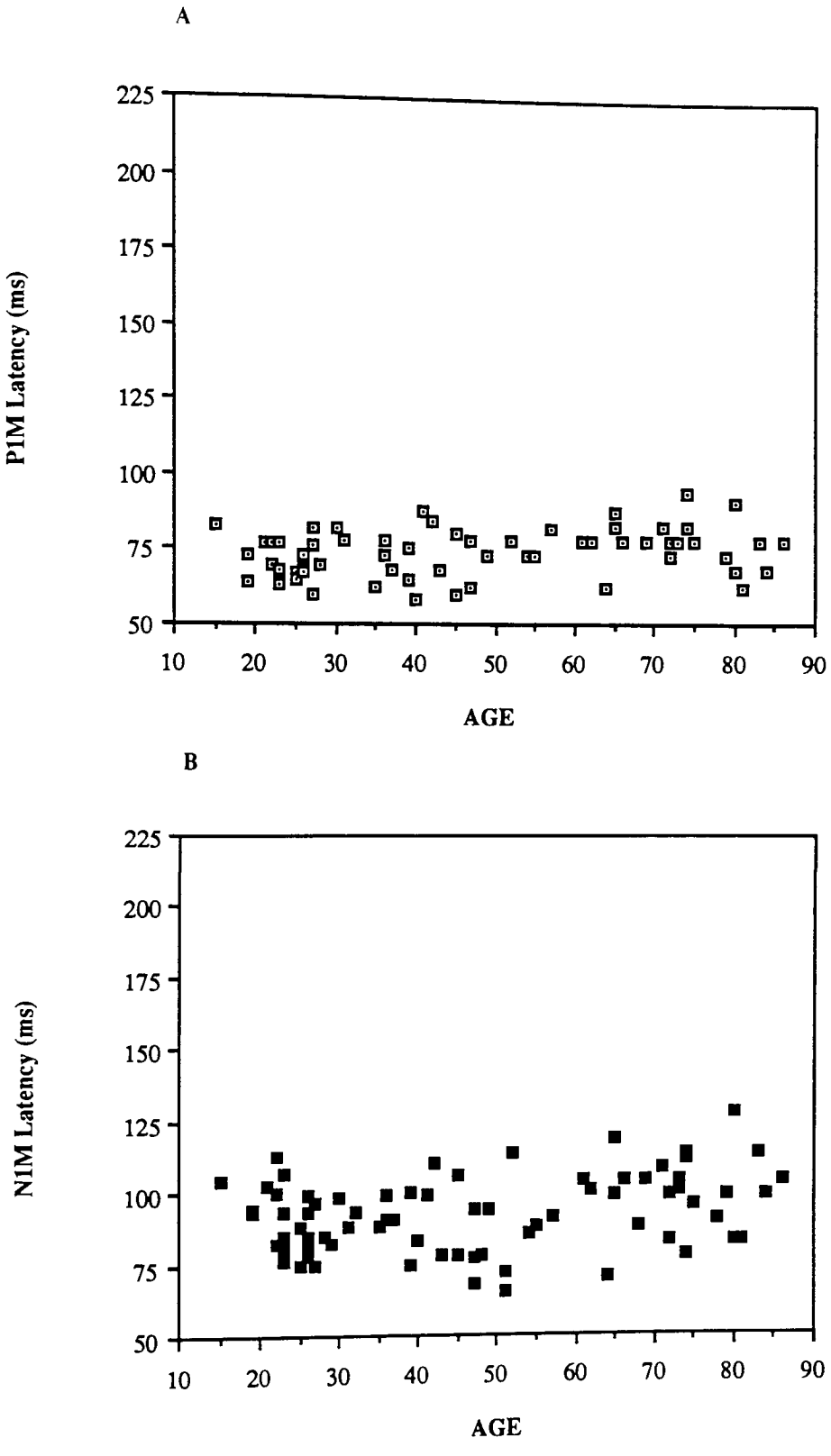

Figure 3.3a : Latency of the flash P1M (A) and N1M (B) in relation to the age of the subject.

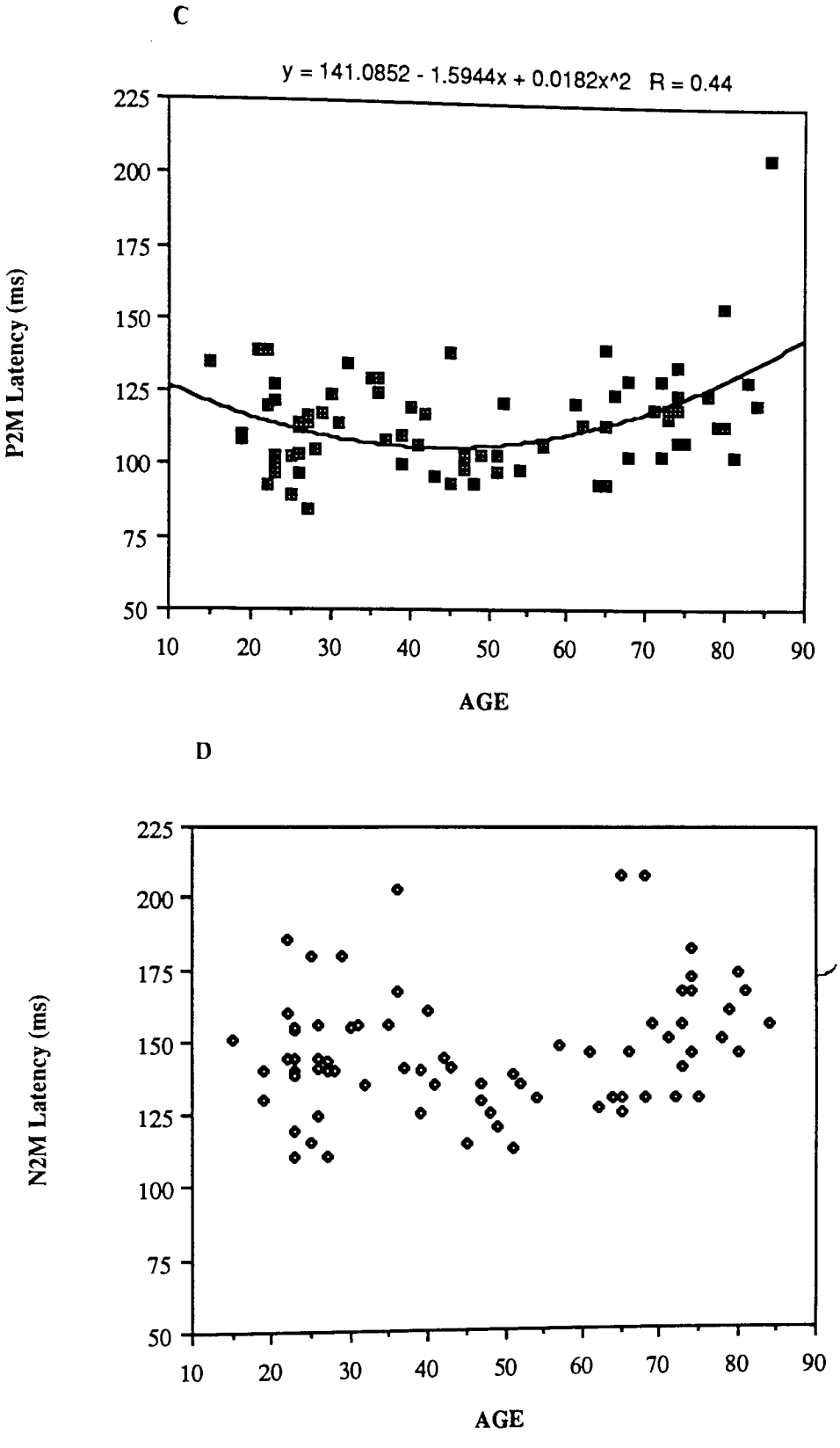

Figure 3.3b : Latency of the flash (C) P2M and (D) N2M in relation to the age of the subject.

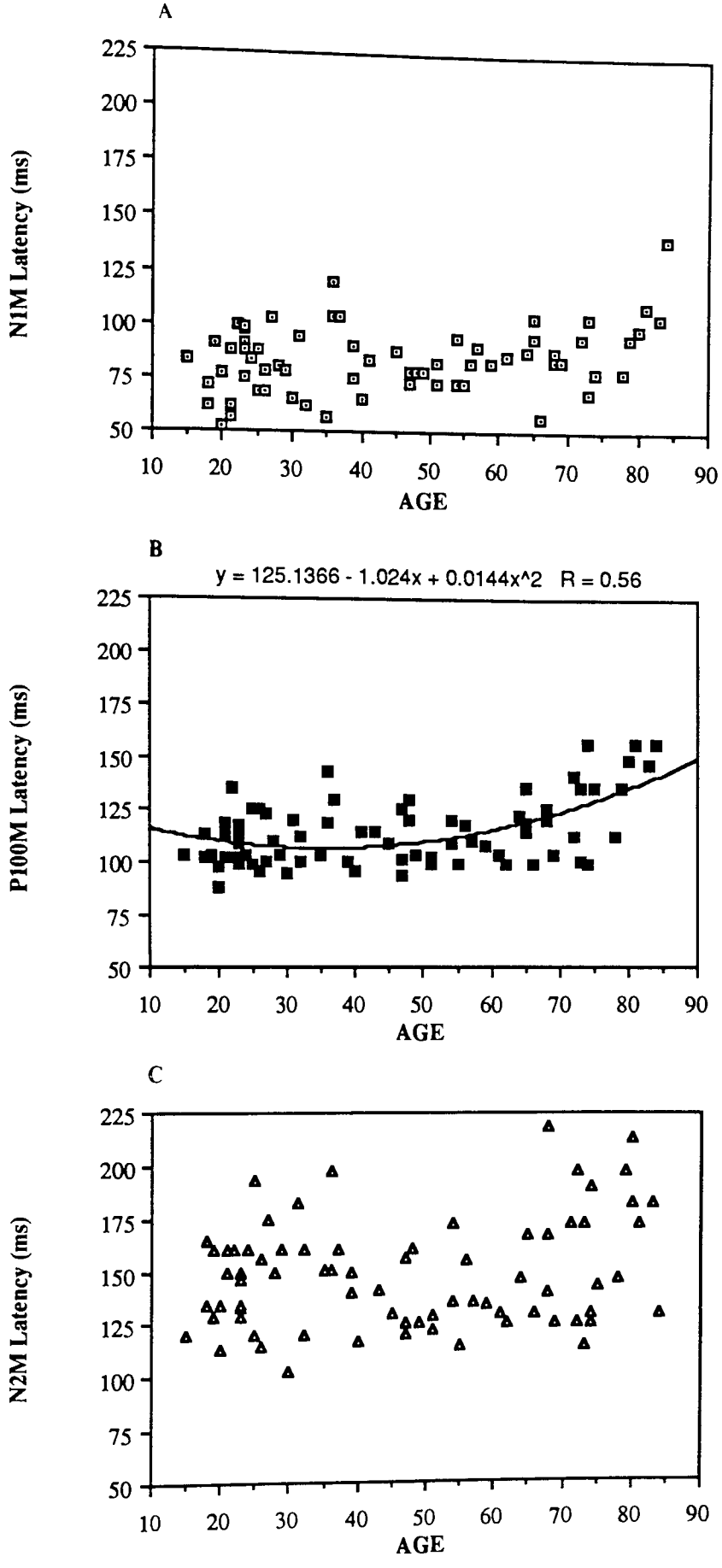

Figure 3.4 : Latency of the pattern reversal components A) N1M, B) P100M and C) N2M in relation to the age of the subject.

Figure 3.1 shows some typical responses to flash stimulation from subjects across the age span. Figure 3.2 shows a similar set of waveforms obtained to pattern reversal stimulation. The most consistent components were the flash P2M and the pattern reversal P100M and these were usually 200-400fT in amplitude. The nomenclature used follows that of Harding (1974). The P100M is an outgoing field occurring between 90 and 120ms and is seen in all subjects from whom an identifiable waveform could be recorded. On visual inspection of the traces there appears to be a decrease in amplitude with age, with it becoming more difficult to discern components after 60 years of age. The response to flash is more complex with a number of components occuring in the first 250ms. The most consistent component, the P2M, occurs between 90 and 140ms. This does not appear to degrade as rapidly as the P100M with age. Other components can be seen to flash (P1M, N1M and N2M) and to pattern reversal (N1M and N2M) although these tend to be neither as consistent nor as high in amplitude.

Figure 3.3 shows the latency of each of the early components to flash stimulation in relation to age and Figure 3.4 the latency of each component produced by pattern reversal versus age. Of the four main components of the flash response it can be seen that the P1M (65-75ms) is the least variable and its' latency remains fairly constant across the age span. The range of the P2M latency is fairly wide with most responses occuring between 90 and 140ms. Visual inspection reveals that there are fewer short latency responses (less than 100ms) amongst the elderly subjects. Curves fitted to the data revealed that the pattern of flash latencies versus age were best fitted by a second order polynomial ie.an initial decrease in latency followed by an increase after the age of 50. A similar, though slightly more marked trend is seen for the N2M (125-155ms). The P1M occurs in 78%, the N1M in 93%, the P2M in 100% and the N2M in 88% of subjects from whom recognisable waveforms could be obtained.

Figure 3.4 shows that of the 3 main components to pattern reversal stimulation, the P100M is the least variable. With most responses occuring between 90 and 120ms this makes the P100M less variable than the flash P2M. There is little change in latency across the age span until around 55 years of age when it begins to increase rapidly. The N1M (65-115ms) and the N2M (110-200ms) are less distinct and more variable than the P100M in most subjects. The N1M occurs in 82%, the P100M in 100% and the N2M in 90% of subjects producing recognisable waveforms. The N2M is often quite pronounced being present even if the P100M is absent in some cases. In fact it can be used as a marker for the presence of the P100M.

Table 3.1 : Normal values for the latency of the P2M component of the VEP and VEMR to flash stimulation. Mean (Standard Deviation).

Age Group	VEP P2* (ms)	VEMR P2M (ms)
10-19	114.5 (9.8)	104 (10.8)
20-29	120.7 (10.99)	109 (14)
30-39	121.7 (7.8)	118 (12.2)
40-49	126.8 (11.26)	109 (14.2)
50-59	122.5 (5.45)	106 (9.7)
60-69	127.29 (11.28)	115 (15.5)
70-79	134.25 (12.72)	119 (9.1)
80-89	--------	125 (19.7)

* Harding and Wright (1986).

Table 3.2 : Normal values for the latency of the P100 component of the VEP and VEMR to pattern reversal stimulation. Mean (Standard Deviation).

Age Group	VEP P100* (ms)	VEMR P100M (ms)
10-19	108.56 (10.9)	105 (4.27)
20-29	101.78 (7.6)	106 (9.3)
30-39	106.78 (4.9)	106 (9.5)
40-49	104.6 (5.2)	109 (13.1)
50-59	102.9 (6.75)	108 (7.9)
60-69	109.2 (10.45)	114 (15.1)
70-79	110.0 (8.7)	119 (16.6)
80-89	--------	153.5 (5.0)

* Harding and Wright (1986).

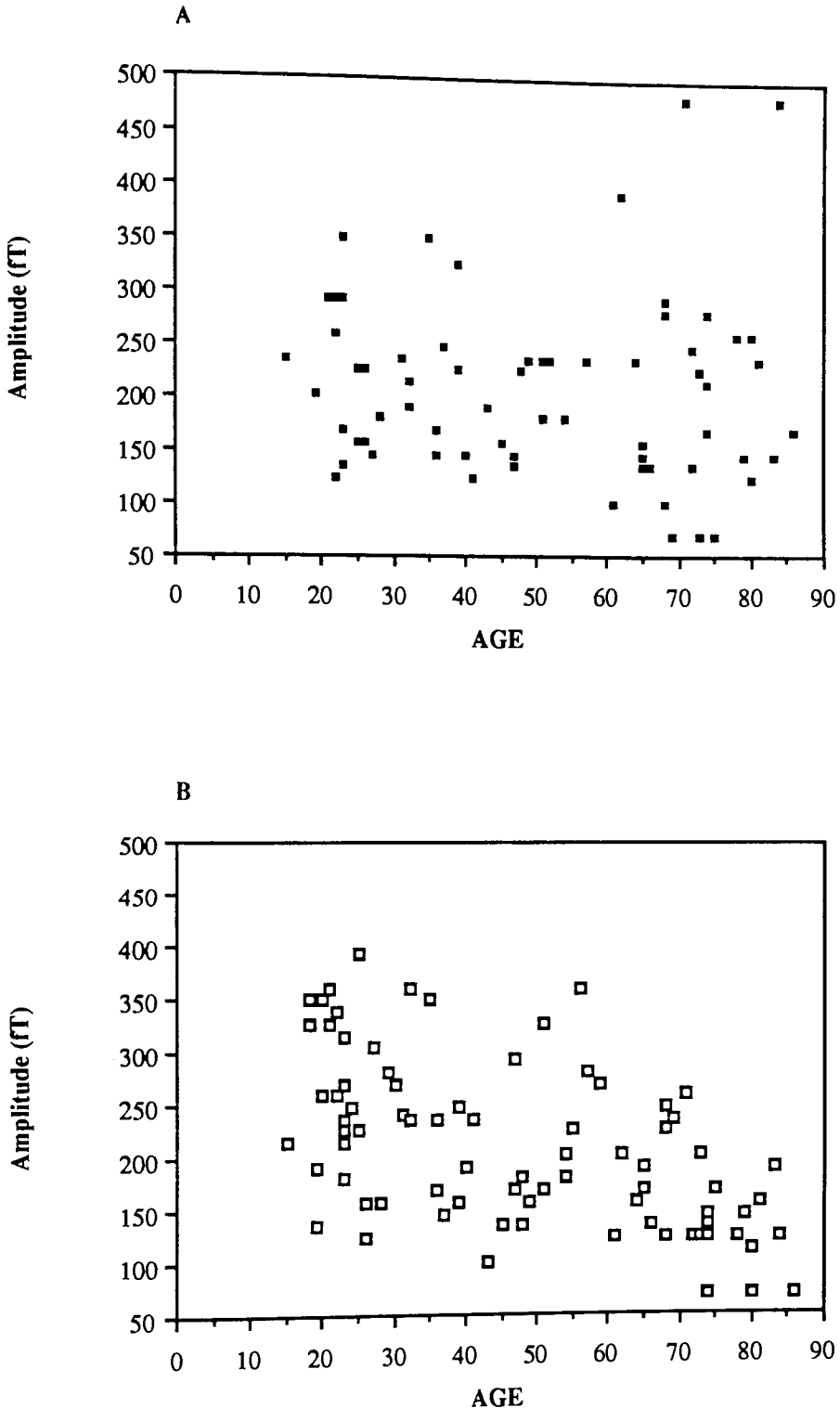

Figure 3.5 : Amplitude of A) P2M and B) P100M components in relation to the age of the subject.

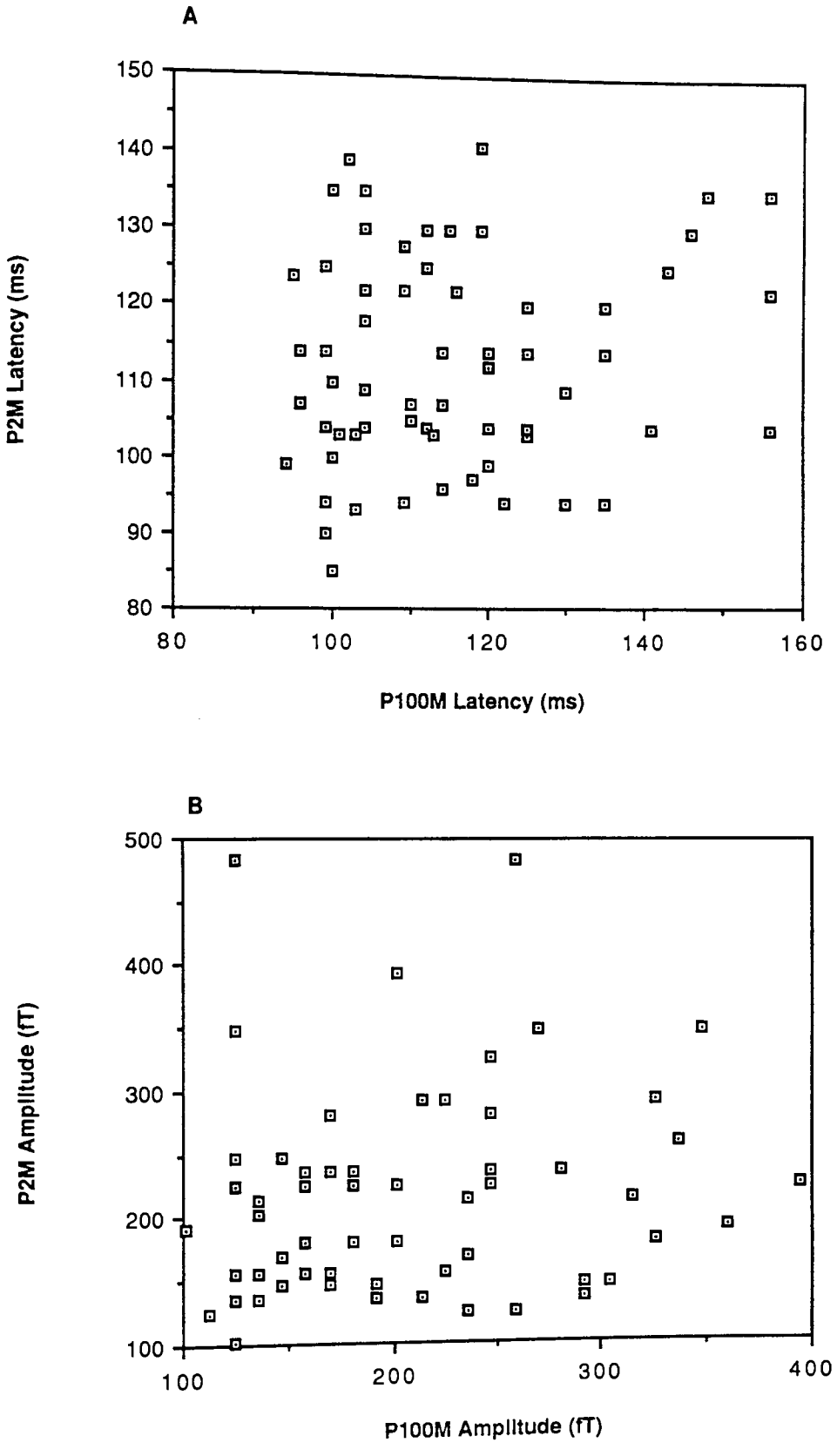

Figure 3.6 : The latency (A) and the amplitude (B) of the P2M and the P100M plotted against each other. Correlation coefficients were not significant in either case (latencies $r = 0.18$, amplitudes $r = 0.18$, $p>0.05$).

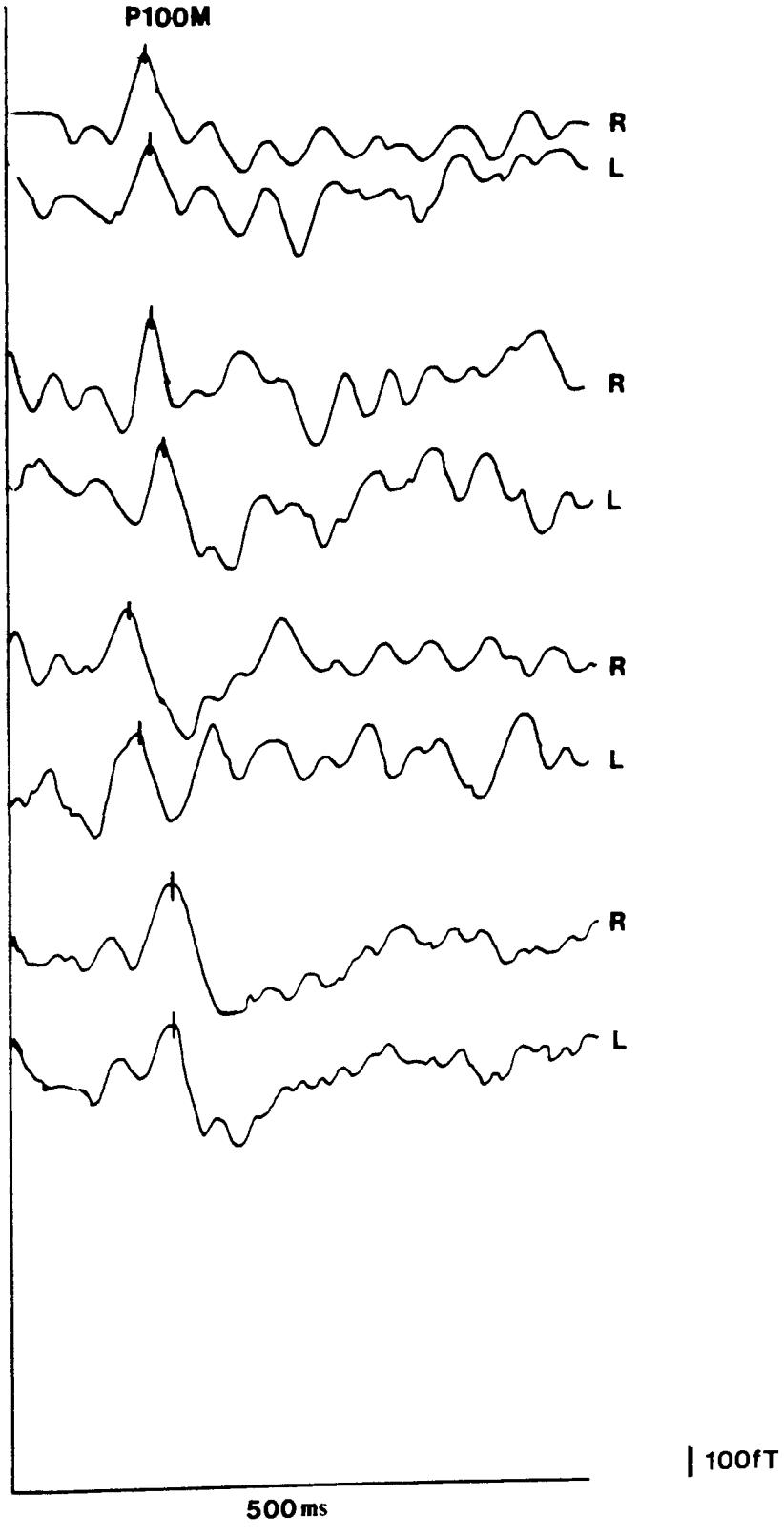

Figure 3.7 : Typical monocular responses to a small check (34')pattern reversal stimulus in four normal subjects (R = right eye, L = left eye).

Table 3.1 shows the mean latency values obtained for the flash P2M component and compares them with values obtained electrically at this unit by Harding and Wright (1986). It can be seen that on the whole the magnetic values are more variable than their electrical counterparts in most age classes.

Table 3.2 shows the mean P100M latency values obtained and compares them with the electrical norms of Harding and Wright (1986). Again the magnetic signals show more variability than the electrical signals.

In subjects up to 60 years of age amplitudes for the P2M range from 100 to 350fT (Figure 3.5a). After 60 years of age there is an increase in the number of low amplitude signals (below 100fT). Three subjects in this age group gave very high amplitude responses - over 350fT. Figure 3.5b shows that up to around 55 years of age most responses fall between 150 and 350fT with more lower amplitude signals - 60 to 250fT - in those over 55 years.

For those subjects producing both a flash P2M and a pattern P100M their latencies (Figure 3.6a) and amplitudes (Figure 3.6b) were plotted against each other . The graphs show that there is no simple relationship between the latency of one component and that of the other.

3.42 Interocular Latency Variation Study

Interocular latency difference was measured in 26 subjects aged between 18 and 47 years. Most subjects used for this study had previously been found to give good binocular signals to the 70' check.

Figure 3.7 shows sample waveforms obtained in response to left eye and right eye monocular stimulation with 34' checks. In the experienced subject (A) the amplitude for all responses is similar and around 300fT. The characteristic ingoing N2M which occurs following the binocular P100M in many subjects is emphasised in the monocular responses. The magnetic data was collected from subjects aged between 18 and 48 years and the mean interocular latency difference is 7.36ms $\pm$ 4.55. Harding and Wright (1986) calculated the mean interocular latency variation of the electrical P100 for ten subjects from each decade between 10 and 80 years of age. The mean latency for the 20 to 29 year olds was 6.7ms $\pm$ 6.49, for the 30 to 39 year olds 2.45ms $\pm$ 1.62 and for the 40 to 49 year olds 3.55ms $\pm$ 2.14. Although the mean is higher than the VEP for all age groups, the variability does not appear large when compared to the electrical data and with improvements in the recording protocol it is

possible that normative data of sufficient quality could be recorded to be of use clinically.

3.5 DISCUSSION

The discussion is divided into 3 sections:- a) the problems encountered during recording, b) a comparison of the results with data for the VEP and c) the clinical implications of the results and further studies.

3.51 Problems of Recording

No satisfactory responses could be obtained from 17 subjects in the study. Of these 7 were rejected on ophthalmic grounds. A further three of the subjects were elderly and gave responses of low amplitude and broad morphology. The present recordings were made in an unshielded environment and hence interpretation of the waveforms may be complicated by a relatively poor signal to noise ratio. A magnetically shielded room (Vacuumschmeltze Model AK1a) has been recently installed (see Chapter 4) and preliminary tests suggest that this will reduce some of the high frequency noise (30Hz and above). Further shielding may be required to reduce the amplitude of lower frequency noise. Another problem which may influence the variability of our data is that the head of the subject is unrestrained and slight movements may occur during the recording, particularly in the elderly. The first gantry system used during the project enabled little movement of the Dewar relative to the subjects head. This meant that on occasion, depending on patient head shape, an unnatural and uncomfortable position was held during the recording. More recent improvements to our gantry system have remedied this problem to a certain extent. Firstly the introduction of a more flexible gantry, allowing the dewar to be tilted to its safe maximum of 45^{o} from the vertical, means that many subjects can be located more comfortably. Secondly, towards the end of the preliminary study a more advanced signal processor became available, the "Biologic Traveller". This system had artifact reject, variable gain and additional filtering. By adjustments of gain and artifact reject, cleaner waveforms were obtained. In addition a reduction in recording time was possible with the number of sweeps reduced to 50 from the original 64-128. However, care needs to be taken when using artifact reject as it can increase the length of the test unacceptably. Fewer sweeps can also mean reduced fatigue for the patient. For example, with early recordings using up to 128 sweeps, an initially sharp signal could be seen which would subsequently broaden and then disappear as the recording proceeded. This may have been a result of fatigue and inattention or owing to the movement of the subject. This observation could also be due to inconsistent appearance of the P100M signal in successive sweeps at a particular recording position. Hence, the number of sweeps taken must be

a balance between an acceptable signal to noise ratio and the attention and fatigue of the subject. In some subjects, from whom no response could be elicited, the fault lay in the subjects' clothing. One problem which occured frequently in young female subjects was that the underwiring present in some bras produces a large, characteristic sinusoidal wave as the subject breathes (breathing artifact). This artifact can be detected by asking the subject to hold her breath momentarily. Few problems occurred with the wearing of metal zippers perhaps because they tend to occur in skirts or trousers and are much further from the detector and less susceptible to body movements. These problems can be solved by sending a request to prospective patients with their appointment cards asking that they avoid wearing clothes with metal fasteners or undergarments (including corsets) with metal supports. A non-magnetic laboratory gown available for the patient should also be considered. Technicians should also be aware of hearing aids and metal framed spectacles. The latter were a considerable problem in some patients and prevented us from recording from a small number of subjects whose refractive error could not be corrected without recourse to them. A non-magnetic set of correction lenses were obtained subsequently to deal with this problem. However, a study is necessary to establish the effects of optical blur on the latency and amplitude of the VEMR because of the ease of recording some subjects without spectacles. Previous electrical studies (Collins et al 1979, Sokol and Moskowitz 1981, Harding 1982) have shown that blur can increase the latency of pattern reversal components (see Chapter 4).

In cases where recording was not possible as a consequence of abnormal head shape, the answer may lie in the use of a different patient support system. After the completion of this study a wooden patient bed was constructed. The subject lies face down and looks through a 'letter box' cut in the head of the bed at the stimulator screen below. Beds have been used sucessfully for visual work (Schmidt and Blum 1984, Maclin et al 1983, Stok 1986). However, preliminary studies using the bed in our laboratory have been less successful than using the chair. Subjects have complained of discomfort and claustrophobia since the patient is enclosed between the bed and the probe; a problem which may be further exacerbated inside a shielded room. It is clear that if the recording system is to be acceptable to patients then some modifications are necessary. Some form of support for the body or head is desirable, particularly for the elderly subjects, to reduce the problems associated with movement. An alternative to the bed may be some form of modified chair. This could be as simple as the addition of a head or shoulder rest to a conventional chair. Alternatively a a kneeling chair could be developed on which the subject kneels upright and leans forward onto a body support system.

The failure to record signals in some subjects may have been a consequence of the probe being located over an inactive region of cortex. In most subjects, a response could be obtained on or to the left of the midline. However, there is some evidence that because of the orientation of the sources in the visual cortex, there may be some cancellation of the visual signal on the midline with full field stimulation (Okada 1983). In addition, magnetic signals are more focally distributed over the scalp than electrical signals (Cohen and Cuffin 1983) and the exact position of the maxima may vary from subject to subject (Stok 1986). This poses a problem when choosing a single recording position using a single channel magnetometer. As recordings from different scalp locations must be made sequentially, it is not practical in the clinical situation to use detailed topographic mapping to locate the magnetic maxima. However it is essential to determine a) how the topography varies from subject to subject within an age group and b) how the topographic maps vary across the age span. A method of avoiding the complications of full field stimulation would be to use half field stimulation since there is evidence that half field responses may be more consistent from subject to subject (Schmidt and Blum 1984). Another consequence of recording from a less active area of scalp is the poorer signal to noise ratio. A poor signal to noise ratio may influence component latency and amplitude. Little is known at present about run to run variability of the VEMR and this is another factor which needs to be studied systematically and will be addressed in Chapter 4.

Explaining the protocol to each subject before recording proved important particularly when using elderly subjects. Many of the subjects relaxed during the explanation particularly when they were given the opportunity to ask questions about the recording technique and protocol. Although it is anticipated that some of the patients, on whom the technique may eventually be applied, may be less co-operative or less able to understand the purpose of the recording for pathological or psychological reasons, the preparatory talk would still be very useful in familiarising the subject with their surroundings. This may be of particular importance when using a shielded room which is an imposing structure, particularly with claustrophobic subjects.

3.52 Discussion of Results

Means (X) and standard deviations (SD) of the VEMR in each age group were compared to the VEP norms currently used in our clinics (Harding and Wright 1986). A limitation of this approach is that recordings of the VEP were made using different stimulus parameters and subject populations. It must also be noted that the relationships between the electrical and magnetic signals have not been demonstrated. Hence, it is an assumption that the P100 and the P100M arise from the same region of

the visual cortex. However despite these limitations, the magnetic data clearly show more latency and amplitude variability with age than is apparent in the VEP (Shearer and Dustman 1980, Allison et al 1983, Harding and Wright 1986). A number of explanations can be proposed to explain this result. Firstly, the number of repetitions contained in an average may have been insufficient to remove spontaneous background activity. Previous electrical work has demonstrated that VEP amplitudes vary with amplitude (Jones and Armington 1977) and phase (Trimble and Potts 1975) of the occipital alpha rhythm. The same may also occur with any rhythmical signal present on the waveforms eg. 50Hz mains frequency, a particular problem of recording in our environment. Another problem is that the magnetic extrema (the positive and negative 'poles') may be the only locations at which the signal can be reliably recorded. However, although topographic mapping of a number of subjects will give some idea of the normal distribution of the extrema it will not be possible to predict accurately the location of the maxima in an unmapped subject. Mapping every patient is not a practical proposition with the current system. Other problems arise when recording from a patient population in which there may be cortical atrophy and as a consequence may exhibit abnormal topography. The VEMR may also be sensitive to defixation, defocussing or inattention. These factors have all previously been shown to effect the VEP and all may deteriorate with age (Snyder et al 1981, Sokol and Moskowitz 1983, Harding 1988). Although fixation was monitored during recording and the subject asked to count reversals to aid attention, subject co-operation cannot be guaranteed. Defocus is unlikely to be a contributary factor using large checks as preliminary studies revealed the effect of blur on P100M latency to be relatively small (See also Chapter 4). The susceptiblilty of the waveform to environmental magnetic and vibrational noise must be noted as these may be important factors in our unshielded environment. Finally the increased variability of the magnetic P100M may be intrinsic to magnetic brain activity and reflect the nature of the signal and its' generators.

Although there are some conflicting results (Celesia and Daly 1977, Dustman and Shearer 1980) the majority of electrical studies agree in suggesting that there is little change in P100 latency until around the fifth decade of life after which there is a 2-5ms latency increase per decade (Asselman et al 1975, Halliday et al 1978, Stockard et al 1979, Allison et al 1983, Wright et al 1985). Sokol et al (1981) demonstrated a more rapid latency increase with age for small (12') checks than for large (48') checks. This difference may go some way to explaining the conflict in reports as to the effects of aging on the VEP. The P100M shows a similar pattern of aging to the P100 in that there is little apparent change in latency until around 55 years of age followed by a progressive increase with age. The latency increase in the elderly appears to be more

rapid than that seen electrically (Harding and Wright 1986). A number of explanations can be proposed for this effect a) waveform interpretation may be more difficult in the elderly b) later positivities may not represent delayed P100M's but new components revealed by atrophy or other changes in visual cortex (Blumhardt 1987) or c) changes in retinal illumination due to senile meiosis (Verma and Kooi 1985, Wright et al 1985) medial or lens opacities. However, the latter is unlikely as the change is thought to be only of the order of 3ms. Degenerative changes to the retina and visual pathways have been reported in the elderly. These include reports of decreased numbers of retinal ganglion cells (Varbec 1965) and optic nerve fibres (Dolman et al 1980) as well as other physiological/biochemical changes (Samuel et al 1983). Sokol et al (1981) surmise that the more rapid increase in latency to small checks than to large checks may reflect a change in the capacity of the visual system to process spatial information with increasing age ie. high spatial frequency channels may age more rapidly than lower spatial frequency channels.

The effects of age on P100 amplitude are less well characterised and the reports somewhat conflicting. Some studies suggest a decrease in amplitude after around 60 years of age (Snyder et al 1981), no change (Celesia and Daly 1977) or an increase (Faust et al 1978). Although the data are variable, the magnetic P100M amplitude does appear to decline with age across the age span particularly after 55 years of age. The VEMR may be more sensitive to the amplitude changes seen in aging as they reflect only a part of the signal seen electrically. For example it is possible that the VEMR is produced by generators oriented more tangentially to the pick-up coil and these may represent the more peripheral parts of the visual field which could be more affected in aging (Dolman et al 1980). As the magnetic signal amplitude is related to the number of activated cells in the cortex it is possible that it may also be more sensitive to the cell losses seen in aging (Wikswo 1983).

The latency of the flash P2M appears to decrease initially and then increase slowly after the age of 50. The increase in latency with age is not as rapid as that seen for the P100M. Electrical studies reveal that the P2 latency increases with age though there is some dispute in the literature. Cosi et al (1982) and Wright (1983) reported an increase across the whole age span of around 20ms whereas others report increased latencies only in subjects over 60 years of age (Straumanis et al 1965, Dustman and Beck 1969). The P2M amplitude shows a greater variability than the P100M particularly in the elderly. Some elderly subjects have unusually high amplitude signals and yet others have amplitudes lower than those seen across the rest of the age span. Electrical findings also vary in this respect with Celesia and Daly (1977) suggesting increased amplitude and Dustman and Beck (1966) minimal change with

age. There was no correlation between the latencies or amplitudes of the P100M versus the P2M which demonstrates the independence of these components from each other. Hence, it is likely that the P100M and the P2M reflect different aspects of visual processing and age differently. Different stimuli may activate different channels in the visual system (Celesia et al 1982). The findings of psychometric tests led to the conclusion that visual information may travel along two channels a) a high spatial frequency or contrast channel and b) a low spatial frequency or luminance channel (Celesia et al, 1982). In the cat these channels may relate to the activity of specific X and Y ganglion cells (For further discussion see Chapter 1). There is speculation that small checks may activate the X cells (Yiannikas and Hammond 1986) which transmit information on contrast via the geniculate pathway to area B17 (V1) whilst flash stimulation may activate the larger, faster Y fibres which transmit luminance/movement information via a cholinergic tectal pathway (Bajalan et al 1986) to the extrastriate cortex areas B18 (V2) and B19 (V3), (Harding and Wright 1986, Armstrong et al 1989). However large checks, as used in this study, may activate both systems hence they may have both pattern and luminance components (Armstrong et al 1991). Since the flash P2 is unaffected by defocus or defixation (Harding 1988), delays in latency tend to be cortical in origin, for example, in Alzheimers disease (Harding et al 1985, Orwin et al 1986). Thus, the increase in P2 latency (and by assumption P2M latency) may be a result of either cell losses in the visual cortex or neurotransmitter changes (McGeer and McGeer 1976). These changes may also explain the low amplitude seen in some elderly subjects. By contrast, the P100 is sensitive to optical factors such as defocussing (Collins et al 1979) and pathological changes to the retina (Bodis-Wollner 1987, Hammond and Yiannikas 1986). The P100 may also be delayed as a result of decreased axonal conduction rate or synaptic delay (Allison et al 1984).

With the exception of the flash P1M all other major early components in our study of the flash and pattern reversal waveforms have greater variability than their electrical counterparts, thus limiting their possible clinical use. This may be expected, particularly for the suceeding N2M components, as electrical studies have demonstrated the greater susceptibility of later components to variations in attention and arousal (Spehlman 1985). The electrical P1 does not appear in all subjects being more consistently recordable in subjects over 40 (Wright et al 1985). Sometimes in the elderly the amplitude of the P1 can approach that of the P2 (Harding 1982). Its presence or absence is not considered to have a diagnostic value although it is sometimes considered to be an indicator of chronic open angle glaucoma (Harding, by personal communication). A number of features of the P1M suggest that it is not the magnetic equivalent of the P1. It did not occur in all subjects although its incidence

was the same across the age range. There is a relatively low latency variability and it is possible that there may be a magnetic artifact from the strobe contributing to the P1M.

Most authors agree that the interocular electrical P100 latency is less than 10ms in normals (Stockard et al 1979, Leuders et al 1980). For the magnetic recordings so far obtained, approximately half of the values were 8ms or greater. Monocular recordings are susceptible to all the problems attending binocular recordings and in addition there is a possible increased sensitivity to refractive error. It is important to establish monocular norms as in patients with an abnormal VEP to monocular stimulation the binocular response produced often falls within normal limits (Shahrokhi et al 1978, Hoeppner et al 1980). Although magnetic recordings may still be useful ultimately, the interlatency variability must be reduced and recordings made across the age span.

3.53 Implications

This study was limited in that a well defined set of stimulus parameters were used to make the magnetic recordings. However, considerable experience of recording a variety of subjects under difficult conditions was obtained. Thus, if magnetic recording is to be used clinically then a systematic investigation of stimulus and protocol variation is essential. It cannot be assumed that the VEMR will behave in the same manner as the VEP and indeed there is some evidence from the data presented in this chapter for differences between them. Patient variables such as refractive error, inattention or inter-trial variability need to be studied as well as variation in stimulus parameters. In addition, increased sensitivity and improved lesion localisation using the VEP has been achieved in a number of ways. The simplest has been the use of monocular and half field stimulation in optic neuritis/multiple sclerosis (Shahrokhi et al 1978, Hoeppner et al 1980). Others have included the use of small bright, foveally presented rectangles (Hennerici et al 1977), low luminance stimuli (Cant et al 1978) and when central scotoma is suspected, the use of smaller stimulus fields (Kriss et al 1982). At the current stage of development of our recording system and stimulators it is not possible to investigate all these aspects in detail. Hence, further study will be limited to :

(1) the effects of optical blur

(2) the effect of check and field size

(3) inter-trial variability

(4) flash intensity

(5) topography of response to full and half field pattern reversal stimulation and flash stimuli of increasing intensity.

The effects of these variables will be described in Chapters 4 and 5.

CHAPTER 4

THE INFLUENCE OF STIMULUS PARAMETERS ON THE VEMR

4.1 INTRODUCTION

It is well established that components of the VEP are influenced by stimulus parameters. For example, the latency of the flash P2 is influenced by flash intensity (Cobb and Dawson 1960, Shipley et al 1966), while the pattern reversal P100 is influenced by check and field size (Bartl et al 1978, Yiannikas and Walsh 1983, Kurita-Tashima et al 1991), pattern luminance (Cant et al 1978), reversal time (Trojaborg and Petersen 1979) and contrast (Bobak et al 1987). In addition, factors such as subject age (Asselman et al 1975, Hennerici et al 1977, Harding and Wright 1986), sex and visual acuity (Collins et al 1979, Sokol and Moskowitz 1981) may influence the VEP. Hence, it is likely that the VEMR will also be affected by stimulus parameters although it may not be possible to predict the response of the VEMR from the VEP because of the differences between magnetic and electrical recording. However, understanding the influence of stimulus parameters on the VEMR is essential prior to clinical use to establish a suitable protocol eg. certain check sizes may be easier to record magnetically than others and may reveal particular aspects of pathology (eg. small checks in optic neuritis). In this study the effects of the following stimulus parameters were studied:-

1) Optical blur

2) Check and field size

3) Temporal variability

4) Flash intensity.

4.2 Optical Blur

It is known that the introduction of blur increases the latency (Collins et al 1979, Sokol and Moskowitz 1981) and decreases the amplitude (Harter and White 1968, Harter and White 1970) of the electrical P100 to pattern reversal stimulation. Since increases in latency are important clinically (Asselman et al 1975, Carroll and Mastaglia 1979, Harding et al 1980) when recording the P100, it is essential to correct for any refractive error. As the VEMR to pattern reversal stimulation (P100M) could be useful clinically it is necessary that the effects of optical blur are established. It was decided to investigate the effects of different degrees of blur on the VEMR to both a

large (70') and a smaller (32') check since the latency (Sokol and Moskowitz 1981, Harding and Wright 1986, Bobak et al 1987) and amplitude (Harter and White 1968) of the electrical P100 is affected more using small than large checks.

4.3 Check and Field Size

The use of a recording protocol incorporating several check sizes is believed to improve the sensitivity of the VEP to pathological changes in the visual system (Asselman et al 1975, Hughes et al 1987, Novak et al 1988). This would be expected since in demyelinating lesions of the optic nerve such as optic neuritis, changes are seen at particular spatial (Regan et al 1982) and temporal (Plant and Hess 1985) frequencies. In addition, it is well established that both the latency and the amplitude of the VEP are influenced by check size (Bartl et al 1978, Ristanovic and Hadjukovic 1981, Sokol et al 1983, Kurita-Tashima et al 1991) and it is possible that the VEMR may be affected similarly.

As with check size, the use of a range of field sizes has improved the diagnostic capability of the VEP (Hennerici et al 1977, Kriss et al 1982, Yiannikas and Walsh 1986). The VEP recorded from a small stimulus field has a different morphology (Cohn and Hurley 1985) and a P100 of longer latency (Yiannikas and Walsh 1983) than that produced by stimulation with a larger field. In addition, a number of studies have shown that the central 0 to 4^{o} of the retina makes the most substantial contribution to the VEP amplitude (Jefferys and Axford 1972, Asselman et al 1975, Yiannikas and Walsh 1983). However, the effects of field size appear to be dependent on the check size used (Harter 1970). Hence, the aim of this preliminary study was to determine how the VEMR P100M responds to changes in the stimulus field size and to compare the results with those reported for the VEP. This parameter is of particular interest since theoretically, there could be a weak or no VEMR in some subjects when using a small stimulus field, as the fovea may be represented at the occipital pole where cells are oriented more radially to the surface of the head (Okada 1983) and hence, produce no externally detectable magnetic field. This may contrast with the VEP which is thought to be dominated by the response of the fovea because of a) its large cortical representation (Rovamo and Virsu 1979) and b) its proximity to the recording electrode (Yiannikas and Walsh 1983).

4.4 Temporal Variation

Serially recorded pattern reversal VEPs may also be useful clinically e.g. they have been used to monitor the progression of optic neuritis (Diener and Schliebler 1980, Walsh et al 1982, Matthews and Small 1983) and Alzheimer's

disease (Orwin et al 1986), the growth of pituitary tumours (Gott et al 1979) and the toxic effects of ethambutol therapy (Yiannikas and Walsh 1982, Yiannikas and Walsh 1983). A proper evaluation of these changes requires information on the degree of natural latency variation over time in the normal subject (Diener and Schiebler 1980, Meienberg et al 1979, Oken et al 1987, Hammond et al 1987). If the VEMR was to be used for a similar purpose, a knowledge of *its* temporal variability would also be needed.

In addition, during the normative data study (see Chapter 3, Armstrong et al 1991) a protocol was used in which the recordings were repeated until two consistent responses were obtained to each stimulus. In this situation, with few stimuli, the recording session was not unnecessarily prolonged. However, if a wider range of stimuli were to be used, incorporating full and half field recordings, this approach would increase the duration of the recording session unacceptably. In our experience this would reduce the concentration of the subject or cause fatigue, which may in turn make the response more difficult to record or more variable. It is therefore necessary to establish the reproducibility of the P100M in successive recordings and over short intervals of time. For example, if the response was most variable over short durations of time (from minute to minute) then it may be a better strategy to record the average latency or amplitude of a number of repetitions. Alternatively, if the response varies most between days then a more appropriate strategy may be to make a series of recording on separate occasions. If the response is highly variable between days in the normal subject then it may not be possible to use the VEMR for serial investigations in the clinical situation. It had been noted previously (Chapter 3) that the latency and amplitude of the VEMR P100M did vary between successive recordings. The responses appeared more variable in the afternoons than in the mornings, and especially at times when environmental noise appeared to be greater.

To investigate this problem, the latency variation of the P100M from minute to minute, between morning and afternoon on the same day and from day to day was investigated in two subjects. The recordings were carried out using a large check ($1^{o}40'$) pattern reversal stimulus, in the unshielded room used for much of the work described in this thesis. In the second part of the study, the three sources of variation were compared between three different environments:- 1) the original unshielded laboratory, 2) a single layer Eddy current shielded room and 3) a two layer magnetically shielded room (Vacuumschmelze Model AK1a). The purpose of this part of the study was to determine the degree to which magnetic shielding might improve the reproducibility of the response. In the final part of the study, the sources of variation were studied using

two identical single channel magnetometers to determine whether variation associated with the recording system would influence the reproducibility of the response.

4.5 Flash Intensity

Although more rarely used clinically than the pattern reversal response, the flash VEP is still considered useful in the monitoring of intraorbital surgery (Wright et al 1973), in pre-operative assessment of cataract patients and more recently in combination with the P100, in the diagnosis of Alzheimer's disease (Visser et al 1976, Harding et al 1981, Wright et al 1985, Philpot et al 1991). It is also possible that the VEMR to flash and pattern could compliment the VEP in the diagnosis of Alzheimer's disease (Armstrong et al 1990).

As with pattern reversal VEMR, it is necessary to characterise the response to flash stimulation. A major parameter of the flash response is its intensity. Studies of the flash VEP show the latency of the P2 to increase (Vaughan et al 1966, Shipley et al 1966, Tepas et al 1974, Whittaker and Seigfried 1983) and the amplitude to increase (DeVoe et al 1968, Tepas et al 1974, Thorpe-Davis et al 1987) or decrease (Dustman et al 1982) in response to increasing flash intensity.

The main aim of this study was to find out how the P2M component of the flash VEMR responds to changes in intensity and to compare the response with that of the VEP.

4.6 METHODS

4.61 Subjects

Six normal subjects participated in these experiments and were experienced members of laboratory staff (RAA, AS, CD, CN, SC and MD). All had corrected vision of 6/6 or better.

4.62 Magnetometer

The experiments were carried out using the single channel BTi magnetometer described in Chapter 3 located in an unshielded environment. An exception is Experiment 3 where a second single channel magnetometer was employed. This equipment was loaned by BTi complete with its own electronics. The original system is designated as Magnetometer A and the new system as Magnetometer B.

4.63 Shielded Room

In one experiment, the effect of different degrees of shielding on the reproducibility of the P100M was studied. These experiments were carried out in a single layer, Eddy current shielded room and then in a 2 layer, magnetically shielded room (Vacuumschmelze Model AK1a). The unshielded laboratory was located on a site chosen as a result of a magnetic survey of the clinical unit. Because of the framework of the building that houses Astons' magnetometry unit, it was not possible to locate the shielded room(s) in the laboratory where the original unshielded work was carried out. As a consequence, another slightly noisier location had to be used for the shielded facility.

Data is available for the shielding factor provided by the 2 layer magnetically shielded room (Figure 4.1). In order to establish this, the room was surrounded by a large set of coils and a signal of known strength and frequency was applied to the coil set. The resultant field was then measured inside the shielding. The difference between the field that should be detected given the size of the signal and that actually detected, gives an indication of how the shielding has attenuated the field at that particular frequency. The attenuation provided by the Eddy current shielding has been calculated and shown for comparison in the same figure. The Eddy current shielding is effective at attenuating the higher frequencies while the magnetic shielding cuts out more of the lower frequencies in addition to improving high frequency attenuation.

4.64 Signal Processing

Signals from the magnetometer were recorded at a sensitivity of x1000 (89pT/V flux to voltage) using a 0.3 to 30Hz (24dB/octave roll off) bandwidth. A 50Hz comb filter was also employed. Signals were attenuated by a factor of 100 before averaging by a Biologic Traveler signal processor which incorporated artifact rejection. The artifact rejection facility works by excluding signals exceeding a set amplitude. It is normal practice to adjust the gain setting so that approximately five percent of the incoming signals are rejected. Fifty sweeps of 500ms each were averaged.

4.65 Stimuli

All stimuli were viewed binocularly. The VEMR, either the P100M or the P2M, was recorded at the positive extremum (outgoing field), the position of which was determined by previous topographic mapping.

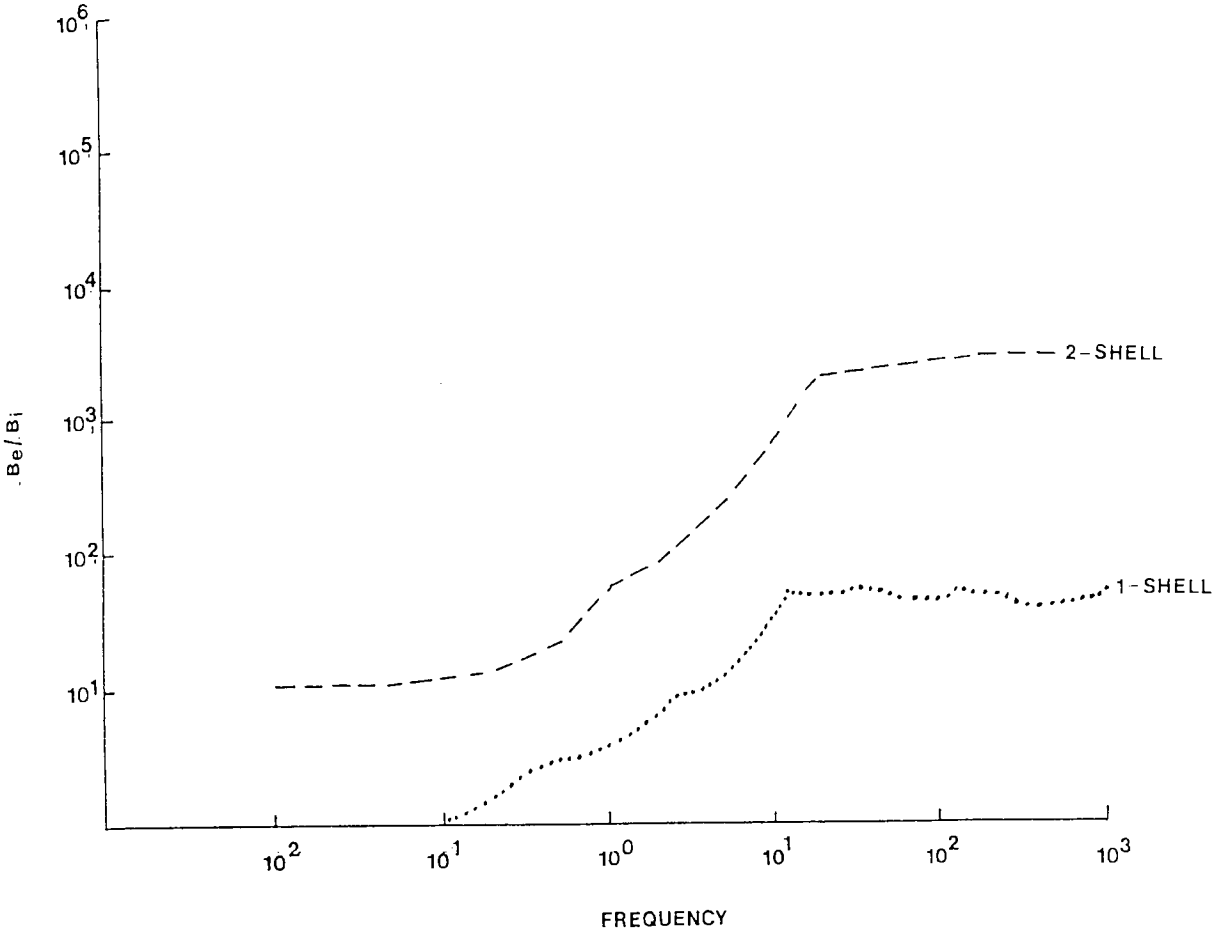

Figure 4.1 : Shielding factors for a 1 shell Eddy current shielded room (calculated) and a 2 shell magnetically shielded room (recorded).

4.66 Statistical Analysis

The data were analysed using various forms of Analysis of Variance (ANOVAR). The check size, field size, and intensity data were analysed using a 2 way (subjects and stimuli) ANOVAR in randomised blocks with differences between individual means determined by calculating the Least Significant Difference (LSD) at $p<0.05$. A limitation of this approach is that too many significant results may be reported if all pairs of means in the experiment are compared (Snedecor and Cochran 1980). In addition, curves were fitted to the response averaged over subjects using a polynomial curve fitting program. A higher order fit was accepted if it resulted in a significant reduction in the sums of squares (Snedecor and Cochran 1980). The temporal variability data were analysed by an analysis of variation of a nested classification. In this analysis, the total variance is partitioned into components attributable to a) variation between recordings on a single occasion, b) between morning and afternoon within days and c) within days.

4.67 Recording Protocol

1. Optical Blur

Three members of laboratory staff (RAA, AS and CD) acted as subjects for this study. Two check sizes were used (32' and 70') and were presented in a circular field of $13^{o}34'$ diameter. The contrast for both the large and small checks was 0.76 and the mean screen luminance was $1050 cd/m^2$. Reversal rate was 2/second. For subjects RAA and CD a trial frame and lens set was used to blur the images while for subject AS, a spectacle wearer, the blurring lenses were attached to the subjects own prescription. The lenses used had dioptric powers (D) between +5D and -5D presented at 1D intervals in a random order.

Subjects were seated comfortably under the magnetometer and the VEMR recorded at the positive extremum for each of the check sizes. The effects of optical blur on the 70' check response was determined first.

The choice of recording location was confirmed by recording two control responses. The subject was then asked to wear the trial frame and the lenses were inserted in a random order. Two responses were recorded under each condition of blur with a short interval between each pair of records. Included in this series was a repeat of the control reading, this being used as the 0D value in analysis.

The experiment was repeated using the same protocol for the 32' check. The major positivity (outgoing field component) was identified for each response and its latency and amplitude (peak to baseline) determined.

2. Check and Field Size

Five subjects were used for this study (RAA, CD, CN, AS and SC). The experiment was in two parts:- 1) the P100M was recorded in response to a 1°40' check presented in circular full fields of the following diameters - 1°45', 3°30', 5°14', 6°59', 11°9', 13°34' and 15°17' and 2) six check sizes were presented in a circular full field of 13°34' diameter. The check sizes used were as follows - 6', 12', 24', 32', 1°6' and 1°40'. Either the check or the field size was presented in a random order. The P100M was recorded for both experiments at the positive extremum of each subjects response to a 1°40' check presented in a circular full field of 13°34' diameter determined previously. Two separate responses were recorded to each stimulus parameter, with subjects remaining in position for each part of the experiment. The latency and amplitude (peak to baseline) of the P100M was determined. The data were then analysed using a 2 way analysis of variance (ANOVAR) in randomised blocks.

3. Temporal Variation

Two members of laboratory staff (RAA and CD) acted as subjects for this study. The VEMR was recorded in response to 70' checks presented in a circular field of 13°34' diameter. The contrast was 0.76, mean screen luminance 1050cd/m^2 and the reversal rate 2/second. Recordings were made using the laboratorys' own system ie. Magnetometer A. On each subject 10 measurements were made at 1 minute intervals in the morning (commencing at 8am) and in the afternoon (commencing at 1pm) for 5 days over a period of approximately 3 weeks. The subject did not move during a sequence of 10 recordings. A similar series of recordings were also made on subject RAA using the second single channel system (Magnetometer B).

In addition two further sets of recordings were made on subject RAA using Magnetometer A, in the one layer and two layer shielded rooms. The major positivity (P100M) on each waveform was identified and its latency and amplitude (peak to baseline) recorded for analysis. The data were analysed using an ANOVAR in a nested classification.

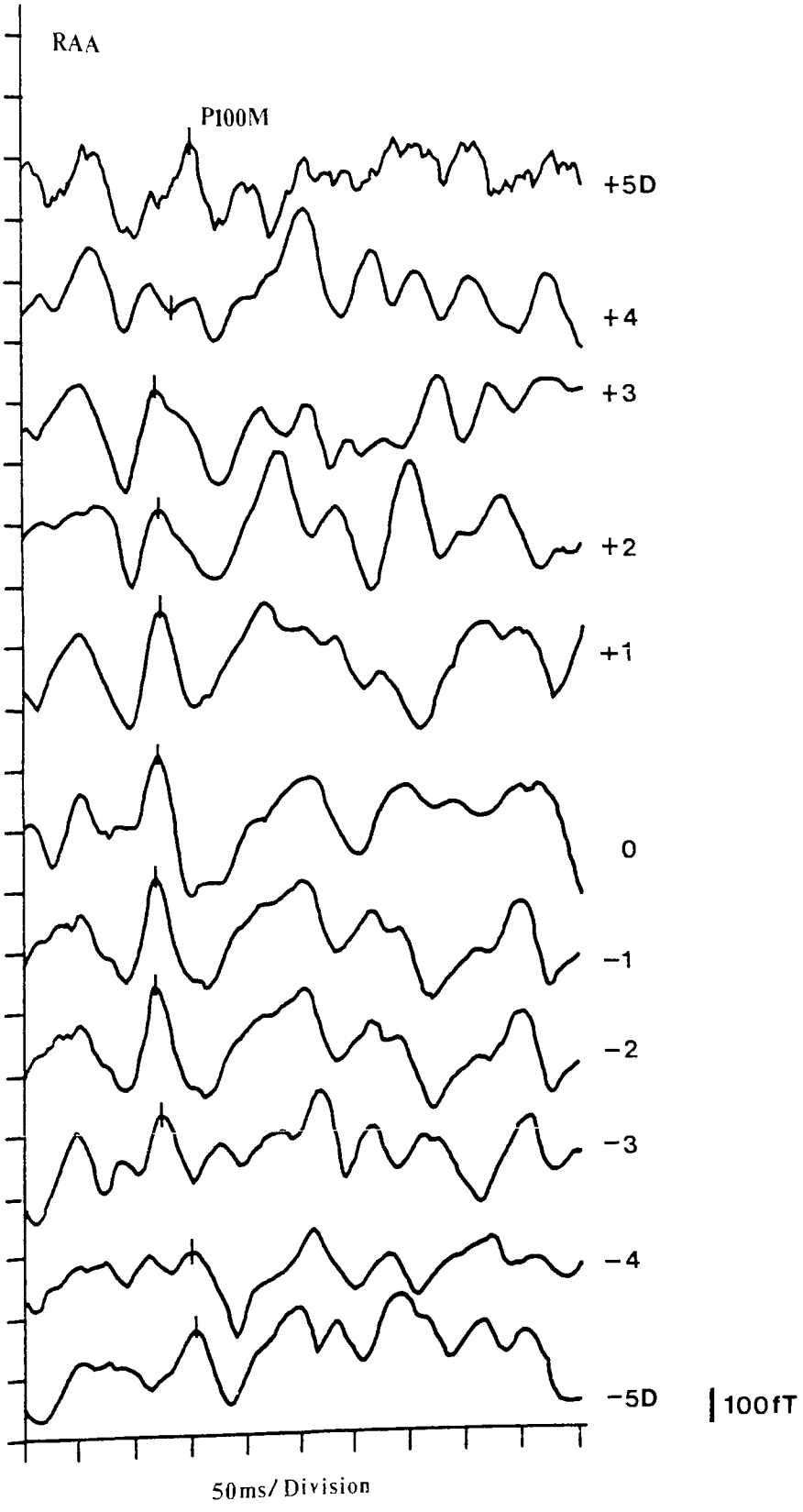

Figure 4.2 : Waveforms obtained from subject RAA in response to blurring of a 32' check pattern reversal stimulus. P100M latency increases with increasing optical degradation of the stimulus.

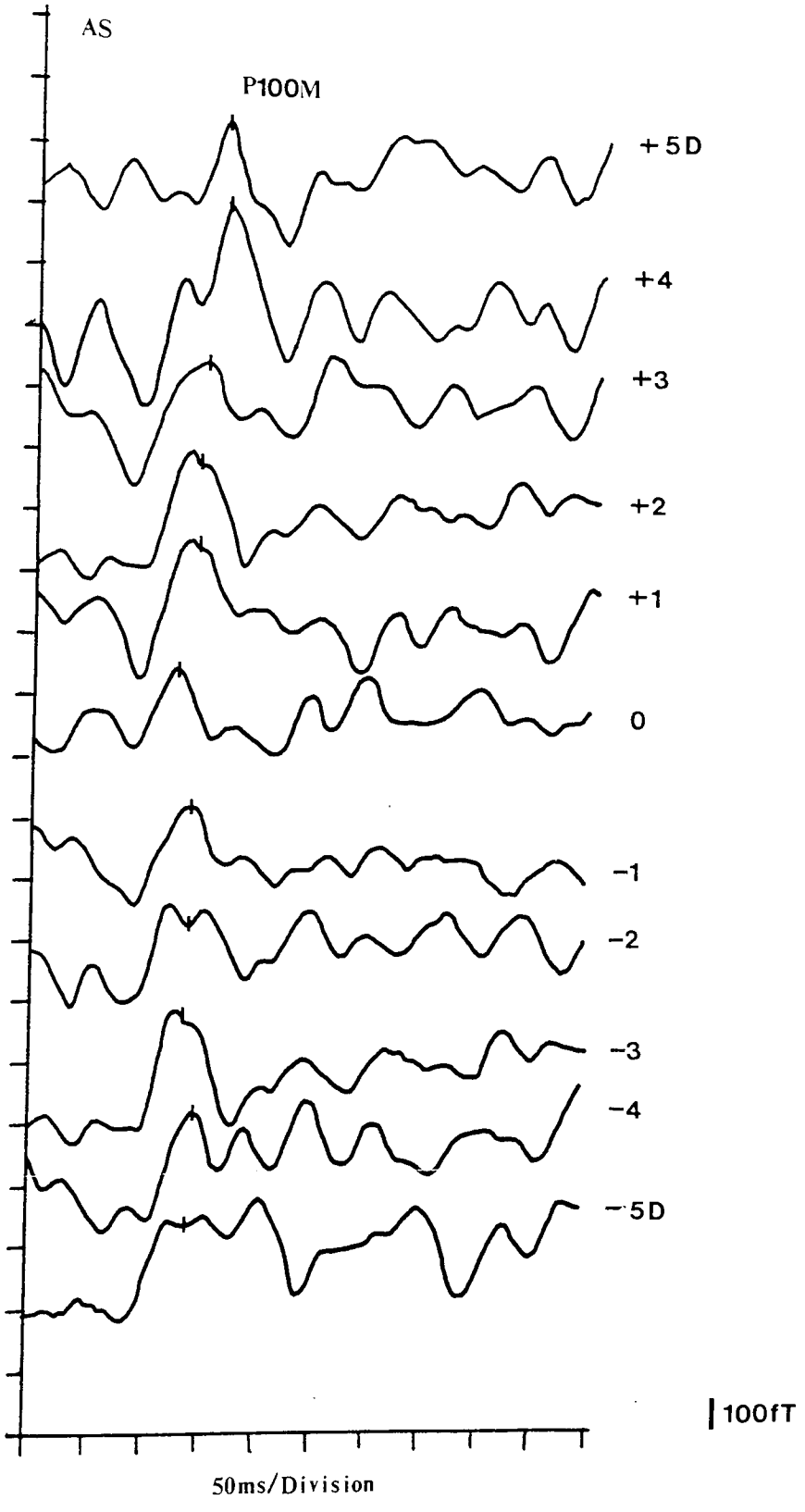

Figure 4.3 : Waveforms obtained from subject AS in response to blurring of a 70' check pattern reversal stimulus. P100M latency increases with increasing optical degradation of the stimulus.

4. Flash Intensity

The VEMR to flashes of varying intensity were recorded in five subjects (RAA, CD, CN, AS and MD). The flash stimulus was generated using a strobe triggered by a Biologic Traveler Signal Processor and a Medelec OS5. The stroboscope was calculated to produce a flash which subtended an angle of 19° at the eye but was located far enough away to minimise artefact produced by its discharge. The VEMR P2M was recorded at the positive extremum determined by previous topographic mapping, using a flash intensity of 8 for each subject. Two responses were recorded from each subject to each of the following flash intensities:- 1(1088cd/m^2), 2 (1363cd/m^2), 4 (1925cd/m^2), 8 (3939cd/m^2) and 16 (9661cd/m^2) presented in a random order. The P2M was identified on each waveform and its latency and amplitude (peak to baseline) determined. The group average was calculated and the results analysed using a 2 way analysis of variance in randomised blocks.

4.7 RESULTS

4.71 Optical Blur

A sample of waveforms obtained in subject RAA to blurring of a 32' check pattern reversal stimulus is shown in Figure 4.2. It is apparent that the latency of the P100M was minimal and its amplitude maximal when the image was clearest ie. at around 0D. Figure 4.3 shows sample waveforms from subject AS in response to blurring of a 70' check pattern reversal stimulus. The latency is shortest at around 0D but the effect on amplitude is less well defined than that seen for the 32' check response. As the power of the positive lenses is increased, the latency of the P100M increases. The responses to the negative lenses are more variable. The latency of the P100M to both 32' and 70' check pattern stimuli with increasing optical blur is shown for subjects RAA, AS and CD in Figure 4.4. In Figure 4.4a (subject RAA) increasing optical blur increases P100M latency for the 32' check pattern. The resulting U shaped curve has its base at around 0D. Neither the positive nor negative lenses appear to affect the latency of the P100M to the 70' check.

In subject AS (Figure 4.4b) the response to both 32' and 70' checks with increasing optical blurring is best described by a slightly flattened U-shaped curve. In subject CD (Figure 4.4c) the response to the 32' check can be described as U-shaped between -2D and +5D but the latency appears to decrease again between -2D and -5D. There does not appear to be any latency trend with increasing blur of the 70' check.

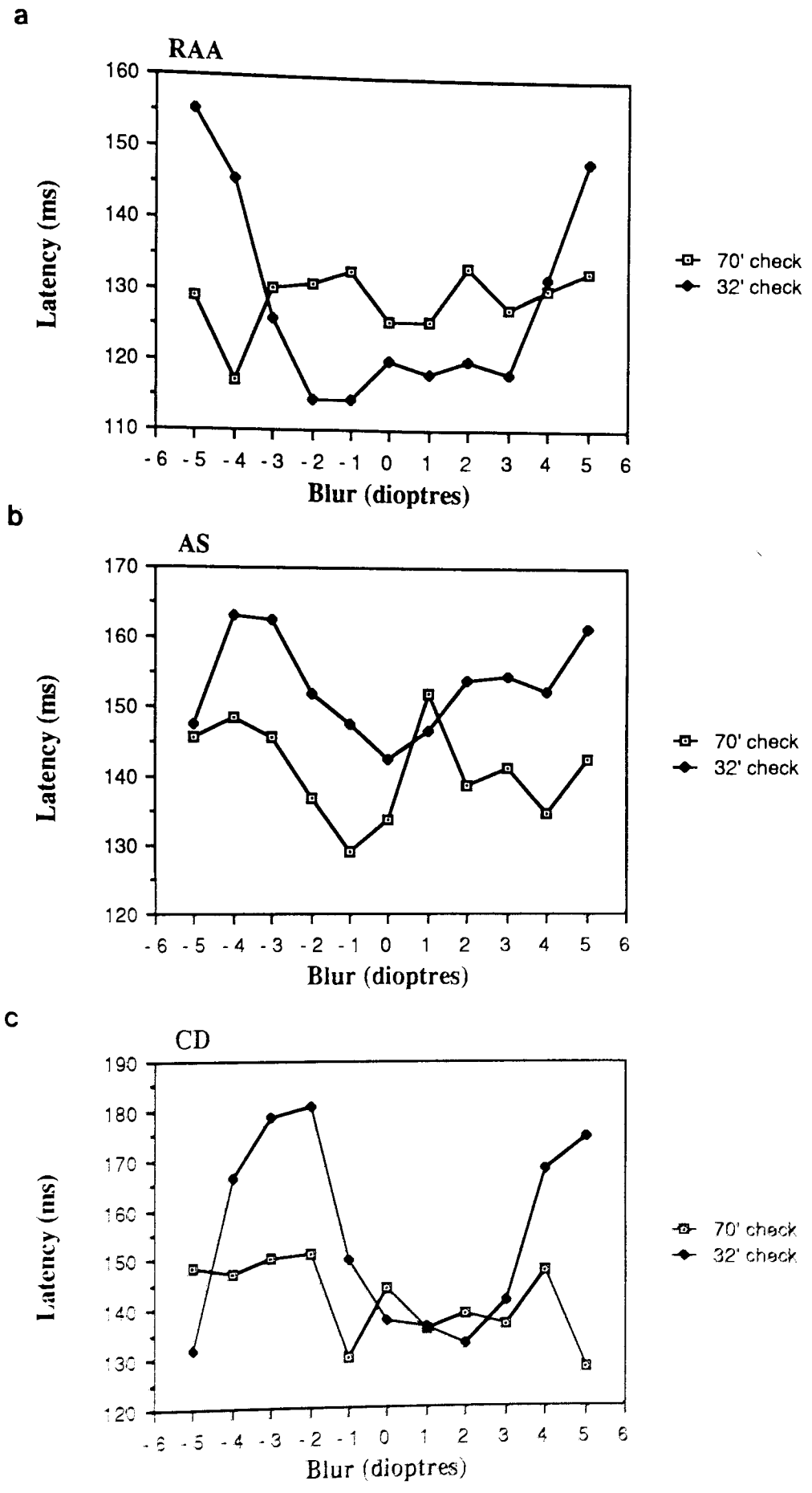

Figure 4.4 : The effects of optical blur on the latency of the P100M to a 32' and 70' check pattern reversal stimulation on a) subject RAA, b) subject AS and c) subject CD.

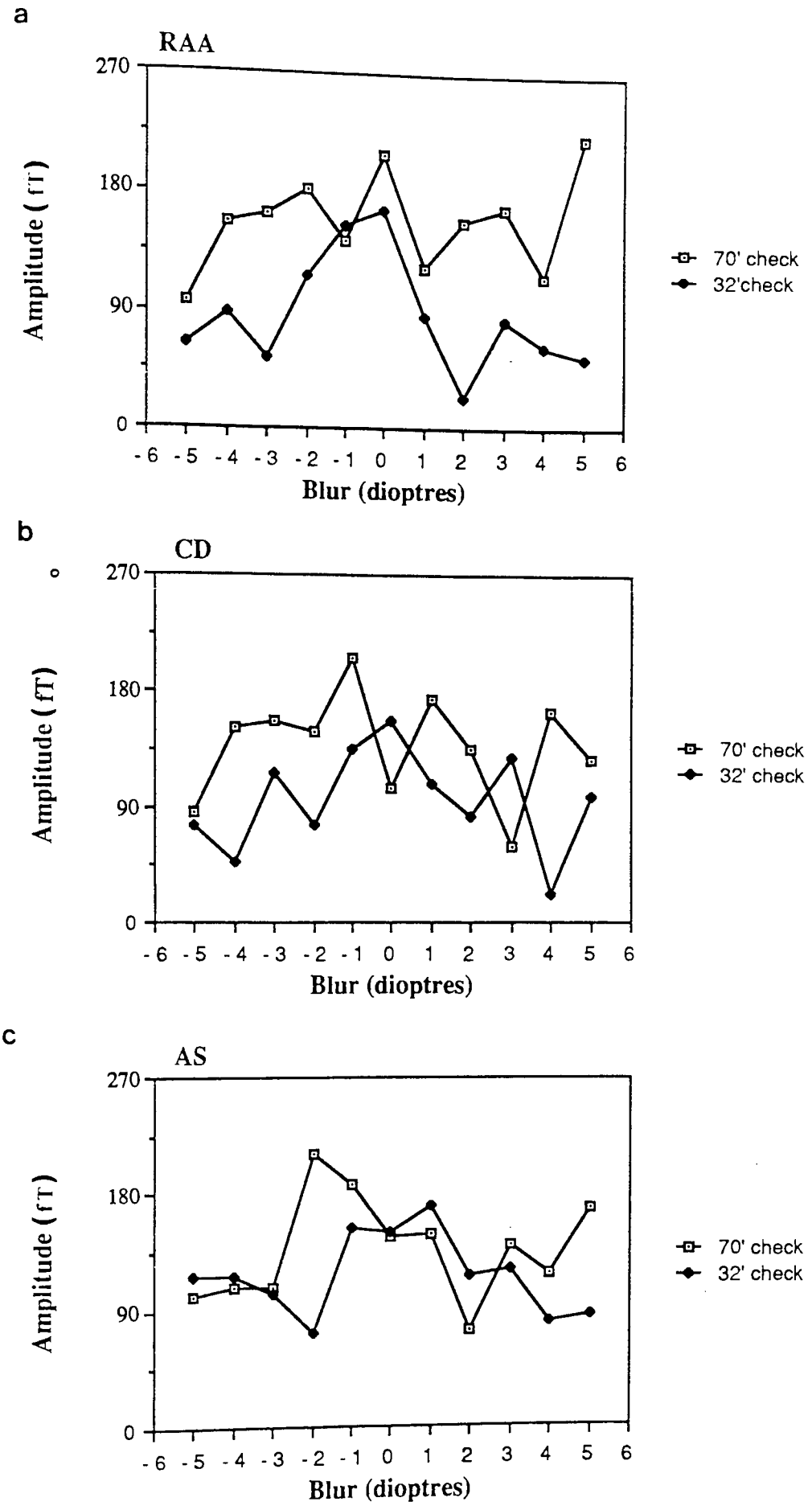

Figure 4.5 : The effects of optical blur on the amplitude of the P100M to a 32' and 70' check pattern reversal stimulation on a) subject RAA, b) subject AS and c) subject CD.

a

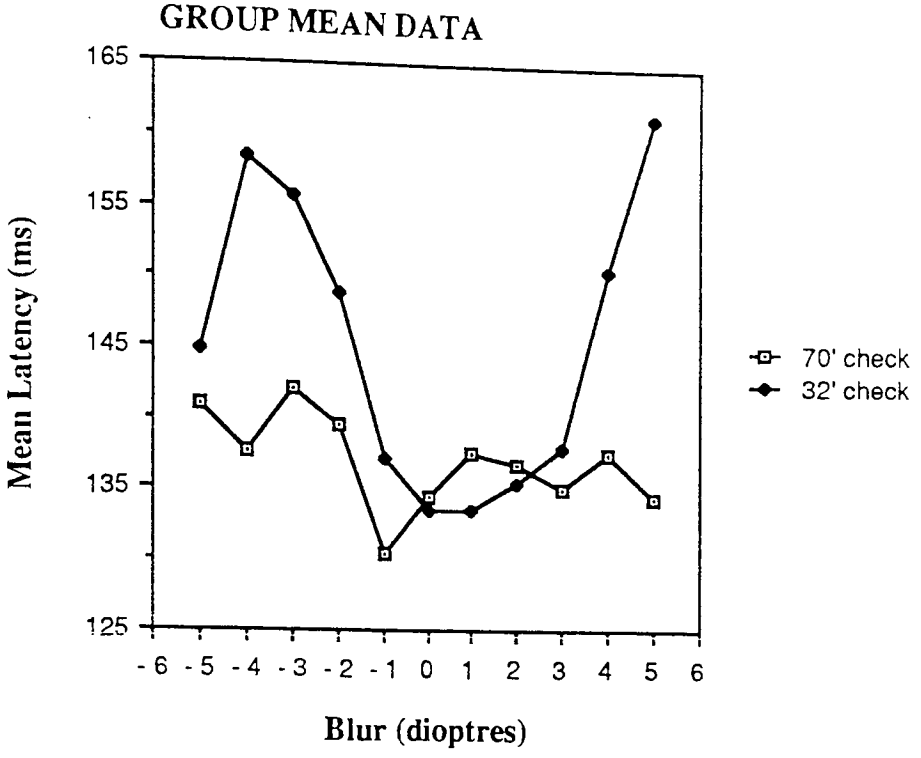

b

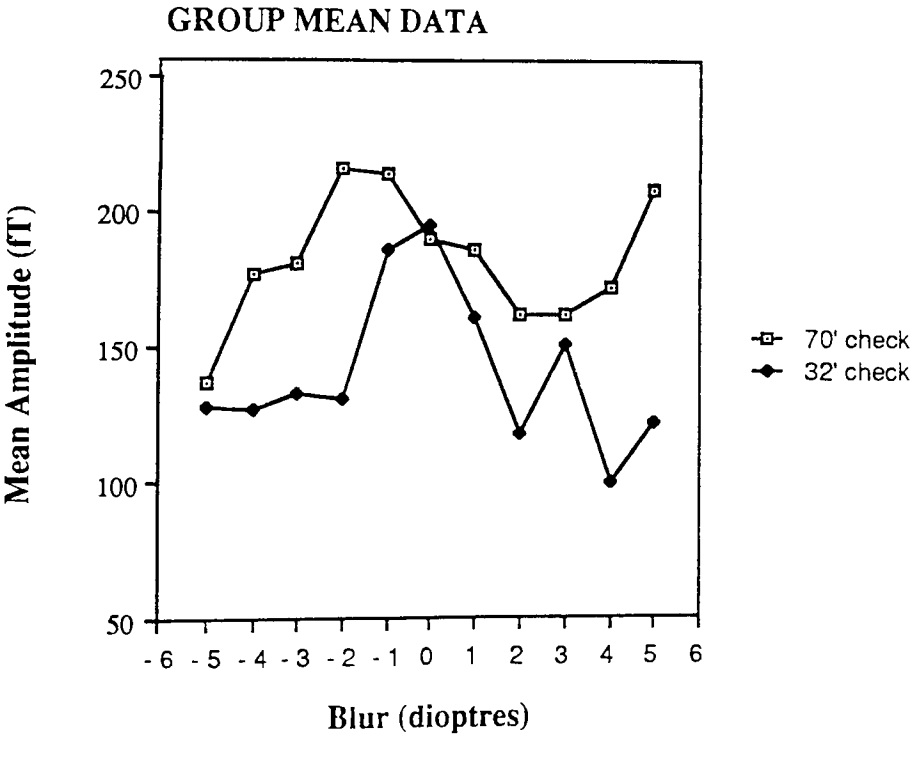

Figure 4.6 : Group mean data showing the effects of optical blur on a) latency and b) amplitude of the P100M to 32' and 70' check pattern reversal stimulation (3 subjects).

The amplitude of the P100M to both check sizes is variable for all subjects (Figure 4.5). However, there may be a tendency for increasing blur to decrease amplitude. The group mean data (Figure 4.6) emphasises the trend suggested in the individual data. The latency of the P100M to the 32' check increases as the image is degraded by both the positive and the negative lenses. With the exception of the response produced with a -5D lens, a U shaped curve results with the base of the U, ie. the shortest latency, occuring at 0 to +1D. The latency of the P100M to the 70' check appears to be little affected by the degradation of the image produced by either the positive or the negative lenses (Figure 4.6a). There is a suggestion that optical degradation decreases the amplitude of the P100M to the 32' check but the responses to both check sizes are quite variable (Figure 4.6b).

4.72 Check and Field Size

A sample of waveforms obtained in subject RAA to varying check size is shown in Figure 4.7. It is apparent that as check size increases, the latency of the P100M decreases. The latency and amplitude of the P100M to variation in check size from each subject is shown in Table 4.1. The analysis of variance (Table 4.2) indicates a significant effect of check size on latency ($F = 13.19$, $p<0.02$) but no significant effect on amplitude ($F = 1.2$, $p>0.05$). A second order polynomial curve was fitted to the group mean data ($R = 0.89$, $p<0.02$) and confirms the trend of decreasing latency with increasing check size. No significant linear or quadratic curve could be fitted to the amplitude data (Figure 4.8).

A sample of waveforms obtained in subject RAA to a 1°40' check presented in fields of increasing diameter (1°45' to 15°17') is shown in Figure 4.9. It can be seen that as the field size increases the latency of the P100M decreases while its amplitude increases. The P100M latency and amplitude for each subject is shown in Table 4.3. The analysis of variance (Table 4.4) indicates a significant effect of field size on both latency ($F = 7.79$, $p<0.001$) and amplitude ($F = 2.71$, $p<0.05$). A second order polynomial curve was fitted to the group mean data for latency ($R = 0.95$, $p<0.01$) and amplitude ($R = 0.94$, $p<0.01$) confirming the trend of decreasing latency and increasing amplitude with increasing field size (Figure 4.10).

4.73 Temporal Variation

Figure 4.11 shows a) a series of consecutively recorded responses to a 70' checkerboard pattern reversal stimulus and b) those same responses overlain to illustrate the stability of the P100M component latency and morphology. The latency of the P100M on consecutive records can vary by 8 to 11ms, with generally greater

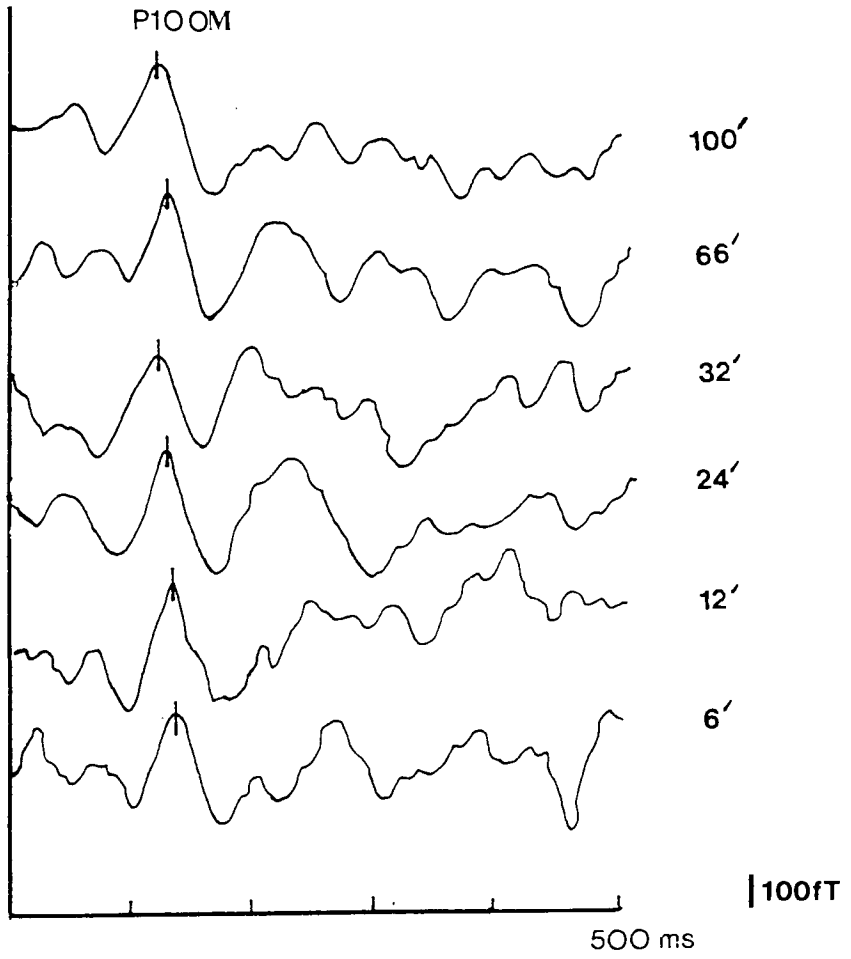

Figure 4.7 : Waveforms obtained from subject RAA in response to pattern reversal stimulation using a range of check sizes. All stimuli were presented in a circular full field of 13°34' diameter.

Table 4.1 : The effect of check size on a) the latency and b) the amplitude of the P100M to a pattern reversal stimulus presented in a circular full field of 13°34' diameter. The table shows the data obtained for each individual and the group mean.

a) Latency (ms)

Check Size

	6'	12'	24'	32'	1°6' (66')	1°40' (100')
RAA	138.67	129.88	127.93	126.95	131.83	120.61
CD	143.55	128.91	121.58	111.33	112.30	111.33
CN	139.16	136.72	132.81	110.35	113.28	101.56
AS	154.30	154.79	125.98	130.86	142.58	134.28
SC	153.32	147.46	112.30	103.52	105.47	100.58
Mean	145.80	139.55	124.12	116.02	121.09	113.67

b) Amplitude (fT)

Check Size

	6'	12'	24'	32'	1°6' (66')	1°40' (100')
RAA	171.25	113.56	176.13	104.49	129.58	204.61
CD	52.78	52.78	122.37	104.84	196.96	121.48
CN	110.00	93.18	33.20	60.70	71.20	98.97
AS	180.58	128.96	155.57	168.21	180.31	190.37
SC	97.19	103.51	10.23	95.76	95.32	54.65
Mean	122.37	98.43	99.50	106.80	134.66	134.03

Table 4.2 : The results of a 2 way analysis of variance (ANOVAR) in randomised blocks of a) the latency and b) the amplitude of the major positivity (P100M) in the response to checks of increasing size presented in a 13°34' field.

a) Latency

Source of Variance	Sums of Squares	Degrees of Freedom	Mean Square
Treatment (Check Size)	4198.60	5	1049.65
Blocks (Subjects)	1690.13	4	338.03
Error	1592.08	20	79.60

F Ratio (Treatments) = 13.19***. Significant at $p<0.001$.

F Ratio (Blocks) = 4.25.

Least Significant Difference = 11.79ms.

b) Amplitude

Source of Variance	Sums of Squares	Degrees of Freedom	Mean Square
Treatment (Check Size)	87.15	5	21.79
Blocks (Subjects)	521.77	4	104.36
Error	362.66	20	18.13

F Ratio (Treatments) = 1.20.

F Ratio (Blocks) = 5.75.

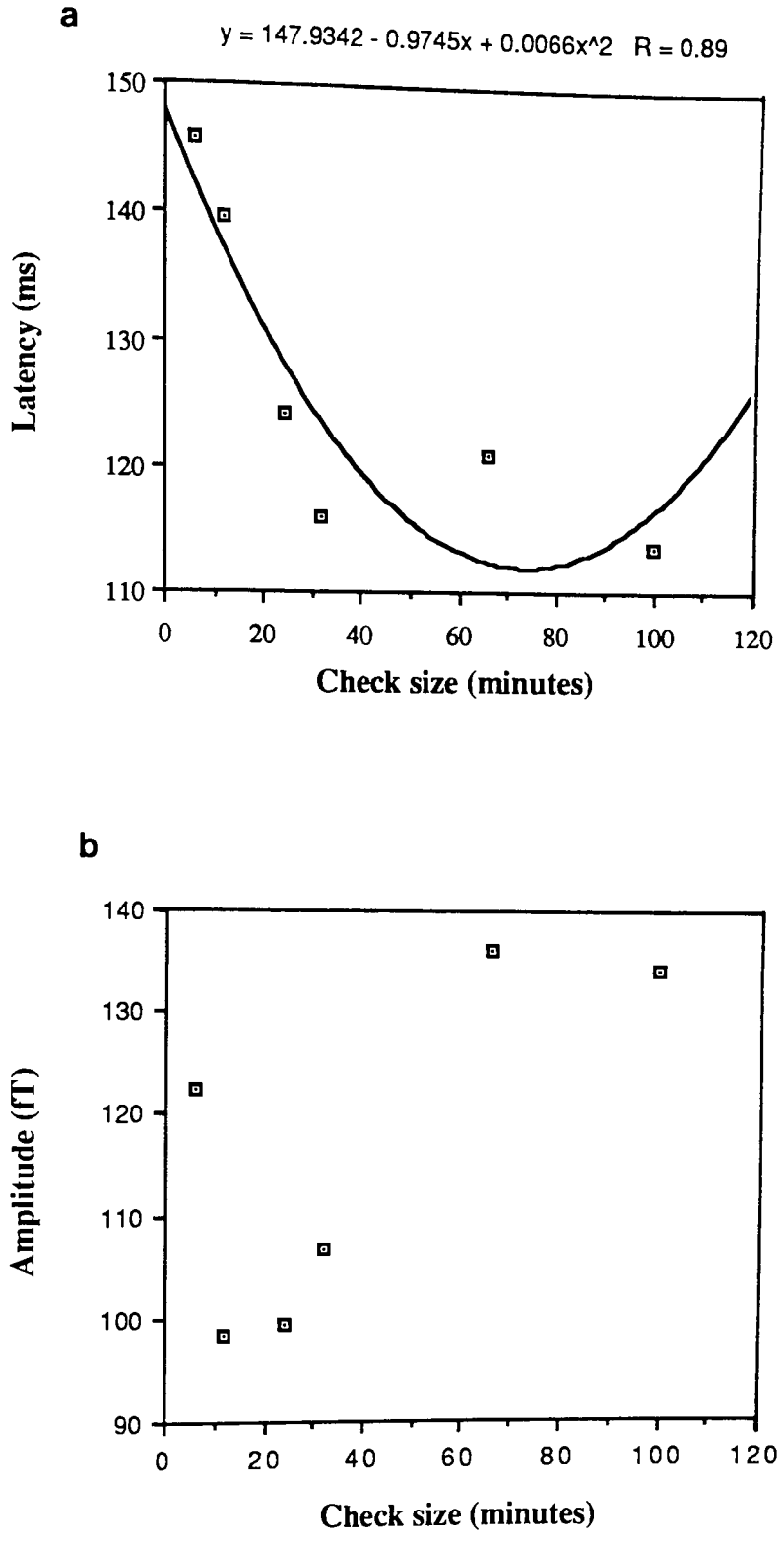

Figure 4.8 : Group mean data showing the relationship between a) latency and b) amplitude of the pattern reversal P100M and check size. The latency data were best fitted by a second order polynomial ($R = 0.89$, $p<0.02$).

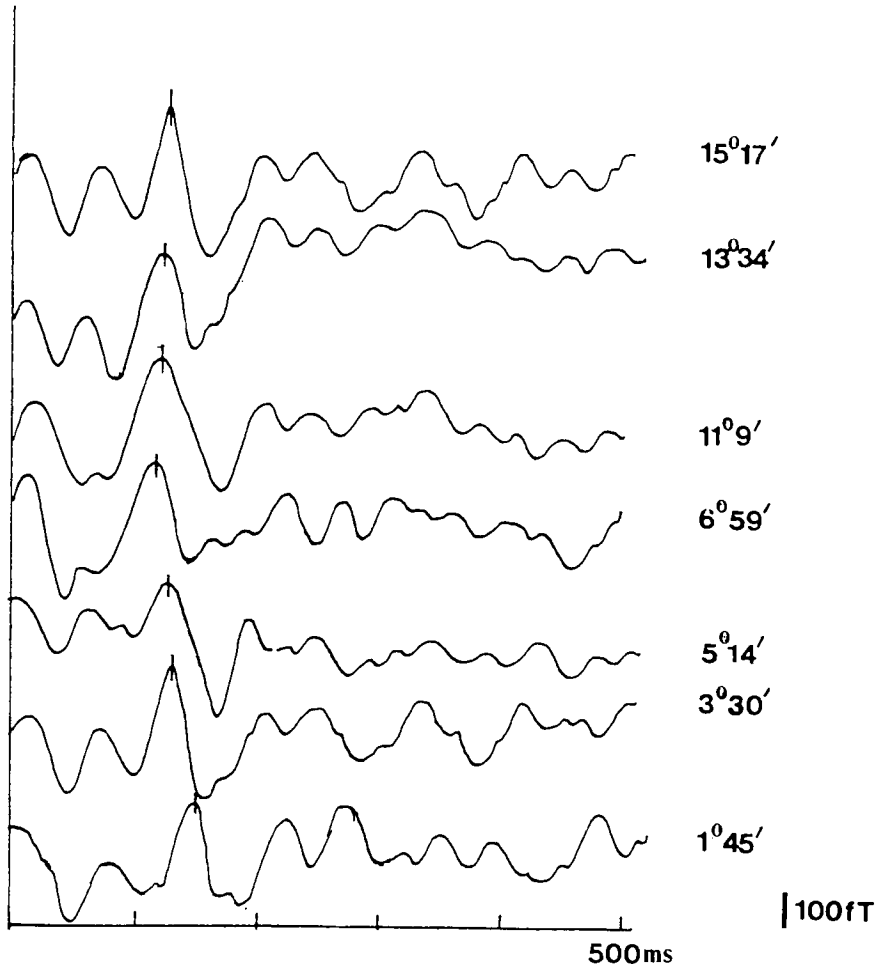

Figure 4.9 : Waveforms obtained from subject RAA in response to 1°40' check pattern reversal stimulus presented in a range of field sizes.

Table 4.3 : The effect of field size on a) the latency and b) the amplitude of the pattern reversal P100M to a 1°40' check. The table shows the data obtained for each individual and the group mean.

a) Latency (ms)

Field Size

	1°45' (105')	3°30' (210')	5°14' (314')	6°59' (419')	11°9' (669')	13°34' (814')	15°17' (917')
RAA	155.86	137.21	133.30	115.73	120.61	123.05	125.98
CD	164.55	108.40	156.25	131.35	145.02	126.46	129.89
CN	146.48	144.53	130.86	139.65	111.82	112.31	109.38
AS	163.09	164.55	151.37	152.35	133.79	137.70	130.86
Mean	157.49	138.67	142.94	134.77	127.81	124.88	124.03

b) Amplitude (fT)

Field Size

	1°45' (105')	3°30' (210')	5°14' (314')	6°59' (419')	11°9' (669')	13°34' (814)	15°17' (917)
RAA	104.22	146.76	78.76	187.88	212.09	204.43	204.61
CD	164.20	111.43	220.27	145.78	183.87	209.33	94.87
CN	154.15	153.26	104.22	133.14	141.33	148.81	342.03
AS	94.61	70.13	109.11	210.75	215.202	243.68	143.65
Mean	129.32	120.42	128.07	171.95	188.06	201.58	196.24

Table 4.4 : A 2 way ANOVAR in randomised blocks of a) the latency and b) the amplitude of the major positivity P100M produced in response to a 1°40' check presented in circular full fields of increasing diameter.

a) Latency

Source of Variance	Sums of Squares	Degrees of Freedom	Mean Square
Treatment (Field Size)	3410.86	6	1136.95
Blocks (Subjects)	1661.93	3	276.99
Error	2626.91	18	145.94

F Ratio (Treatments) = 7.79*** Significant at $p<0.001$.

F Ratio (Blocks) = 1.9.

Least Significant Difference = 17.94ms.

b) Amplitude

Source of Variance	Sums of squares	Degrees of Freedom	Mean Square
Treatments (Field Size)	375.12	6	125.04
Blocks (Subjects)	7.35	3	1.23
Error	830.18	18	46.12

F Ratio (Treatments) = 2.71* Significant at $p<0.05$.

F Ratio (Blocks) = 2.66

Least Significant Difference = 89.80fT

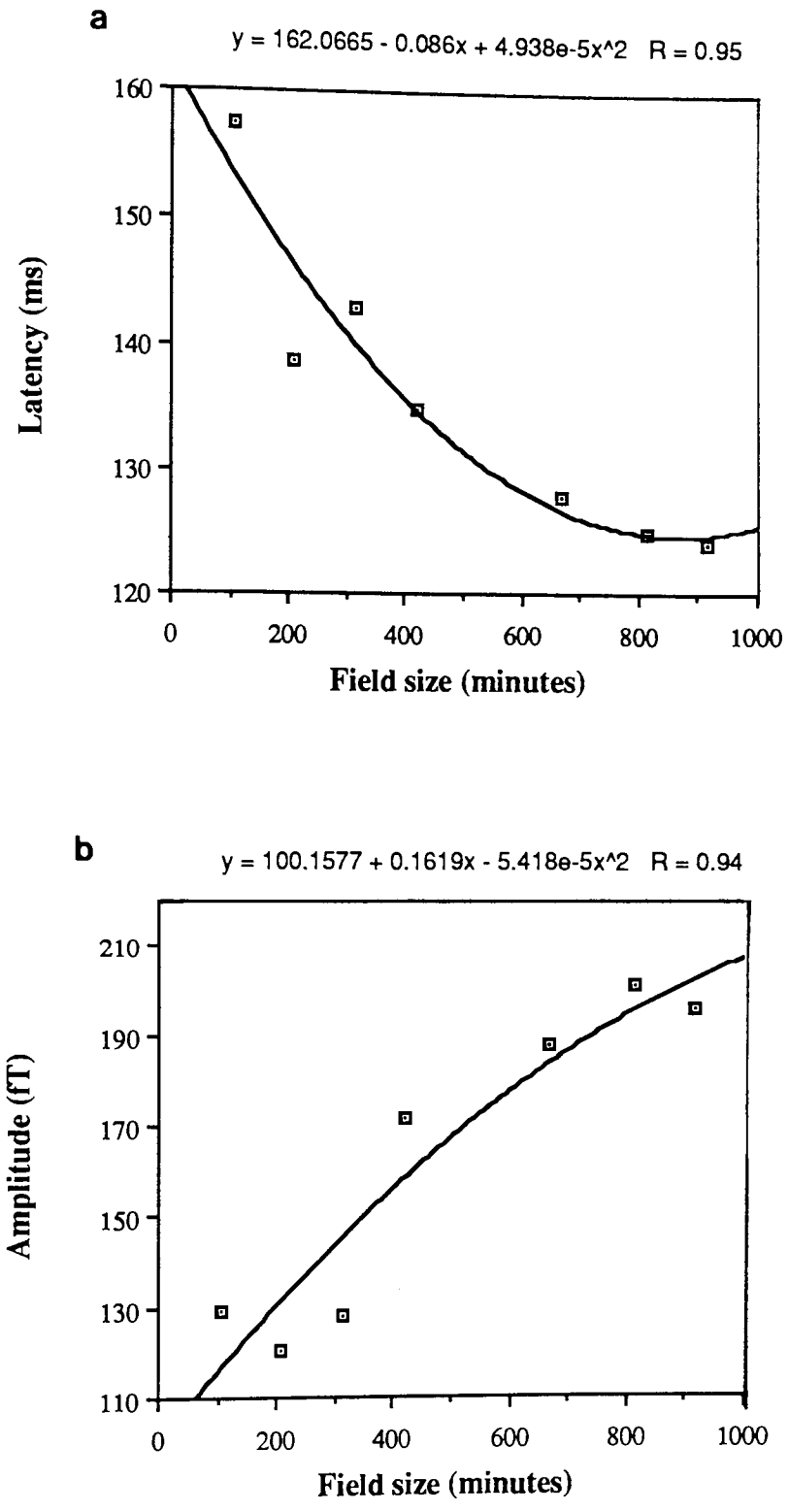

Figure 4.10 : Group mean data showing the relationship between a) latency and b) amplitude of the pattern reversal P100M and field size. Both the latency and the amplitude data were best fitted by a second order polynomial - a) latency $R = 0.95$, $p<0.01$ and b) amplitude $R = 0.94$, $p<0.01$.

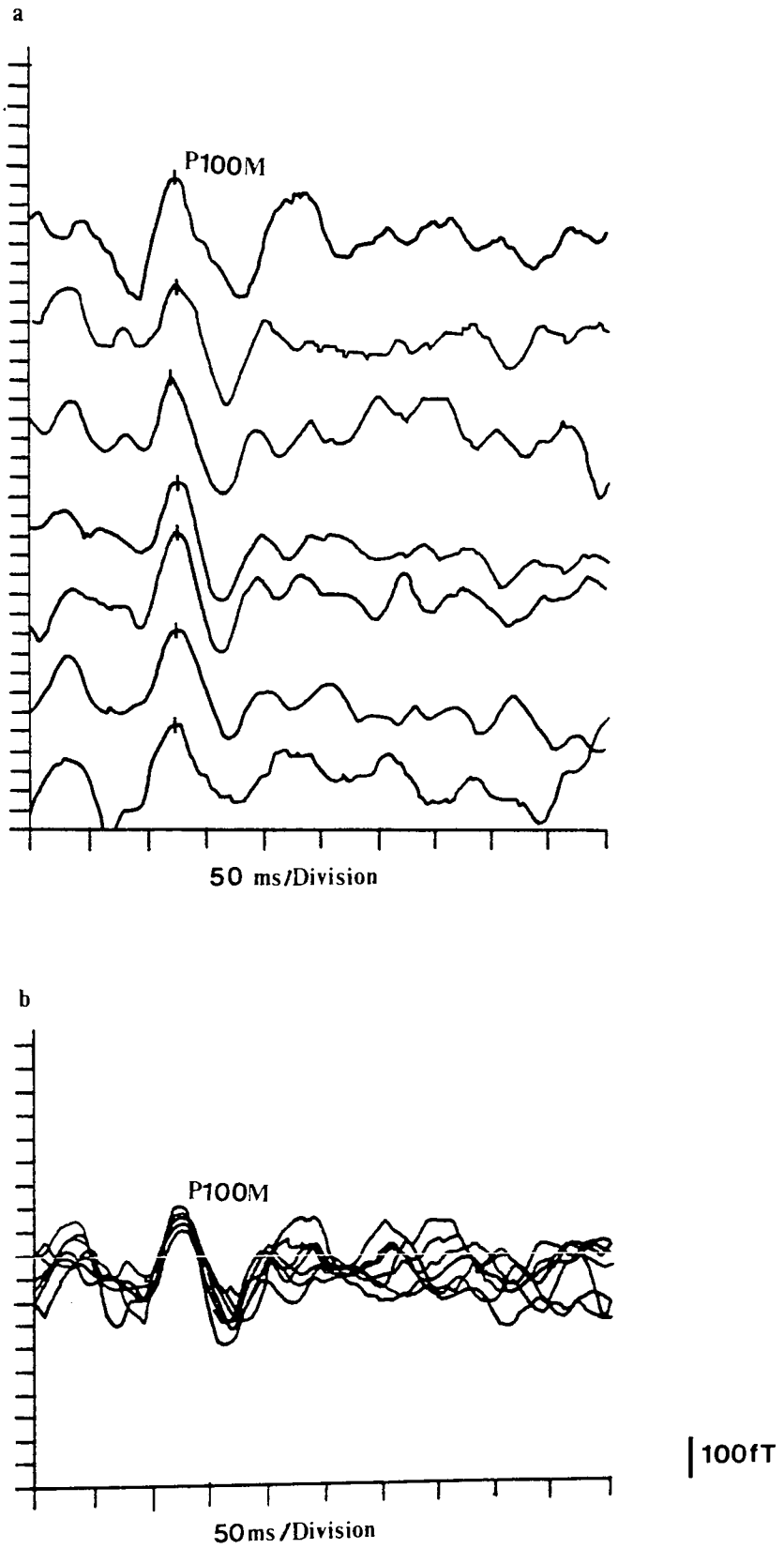

Figure 4.11 : Responses to a 70' check pattern reversal stimulus a) recorded consecutively approximately 1 minute apart and b) shown overlaid to illustrate stability of P100M component.

variability being seen in the afternoon. Also present, although prominent to a varying degree on each waveform , are the ingoing field components N1M and N2M.

Table 4.5 shows the results of a 3 block ANOVAR of a nested classification of the latency of the P100M to a 70' check, pattern reversal stimulus in subjects RAA and CD. In this analysis, variance is attributed to different sources ie. that occuring from minute to minute, from morning to afternoon and between days. The data on which this analysis is based can be found in Appendices 4 and 5.

Table 4.6 shows the results of a 3 way ANOVAR of a nested classification on the latency of the P100M to a 70' check, recorded from subject RAA in an unshielded environment, and in a one layer and two layer magnetically shielded room. The data on which this analysis is based can be found in Appendices 4 and 6.

The mean latency for RAA is 124.92ms and the range of standard deviations 1.52-4.8. The mean latency for CD is longer (127.16ms) and the range of standard deviations wider (6.31-14.4) than for subject RAA. In both subjects, most of the variance can be attributed to the variation in the response from minute to minute. However, while in RAA time of day and date have little effect on response latency, it appears that for subject CD the day of the recording made a significant contribution to the variance. Little variation was associated with differences between morning and afternoon sessions.

The mean latency of the P100M was almost identical in the unshielded and magnetically shielded environments. In the Eddy current shielded room the mean latency was slightly shorter but, as indicated by the range of standard deviations and coefficients of variation, it was also more variable. In the three environments, most of the latency variation occured from minute to minute. In the unshielded environment little of the variability could be attributed to either differences between recording sessions on the same day or between days. In the Eddy current and magnetically shielded rooms variance was negligable between days, but of increasing importance, between recordings made on the same day.

The overall variability in the latency of the P100M was smallest in the magnetically shielded room as illustrated by the smaller overall standard deviation (3.73) and coefficient of variation (3.0%) for this environment. However, this is only slightly better than for the data recorded in the unshielded environment ($F = 1.08$, no significant difference) where overall standard deviation (SD) was 4.04 and the coefficient of variation (CV) 3.2%. The Eddy current shielded room performed worst in these terms (SD = 6.66, CV = 5.4%). When the variability of the data recorded in

Table 4.5 : The results of a 3 block nested classification ANOVAR on P100M latency (70' check, pattern reversal stimulus) data obtained from subjects RAA and CD in an unshielded environment.

	RAA	CD
Mean Latency	124.92ms	127.16ms
Range of Standard Deviations	1.52-4.8	6.31-14.4
Range of Coefficients of Variation	1.2-3.8%	4.1-11.7%
Variance (Minute to Minute)	15.42	88.25
Variance (Morning to Afternoon)	-0.17	7.06
Variance (Between Days)	1.36	71.55

Table 4.6 : The results of a 3 block ANOVAR of a nested classification of data recorded in an unshielded, an Eddy current shielded and a magnetically shielded room. The data was obtained from subject RAA in response to a 70' check pattern reversal stimulus.

	Unshielded Room	Eddy Current Shielding	Full Magnetic Shielding
Mean Latency	124.92ms	122.50ms	124.24ms
Range of Standard Deviations	1.52-4.8	2.95-7.95	1.60-4.3
Range of Coefficients of Variation	1.2-3.8%	2.3-6.6%	1.3-3.6%
Variation (Minute to Minute)	15.42	38.71	10.29
Variation (Morning to Afternoon)	-0.17	12.19	4.73
Variation (Between Days)	1.36	-5.55	0.83
Overall Standard Deviation	4.04	6.66	3.73
Overall Coefficient of Variation	3.2%	5.4%	3.0%
Total Number of Records	100	60	100

Unshielded room v 1^{O} shielded room F = 1.65*. Significant at $p<0.05$

Unshielded v 2^{O} shielded room F = 1.08.

1^{O} shielded room v 2^{O} shielded room F = 1.78*. Significant at $p<0.05$

the unshielded room was compared with that from the Eddy current shielded room and the magnetically shielded room, F ratios of 1.65 and 1.78 were obtained respectively , both significant at $p<0.05$.

Each set of 10 records was examined for evidence of any latency or amplitude trend. A polynomial curve fitting program was used to determine whether there was a significant linear or quadratic response. Data obtained inside the magnetically shielded room can be seen in Table 4.7. Figures 4.12 and 4.13 show some of these data fitted with regressions.

In most cases no significant trends were apparent. Statistically significant trends in both latency and amplitude occurred more frequently in the afternoon than in the morning and more significant fits were obtained with latency than compared with amplitude data.

Figure 4.12 shows curves fitted to the P100M latency data obtained at 3 different recording sessions. The latency of the P100M is plotted against the order of the record and curves fitted to the data. Figure 4.12a shows an occasion on which a significant latency trend was observed. These data were best fitted by a second order polynomial ($R = 0.77$, $p<0.05$) with the longest latency observed at the start of the experiment, then decreasing and increasing again towards the end of the sequence. Figure 4.12b also shows an occasion on which a significant latency trend was observed during the recording session, again the data was best fitted by a second order polynomial function ($R = 0.71$, $p<0.05$). However, in this instance the latency of the P100M is longest at the start of the experiment and falls towards the end. The final graph (Figure 4.12c) shows an occasion on which no significant latency trend could be observed, the case in the majority of instances.

Figure 4.13 shows curves fitted to the P100M amplitude data obtained at 3 different recording sessions. Figures 4.13a and 4.13b show occasions on which a significant amplitude trendwas observed ($R = 0.63$, $p< 0.05$; $R = 0.71$, $p< 0.05$ respectively). Again the shapes of the curves fitted vary with normal and inverted parabolas apparent. Figure 4.13c shows an occasion on which no amplitude trend could be discerned, this again being the case in most instances.

The final table in this section shows the results of a 3 way ANOVAR of a nested classification carried out on the data obtained for a) the latency and b) the amplitude of the P100M to a 70' check pattern reversal stimulus in the unshielded room using two single channel systems (Table 4.8). Ten recordings were made with each system, on subject RA, morning and afternoon on five separate days. The two systems varied in

Table 4.7 : A regression analysis of the trends in P100M latency and amplitude in sets of 10 successive runs on the data recorded from RAA inside the magnetically shielded room . * and ** denote a significant fit ($p<0.05$ and 0.01 respectively).

a) **Latency Trends**

		1/10/91	2/10/91	3/10/91	7/10/91	8/10/91
AM	Linear	-0.25	-0.66*	-0.32	0.24	0.51
	Quadratic	0.43	0.71*	0.47	0.25	0.76
PM	Linear	0.34	-0.29	-0.86*	-0.40	-0.29
	Quadratic	0.40	0.29	0.91**	0.77**	0.51

b) **Amplitude Trends**

		1/10/91	2/10/91	3/10/91	7/10/91	8/10/91
AM	Linear	0.42	0.40	-0.04	0.39	0.55
	Quadratic	0.42	0.43	0.28	0.49	0.58
PM	Linear	0.67*	-0.66*	-0.37	0.33	0.61
	Quadratic	0.69*	0.71*	0.37	0.48	0.63*

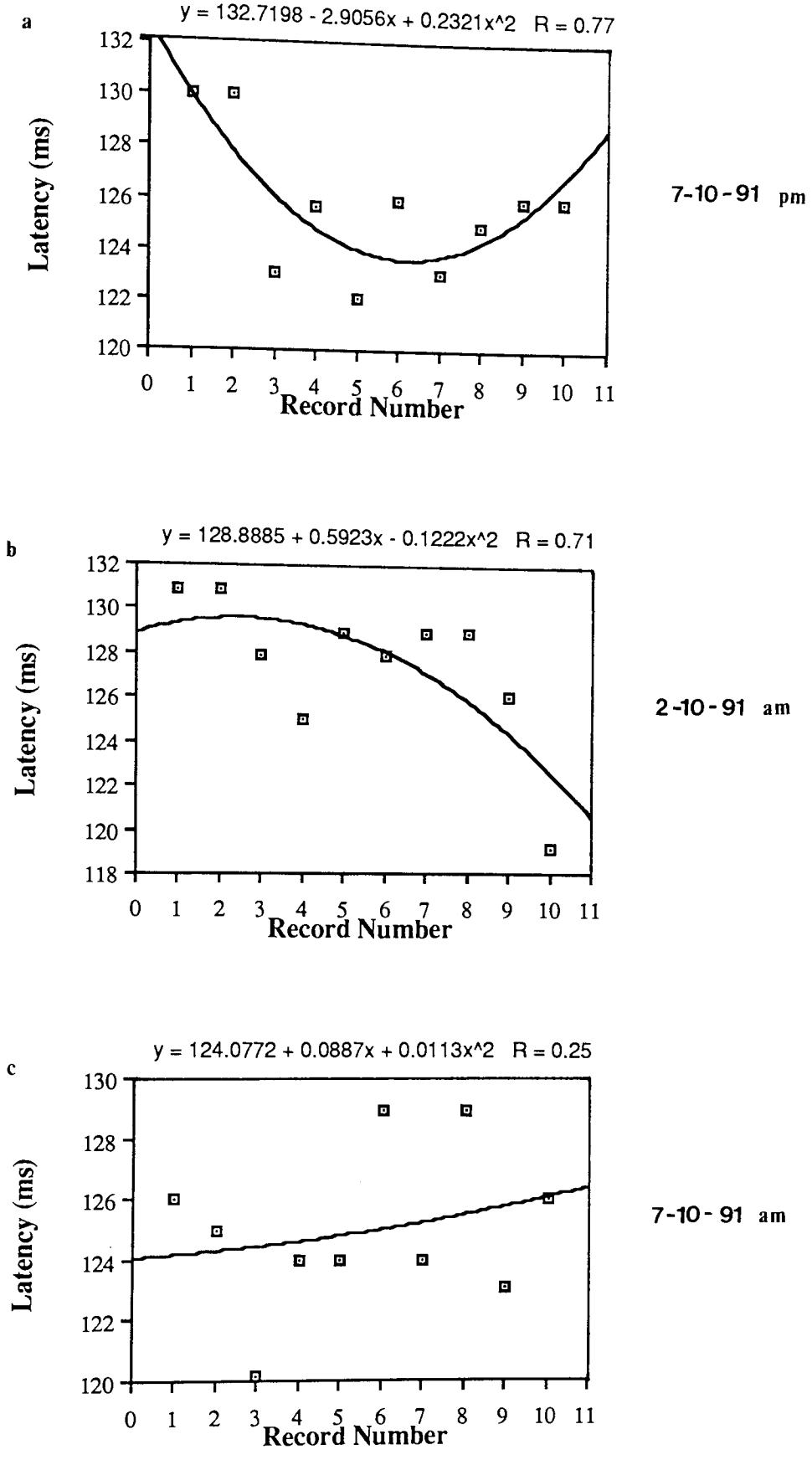

Figure 4.12 : Regressions fitted to latency data obtained on 3 different occasions. a) and b) show occasions when a significant trend in P100M latency could be seen during the recording session ($R = 0.77$, $p<0.05$ and $R = 0.71$, $p<0.05$ respectively). c) shows an occasion on which no trend was discernable, this being the norm.

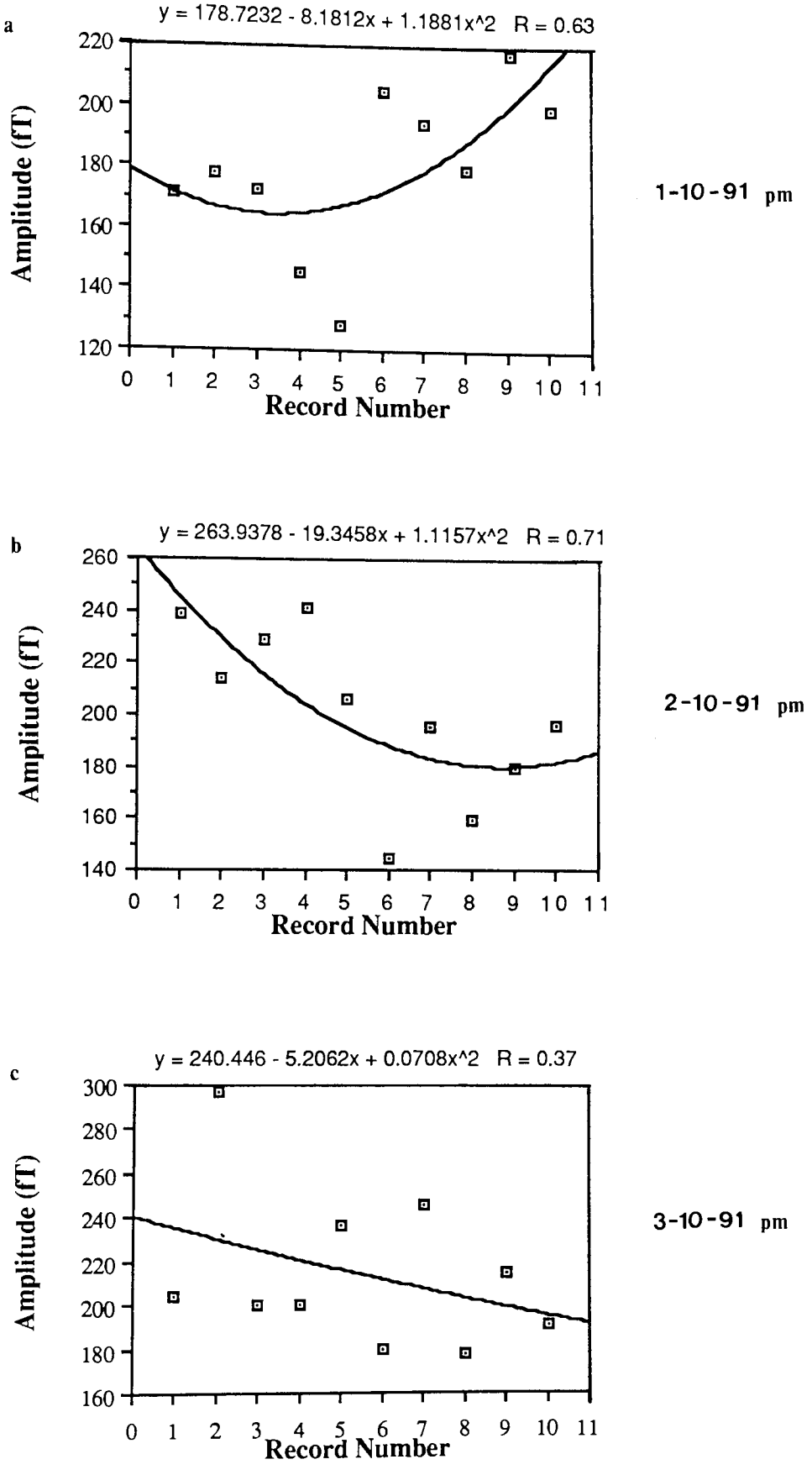

Figure 4.13 : Regressions fitted to amplitude data obtained on 3 different occasions. a) and b) show occasions when a significant trend in P100M amplitude could be seen during the recording session ($R = 0.63$, $p<0.05$ and $R = 0.71$, $p<0.05$ respectively). c) shows an occasion on which no trend was discernable, this being the norm.

Table 4.8 : An analysis of the components of variance of the latency and amplitude of the VEMR P100M to a 70' check pattern reversal stimulus measured using two different magnetometers on subject RAA.

	Magnetometer A		Magnetometer B	
	Latency	**Amplitude**	**Latency**	**Amplitude**
Mean	124.92ms	154.50fT	114.94ms	160.25fT
Range of Standard Deviations	1.52-4.8	32.93-56.07	2.23-8.9	20.38-80.08
Range of Coefficients of Variation	1.2-3.8%	16.37-51.35%	1.91-7.59%	13.58-44.22%
Variance (Minute to Minute)	15.42	26.13	24.82	24.36
Variance (Morning to Afternoon)	-0.17	4.72	1.15	2.22
Variance (Between Days)	1.36	15.36	5.47	2.32

mean latency by around 10ms (A>B) although mean amplitude values were similar. The ranges of standard deviations for both latency and amplitude were smaller for magnetometer A than for B. For both systems, latency and amplitude varied most from minute to minute within a recording occasion. With the exception of the amplitude variance between days for magnetometer A, little latency or amplitude variation could be attributed to the differences between morning and afternoon recordings or between days, for either magnetometer. The largest component of latency variance for both magnetometers was attributable to the variation from minute to minute. The variance due to differences between morning and afternoon sessions and between days was small. The largest component of amplitude variance was also attributable to the variability from minute to minute for both magnetometers although a proportion of the variance can be accounted for by the variation between days for Magnetometer A.

4.74 Flash Intensity

A sample of waveforms obtained from subject CD in response to flash stimuli of increasing intensity is shown in Figure 4.14. It is apparent that as flash intensity increases, the latency of the P100M decreases while its amplitude increases. In addition, increased intensity apparently leads to better definition not only of the P2M component but also of the preceeding (N1M) and suceeding (N2M) components. The latency and amplitude variation with intensity for each subject is shown in Table 4.9. The analysis of variance (Table 4.10) indicates a significant effect of intensity on latency ($F = 8.24$, $p<0.01$) and amplitude ($F = 8.75$, $p<0.01$). There is also a significant difference in latency ($F = 95.61$, $p<0.001$) but not amplitude ($F = 2.11$) between subjects attributable mainly to the results from one subject (MD). A second order polynomial curve was fitted to both the group mean latency ($R = 0.99$, $p<0.001$) and amplitude ($R = 0.87$, $p<0.05$) and confirms the trend of decreasing latency and increasing amplitude with increasing flash intensity (Figure 4.15).

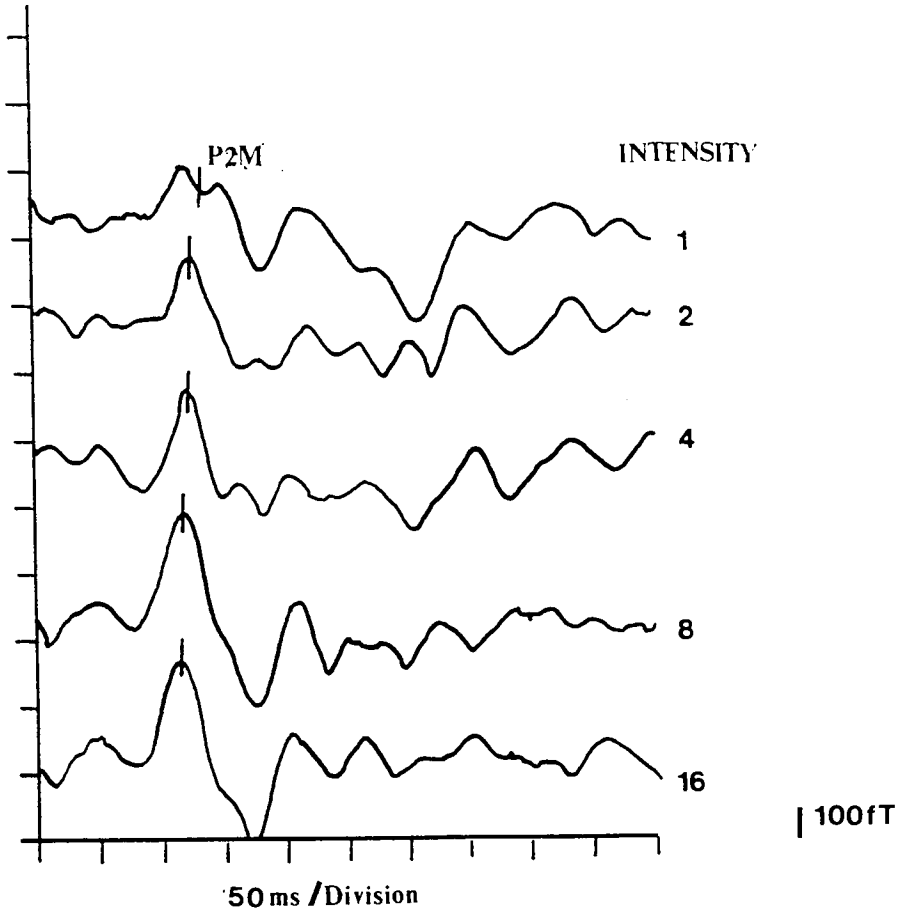

Figure 4.14 : Waveforms obtained from subject CD in response to flash stimuli of increasing intensity. P2M latency decreases and the amplitude increases with increasing stimulus intensity.

Table 4.9 : The effect of flash intensity on the a) latency and b) the amplitude of the flash P2M. The table shows the data obtained for each individual and the mean values.

a) Latency (ms)

	Intensity				
	1 (1088cd/m^2)	2 (1363cd/m^2)	4 (1925cd/m^2)	8 (3939cd/m^2)	16 (9961cd/m^2)
RAA	123.04	125.00	119.14	114.26	114.26
AS	127.40	122.56	125.48	126.97	118.65
CD	136.72	127.93	123.53	119.63	119.14
MD	165.53	166.51	165.04	151.86	156.25
Mean	138.17	135.50	133.30	128.18	127.07

b) Amplitude (fT)

	Intensity				
	1 (1088cd/m^2)	2 (1363cd/m^2)	4 (1925cd/m^2)	8 (3939cd/m^2)	16 (9961cd/m^2)
RAA	110.72	129.58	146.23	109.29	184.05
AS	82.68	123.26	123.71	124.78	156.73
CD	106.53	112.41	143.91	192.42	182.36
MD	70.13	74.31	147.65	69.49	167.50
Mean	92.56	109.83	140.53	123.98	172.66

Table 4.10 : An analysis of the variance of the flash P2M latency and amplitude in response to increasing flash intensity in four subjects.

a) Latency

Source of Variance	Sums of Squares	Degrees of Freedom	Mean Square
Treatment (Flash Intensity)	359.56	4	119.85
Blocks (Between Subjects)	5560.69	3	1390.17
Error	174.47	12	14.54

F Ratio (Treatments) = 8.24** ($p<0.01$)

F Ratio (Blocks) = 95.61*** ($p<0.001$)

Least Significant Difference = 6.43

b) Amplitude

	Sums of Squares	Degrees of Freedom	Mean Square
Treatment (Flash Intensity)	189.46	4	63.15
Blocks (Between Subjects)	61.06	3	15.26
Error	86.61	12	7.22

F Ratio (Treatments) = 8.75** ($p<0.01$)

F Ratio (Blocks) = 2.11 (n.s.)

Least Significant Difference = 18.78fT

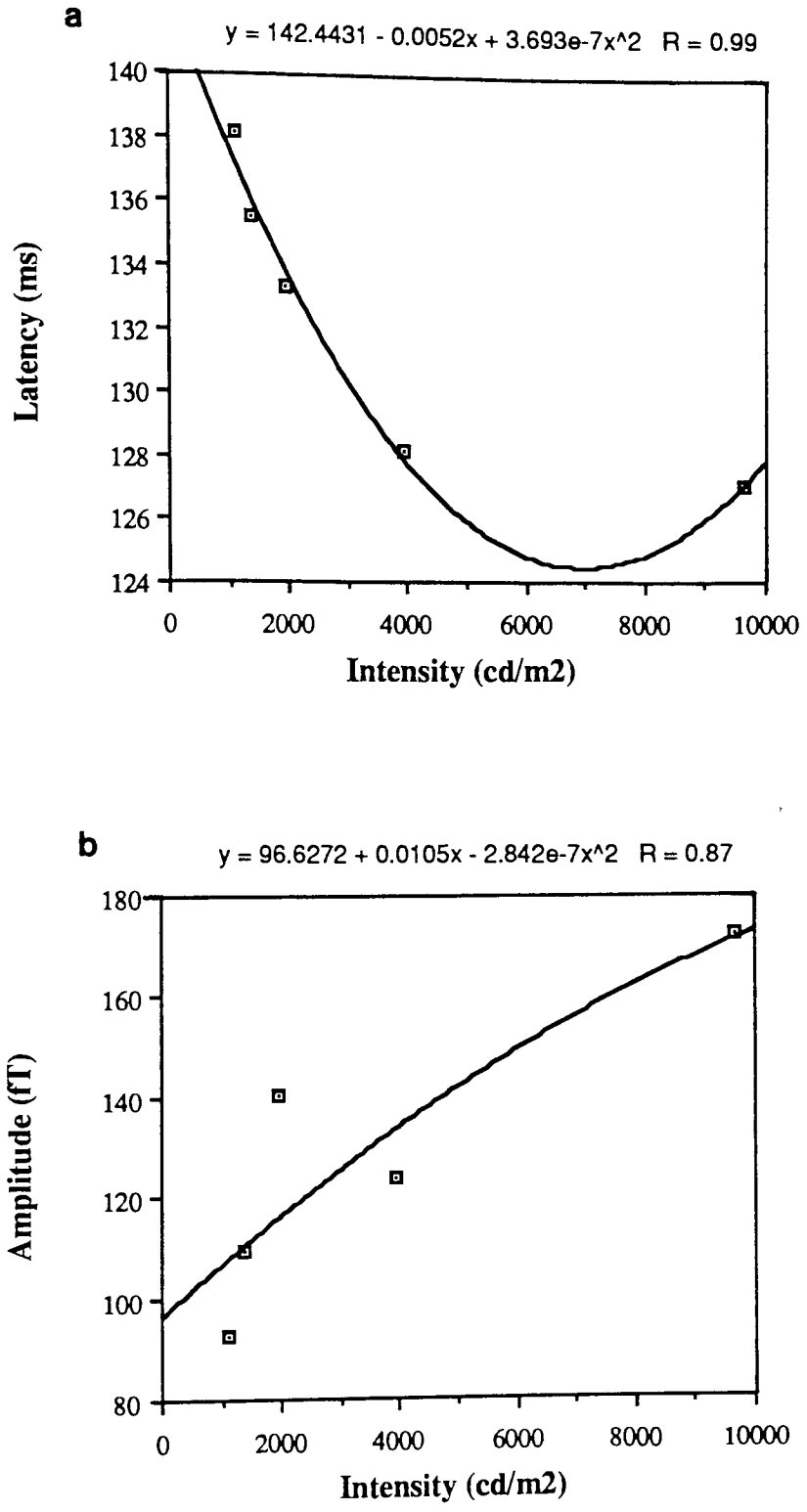

Figure 4.15 : Group mean data showing the relationship between a) latency and b) amplitude of the P2M and flash intensity.. Both the latency and the amplitude data were best fitted by a second order polynomial - a) latency $R = 0.99$, $p<0.001$ and b) amplitude $R = 0.87$, $p< 0.05$.

4.8 DISCUSSION

4.81 Optical Blur

No previous studies have been reported of the effects of blurring a patterned stimulus on the VEMR. However, the magnetic results appear to be in agreement with the VEP in that pattern defocus increases latency (Collins et al 1979, Sokol and Moskowitz 1981, Harding and Wright 1986, Bobak et al 1987) and decreases amplitude (Harter and White 1968, 1970, Sokol and Moskowitz 1981). These effects are greater for small than large checks (Harter and White 1968, Sokol and Moskowitz 1981, Harding and Wright 1986, Bobak et al 1987).

A number of hypotheses have been advanced to explain the effects of blur on the VEP P100 to a pattern reversal stimulus. The VEP may be particularly sensitive to the sharpness of contour and the number of edges present within a defined stimulus field (Harter and White 1970). Hence, blurring reduces the number of sharp edges and hence, reduces the effectiveness of the stimulus. In addition, it has been suggested that blurring reduces the contrast of the stimulus and that this is responsible for the increased latency and decreased amplitude (Sokol and Moskowitz 1981, Bobak et al 1987). This effect could also explain the difference between large and small checks. However, Bobak et al (1987) found that reducing the contrast of a patterned stimulus by as much as 50% produced an increase in response latency of approximately 3ms and this was too small to be the sole reason for the increase in latency. In addition, Sokol and Moskowitz (1981) found that blurring a checkerboard stimulus using a cylindrical lens oriented along one of the oblique axes reduced stimulus contrast but did not produce an increase in response latency.

The latency of the response may also depend on the integrity of various spatial frequency components of the checkerboard stimulus. Sokol and Moskowitz (1981) suggested that the increase in latency was attributable to defocussing the oblique fundamental frequencies while there was no change in latency if only the fundamental was attenuated. Bobak et al (1987) suggested that the latency increase produced by blurring larger checks (2.3cpd) was due to an interaction between the fundamental and higher spatial frequency harmonic components while the effect on small checks was mediated via attenuation of the fundamental frequency alone. These conclusions are based on the results of a comparison of the effects of blur on bar gratings and checks of equivalent fundamental spatial frequency. With unblurred stimuli, the latency of the P100 to both checks and bar-gratings was similar. However, when the low spatial frequency stimuli were blurred, the latency of the response to the check stimulus increased more than that to the corresponding bar grating. At the higher spatial

frequency (6.9cpd) however, the difference in response latency for the two stimulus types was insignificant.

Several other factors which have been proposed have been discounted by more recent studies. These include pupil size, accommodation and retinal image size effects (Harter and White 1968, 1970). The reduction in amplitude observed may reflect a decrease in the number of active neurons as a result of an increasingly less effective stimulus.

Our results suggest that if the P100M is recorded to a large check then blurring the stimulus has relatively little effect on latency and amplitude over a wide range of dioptres. Hence, patients can remove spectacles which produce an excessive magnetic artifact. However with smaller checks, the effects of blur on latency are considerable and it is essential, as for the VEP, that vision is corrected prior to recording with non-magnetic spectacles.

4.82 Check and Field Size

The objective of this study was to determine how the latency and amplitude of the P100M recorded from a single position on the head varied with check size. The recording location was chosen from topographic mapping of the response of each individual subject to a $1^{o}40'$ check presented in a $13^{o}34'$ diameter field (See Chapter 5). The point at which the outgoing field was maximal was used for both the check and field studies. The study should provide information on a) whether a single recording point could be used in a clinical investigation requiring the use of more than one check size and b) whether the magnetic data behaved similarly to the VEP. However, few studies of the VEMR have been published and direct comparisons with other data are difficult. In addition, few studies of the VEP appear to have been carried out with similar aims or design. In addition, literature for the VEP suggests that the effects of check and field size on latency and amplitude are interdependent making studies which use different experimental parameters difficult to compare (Harter 1970, Bartl et al 1978, Meredith and Celesia 1982, Yiannikas and Walsh 1983).

The results of this study suggest that the P100M latency increased and the amplitude decreased with decreasing check size. Comparison with the previous magnetic studies is complex because such studies a) used sinusoidal bar gratings rather than checks and b) used steady state rather than transient evoked responses. While the spatial frequency of a bar grating can be expressed in terms of cycles per degree (cpd), a checkerboard stimulus is more complex comprising a mixture of spatial frequencies (Spehlmann 1985). However, the major Fourier component of a checkerboard

stimulus is oriented at 45° (diagonally) to the squares and this frequency component can be calculated using 1.4 times the side length of the checks as the wavelength. A further problem arises in the study of the steady state rather than the transient evoked response in that the response latency cannot be directly measured. However, an estimate of this latency can be calculated from the waveform ie. latency can be calculated using the slope of the function relating the response phase lag to the spatial frequency of the stimulus (Okada et al 1983).

Despite these problems, the mean latencies obtained in this study using a checkerboard stimulus are similar to those obtained using bar gratings of a similar spatial frequency (Williamson et al 1978, Okada et al 1983). However, the finding that P100M amplitude decreased with decreasing check size is not in agreement with that of Okada et al (1983) who found that the response amplitude versus check size data could be fitted by an inverted parabolic function, with maximal amplitude occuring at intermediate spatial frequencies (1-3cpd). This disagreement may be due to a combination of the following reasons:- a) the use of different field sizes, b) the different method of measuring response amplitude ie. peak to peak rather than peak to baseline, c) the study of steady state rather than the transient response and d) the use of bar gratings rather than checks whose spatial frequency content is more complex.

There is also disagreement in the electrical literature regarding the effect of check size on latency although much of this may be attributable to the choice of field size used (Kurita-Tashima et al 1991). The majority of studies find an exponential decrease in latency with increasing check size (Ristanovic and Hadjukovic 1981, Plant et al 1983, Novak et al 1988) although a more extensive study by Kurita-Tashima et al (1991) found that the response was best described by a U-shaped, parabolic curve, with the shortest latency occuring at a check size of 35'. This study however, used a comparatively small field of only 8° diameter. It would appear, therefore, that the VEMR results are in general agreement with the VEP. However, it is apparent that the latency change of the VEMR is steeper than that seen electrically. An attempt to quantify this was made by comparing directly the magnetic P100M latency versus check size data with VEP data. The most comparable study was that of Kurita-Tashima et al (1991) who used a similar range of check sizes produced by a back projection system. The steepest part of the latency curve for both the electrical and magnetic data was measured and found to occur between 6' and 32'. It was found that the change in latency for the magnetic data was 2ms per minute of stimulus arc compared with 1ms per minute of stimulus arc for the electrical data.

There is also some controversy over the effect of check size on amplitude. However, the majority of studies suggest that amplitude varies as an inverted U-shaped function with check size, maximal amplitude occuring at a particular check size (Bartl et al 1978, Ristanovic and Hadjukovic 1981, Sokol et al 1983, Novak et al 1988). Kurita-Tashima et al (1991) however, found no effect of check size on amplitude but this may again have been a consequence of the small field size chosen. The magnetic data obtained in this study do not appear to be in agreement with the electrical data, showing instead, with the exception of the 6' check, a sigmoidal increase in amplitude with increasing check size.

There are, apparently, no previous single point magnetic studies of the effects of field size on the latency and amplitude of the P100M although Maclin et al (1983) recorded the field pattern produced by eccentrically placed annuli in order to study the retinotopic organisation of the visual cortex. In addition, his study of the sustained rather than the transient response means that there is no latency information available for direct comparison.

Our study suggests that for a large check (1°40') the latency decreased with increasing field size while the amplitude increased. Comparison with the electrical data are again problematic as most studies had the objective of studying the retinotopic organisation of the visual cortex and so used a combination of check and field sizes presented at increasing eccentricities. However, Yiannikas and Walsh (1983) studied the effect on latency and amplitude of field sizes between 2° and 32° diameter. They found that the latency of the electrical P100 to a 55' check was significantly longer when presented in a 2° ($p<0.001$) and a 4° ($p<0.01$) field than when presented in a 32° stimulus field.

An attempt was made to record the VEMR to checks of varying size presented in a small field (5°14' diameter). However, unlike the large field data, the response at a single recording position was poor and no consistent waveforms were obtained.

The increase in P100M amplitude with increasing check size could be due to retinal physiology and the representation of the retina on the visual cortex. Smaller checks may stimulate the foveal retina more optimally than larger checks; the large checks may be a better stimulus for the parafoveal or more peripheral retina (Hammond and Yiannikas 1986). This may be due to the relative sizes of the receptive fields at various retinal eccentricities. Although the fovea is believed to have the largest cortical representation (Rovamo and Virsu 1979), the orientation of the active neurons in this area of cortex, ie. the degree to which they may be radial to the magnetometer, may be such that the contribution it makes to the magnetic signal recorded at the scalp is small. Alternatively, although the peripheral retina has a much smaller cortical representation,

the sources activated by its stimulation may be more favourably oriented ie. tangentially with respect to the detector, and hence produce a larger amplitude signal. The anomalous result seen for the 6' check may be a consequence of a significant change in field topography.

The difference in latency observed for small versus large checks may arise from one, or a combination of three source:- a) the retina, b) transmission along the optic nerve or c) processing at the cortical level. Celesia et al (1987) and Lowitsch et al (1989) report no differences in the latency of the ERG 'b' wave for a large compared to a small check despite differences in P100 latency to the same stimuli. This would suggest that the latency difference is not of retinal origin. However, the fibres of the optic nerve do not have a uniform conduction velocity; the smaller diameter central fibres conduct more slowly than the larger diameter peripheral fibres (Carpenter 1990, Hinton et al 1986). It is possible that the longer latency resulting from stimulation with small checks reflects the proportion of the more slowly conducting fibres activated. In addition, the large checks activate more shorter latency fibres and produce a P100M of correspondingly shorter latency. However, it is unlikely that this difference in conduction velocity alone is sufficient to explain this effect on latency and hence, there may be some contribution from processing at the cortical level.

Similar arguments may apply to the effects of field size on the latency and amplitude of the P100M. The increase in amplitude observed with increasing field size is likely to be due first to the greater area of retina stimulated and secondly to the large check being a more effective stimulus for the peripheral retina. The latter may be represented further down the calcarine fissure, a region which may contribute more to the response recorded at the scalp by virtue of its' more tangential orientation to the detector. Hence, the difference in latency may be the result of the preferential activation of central versus peripheral retina - the longer latencies seen with small fields being due to the optimal activation of the fovea and hence more slowly conducting fibres while the larger fields stimulate correspondingly more of the faster peripheral fibres.

Comparison of the VEMR and the VEP data by other authors under similar conditions suggests that the latency change was greater for the magnetic than the electrical data. This difference between the electrical and magnetic response has been reported previously by Teyler et al (1978) who found that the amplitude of the magnetic P2M increased more rapidly than that of the electrical P2 to flash stimuli of increasing intensity. This effect could be due to differences in the neuronal populations contributing to the electrical and magnetic responses. Alternatively, it is possible that the topography of the VEMR changes as different neuronal populations are activated

by different check sizes. The effect of a shift in the sources activated on the response topography would be greater for the magnetic than the electrical response because of the more focal distribution of the former. Hence, a change in amplitude may reflect either activation of a smaller population of neurons at approximately the same location or activation of a different source with a maximum at a different location. In addition, a change in latency may be an indication that a change in topography has occurred and a different source has been activated. Hence, detailed study of the topography of the VEMR using different check and field sizes will be essential to explain the magnetic response more fully (see Chapter 5).

The failure to obtain useful data when using a small field (5°14') and various check sizes probably results from a combination of factors. First, the topography of the response to this predominantly foveal stimulation may change too much for a single recording position to be used to record for all check sizes. In agreement with this suggestion, Aine et al (1990) found using a 2° x 4° stimulus field a statistically significant difference in the topography of the response to a 2cpd stimulus compared with a 6cpd stimulus. Secondly, the fovea despite its large cortical representation, may activate a part of the cortex which may not contribute much to the magnetic signal detectable on the scalp. In addition, the extent of foveal representation on the occipital pole can vary widely between subjects (Polyak 1957) and this could make the topography more variable between subjects than for a larger field.

Hence, it is possible to record an outgoing magnetic field component between 100 and 150ms to a variety of check sizes presented in a large stimulus field and a number of field sizes using a large check stimulus. This could be of use clinically, particularly in circumstances where disease may influence the peripheral retina e.g. some forms of optic neuritis and possibly vascular disease. However, before these measurements can be used clinically, it would be necessary to study the topography of the response to a wide range of check and field sizes and to determine in detail the magnetic components which are present.

4.83 Temporal Variability

The aim of this study was to determine the degree of reproducibility of the magnetic P100M over short and longer periods of time. The only previous work on the temporal variability of the VEMR has been limited to the study of the trial to trial amplitude variability of single unaveraged sweeps (Lewis et al 1989).

However, the temporal variation of the VEMR can be compared with that of the corresponding VEP. Since the VEP and VEMR components may reflect activity in

different, though overlapping, neuronal populations, electrical summation may mask features observed in the magnetic response. The response of the VEMR to stimuli of increasing check/field size and flash intensity where changes in latency were greater than has been observed for the VEP may be consistent with this suggestion.

In addition, there are no directly comparable studies of the VEP. Electrical studies concentrated on a specific individual source of variation e.g. minute to minute (Van Lith et al 1978, Shors et al 1986), diurnal (Stolz et al 1988, Lu and Spafford 1989, Padhiar and Harding 1991) and long term test-retest variability (Diener and Scheibler 1980, De Weerde and Jonkman 1982, Hammond et al 1987, Oken et al 1987).

The data suggest that the largest component of variance in latency and amplitude of the VEMR P100M is associated with variation from minute to minute within a recording session. In addition, in one of the subjects (CD) a significant difference between days was also apparent. By contrast, minute to minute variation in the VEP P100 latency has been reported to be insignificant and less than that recorded between between occasions weeks or months apart. Some authors have emphasised this point by superimposing consecutively obtained waveforms (Maurer et al 1989). The amplitudes of the magnetic response were more variable generally than latencies which is in agreement with the VEP (Meienberg et al 1979). Shors et al (1986) studied run to run variability of the P100 amplitude in a number of subjects. If this variation is expressed as a percentage of the mean amplitude (Coefficient of Variation), then subjects show run to run variabilities ranging from 10 to 29%. This figure is considerably lower than that obtained for VEMR amplitudes which varied on average by around 30% but on occasion by as much as 44-51%. Hence, in general, both latency and amplitude of the magnetic component appear to be more variable than the electrical component.

Recordings of the VEMR variability were made in the morning and afternoon of each day to determine whether the level of environmental noise influenced run to run variabililty; a greater level of background noise being recorded in the afternoons. In addition, a comparison between responses in the morning and afternoon would indicate the presence of variation throughout the day. However, the results suggest that there is no significant variation associated with morning and afternoons. Hence, the magnetic data are in agreement with the VEP in that studies of the diurnal or circadian variation of electrical P100 latency have suggested there is no effect of time of day on latency during normal working hours (Stolz et al 1988, Lu and Spafford 1989, Padhiar and Harding 1991). The magnetic data is in agreement with this finding, as far as it is applicable. However, more detailed study of variation of the

VEMR over 24 hours would be necessary to determine if diurnal or circadian variation were present.

The long term test-retest variability of the VEP has been studied more frequently because of the possible clinical implications for longitudinal studies. The test-retest interval varies between studies from around 2-4 weeks to periods of up to 3 years. The mean latency change between recordings for most studies is around 2.5 $\pm$ 2.4ms but maximum latency changes of between 6ms (Becker and Richards 1984, Hammond et al 1987) and 10-12ms (Meienberg et al 1979, Diener and Scheibler 1980, Oken et al 1987) have been recorded. However, if the mean values for sets of 10 consecutive recordings are compared for different days it can be seen that the average latency change is 1.6ms for RAA and 10.36ms for subject CD. The maximum latency change observed on any day was 11ms for RAA and 27ms for CD. The wide difference between the two subjects means that there may be considerable variations in response reproducibility between subjects and thus this needs to be investigated further. An estimate of the number of repeat measurements necessary on a single occasion to obtain a stable estimate of component latency suggested that 5 to 7 repeats would be necessary for subject CD and 4 to 6 repeats for RAA where variability was lower. However, the test-retest interval used in the present study was much shorter than that used in VEP studies. Longer term studies of temporal variation are essential prior to clinical use of the VEMR.

The variability of the magnetic P100M may originate from a combination of three possible sources : the subject, the environment and the recording system.

It is possible that the level of subject arousal varies from minute to minute as well as between recording sessions or different days. In the present study although the subject was observed for signs of inattention during recording, it may not be possible to detect small changes in arousal. The level of arousal may affect the background brain activity and this could affect VEP latency and amplitude (Ciganek 1969, Jansen and Brandt 1991). Lu and Spafford (1989) also reported studies which illustrate that attention span and concentration can affect the VEP although they failed to see evidence of this in their own subjects. The same may be true for the VEMR. The trends with time seen in some sets of 10 repeats could be indicative of these short term fluctuations in arousal level and hence background brain activity.

The influence of background brain activity on the evoked response may be reduced by increasing the number of sweeps averaged. The background activity is assumed to be unrelated to the stimulus and this being random will, when averaged, tend to zero. However, when recording the VEMR a compromise is necessary since an increase in

the duration of the run by increasing the number of sweeps averaged may itself increase background brain activity, in particular the amount of alpha rhythm and so could increase rather than decrease variability. The number of responses to be averaged also depends on the signal to noise ratio. Hence the number of sweeps in an average is a complex function of 1) the magnitude of the stimulus evoked brain activity, 2) the level of the environmental noise and 3) the level of attention of the subject. More detailed study of each of these factors is necessary for the VEMR.

The morphology of the waveform may also influence variablility. If the component is broad, distorted by high frequency noise or bifid as a result of refractive error or pathological changes then the identification of the peak latency may become more subjective. The P100M of subject CD was usually well defined but the peak was broad. As a result it was more difficult to mark the position of the peak for subject CD than for RAA where the P100M was much sharper in morphology. This could have contributed to the wider range of variability seen for subject CD than for RAA although Oken et al (1987) remarked on this aspect of variability but came to the conclusion that it made an insignificant contribution to variability of the VEP. Magnetometer location may also contribute to the level of variability. Magnetic recordings do not have the problems of variability associated with the choice of reference (Van Lith et al 1978). However, the positioning of the field detector is more critical than the placement of the active electrode since the field extrema are more focal than their electrical counterparts (Cohen and Cuffin 1983). As a result, moving the detector a short distance away from the extrema may decrease the signal to noise ratio and hence, increase variability. The recording locations used in this study were chosen as a result of mapping the P100M over the scalp for each subject (see Chapter 5). However, the position of the extremum determined by this method would not be entirely accurate since the points of the mapping grid were approximately 3cm apart. Hence, the recording location chosen for one subject may have been closer to the true field maximum than for the other. This factor may also contribute to the greater variability in response seen for CD compared with RAA. Additionally, slight variations in positioning of the detector to the scalp on each occasion cannot be ruled out. Subjects remained in position during each series of ten recordings, but some slight movement of the subject relative to the detector could have occurred.

Two final sources of subject variability are 1) adaptation to the stimulus and 2) variability in the response of the neural populations themselves. In addition to the subject, the environmental noise level may also contribute to the response variability. Recordings were made in 3 different environments of the frequency distribution of noise between 0 and 100Hz (Figure 4.16). These locations were a) the original

unshielded location, b) a single Eddy current shielded room and c) a two layer shielded room. In the original unshielded laboratory the background noise level was approximately -79.5dBV/ Hz and prominent peaks can be seen at 50, 60 and 70Hz frequencies. In the centre of the Eddy current shielded room the background noise level is higher at approximately -74.5dBV/ Hz but the 50Hz peak is much reduced while the 60 and 70Hz peaks are absent. However, more low frequency noise was recorded in the 0 to 5Hz range and it is possible that this noise contributed to the wider variability seen in this environment. Noise spectra were also recorded adjacent to the shielded room (Figure 4.16c) and indicated that this location was magnetically noisier than the original unshielded room (Figure 4.16a). Although the 50Hz peak appears to be of a larger amplitude in the unshielded location than adjacent to the shielded room, there appears to be less noise in the 0-5Hz range. This location was noisier than both the original unshielded and Eddy current shielded rooms (-70.2dBV/ Hz). This may be due to 1) the centre of the shielded room being closer to the generator of the noise or 2) the room itself generating 0-5Hz noise, possibly as a result of vibration.

At the time of writing, a frequency spectrum is not available for the two layer shielded room. However, the shielding factor of the two layer room was measured by applying a signal of known strength and frequency to a large set of coils around the room (Figure 4.1). The strength of the resulting field is measured inside the shielding. The ratio between the field that should be detected given the size of the signal in the coils and that actually detected, gives an indication of how the shielding has attenuated the field at that particular frequency. The attenuation provided by the Eddy current shielded room has been calculated and is shown for comparison. The Eddy current shielding is most effective at attenuating the high frequencies , while the magnetic shielding cuts out more of the lower frequencies and further attenuates the high frequencies.

Considering the results of the reproducibility of the P100M in the different environments - latency variation was maximal in the single shielded room. However, in the two layer room variation was reduced to a degree below that of the original unshielded environment. Hence, the noise environment does appear to affect the reproducibility of the response but increasing the shielding may only improve reproducibility of the P100M to a particular level. Other factors were probably responsible for the maintained or only slightly improved level of variability observed. In addition, comparison of the responses of two single channel magnetometers revealed 1) a difference of 10ms in the mean P100M latency and 2) that the latency variability was much greater in one system than the other. Thus, the magnetometer itself and/or its electronics may contribute to P100M variability.

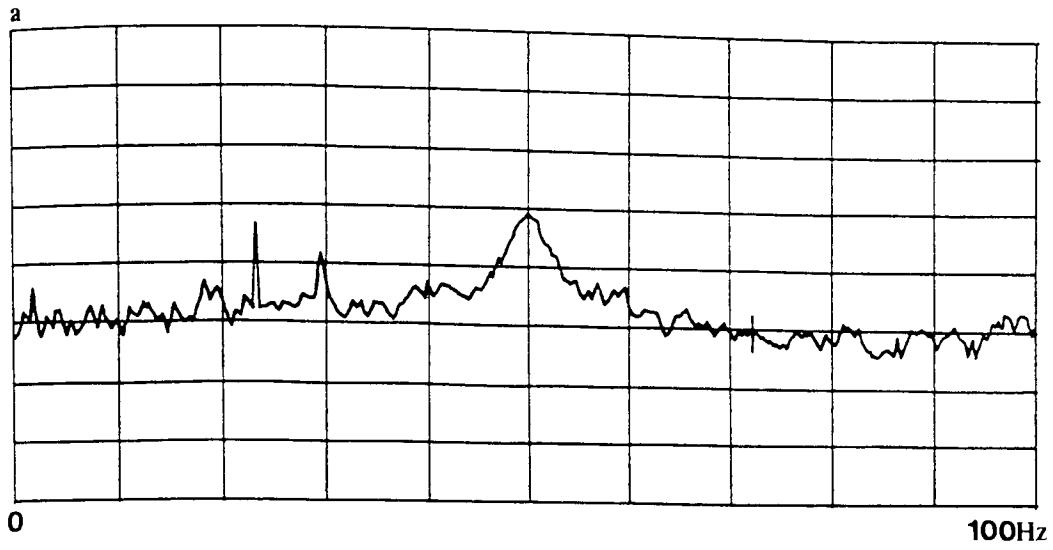

Background Noise
-79.5dB

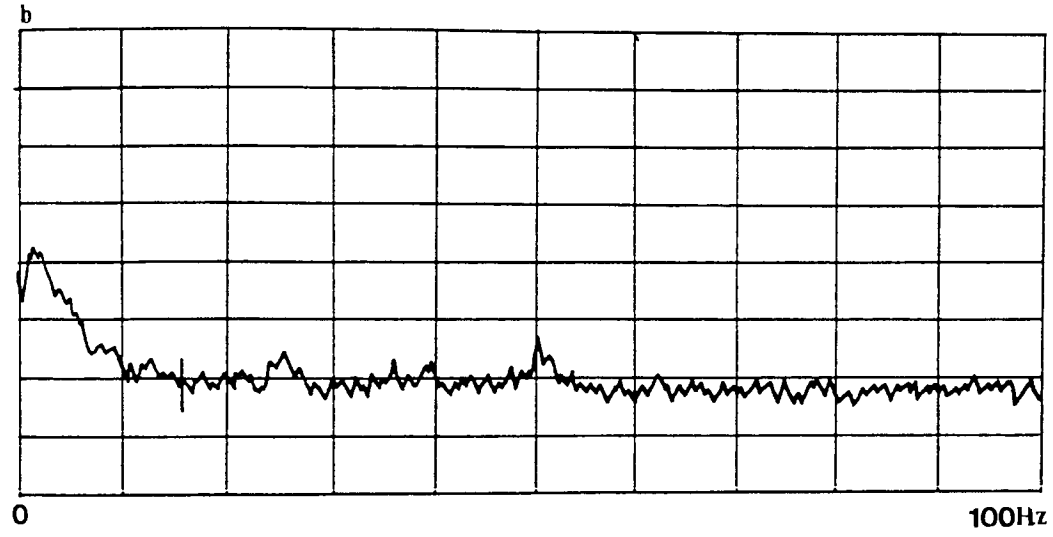

Background Noise
-74.5dB

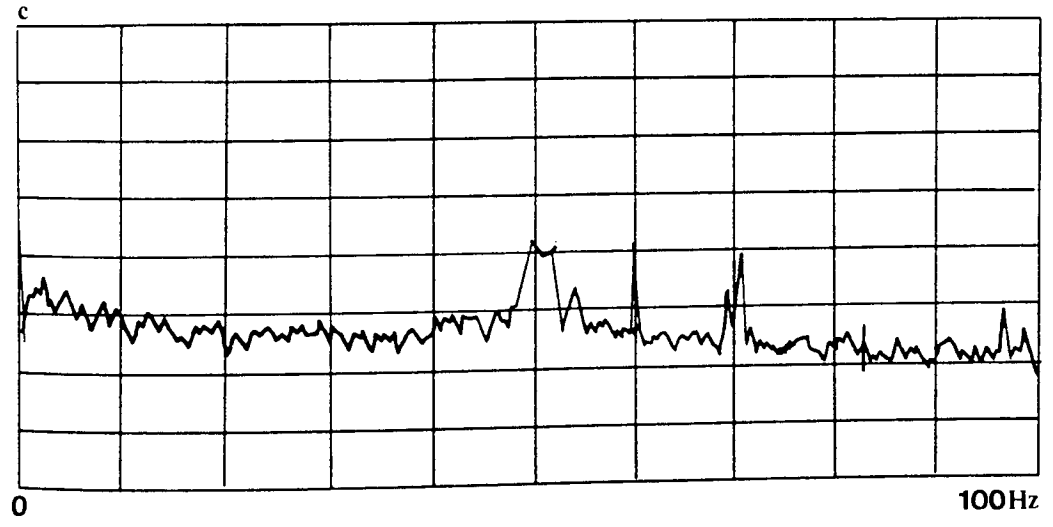

Background Noise
-70.2dB

Figure 4.16 : Frequency distributions of the noise obtained in a) the unshielded environment, b) the 1 layer Eddy current shielded room and c) adjacent to the 2 layer magnetically shielded room.

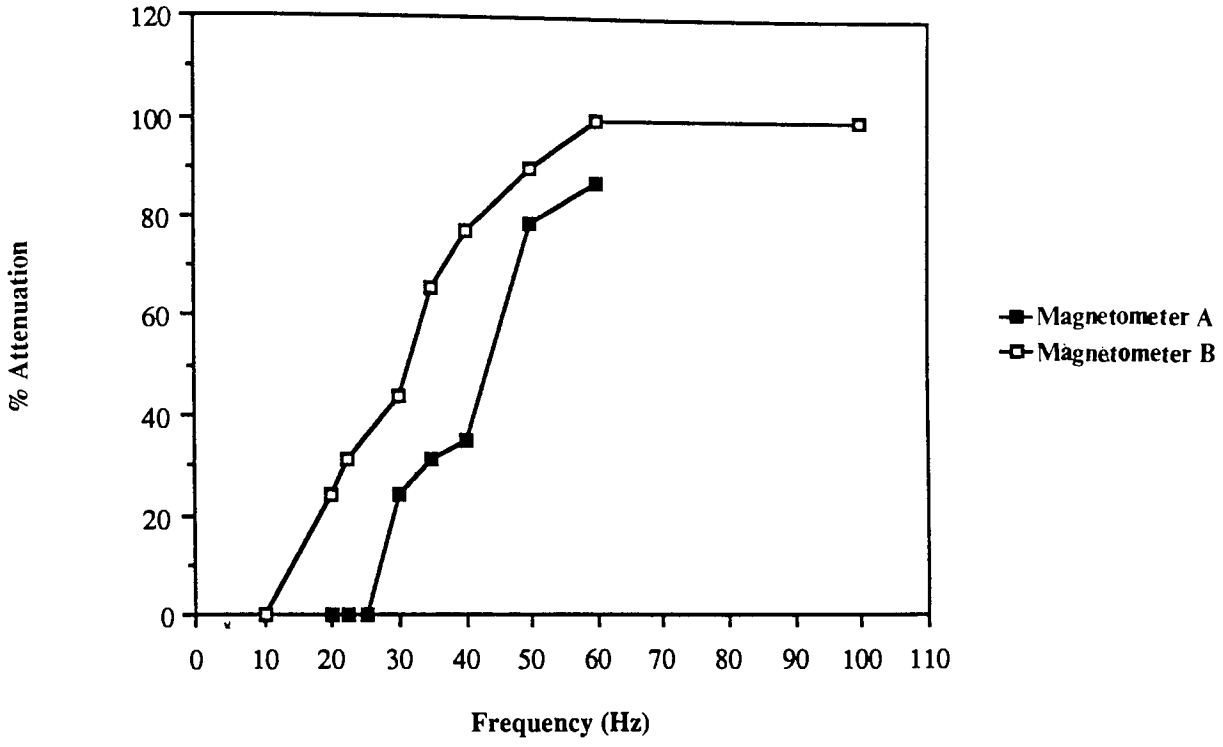

Figure 4.17 : A Bode plot of the filter responses for Magnetometers A and B. The curve for Magnetometer A is shifted to the right of that for Magnetometer B.

One source of this system based variability may be the filters used. Although the two systems were equiped with supposedly identical electronics, there was evidence of differences in filter performance which could be due to the tolerances of the components used in constructing the filters. Filters can be characterised in terms of their attenuation of signals of various frequencies. Typically this information is plotted as the percentage attenuation versus the frequency (Bode plot). Figure 5.17 shows a Bode plot of the filter responses (bandpass 0.3 to 30Hz) for both magnetometers. The plot shows that although the filters have approximately the same roll-off characteristics (slope), the curve for Magnetometer A is shifted to the right of that for Magnetometer B giving the two machines different frequency cut off characteristics. Such a difference could contribute to the different responses recorded from the two magnetometers.

Another factor which may influence variability is the bandwidth. The optimal bandwidth for recording the VEMR, as for the VEP, has not been standardised in different laboratories. It should reflect the frequencies of the signal to be recorded. For the VEP most of the signals' energy is believed to lie in the 8 to 50Hz range. However, the bandwidth used in the original unshielded location was 0.3 to 30Hz. The low pass filter was set at 30Hz to remove as much as possible of the high frequency noise in the unshielded environment. It was not possible to record any recognisable waveforms with a low pass filter set at greater than 50Hz. Systematic study of the effects of filter settings and bandwidth show that the settings of the high and low pass filters can increase or decrease the electrical P100 latency and, if the bandwidth is too narrow, an increase in variability occurs (Yiannikas and Walsh 1983, Maurer et al 1989, Skuse and Burke 1990). Although our filters had a steeper roll off (24dB/octave versus 6dB/octave) which should mean less variability according to Skuse and Burke (1990), the narrow bandwidth is likely to be a factor contributing to the overall variability.

Gradiometer balance in both magnetometers may differ and could contribute to the P100M variability. Less than optimal balancing of the gradiometer coils will lead to reduced signal sensitivity and decreased noise rejection. The two machines were originally balanced to the same degree by BTI prior to transportation to the laboratory. However, the rigours of transport and successive "cool downs" may influence gradiometer balance.

Conclusions

In conclusion : 1) Minute to minute variation is the most significant source of variation for the VEMR P100M, 2) some evidence was also found for significant day to day

variation in one subject and 3) the degree of minute to minute variation is machine dependent and could depend primarily on the filters, 4) the bandwidth of the filters may influence variability and 5) the degree of minute to minute variation can be reduced, and hence reproducibility improved by magnetic shielding. These findings have a number of implications for the establishment of protocols, particularly for clinical recording, and these will be discussed in the final chapter.

4.84 Flash Intensity

The results indicate that with increasing flash intensity, the latency of the P2M decreased while the amplitude increased. This result is not in agreement with the study of Teyler et al (1975) who found that while the amplitude increased with increasing flash intensity, there was no significant change in latency. The failure of the component identified by Teyler et al (1975) to show a systematic change in latency with increasing flash intensity was attributed to noise which could shift a peak from it's normal location. Most of the noise was considered to come from the recording system itself since the experiment was made in a shielded room. However, inspection of the waveforms reported in Teyler et al (1975) suggest that the component identified, although a prominant positivity, was not analogous to the electrical P2. In addition, the smaller peak immediately preceeding the component marked showed both an increase in amplitude and a decrease in latency with increasing flash intensity.

Most of the previous work on the flash VEP was carried out in the 1960s. In general the results reported in this thesis agree with the electrical studies of the P2 (Cobb and Dawson 1960, Tepas and Armington 1962, Shipley et al 1966, Vaughan et al 1966, Lenders et al 1980, Hobley 1988). The increase in amplitude of the P2M with increasing flash intensity could be owing to an increase in the number of active neurons in the visual cortex. Vaughan et al (1966) found that at low flash intensities the fovea (central 1.5^{o}) produced little response. This led to the conclusion that the P2 was probably a response originating from the rod cells of the retina. Thus, at low flash intensities the response may be solely to rod cell activation while at higher intensities the cone cells may also be active and hence, the result would be an increase in amplitude. However, amplitude changes recorded at a single recording position may also be owing to a change in the position or orientation of the source (see Chapter 5).

The effect of intensity on the latency of the P2M is more difficult to explain. If the increased amplitude at higher intensities was due to activation of central cones, an increase in latency would be expected. An alternative explanation is that higher intensity flashes stimulate a portion of the peripheral retina. Hence, this reponse

was probably a response originating from the rod cells of the retina. Thus, at low flash intensities the response may be solely to rod cell activation while at higher intensities the cone cells may also be active and hence, the result would be an increase in amplitude. However, amplitude changes recorded at a single recording position may also be owing to a change in the position or orientation of the source (see Chapter 5).

The effect of intensity on the latency of the P2M is more difficult to explain. If the increased amplitude at higher intensities was due to activation of central cones, an increase in latency would be expected. An alternative explanation is that higher intensity flashes stimulate a portion of the peripheral retina. Hence, this reponse would tend to be mediated by a higher proportion of faster conducting axons as the intensity increased. A number of experimental subjects commented that lower intensity flashes appeared to be more focal. At higher intensities the flash appeared to spread more peripherally. Vaughan et al (1966) reported that an increase in stimulus area produced shorter latency reponses to the same stimulus intensity. This would appear to support the idea that stimulation of more peripheral retina may be responsible for the decrease in latency.

Hence, if it is proposed to use the P2M clinically in addition to the P100M, it would be reasonable to use a higher intensity flash since the larger amplitude signals would be recorded more consistently. However, a weakness of studying variations in stimulus parameters at a single recording position is that effects due to changes in the same source and those due to a change in source are confounded. Hence, it is necessary to study the topographical distribution over the scalp of the VEMR and this aspect will be investigated in Chapter 5.

CHAPTER 5

TOPOGRAPHICAL STUDIES OF THE VISUAL EVOKED MAGNETIC RESPONSE

5.1 INTRODUCTION

To record the VEMR clinically using a single channel magnetometer or a magnetometer with few channels, requires knowledge of the topography of the magnetic components over the scalp. Since magnetic signals are more focally distributed over the scalp than their electrical counterparts (Cohen and Cuffin 1983), and there may be more variability in the location of extrema between subjects, the maximum activity of a component may be difficult to find. In addition, the constraints of time and patient co-operation mean that it is not practical to map the response of each patient to each stimulus that may be used in a clinical investigation. Hence, a study of the VEMR topography in normal subjects is needed to establish the location of extrema for single channel recording. Such a study should be able to identify regions of scalp where, in most subjects, it would be possible to record the desired response.

Relatively few studies have been made of the topographic distribution of the VEMR over the scalp. Most studies of VEMR topography have concentrated on sinusoidal gratings (Brenner et al 1975, Maclin et al 1983), pattern onset-offset (Kouijzer et al 1985, Stok 1986, Degg et al 1991) and flashed pattern (Richer et al 1983) stimulation. Fewer studies have been made using strobe flash (Teyler et al 1975) and pattern reversal stimuli (Janday et al 1987, Okada 1991) and in addition, most of these studies have involved relatively small numbers of subjects.

This study examines the topography of the VEMR to a full field, large check (70') pattern reversal stimulus (12 subjects), full, left and right half field responses to large check pattern reversal (6 subjects) and to a flash stimulus (9 subjects). In addition, the effects of central scotomata on the pattern reversal response were studied to obtain information on the contributions of central and more peripheral retina to the P100M. The effect of flash intensity on the topography of the P2M was also studied. Topographic maps were also recorded with a more detailed sampling grid over the scalp, so that a simple source localisation procedure could be carried out and the origin of the P100M and P2M determined.

Although in this study variations in topography were of primary interest, much of the recent work in biomagnetism has concentrated on the possibility that it may provide a

more accurate method of source localisation. The accuracy of source localisation depends on a large number of variables, the models of the head and the source models employed (Okada 1983, Barth et al 1986, Cuffin 1990), the choice of recording surface (Meijs et al 1987) and the size and configuration of the sensing device used (Williamson and Kaufman 1981, Hari et al 1988). Thus accordingly, the following section provides a brief discussion of current head and source models and their adequacy, the main methods of source localisation and the problems of each of the possible mapping strategies that can be employed. Discussion is necessarily limited to those models most relevant to the study of the visual system.

5.11 Head Models

Three major models of the head have been proposed (Baule and McFee 1965, Cuffin 1990). These are a) the single homogenous sphere model, b) the concentric homogenous spheres model and c) the realistically shaped, compartmentalised head model. They differ mainly in terms of their complexity and the contribution of the primary and secondary sources to the field detectable at their surface.

The magnetic field detectable outside the head can be considered to result from the activity of both primary and secondary sources (Nunez 1986). The primary source is the intracellular current flow from dendrite to soma in activated neurons, while the secondary sources or volume currents, arise at the boundaries between tissues of differing conductivity (see Chapter 1). The secondary sources are a consequence of the primary source activation and the current spread through the conducting media of the head. The primary source is modelled frequently as a current dipole, producing a magnetic field with both radial and tangential components (Tripp 1983).

The simplest model of the head is that of the homogenous conducting sphere. Most of the early studies of source localisation were made using this model (Baule and McFee 1965). A dipolar source oriented radially to the surface of a sphere produces no detectable magnetic field outside the sphere (Tripp 1981, Okada 1983). This is because a) the radial field components are zero as a result of the conductors' spherical symmetry and b) the tangential component is zero because the primary and secondary sources produce tangential field components of equal magnitude and opposite sign, and tend to cancel (Baule and McFee 1965, Nunez 1986).

Hence, a tangentially orientated dipolar source located in a sphere should, in theory, produce a radial field outside the sphere that is due to the activity of the primary source alone. However, the tangential component of the field contains contributions from both primary and secondary sources. It has been concluded from these results that the

radial field component recordable outside the head by a detector located normal to its surface, arises mainly from tangential rather than radial sources and, that the radial component is the least complex component of the magnetic field to record and interpret.

However, the single sphere model of the head has a number of limitations. Firstly, the head is not a perfect sphere (Barth et al 1986, Weinberg et al 1986, Kobayashi et al 1991). Deviations from sphericity mean that some mapping locations on the scalp are further from the centre of the model sphere used for source localisation than others and hence, influence the accuracy of localisation. Weinberg et al (1986) found that these errors could be reduced by fitting separate spheres (with the same origin but varying radii) to each mapping point, a procedure requiring little extra computational power. A second limitation of the single homogenous sphere model is that no account is taken of the differing conductivities of the brain, skull or scalp. Although these tissues are considered essentially transparent to magnetic fields up to 1KHz (Kaufman and Williamson 1982), the boundaries between differently conducting media affect the secondary sources or volume currents (Romani 1989). This is particularly true for the skull which has a conductivity some eighty times lower than that of the other tissues. This would not be important if it was possible, when mapping the head, to adhere to a strictly spherical mapping surface. However, in regions of the head where the detector cannot be located normal to the scalp easily, then the primary source may be less tangential and the influence of the secondary sources greater (Barth et al 1986, Meijs et al 1987). The importance of these secondary sources increases with increasing primary source depth (Nunez 1986, Meijs et al 1987, Hari et al 1988). As the primary source gets deeper its contribution to the external field is decreased, while the contribution from the secondary sources, which are generated much closer to the detector, remain undiminished. Again any deviations from the spherical mapping surface will exaggerate this effect.

In the concentric spheres model the brain, cerebrospinal fluid, skull and scalp are represented as having different conductivities and is therefore, in one sense, more realistic than the single homogenous sphere model. However, this model still does not take into account non-concentric variation in conductivity or the effects of head asphericity. Cuffin (1990), using a concentric spheres model of the head, found that although asphericity can produce significant changes in the maps produced for some sources located in some regions, this did not produce locational errors of greater than 1cm. However, this work was carried out using a spherical mapping surface. Meijs et al (1988) looked at the effect of head model on the accuracy of source localisation. Source localisations were compared using both a concentric spheres model and a

realistic compartment model of the head. The latter comprises four compartments representing the brain, cerebrospinal fluid, skull and scalp. Each compartment was assumed to be homogenous and was given its own conductivity. The model was constructed using MRI data obtained from a real head. In comparing these models, the authors investigated the effects of non-concentric variations in conductivity and head asphericity on localisation accuracy. The mapping was carried out on a spherical surface of a slightly larger radius than the scalp shell of the concentric spheres model. This means that for the concentric spheres model of the head there is no secondary source contribution to the field component measured normal to the surface. In addition, secondary source contributions although not zero, are also small in the case of the realistically shaped head model (Meijs et al 1987). The accuracy of the realistic head model relative to that of the concentric spheres model, increased with increasing source depth. This occurs for the reasons mentioned earlier and in part, as a consequence of the accuracy of the algorithms used for source localisation, being poorer for deeper sources. In this case, differences of up to 16mm were found for deeper sources but the error was only 3mm for shallow sources. There was a negligable effect on the accuracy of determining the source orientation in this study. Hence, it can be concluded that although there are some errors in locating the detector caused by using a spherical model of the head, these are within acceptable limits for shallow cortical sources, particularly those located in brain areas which approximate to a sphere (for example the occiput), at least when a spherical mapping surface is used.

Even the most complex head model does not take into consideration the effects of the folds and fissures of the brains surface (Cuffin 1985), in particular the complex geometry of the calcarine fissure (Kaufman et al 1991), the non-homogeneity of the ventricles, sinuses or even brain lesions (Ueno et al 1985) or the number, nature or geometry of the source itself (Okada 1983, Nunez 1986, Kaufman et al 1991, Muresan et al 1991). All of these factors have a demonstrable effect even when the simplest head model, that of a single sphere, is used. Their effects may be more complex still in the real head.

5.12 Adequacy of the Single Dipole as a Source Model

The most commonly used source model is that of a single current dipole (Wood 1985, Pantev et al 1989, Sutherling et al 1989, Harding et al 1991). The adequacy of the single dipole as a source model is often evaluated in terms of spatial resolution. Under the ideal conditions of shallow sources, optimal coil diameter and configuration, sufficiently dense mapping matrix and low noise, it may be possible to separate two simultaneously active sources just a few millimetres apart (Hari et al 1988). However

with more realistic noise levels it becomes possible to separate two sources providing that they are no closer than 1cm (Muresan et al 1991) or 1 to 2cm apart (Okada 1985). These values have been obtained for shallow sources, with poorer resolution resulting from deeper sources (Hari et al 1988, Muresan et al 1991). In these instances the sources were localised using the least squares method, the situation is somewhat worse if the bisection or peak location method is used (Nunez 1986).

Okada (1985) studied the magnetic field patterns produced by extended or multiple generators and found that under a wide variety of conditions they were statistically indistinguishable from that produced by a single dipole source. His main conclusions were that the single dipole may therefore be an adequate source model for many magnetic components but that occasionally field patterns deviate from the dipolar sufficiently to allow identification of distributed or multiple source generators.

Although studies indicate that in most instances we cannot justify the fitting of more than a single dipole it may eventually be necessary, if we are to learn more about visual processing, to implement complex, geometrically accurate head models and multiple source generators.

5.13 Mapping Matrices

Meijs et al (1987) carried out a fairly comprehensive study of the three mapping matrices (sphere, contour or plane) using a realistically shaped head model and dipolar sources located in the occipital region.

Of primary concern is the ease with which field maps can be interpreted. This means that it is best practice to map using the surface least affected by contributions from secondary sources. In practice this turns out to be the spherical surface because the secondary source contribution is small (approximately 10%). However, since the head is not spherical, the mapping surface must be located away from the scalp and thus there may be some, possibly unacceptable, loss of sensitivity (Barth et al 1986). In addition, to obtain the degree of accuracy desired in locating the detector, it is necessary that the gantry supporting the magnetometer and the patient support system, are highly flexible and capable of fine adjustment.

Mapping in a plane over the back of the head, although probably the simplest in terms of physically manipulating the patient or the detector, is least acceptable in mapping terms as the contribution of secondary sources to the field recorded may be as high as 80% (Meijs et al 1987). In addition, at the extreme points of the mapping grid

information is lost because the distance between the source and detector may be impractically large.

Mapping following the natural contours of the head, although a compromise, was considered the most practical option using our magnetometer. We could not locate on a spherical surface using our current system. The limitations of following the contours are that secondary sources may contribute up to 20% of the field. As with the planar mapping surface, distortion is maximal for the outer points of the mapping grid towards the edge of the head. For example, it is difficult when recording the outer points of a grid located over the occiput to locate the detector normal to the head, without moving the head itself. In this study a compromise was achieved by using a combination of small movements of both the magnetometer and the head of the subject. At various recording positions these small movements of the head were shown not to significantly affect the amplitude or latency of the VEMR at that recording position.

5.14 Methods of Source Localisation

Two main methods of source localisation have been used. The simplest and least accurate is the peak identification method. The source is considered to lie midway between the two extrema in a direction consistent with the orientation of the fields. If the extrema are separated by a distance 'd' then it can be shown that the source is located approximately $d/\sqrt{2}$ below the detector (Tripp 1983).

The second method is the Least Squares Method. This is based on the inverse problem ie. the calculation of the current distribution inside a volume conductor (the head) based on the distribution of the field outside the volume conductor. There is no unique solution to the inverse problem, but it may be solved in a restricted form by placing constraints on the source (dipole) and the volume conductor (sphere). Using a computer, sources are fitted to the field data using the inverse problem solution. A test is made of the goodness of fit of the fields generated by these theoretical sources to the fields actually recorded (Stok 1986). An acceptible fit is achieved when the least squares difference between the calculated and measured fields is minimised.

5.2 METHODS

5.21 Subjects

All the subjects participating in the following studies were without ophthalmological or apparent neurological problems and had corrected vision of 6/6 or better. Subjects were aged between 22 and 41 years of age and all were alert and co-operative.

5.22 Mapping Grid

The following studies were carried out using either a 20 or a 42 point grid on the scalp. The 20 point grid consisted of four rows of five points per row located over the occipital cortex with the inion (I) as the centre point of the bottom row (Figure 5.1). The spacing between the points was calculated as 10% of the measured half circumference of the subjects head. This spacing varied between 2.7 and 3.1cm in the subjects used.

For the more detailed mapping study a 42 point grid was used. This comprised six rows of seven points per row, with the inion as the centre point of the penultimate row (Figure 5.2). Hence, a greater area of scalp was sampled with a greater density of recording positions. Recording positions were separated by 2cm in all subjects.

5.23 Recording Protocol

The subjects were comfortably seated under the magnetometer with the Dewar tail positioned approximately normal to the scalp. The recordings were made sequentially from each point on the grid as indicated in Figures 5.1 and 5.2. At a sample of locations, repeat recordings were made to ensure consistency of the magnetic response.

5.24 Stimulus Parameters

Pattern reversal stimulation was provided using a projection system (Drasdo 1976) and flash stimulation via a Grass PS22 stroboscope triggered by the Biologic Traveler signal processor, via a Medelec Sensor OS5. All stimuli were viewed binocularly and centrally fixated unless otherwise stated. In all of the experiments, the pattern reversal rate was 2/second and the flash rate 1.6/second.

5.25 Protocols

Study 1

Twelve subjects were used including both experienced laboratory staff and previously untested volunteers. The stimulus was full field (13°34' diameter circular field) pattern reversal. A 70' check was used with a mean screen luminance of 1050cd/m^2 and a contrast of 0.76. Subjects were mapped using the 20 point grid.

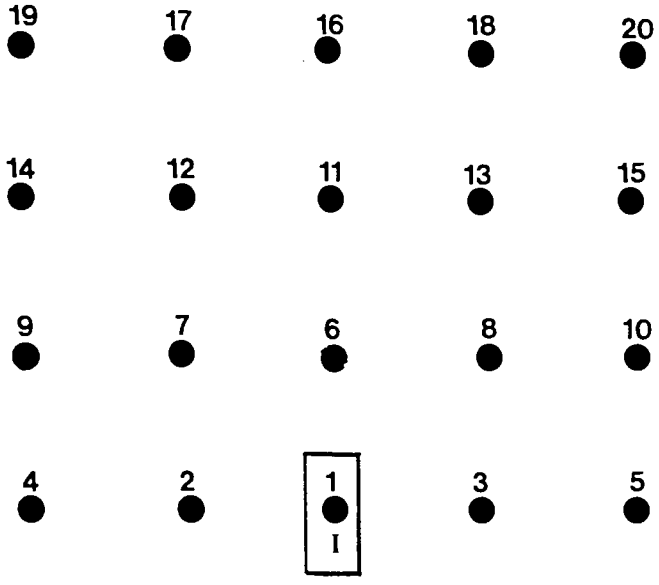

Figure 5.1 : The 20 point mapping grid. I represents the inion. The points were 10% of the measured half circumference of the head apart and were recorded in the sequence indicated by the numbering.

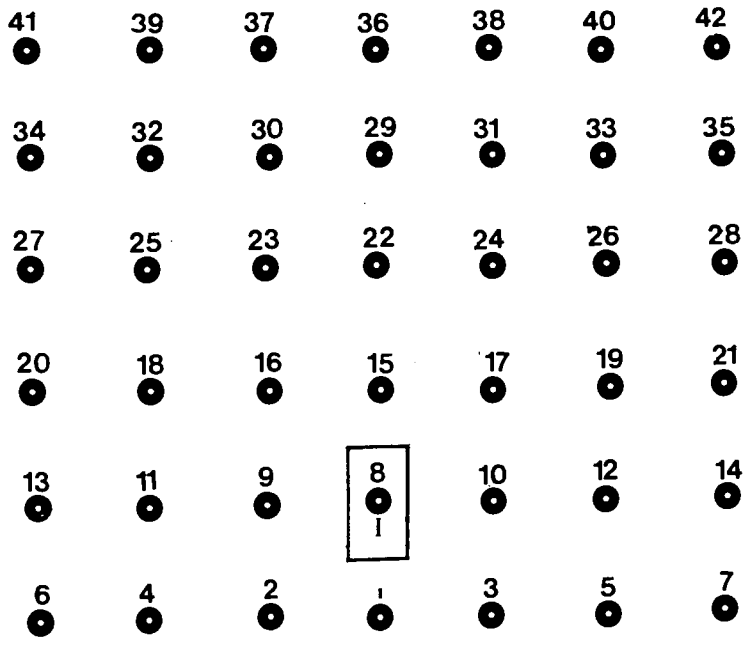

Figure 5.2 : The 42 point mapping grid. I represents the inion. Points 1 to 7 are on a line below the inion. The points were 2cm apart and were recorded in the sequence indicated by the numbering.

Study 2

Nine subjects were used. The stimulus was a diffuse flash of light produced by a Grass PS22 stroboscope gun set at intensity 8 (3939cd/m^2), subtending a visual angle of 19^o at the eye. Subjects were mapped using the 20 point grid.

Study 3

Six experienced subjects participated in this study (RAA, AS, CD, CN, SC and GB). The stimulus was pattern reversal using a 70' check (as for Experiment 1) presented as a full field and presented in the left and right half field. A circular field (diameter $13^o34'$) was used with left or right half stimulation achieved by covering the relevant half of the screen. Subjects were mapped using the 20 point grid.

Study 4

Two subjects (RAA and CD) were used for this study. The stimulus was pattern reversal using a $1^o40'$ check (mean screen luminance of 1050cd/m^2 and the contrast 0.76). 20 point maps were recorded to a) a $13^o34'$ full field, centrally fixated, b) a $13^o34'$ field with a circular, centrally located, 4^o scotoma and c) a $13^o34'$ field with a circular, centrally fixated 7^o scotoma.

Study 5

Three experienced subjects (RAA, AS and CD) were used for this study. 20 point maps were recorded in response to flash stimuli of the following intensities:- 1 (1088cd/m^2), 2 (1363cd/m^2), 8 (3939cd/m^2) and 16 (9661cd/m^2). The stimulation rate was 1.6/second.

Study 6

A series of 42 point maps were recorded from subject RAA in response to a) full field and b) right half field pattern reversal ($1^o40'$ check, $13^o34'$ field diameter) and c) a flash stimulus (Intensity 8, 3939cd/m^2). The Pathfinder II is limited in the number of recording positions that can be used as mapping input. Hence, only 31 points were used to construct the coloured images. This was achieved by eliminating the bottom row and the extreme point on each side of the top and inion rows of the grid. However, all 42 points were used for the source localisation procedure.

5.26 Signal Processing

Signals from the magnetometer were recorded at a sensitivity of x1000 (89pT/V flux to voltage) and were bandpassed between 0.3 and 30Hz (24dB/octave roll off). A 50Hz comb filter was also used. Signals were attenuated by a factor of 100 before input into a Biologic Traveler signal processor, incorporating artifact rejection. Fifty signals were averaged at each point with a time base of 500ms.

Unless otherwise indicated, it is the largest and most consistent component within the first 150ms which was mapped. In most subjects, this occurs between 90 and 120ms to pattern reversal stimulation (P100M) and between 90 and 140ms to flash stimulation (P2M : See Chapter 3). The amplitude of this signal (peak to baseline) at each location on the grid was used as mapping input. Topographic mapping was carried out on a Nicolet Pathfinder II using a rectangular grid and linear interpolation between points. The detailed 42 point maps were inspected for dipolar distributions and source localisations performed at the Open University using a simple dipole in a sphere model and the least squares method (Janday et al 1987).

5.3 RESULTS

Figure 5.3 shows waveforms recorded at the 20 locations of the mapping grid (numbered 1 to 20 from top to bottom and left to right) from subject RAA in response to a 70' check pattern reversal stimulus presented in a circular field of 13°34' diameter. The P100M component can be seen most clearly on waves 7 and 8.

Figure 5.4 shows the topographic field map from the same data printed using the Pathfinder II, using both symmetrical and asymmetrical colour scales. White/red represents an outgoing magnetic field or 'positivity', while blue/green represents an ingoing field or 'negativity'. Hence the topographic maps represent the surface magnetic field pattern of the pattern P100M or flash P2M at a latency as indicated underneath each map.

Figure 5.4a shows an individual map printed i) on an asymmetrical amplitude scale and ii) on a symmetrical amplitude scale. In this case the amplitudes of the ingoing and outgoing extrema are similar and so there is little difference between the maps. However, in Figure 5.4b, where the ingoing and outgoing field extrema are of different magnitudes, the effects of scale can be seen more clearly. On an asymmetrical scale (Figure 5.4b(i)) the pattern appears essentially 'dipolar' while this effect is less apparent when printed out on a symmetrical scale (Figure 5.4b(ii)). In order to avoid the false impression of a dipolar field pattern all of the maps in the

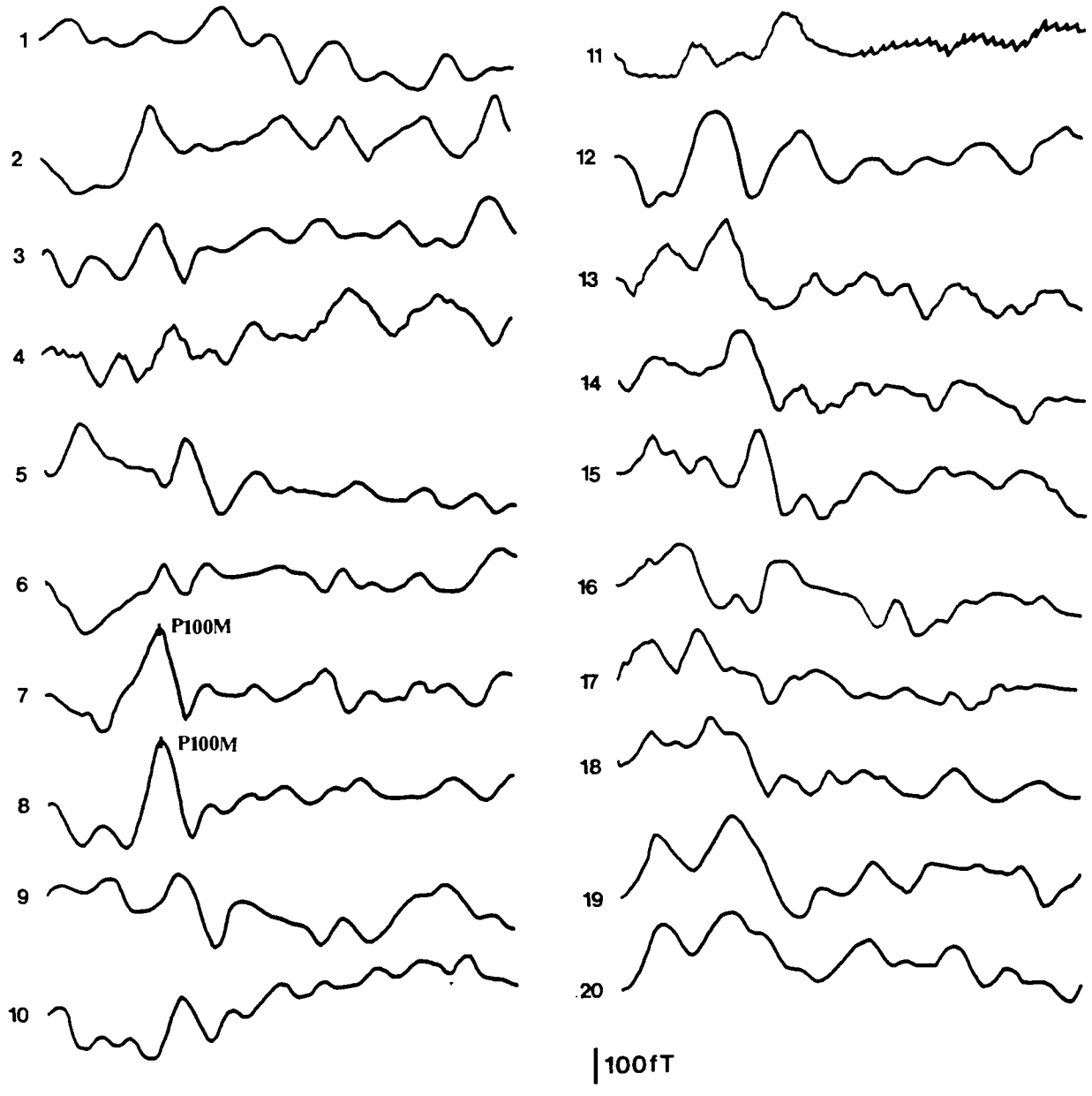

Figure 5.3 : Waveforms recorded at the 20 locations of the mapping grid (numbered 1-20 from top to bottom and left to right) from subject RAA in response to a 70' check pattern reversal stimulus presented in a 13°34' diameter full field. The P100M appears prominent on waves 7 and 8.

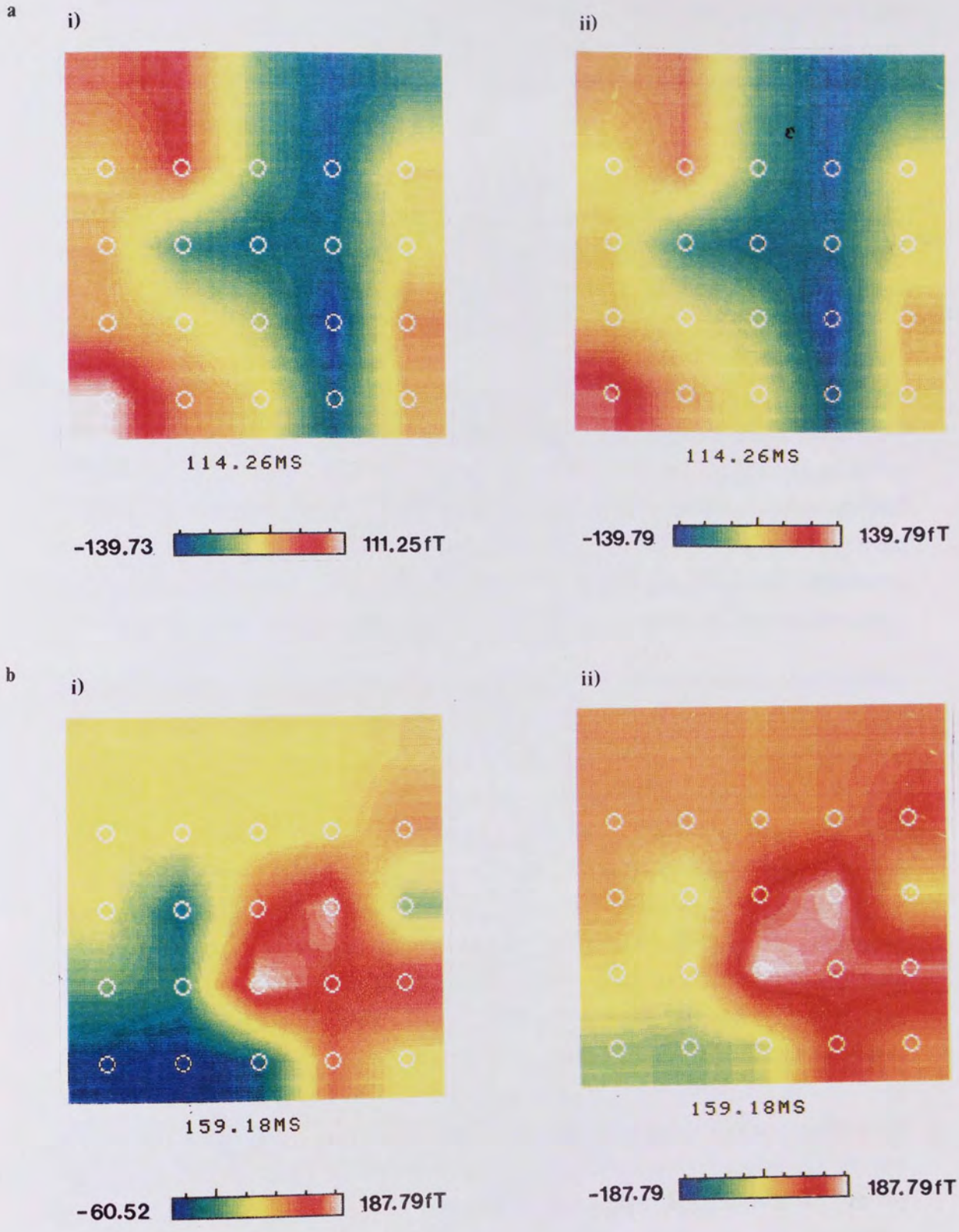

Figure 5.4 : Two different topographic maps (a and b) are printed on both asymmetrical (i) and symmetrical (ii) amplitude scales. Where the ingoing and outgoing extrema are of similar amplitude (a), there is little difference between the maps while in a case where the extrema are of different amplitudes, on the asymmetrical scale (i) the field appears essentially dipolar while on the symmetrical scale (ii) this is less apparent.

following section were printed using a symmetrical scale. This approach has the additional advantage in that it allows easy identification of the areas of scalp over which the field is maximal, one of the primary aims of the present topographic mapping study.

Figure 5.5 shows topographic maps of the pattern reversal P100M component (70' check, 13°34' circular field) recorded on two subjects approximately two years apart. The maps shown in Figures 5.5a(i) and (ii) were recorded from subject RAA. The overall field pattern of the two maps is similar; the strongest field is outgoing and occurs approximately 6cm above the inion, 3cm to the left of the midline.

The maps shown in Figure 5.5b(i) and (ii) were recorded from subject CD to a pattern reversal stimulus (70' check, 13°34' circular field). These maps have similarities and differences. The amplitudes of the outgoing field extremum are similar, as is the P100M components' latency. In addition, in both maps the strongest outgoing field occurs approximately 3cm above the inion, 3cm to the left of the midline. However, in the second map (Figure 5.5b(ii)), there are areas of strong ingoing field 3cm above the inion, 3cm to the left of the midline and 9cm above the inion and 3cm to the right.

Figure 5.6 shows topographic maps of the VEMR P100M obtained from twelve subjects in response to a full field (13°34'), large check (70') pattern reversal stimulus (maps 1 to 12). Maps 13 and 14 show the distribution of the mean and standard deviation of the amplitudes at each recording position in the 12 subjects. The most commonly observed pattern is that shown by the group mean map (map 13). This map can be divided into four quadrants. On the left there is an upper positivity and lower negativity while on the right an upper negativity and lower positivity. Individual maps 4, 6, 8, 10, 11 and 12 show this pattern most clearly. However, some variations occur in individual subjects. For example, in maps 2, 3, 5 and 7 the pattern appears to be displaced more posteriorly on the head. In addition, in map 1 the general pattern is discernable but the response appears shifted to the left and more dominant over the left hemisphere. In the remaining map (map 9), only two extrema are visible - an outging field over the upper left quadrant/midline and an ingoing field over the lower right quadrant. This particular subject had an asymmetrically shaped head with an inion displaced to the right. This could have resulted in a shift of the pattern to the right, so that the right hemisphere half of the response was not recorded.

Figure 5.7 shows waveforms recorded at the 20 locations of the mapping grid from subject CD in response to a flash stimulus (Intensity 8, 3939cd/m^2). The P2M positive extremum can be seen most clearly on waves 1, 19 and 20.

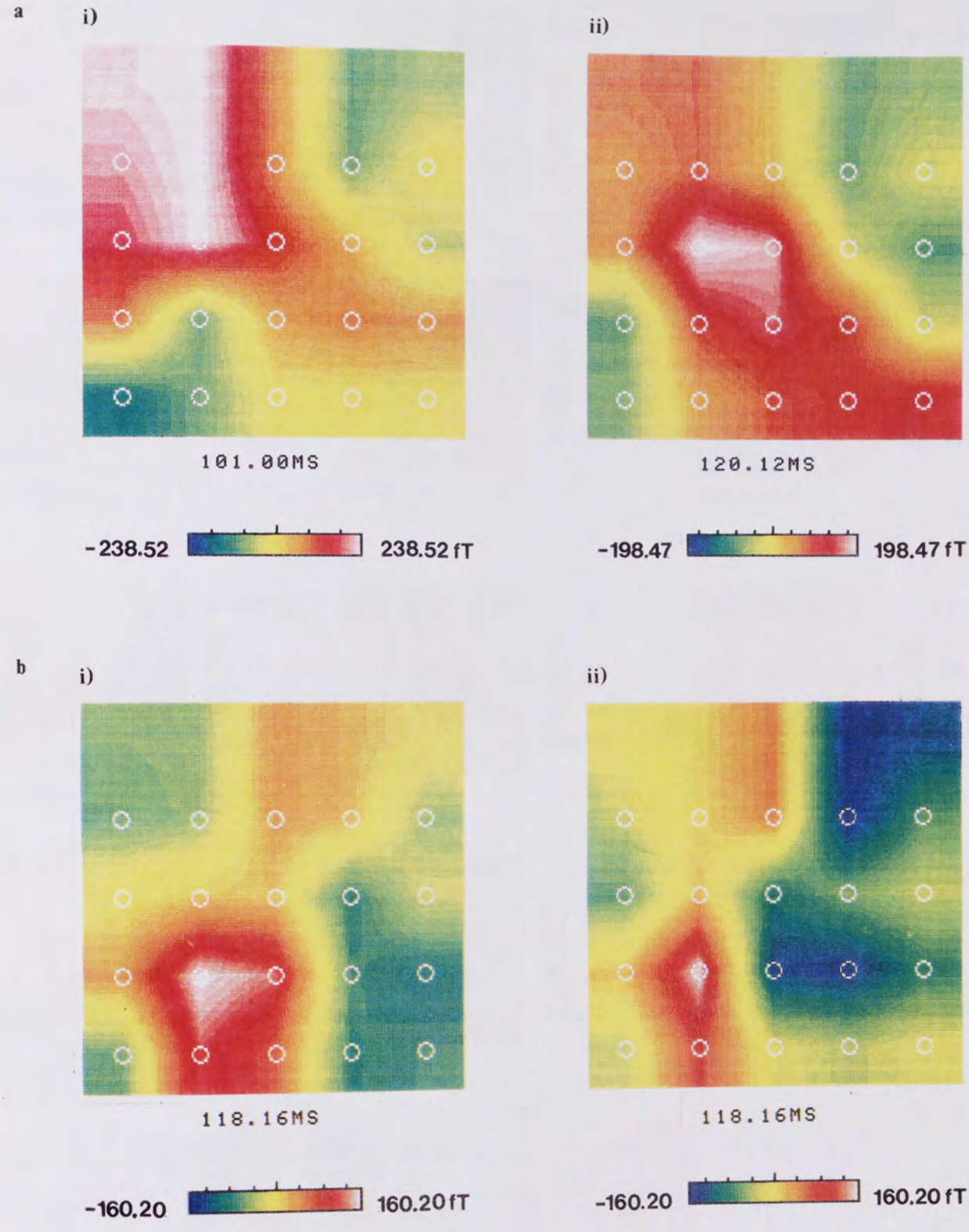

Figure 5.5 : Topographic maps recorded from the same subjects two years apart. The maps were recorded in response to a 70' check pattern reversal stimulus presented in a circular full field of 13°34' diameter from a) subject RAA and b) subject CD.

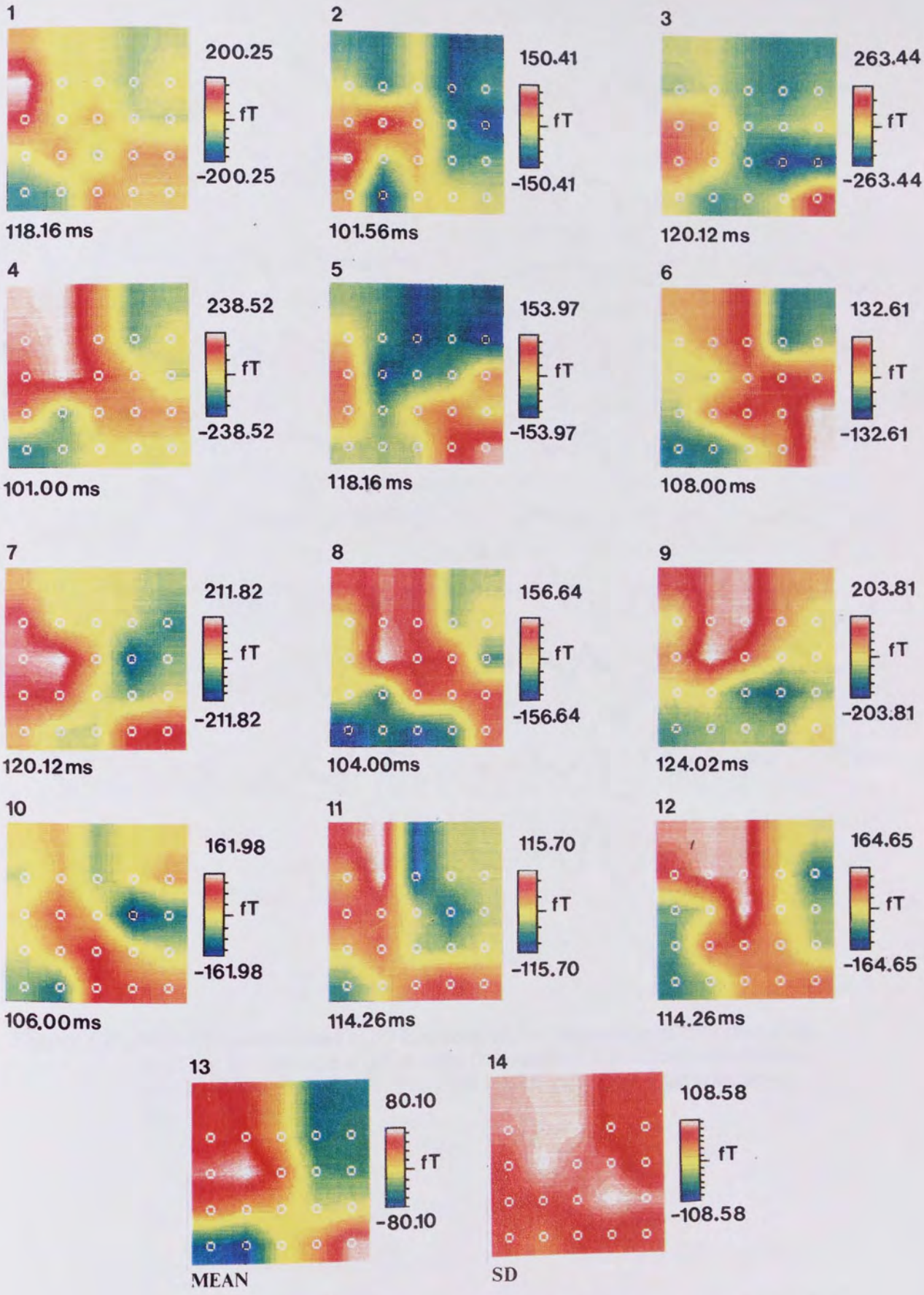

Figure 5.6 : Topographic maps of the P100M to a 70' check pattern reversal stimulus presented in a 13°34' diameter full field, recorded from twelve subjects. Maps 13 and 14 show respectively the group mean and Standard Deviation (SD) maps.

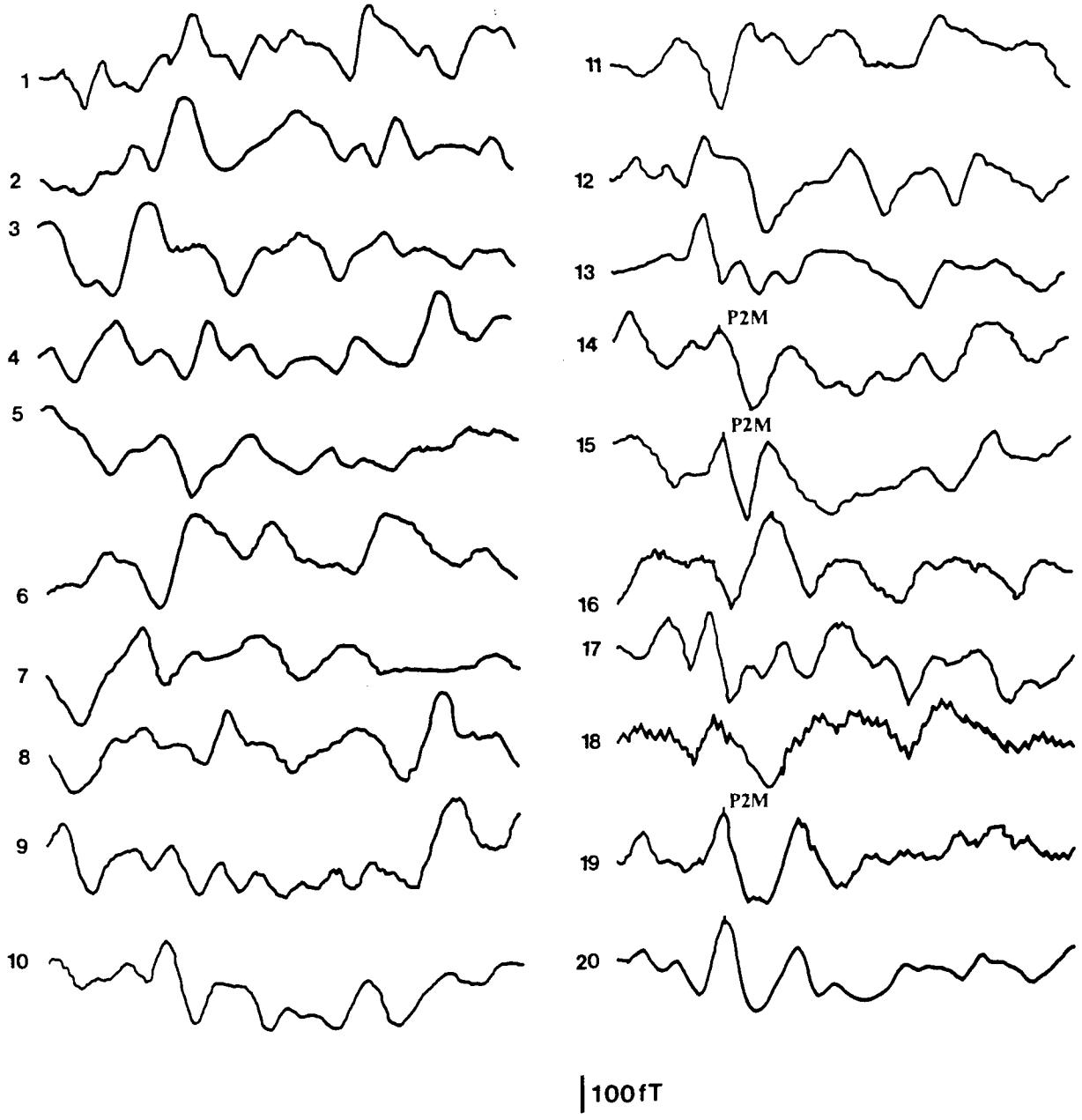

Figure 5.7 : Waveforms recorded at 20 locations of the mapping grid (number 1-20 from top to bottom and left to right from subject CD in response to flash stimulation at intensity 8. The P2M can be seen most clearly on waves 14, 15, 19 and 20.

Figure 5.8 shows topographic maps of the P2M to a flash stimulus (Intensity 8, 3939cd/m^2) obtained from 9 subjects (maps 1 to 9). Maps 10 and 11 show the mean and standard deviation of the first nine maps. The individual maps to flash stimulation appear more variable than those to pattern reversal and this is illustrated by the greater range of standard deviations (map 11). However, the group mean map of the P2M appears to be similar to that seen for the P100M to a pattern reversal stimulus ie. on the left upper positive and lower negative and vice versa on the right. On average, the field appears stronger over the left hemisphere than the right. Individual maps 4, 8 and 9 are the clearest examples of this pattern. Variations between subjects were observed. For example, in map 3 the pattern appears lower on the head. The field patterns of several of the maps are more complex. Maps 5 and 7 show an upper left quadrant outgoing field and an upper right ingoing field, with only slight evidence of activity over the lower quadrants as seen in the group mean map (10). Maps 2 and 6 show similar patterns. There is an area of outgoing field over the bottom right quadrant and over the point approximately 9cm above the inion on the midline on both maps. An area of ingoing field can be seen over the left hemisphere for both subjects with the peak amplitude occuring to the left hand edge of the grid in map 2 and around the midline, slightly to the left, in map 6. Map 1 appears to be similar to the group mean map (map 10), except that there is no evidence of the ingoing field expected over the upper right quadrant.

Similarities were found in the maps produced by pattern reversal and flash stimuli in the same subject. Map 2 (subject CD) shows the least similarity between the two stimuli. However, the remaining maps show striking similarities. For example, subjects 3 and 7 show magnetic field patterns low on the head to both stimuli while subjects 1 and 4 appear to have a dominant left hemisphere response to both stimuli.

Figure 5.9 shows the topographic field distribution of the P100M recorded from 6 subjects in response to full field (FF), left (LHF) and right (RHF) half fields stimulation using a 70' check pattern reversal stimulus. The mean map shown for each subject is the sum of their left and right half field maps. The full field had a diameter of 13°34' and the half fields were produced by covering the appropriate half of the screen with white card. Figure 5.9a shows the responses of subjects RAA, AS and CN while Figure 5.9b shows those of subjects JY, GB and CD. Group mean maps of the FF, LHF and RHF for these subjects can be seen in Figure 5.10.

The latency of the component mapped (P100M) varied between 101 and 124ms for the FF, 102 and 118ms for the LHF and 99 and 120ms for the RHF. With the exception of GB (Figure 5.9b), the latencies of the FF and both half field maps do not vary by

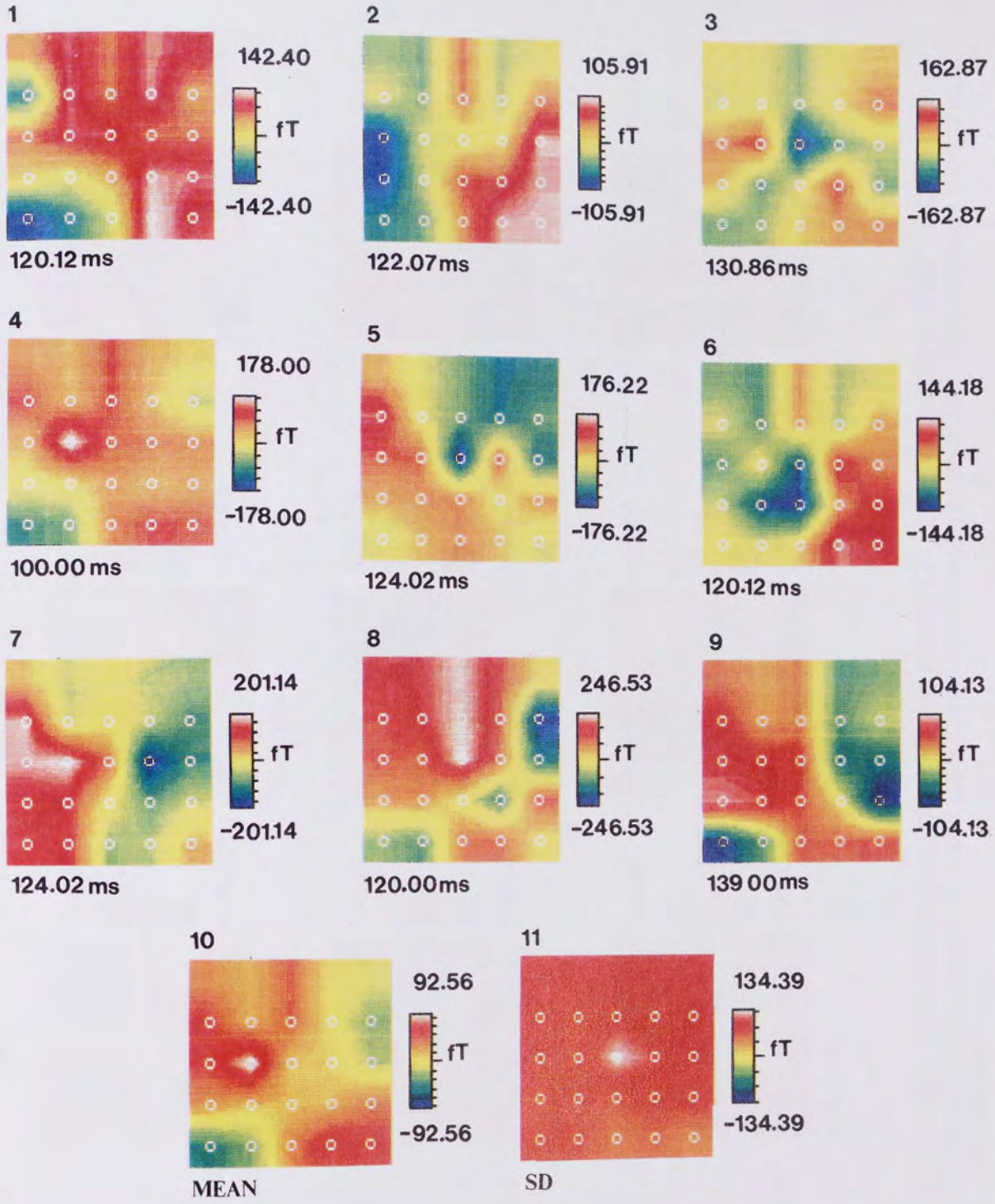

Figure 5.8 : Topographic maps of the P2M to a flash stimulus (Intensity 8) recorded from 9 subjects. Maps 10 and 11 show respectively the group mean and Standard Deviation (S.D.).

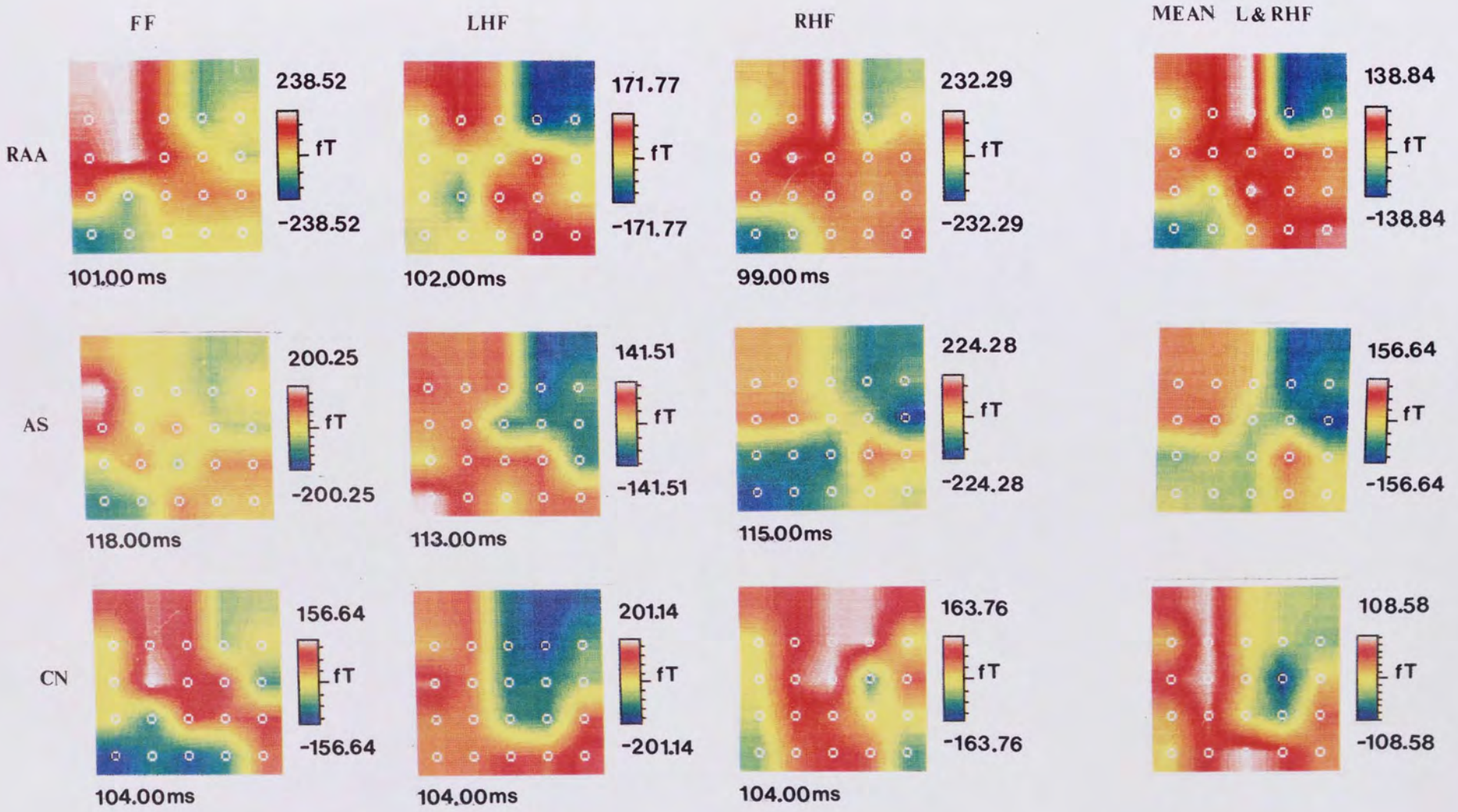

Figure 5.9a : Topographic maps of the P100M recorded from subjects RAA, AS and CN in response to full field (FF), left (LHF) and right half field (RHF) stimulation using a 70' check pattern reversal stimulus. The mean map, shown for each individual, is the sum of the LHF and RHF maps.

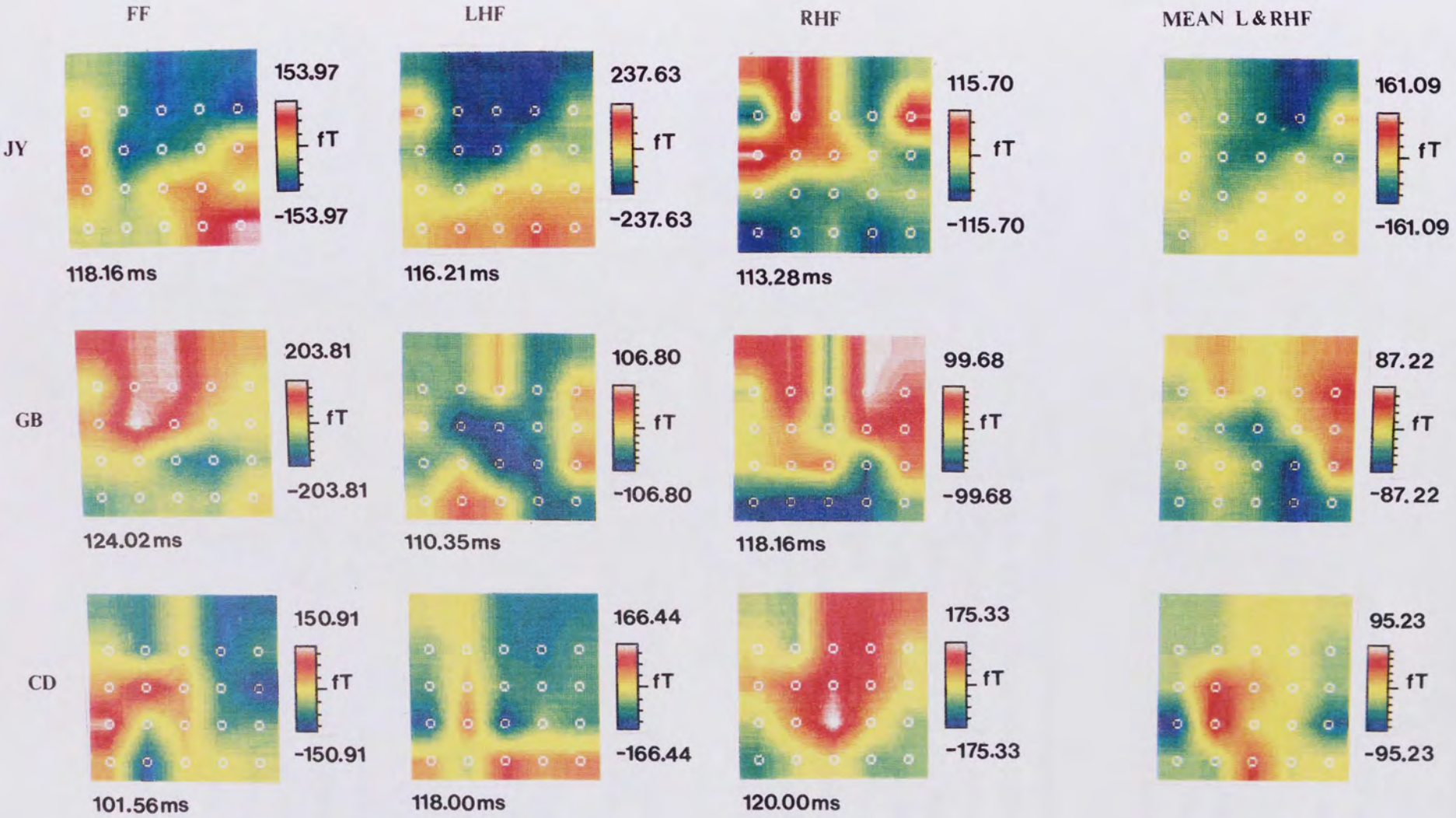

Figure 5.9b : Topographic maps of the P100M recorded from subjects JY, GB and.CD in response to full field (FF), left (LHF) and right half field (RHF) stimulation using a 70' check pattern reversal stimulus. The mean map, shown for each individual, is the sum of the LHF and RHF maps.

more than 5ms for an individual. For subject GB there is a maximum latency difference of 14ms between the FF (124.02ms) and the LHF (110.35ms) and 8ms between half fields.

The amplitude varies between 153 and 238fT for the FF, 106 and 237fT for the LHF and between 99 and 232fT for the RHF. There does not appear to be a tendency for any particular field presentation to have a higher amplitude.

The group mean FF map (Figure 5.10) shows a similar field pattern to that described previously in Figure 5.6 (map 13) for the larger group of 12 subjects. The pattern is discernable in the individual maps (Figure 5.9), being well defined for subjects RAA, AS, CN and JY, but less so for GB and CD.

The group mean maps for LHF and RHF also have a distinctive topography. Activity is maximal over the contralateral hemisphere in both instances, with activity over the ipsilateral hemisphere tending to zero in the group mean average. For the LHF there is a strong ingoing field over the upper right quadrant and an outgoing field over the lower right quadrant. For the RHF there is an outgoing field over upper left quadrant and an ingoing field over the lower left quadrant. These patterns can be seen in the individual maps (Figure 5.9) although with some variation. In some individuals, there is a tendency for the RHF to be located more over the midline than the left hemisphere (subjects RAA, CN and CD). In addition, activity over the ipsilateral hemisphere was often observed which could be due to poor subject fixation.

The summated maps of the LHF and RHF are usually similar to that produced by the FF response. One exception is the complex field distributions recorded in subject GB.

Figure 5.11 shows P100M maps produced in response to a $1^{o}40'$ check pattern reversal stimulus presented a) in a circular full field of $13^{o}34'$ diameter and the same field with a circular, centrally located scotoma of b) 4^{o} diameter and c) 7^{o} diameter. Two subjects were used for this experiment viz. RAA and CD. In subject RAA, occlusion of the central field with 7^{o} scotoma reduced the amplitude of the P100M. The field pattern produced by a 4^{o} scotoma (Figure 5.11a(ii)) appeared similar to the full field map (Figure 5.11b(ii)) but was more diffuse and less defined. The 7^{o} scotoma (Figure 5.11c(ii)) produced a map, the major features of which are an outgoing field approximately 6cm above the inion, 3cm to the left of the inion and an ingoing field extremum approximately 6cm above, 3cm to the right of the inion. This field is more diffuse than that produced by the 4^{o} scotoma. In subject CD the outgoing field extremum for the 4^{o} scotoma map (Figure 5.11b(i)) remains over the same point that it occupies for the full field map (Figure 5.11a(i)). However, the

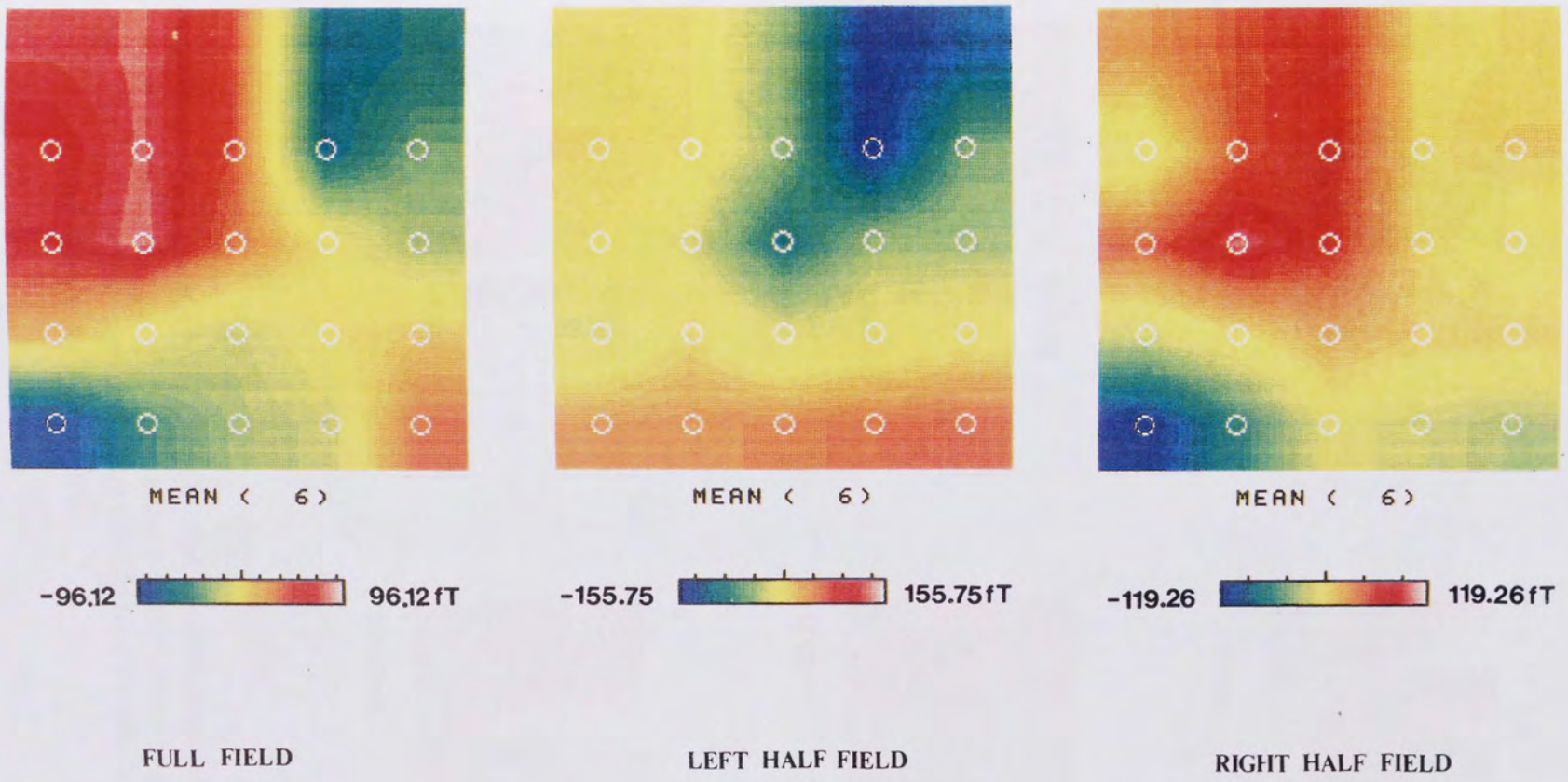

Figure 5.10 : Group mean maps to full field (FF), left (LHF) and right half field (RHF) stimulation using a 70' check pattern reversal stimulus. The half field responses appear over the contralateral hemisphere.

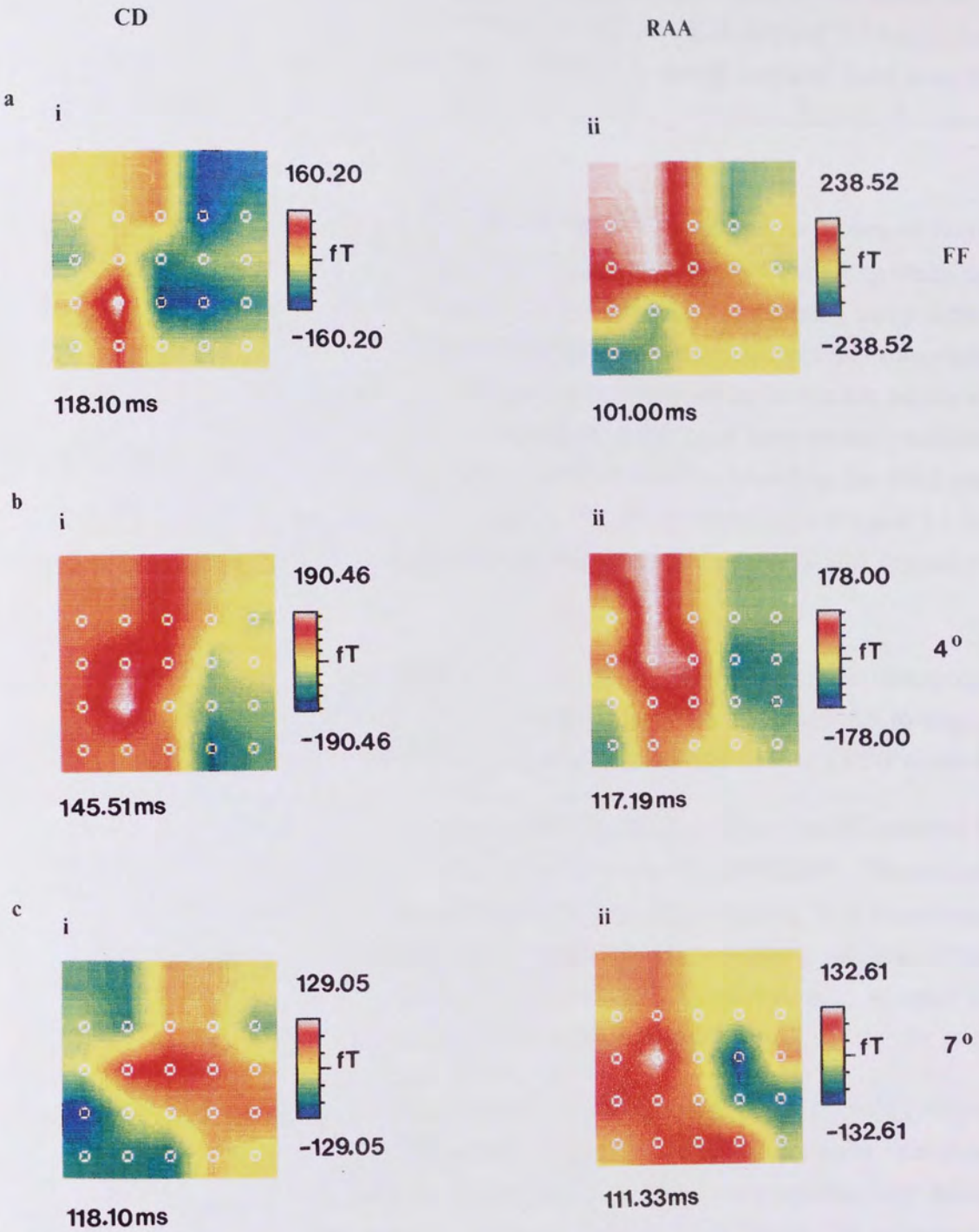

Figure 5.11 : Topographic maps of the P100M recorded from i) CD and ii) RAA in response to a 1°40' check pattern reversal stimulus presented in a 13°34' diameter field a) full field, b) with the central 4° occluded and c) with the central 7° occluded.

ingoing field appears over the same hemisphere but much lower down on the 4° scotoma map. The 7° scotoma map for subject CD (Figure 5.11c(i)) does not resemble either of the other maps. There is a strong ingoing field over the left hemisphere and an outgoing field over the midline, maximal at around 6cm above the inion.

Figure 5.12 shows topographic maps of the P2M produced to flashes of increasing intensity for subjects CD, AS and RAA. Figure 5.13 shows the group mean map for each flash intensity. These maps are particularly complex showing many differences and few similarities. For intensities 2, 8 and 16 responses from the lower halves of the head show most similarity. Recording positions in the lower left corner usually give an ingoing field component while those at the right hand corner yield show an outgoing field . The midline is also a good location for recording the P2M outgoing field. This tendency can also be seen in the group mean maps (Figure 5.13). The upper portions of each map are variable between subjects and between flash intensities.

Figure 5.14 shows waveforms recorded at 42 locations of the mapping grid (numbered 1-42 from top to bottom and left to right) from subject RAA in response to a 1°40' check pattern reversal stimulus, presented in a full field of 13°34' diameter.

Figure 5.15 shows 31 point maps to a FF and a RHF pattern reversal stimulus (1°40' check, 13°34' field) and flash stimulation (Intensity 8, 3939cd/m^2). The subject was RAA. The most prominant feature of the FF map is an outgoing field extremum, 4cm above the inion on the midline. This extremum is surrounded by an area of weaker field that spreads across the left hemisphere and slightly downwards. Another area of outgoing field can be seen on the midline, 2cm below the inion.

The response to RHF pattern reversal stimulation shows an outgoing extremum occuring over the point 4cm above and 2cm to the left below the inion. Another area of strong outgoing field can be seen over the ipsilateral hemisphere, 2cm below the inion. Areas of weak ingoing field can be seen both below the outgoing field extremum over the left hemisphere and over parts of the ipsilateral side.

The subjects response to flash stimulation is the best defined of the three maps. The map shows the distribution described previously in relation to the group mean flash map (9 subjects) and is very similar to the 20 point map recorded on this subject (Figure 5.8, map 4).
The final figure shows the results of source localisation carried out on the 42 point data (Figure 5.16). The localisation carried out on the full field (FF) pattern reversal

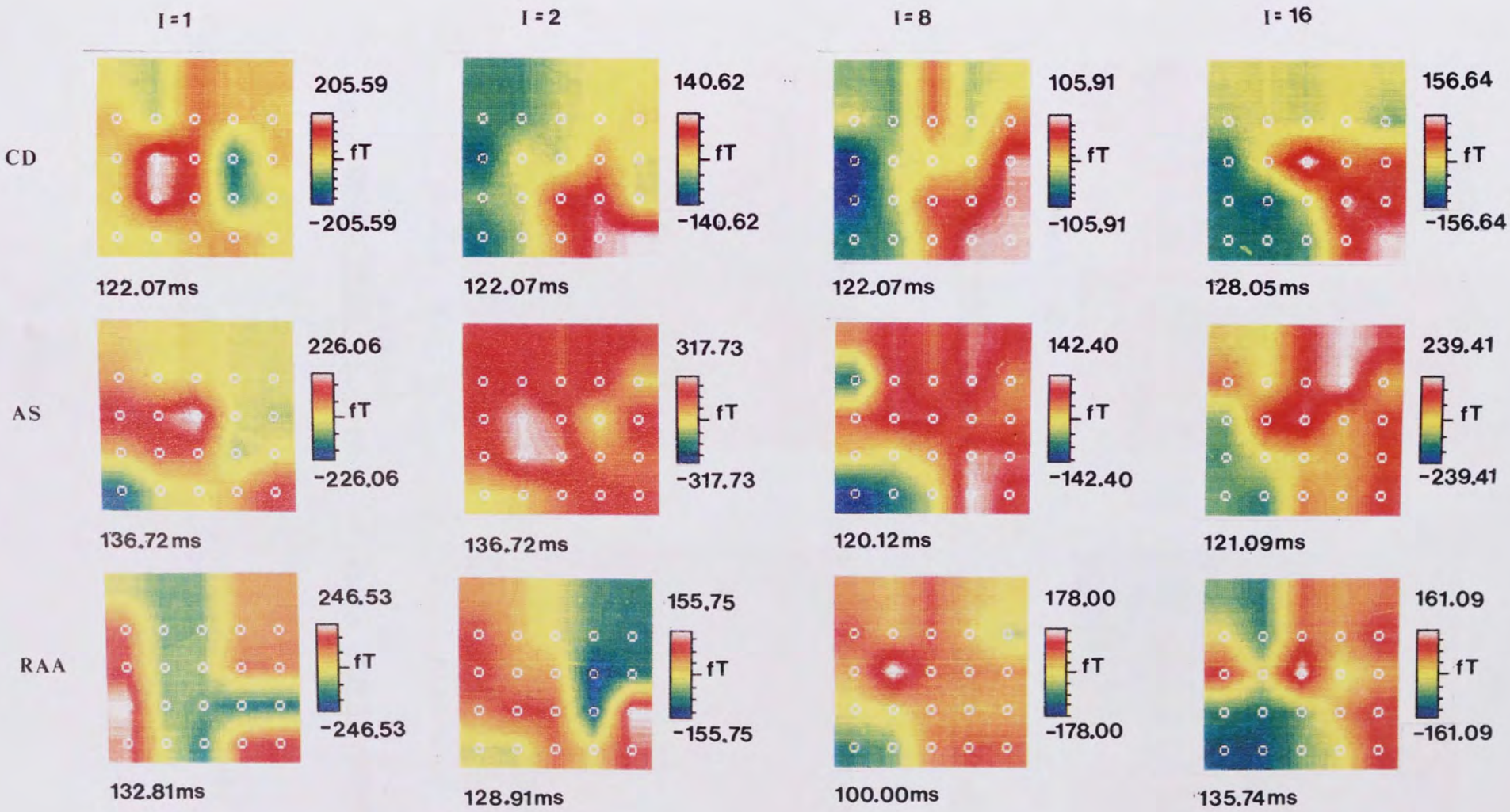

Figure 5.12 : Topographic maps of the P2M recorded from 3 subjects in response to flash stimulation at intensities 1, 2 , 8, and 16.

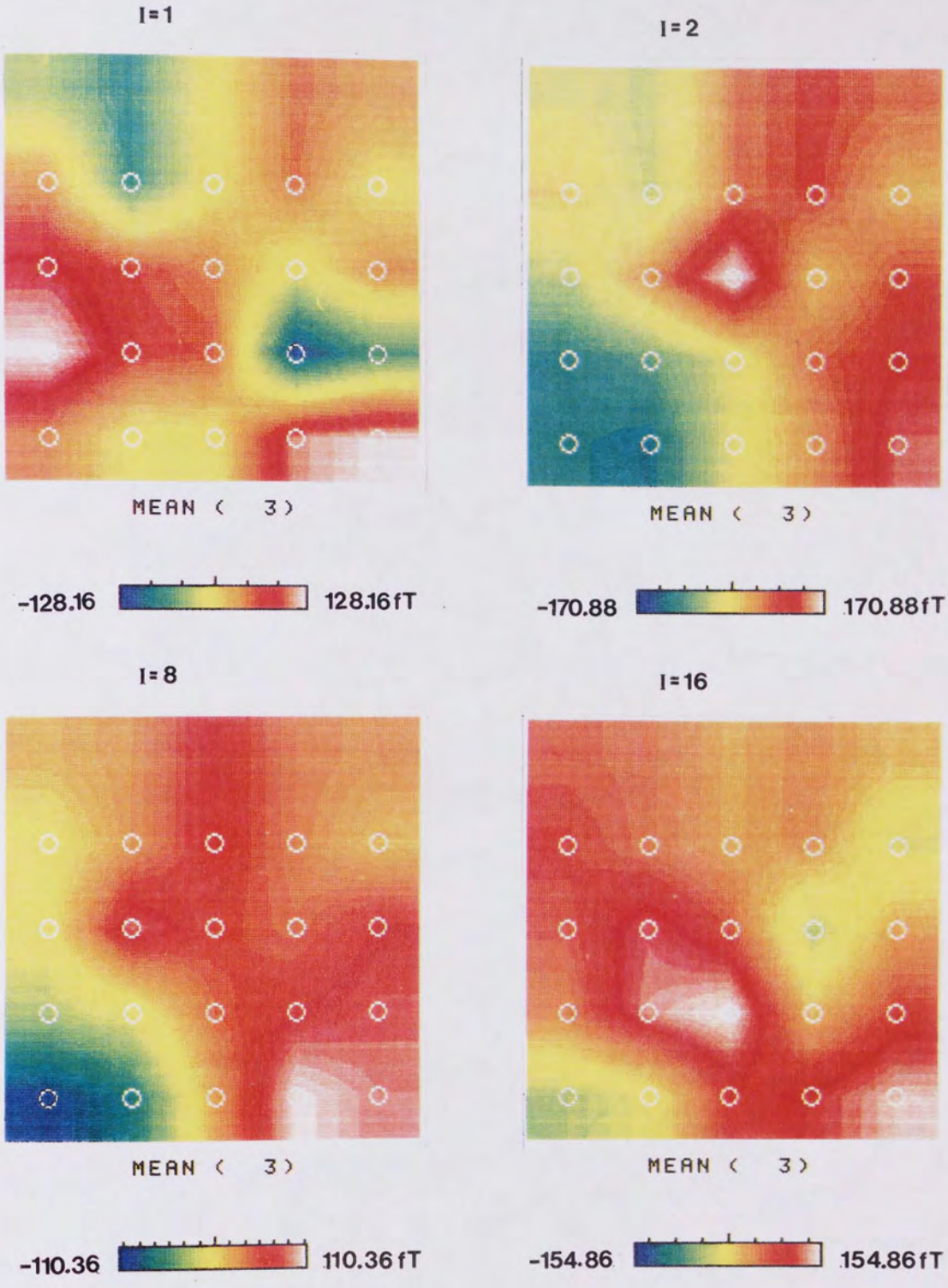

Figure 5.13 : Group mean maps of the P2M produced in response to flash stimulation at intensities 1, 2 , 8, and 16.

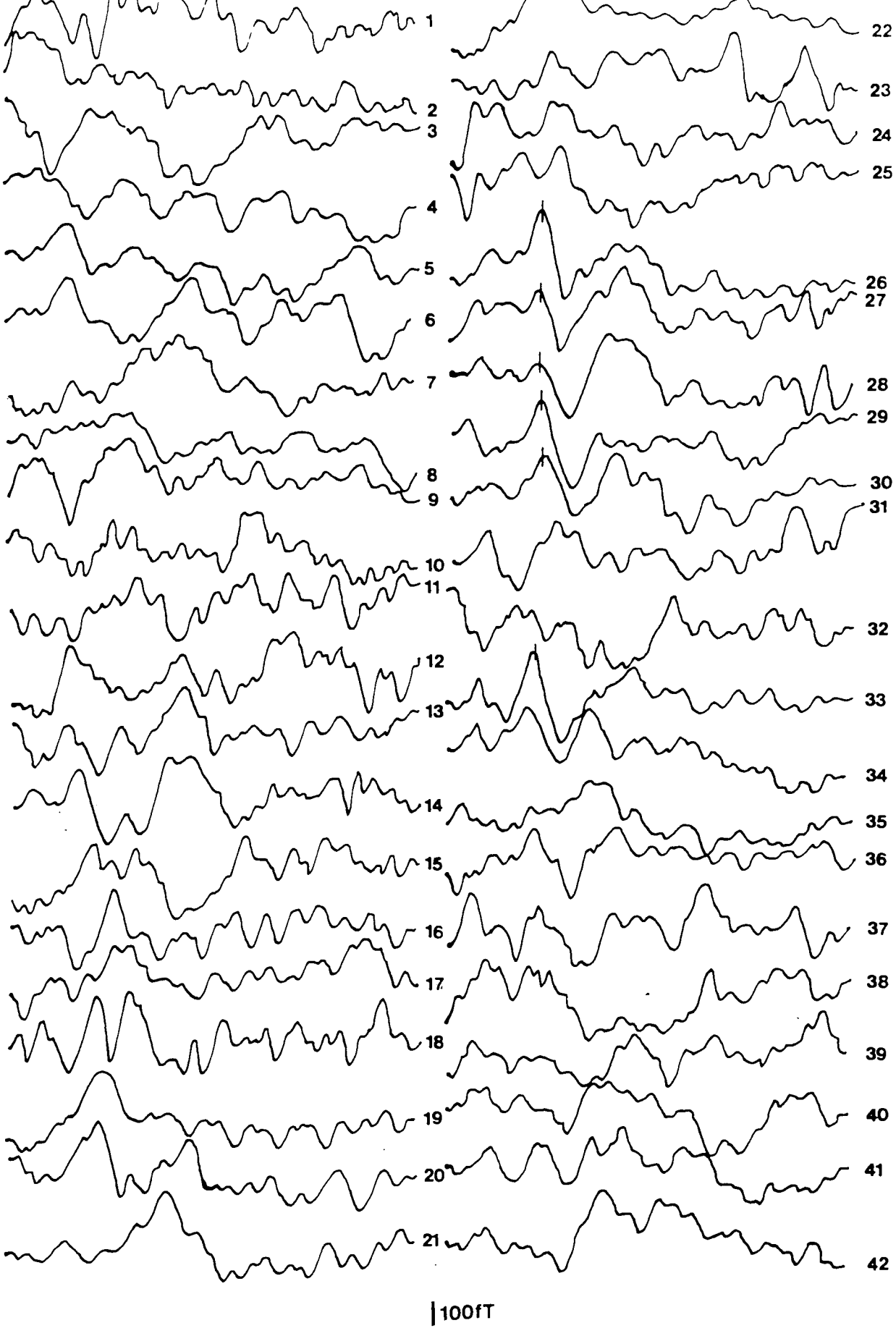

Figure 5.14 : Waveforms recorded at 42 locations of the mapping grid (numbered 1-42 from top to bottom and from left to right) from subject RAA in response to a 1°40' check pattern reversal stimulus presented in a 13°34' diameter field.

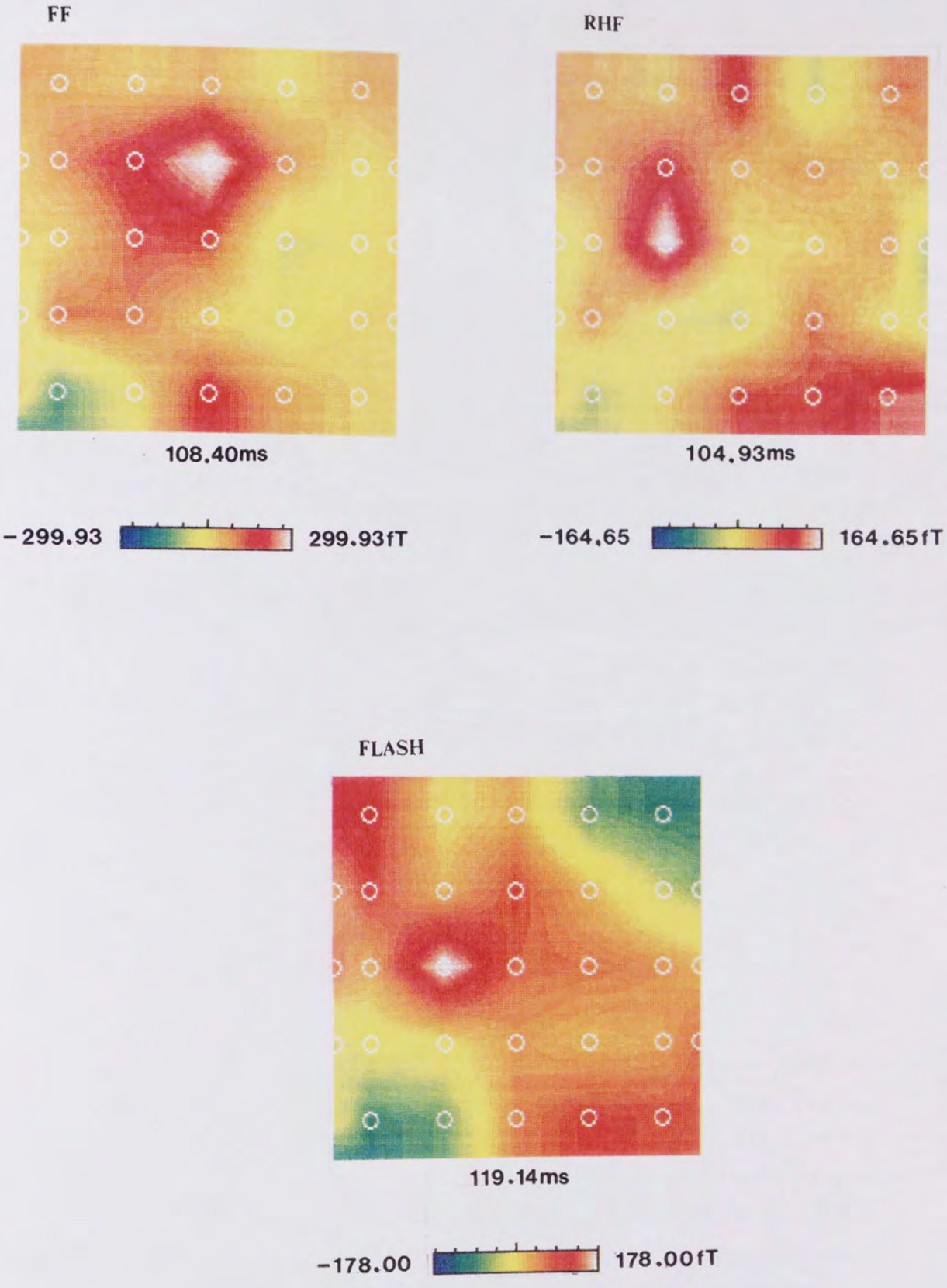

Figure 5.15 : 31 point topographic maps of the P100M to full field (FF) and right half field (RHF) pattern reversal stimulation (1°40' check) and to a flash stimulus (Intensity 8).

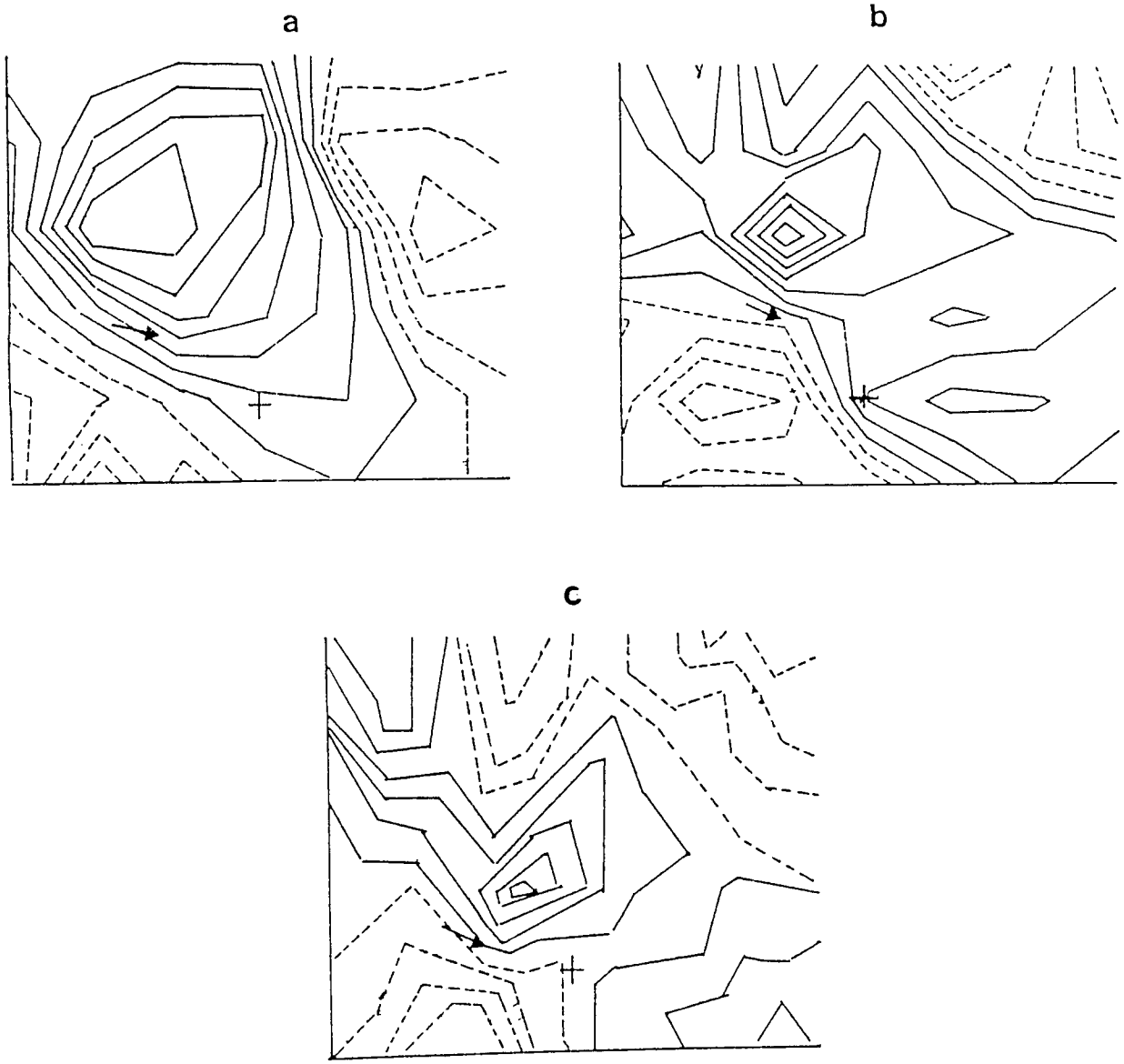

Figure 5.16 : Some localisation for the 42 point mapping data (subject RAA). a) pattern reversal full field response. The source is located 4cm below the scalp (dipole orientation 290°, strength 3.1×10^{-7} A). b) pattern reversal right half field response. The source is located 2.0cm below the scalp (orientation 92°, strength 3.4×10^{-7} A). c) flash response. The source is located 2.0cm below the scalp (dipole orientation 300° strength, 10.7×10^{-7} A). Co-ordinates are relative to the inion marked (+).

map suggests a source in the left hemisphere in which the current flows towards the midline at a depth of around 4cm. For RHF stimulation the source appears to be located in the left hemisphere, more posteriorly than for the FF , 2cm below the scalp. The direction of current flow is towards the midline. Localisation of the flash P2M suggested a source located in the left hemisphere and at a depth of 2cm. The source is lower on the head than that seen for pattern reversal, possibly suggesting activation of polar areas of the cortex.

5.4 DISCUSSION

The topography of the VEMR to both flash and pattern reversal stimulation varies from subject to subject. The standard deviations of the latencies and amplitudes suggest that flash topography is more variable than the pattern reversal topography to a large check. However, the group mean maps to both stimuli are very similar; an upper outgoing and a lower ingoing field over the left hemisphere with the opposite pattern over the right hemisphere. The majority of individual maps show this pattern but they vary in the hemisphere which shows the strongest response and in whether the response is more lateral or more posterior on the scalp. In addition, similarities are apparent when comparing the flash and full field pattern reversal maps from the same subject.

The full field pattern reversal reponse appears to be approximately the sum of the two half field responses (Okada 1983, Harding et al 1991). The half field response appears over the contralateral hemisphere as predicted from the cruciform model (Okada 1983, Maclin et al 1983) and previous experimental work (Maclin et al 1983, Richer et al 1983, Kouijzer et al 1985, Janday et al 1987). However, there is a tendency for the right half field response to be distributed more towards the midline than the left half field reponse. By contrast, studies of the VEP show a paradoxical ipsilateral lateralisation, the positive maximum of the P100 occuring over the hemisphere ipsilateral to the visual field stimulated (Barrett et al 1976, Rowe 1982, Hammond et al 1987). That this component originates in the contralateral hemisphere as predicted by the anatomical organisation has been demonstrated in patients with hemispherectomy and in whom paradoxical lateralisation may still be observed (Barrett et al 1976, Blumhardt et al 1979). Blumhardt and Halliday (1979) postulate that this effect is a result of the ipsilateral recording electrode being positioned almost perpendicular to the current sources which are located mesially in the contralateral hemisphere.

In the present study, latency differences between hemispheres of up to 8ms were seen, which compares favourably with the 12ms found in a study of VEP half fields by

Haimovic and Pedley (1982). It is possible that this effect is due to the maximum amplitude of the P100M occurring at a different latency in each hemisphere as has been recently demonstrated for the VEMR to a pattern onset stimulus in some subjects (Degg et al 1992; in press).

Despite the variation observed in response topography between subjects, the data suggest that a region of the scalp can be identified in which there is a good chance of successfully recording the P2M or P100M using a magnetometer with one or a few channels. The data suggests that a good position would be either 6-9cm above the inion, on the midline or alternatively 2-3 cm to the left of the midline at the same level on the head for both the P2M and the P100M.

The similarity between the P2M and full field P100M maps from the same subject suggest that both stimuli activate similar areas of the visual cortex. This appears to confirm the suggestion that a large check stimulus has a significant luminance component (Celesia et al 1987). However, when the latency of the P2M was plotted against the P100M recorded from the same subject (See Chapter 3), no significant correlation was observed. This suggests that although they may originate in similar regions of visual cortex, the P2M and P100M probably reflect different aspects of visual processing.

Full field stimulation results in a response from both hemispheres of the brain. This may lead to a complex pattern of field topography particularly if small checks are used (Harding et al 1991). However, to evaluate each hemisphere separately requires stimulation of the relevant half field. When recording the response to right half field stimulation, a position 6-9cm above the inion on the midline or, in some patients, 2-3cm to the left, appears to be an appropriate location. For the response to left half field stimulation, it is easier (more comfortable for the subject) to record the more anterior ingoing field component than the more posterior outgoing field. This appears maximally 6-9cm above the inion on the midline or 2-3cm to the right. This reponse is of higher amplitude generally than the outgoing part of the field, possibly because it is easier to locate the probe normal to the scalp in this region.

The preliminary study of the effects of central scotomata on the topography of the response to large check pattern reversal stimulation yielded different results in the two subjects studied. In subject RAA, increasing central occlusion resulted in a more diffuse, but essentially similar field topography in which the amplitudes of the extrema were significantly reduced. This would appear to suggest that both central and peripheral parts of the visual field make a contribution to the full field response. In subject CD the 4^{o} scotoma resulted in a more diffuse field pattern with higher

amplitude extrema, while the 7° scotoma resulted in a field pattern that bore little resemblence to either the full field or 4° scotoma maps. Hence, magnetic reponses to scotomata in individual subjects may be complex. It is assumed that the component chosen for mapping in the case of the scotomata is analagous to the P100M. The longer latency and higher amplitude of the component mapped to a 4° scotoma for subject CD suggests that a component other than the P100M may have been chosen as mapping input. Alternatively, variations in the morphology of the calcarine fissure between the two subjects may have influenced the results. Further investigations of the effects of scotomata on the VEMR are essential to resolve these questions.

The topography of the response to a flash stimulus of increasing intensity are complex and vary widely between individuals. The most consistent location for recording the P2M at all luminance intensities studied would appear to be to be 3-6cm to the right of the inion point. However, with seated subjects it is difficult to locate the detector normal to the scalp at this position. To overcome this problem either a patient bed could be used in which this recording location can be readily reached or an alternative recording location should be used. A more acceptable location, although showing more inter-individual variation, is 3-6cm above the inion on the midline or 2-3cm to either side. This is approximately the location that was used for the population study described in Chapter 3.

A large part of the variation seen between subjects is likely to arise from individual differences in brain morphology. Since the fields detected in magnetometry are neither smeared nor attenuated by the intervening tissues (see Chapter 1) it is to be expected that these morphological differences would be magnified when recording the VEMR compared with the VEP. Before considering this morphological variation, it is necessary to consider how the visual field is represented on the visual cortex. The interpretation of both electrical and magnetic signal is made in relation to the cruciform model of the visual cortex (Okada 1983, Maclin et al 1983, Harding et al 1991). In this model the visual field, divided into octants, is shown to project systematically onto the visual cortex (Figure 5.17). The left visual field is seen to project onto the right hemisphere and conversely for the right visual field. In addition, the lower visual field projects to the upper, cuneal gyrus while the upper visual field projects to the lingual gyrus. There also a retinotopic organisation such that the central visual field is represented on or at the occipital pole while more eccentric retinal locations project progressively deeper along the medial surface of the occipital lobe.

However, this interpretation is complicated by the wide variation seen in occipital morphology in normal subjects. Polyak (1966) commented that "Altogether the

configuration of the calcarine fissure shows almost an infinity of individual variation.....No two brains, or two hemispheres of the same brain are exactly alike".

The angle of the calcarine fissure with respect to the scalp is one of the most obvious sources of variation (Steinmetz et al 1989). This angle exhibits variation both between individuals and also between hemispheres of the same brain (Myslobodsky et al 1991). The angle of the fissure determines not only the extent to which sources are oriented radially or tangentially with respect to the detecting device, but also the distance between the magnetometer and the source, thus influencing the field topography and extrema amplitudes.

If the angle of the calcarine fissure is steep with respect to the scalp (Figure 5.18a) then the sources in the occipital pole, which should theoretically be radially oriented (Z), may have a tangential orientation with respect to the probe at higher locations on the head. Sources in the calcarine fissure (X) would tend to be radial while those lining the cuneal and lingual lips of the gyri (Y) would be more tangential with respect to the scalp. Thus, the sources in the fissure (X) could produce a weaker field than those lining the gyri (Y) which would dominate the field recorded by a probe located normal to the scalp (Harding et al 1991).

In Figure 5.18b the angle of the fissure is much shallower. The sources at the occipital pole are more radial with respect to the scalp. Both the sources in the calcarine fissure (X) and those in the cuneal and lingual gyri (Y) are more tangential with respect to the scalp and so should therefore contribute to the field detected. However, it is also likely that the sources above and below the fissure produce magnetic fields which may mutually cancel (Okada,1983) because they are oppositely directed while those in the cuneal and lingual gyri summate.

Thus, the angle of the calcarine fissure may be a factor which determines the relative contribution made by the different neuronal populations in the visual cortex to the VEMR. In the case of a steep calcarine fissure, there may be a considerable contribution from neurons at the anterior end of the fissure to a large check stimulus and the response may appear higher on the head than that produced by an analogous neuronal population in a shallow fissure. It was also noted that the full field reponses were of higher amplitude over the left than the right hemisphere. This is of interest since Myslobodsky et al (1991) found that the angle of the calcarine fissure could be steeper in the left than the right hemisphere in some subjects, although this trend failed to reach statistical significance in the subject group as a whole.

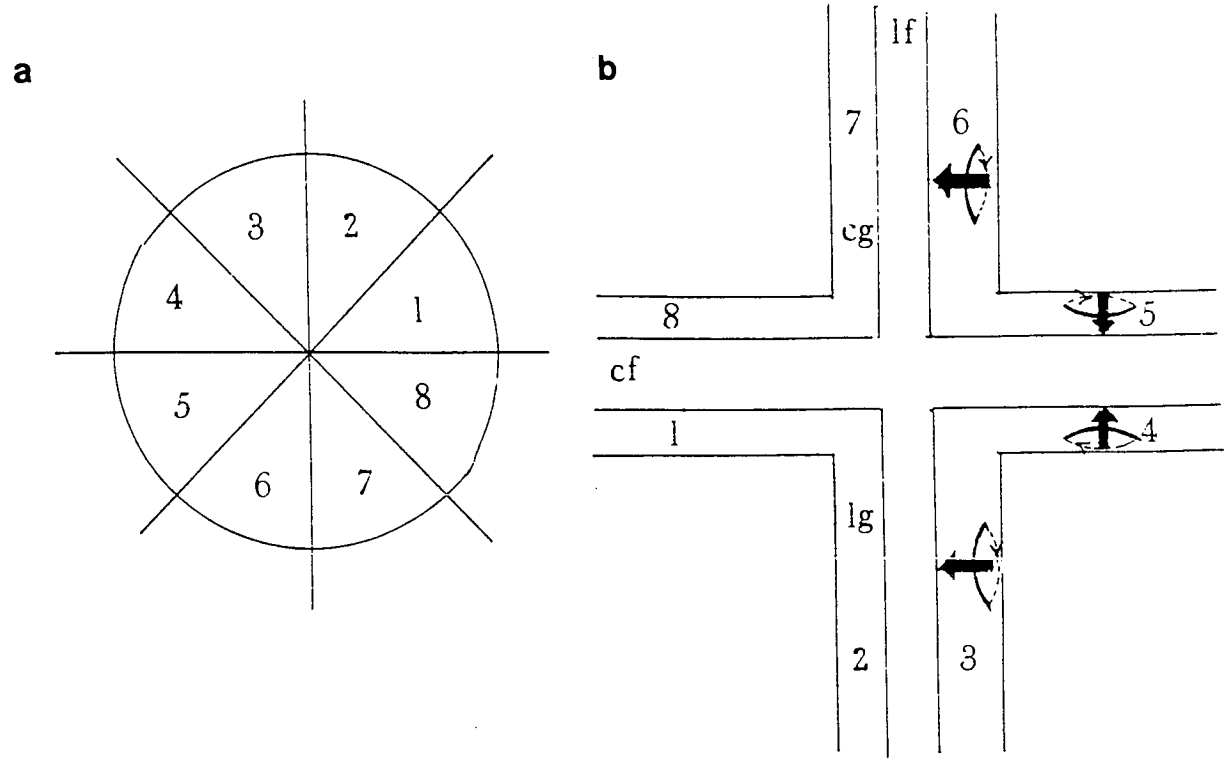

Figure 5.17 : Projection of the visual field, divided into octants (a), onto the visual cortex (b). The arrows indicate dipolar current sources with their associated magnetic field.

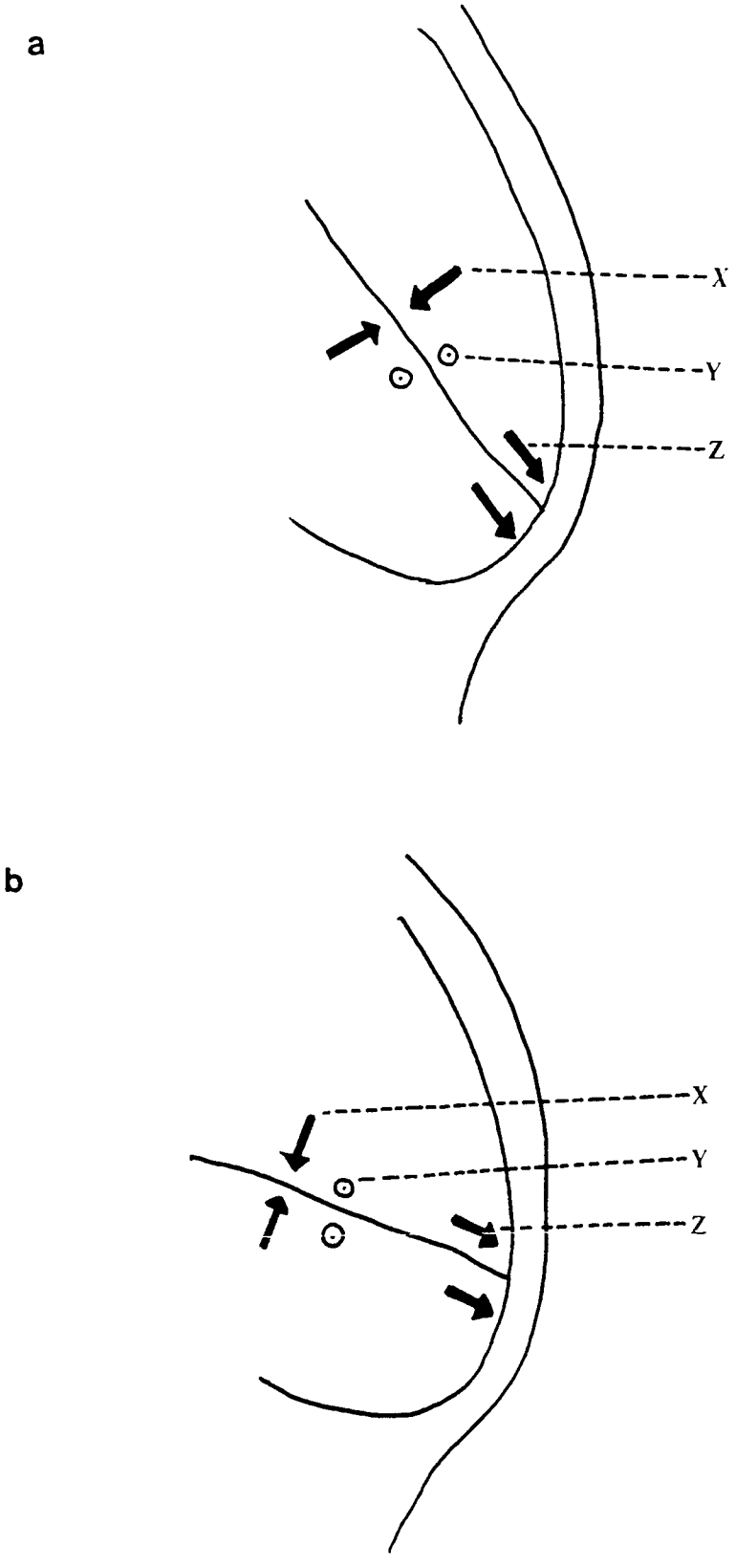

Figure 5.18 : Orientation of sources in the visual cortex as seen in a medial sagittal view of the right hemisphere. a) shows a calcarine fissure with a steep angle while b) shows one of shallower inclination. X = sources in the calcarine fissure, Y = sources in the cuneal and lingual gyri and Z = sources at the occipital pole. ⊙ represents positivity towards the viewer.

However, there may be other reasons for this asymmetry which include differences in the way in which each hemisphere processes information. Spinelli and Mecacci (1990) found evidence of hemispheric differences in the processing of primary visual information. In studies of the pattern reversal VEP, they found that the hemisphere producing the largest response was related to handedness and dependent upon stimulus parameters. In addition, a study by Degg et al (1992; in press) on the VEMR to pattern onset-offset stimulation may support this suggestion. Responses were mapped at 5ms intervals along the waveform for the left and right half field responses. In two male subjects the duration of the response was longer in one hemisphere than the other. In one subject, the persistence occured in the left hemisphere while in the other subject it was in the right hemisphere. There was no evidence of such a difference in the female subjects recorded Cohn et al (1985) cite a number of studies which suggest that there is a greater lateralisation of function in the male than the female brain which could explain this effect. However, the sample size was too small for any significant conclusions to be drawn. The longer duration of the response in one hemisphere may be due to the phenomenon described by Spinelli and Mecacci (1990) who state that although " sensory analysis may sometimes be handled more efficiently by one hemisphere .....such asymmetries are more fragile than higher order ones".

There are further problems in using the cruciform model to interpret magnetic data. Firstly, the calcarine fissure may be neither straight nor continuous (Polyak 1966, Steinmetz et al 1989) and secondly, there may be variations in the extent to which the primary visual cortex (Area B17 or V1) is represented on the outer face of the occipital pole. At the pole the gyri may show wide morphological variation (Polyak 1966, Brindley 1972) and this may have a profound effect on the orientation of the active sources and hence on the response topography.

The central visual field is believed to be represented on or near the occipital pole (Rovamo and Virsu 1979). Sources at the occipital pole are for the most part radially oriented with respect to the scalp and so theoretically should contribute little to the magnetic field recorded. However in some subjects there may be no polar representation of the fovea at the pole (Polyak 1966). Instead the fovea is represented at the posterior end of the calcarine fissure on the medial surface of the occipital lobe. Here the sources may assume a more tangential orientation with respect to the scalp and therefore should contribute to the magnetic field. Moreover, as this area of cortex is closer to the scalp, it may make a significant contribution to the field. This effect should be more apparent using a small check stimulus which is thought to stimulate

the fovea more optimally. If flash stimulation activated primarily foveal sources this may also explain the wider intersubject variation observed in our data.

The results of occluding the central visual field for RAA suggests that part of the reponse to the large check is non-polar in origin. The scotoma prevents stimulation of the central retina and the resultant topography may reflect activity produced by more peripheral retina, and hence, located deeper in the calcarine fissure. Maclin et al (1983) found that annular stimuli presented at various retinal eccentricities gave sources that localised deeper for more peripheral stimulus presentations, a result consistent with this suggestion.

The use of the inion as a reference point for any mapping matrix can also be criticised. Steinmetz et al (1989) found that the variation in the position of the calcarine fissure, around the inion, was approximately 4cm which is twice that seen for the other major fissures. In addition, Myslobodsky et al (1991) found a similar degree of variation in their study and noted a tendency (not reaching statistical significance) for the right calcarine fissure to begin higher up the occiput than the left. In some subjects, the brain may be shifted laterally with respect to the inion or the inion may be located one side of the head. The resultant magnetic fields may be shifted laterally or anteriorly. Without the aid of MRI or CT scans it is not possible to determine the location of the central commissure relative to the nasion-inion line. In subjects where the fissure is high with respect to the inion, particularly if it is steep, then it is possible that the magnetic extrema may lie outside the area covered by the mapping grid.

In some subjects one occipital pole may overlap the other. This could have a number of effects depending on the degree of cortical representation of the central visual field and the nature of the overlap. Hence, a field distribution for one half field may suggest a shallower source than in the hemisphere which is overlapped. In addition, with such an overlap there may be an increased chance that fields produced in the two hemispheres would mutually cancel.

Finally, the shape of the head may also play a role in topographic variation since this influences the location of the detector relative to the scalp. Variation in head shape may be a factor determining the contribution to the external field from secondary sources (see Chapter 1). The problems of each type of mapping matrix have been discussed more fully in the introduction to this chapter. For example, Meijs et al (1987) estimated that a mapping regime which followed the contours of the head could result in secondary sources contributing up to 20% of the field recorded. With the current recording system, the contribution from secondary sources are likely to be greatest at the lower and lateral points where location of the detector normal to the scalp is

especially difficult. Hence, individual differences in head curvature could lead to significant intersubject variation in topography, particularly at the peripheral points of the mapping grid.

In view of the wide range of morphological variations possible, there is a surprising degree of similarity between topographic maps recorded from different individuals. Hence, it may be possible to establish topographic 'norms' and to use them to determine optimal areas of scalp for single channel recording and utimately for clinical diagnosis. However, since there is also variability between subjects, failure to record a response at the expected location may be not a sign of pathology but an indication of unusual occipital topography. These studies suggest that it would be essential to collect topographic 'norms' from across the age span by using a multi-channel magnetometer system to assess and quantify these variations.

Both the group mean maps for the flash P2M and pattern reversal P100M would appear to be consistent with the predictions of the cruciform model. The pattern suggests, for both stimuli, the presence of a source located in each hemisphere with current flow directed towards the midline. The similarity in topography of the P2M and P100M suggests that these responses may reflect activity in a) closely adjacent neuronal populations, b) different neurons in approximately the same location and c) a different aspect of processing in the same neuronal population. The half field maps also appear essentially dipolar and occur over the hemisphere contralateral to the visual field as predicted by the cruciform model.

At the cellular level, the most likely source of these essentially dipolar field patterns are the long apical dendrites of the pyramidal cells which run perpendicular to the surface of the cortex (Okada 1982). These are present in sufficient numbers and have the open field configuration necessary for their activity to summate to produce externally detectable fields (see Chapter 1).

Source localisation carried out on the 20 point mapping data using a single dipole in a sphere model and the least squares method of fitting, gave poor results. One problem of this approach is that a full field stimulus is likely to activate sources in both hemispheres. When dipoles were fitted to the fields over the left and right hemispheres separately the fits achieved were better, but still poor. Previous magnetic studies using visual stimuli appear contradictory with Maclin et al (1983) suggesting adequate single dipole fits while others explain their results as arising from at least two sources in each hemisphere (Brenner et al 1981, Okada 1982, Okada et al 1982).

Problems may also arise from the use of a mapping matrix which followed the head contour because secondary sources contribute to the recorded responses. Where a full field stimulus has been used, a pair of extrema may appear over each hemisphere. However, if the upper extrema are stronger by virtue of the detector being located closer and more normal to the scalp at these locations, then a source localisation program directed to fit a single dipole, may result in a spurious fit to the data.

It is also possible that a 20 point mapping grid is too coarse for accurate source localisation. With a coil diameter of 2cm, recording at points 2.8 to 3.1cm apart means that field information is being lost between recording positions since the gradient of the magnetic field can change rapidly over the scalp. The resolution should be better for the 42 point maps where the recording points were only 2cm apart.

Another problem is the sequential recording of magnetic signals at different locations on the scalp which is inevitable when using a single channel system. It is an assumption of such recording that environmental conditions are duplicated exactly while recording at each location. However, subject and environmental noise and subject arousal and concentration may vary systematically over a recording session and influence the recording of a topographical map. Clearly, a multi-channel system employing sufficient channels to construct a map using one or a small number of runs is essential to eliminate this source of error.

Source localisation carried out on the 42 point mapping data (full and half field pattern reversal P100M and flash P2M) gave slightly better dipole fits but the proceedure was still susceptible to the aforementioned problems associated with the 20 point maps. The source producing the right half field response was localised to the left hemisphere at a depth of approximately 2cm below the scalp. However, the full field pattern reversal P100M and flash P2M maps were more problematic. Both stimuli are likely to produce activity in both hemispheres and so one would expect that a least two sources would need to be fitted to produce a statistically adequate fit. However, the best fits were achieved with a single dipole in each case. This may be a consequence of the activity in the left hemisphere being more dipolar and of higher amplitude than that in the right hemisphere. The source localised for the full field pattern reversal map appeared to be in the left hemisphere at a depth of around 5cm below the scalp while that producing the flash P2M again localised to the left hemisphere, 2cm below the scalp, and lower on the head than the P100M. Although the data are not accurate enough to allow distinction to be made between Areas B17 and 18, the data may suggest that the flash stimulus activates more foveal sources than the large check pattern reversal stimulus.

Hence, it is possible to recommend a region of scalp over which is likely that a response may be recorded to large check pattern reversal full and half fields and flash stimuli in an unknown subject. As an extension to this work, topographic studies are needed to quantify changes in topography across the age span. In addition, the presence of a central scotoma may affect the topography of the magnetic response even when a large check is used and this could have possible clinical relevance. The 20 point maps were adequate for the purpose of indicating the variation in response topography between individuals but the source localisations carried out on them were too poor to yield useful information about visual processing. Although the 42 point mapping grid may provide more adequate coverage of the occipital scalp, source localisation remained poor. For studies of the origins of the P2M and P100M a specific mapping protocol needs to be designed for source localisation. This may necessitate the use of a shielded room and mapping on a spherical surface. The latter would require a versatile gantry and the ability to locate the detector accurately.

CHAPTER 6

GENERAL CONCLUSIONS, FURTHER WORK AND PROTOCOL RECOMMENDATIONS

6.1 INTRODUCTION

Compared with the auditory system, there have been relatively few studies of the visual system using MEG. This is probably due to the problem of generating a magnetically quiet and visually adequate stimulus and to the problems of relating magnetic responses to the complex and variable morphology of the occipital lobe. In addition, many of the currently important questions which relate to visual processing are concerned with locating precisely in the cortex where various aspects of visual information are processed. A single channel magnetometer system, the commonest system in use to date, would appear unequal to the task of accurate source localisation. Hence, many current and future research applications require a multichannel system. The cost of such a system with its associated hardware (ie. a magnetically shielded room) would probably prove prohibitive. In addition, maintaining and running such a system requires personnel trained in a variety of specialised fields. These factors will limit the clinical application of MEG unless a unique diagnostic role is found. Although not divorced from these problems the single channel system may be more likely to see clinical use at least in the short term.

The major objective of this thesis was to investigate a number of the fundamental problems of using a single channel MEG system in an unshielded clinical environment. Many of these questions may also apply to the use of a multichannel system. In the following section, the major findings of this thesis are summarised. Subsequently protocol recommendations for the recording of patients will also be made and areas requiring further investigation emphasised.

6.2 GENERAL CONCLUSIONS

1. There may be a significant increase in latency of the pattern reversal P100M in normal subjects after 55 years of age. This result requires confirmation with further more detailed age series. If confirmed, it would imply that norms in the elderly would have to be established for shorter age intervals than each decade. In addition, since there is evidence that the latency of the electrical P100 increases more rapidly with age for small than large checks (Sokol et al 1981), this would also have to be tested magnetically since a small check stimulus could be useful in certain clinical protocols.

In elderly subjects there was a tendency for the VEMR to be of small amplitude. It was assumed that the largest positive component within 200ms was the true P100M in each case. However, this may not be the case since there may be a difference in the topography of the P100M response in the elderly or possibly, the appearance of a new component as a result of brain atrophy (Blumhardt 1987). Topographic studies across the age span are therefore essential to allow better component identification in the elderly especially.

2. There is significant minute to minute variation in the latency and amplitude of the P100M. Although magnetic shielding may improve the reproducibility of the P100M to a degree, there may be other causes of this variation which need to be identified and possibly taken into account. However if significant variation is present, two strategies can be adopted a) record until two consecutive P100Ms are consistent or b) take an average of several responses. If the latter is used then the number of responses needs to be established and this would have to take into account the number of different stimuli used in the clinical test.

In addition, longer term temporal variability needs to be studied over months or even years to test whether the VEMR is stable and therefore, whether it can be used in longitudinal studies.

3. The absolute latency of the P100M and the degree of run to run variation may be dependent upon the system used. This means that each laboratory must establish its own set of normative data. Further work is necessary to establish the source(s) of this variability.

4. The most successful VEMRs were obtained to a large check pattern reversal stimulus presented in a large field. It was more difficult to record consistent VEMR to small check stimuli presented in a small field in the unshielded environment. Magnetic shielding may be of some help in reducing the extent of this problem, otherwise the diagnostic use may be limited if norms are difficult to establish with small checks. However, large checks could be useful for studying conditions which affect the more peripheral parts of the retina, eg. in some cases of optic neuritis or vascular diseases of the retina.

5. The optical blur data indicate that it is unnecessary to correct vision in subjects when using a large check stimulus. Optical blurring of the stimulus produced little effect on the latency and amplitude of the P100M when large checks were used. However, significant increases in latency were observed with increased blurring of small checks. If correction of vision is necessary then this could

be accomplished best using a non-magnetic trial frame and lens set since many normal spectacles create excessive magnetic artifacts.

6. The flash intensity data suggests that if flash is to be used as a stimulus then the flashes should be of relatively high intensity. At high stimulus intensities the flash P2M was of higher amplitude and the shape of the component was better defined. This may be of particular advantage in elderly subjects in which the response amplitude appeared to decline with increasing subject age. As has been noted previously, a flash stimulus in combination with a pattern reversal stimulus may be of use in the diagnosis of Alzheimer's disease (Armstrong et al 1989).

7. The topography of the VEMR over the scalp to full and half field pattern reversal stimulation varied between subjects. Group average maps can be used to suggest recording positions at which it is probable that the P100M can be recorded in a new patient. However, individual variations in topography imply that the absence of a response is not necessarily an indication of pathology. If a magnetometer with a single or few channels is used, the recording protocol must take this variation into account. The half field responses may be more consistent between subjects than the full fields and could possibly give more consistent normative data. Since topography may also vary across the age span, topographic variation with age needs to be studied preferably using a multichannel system to establish the extent of this variation.

8. The topography of the flash P2M is similar to that for large check full field pattern reversal stimulation. In addition, flash and pattern maps for the same individual show considerable similarity. This may result from the large check pattern reversal stimulus having a significant luminance component (Celesia et al 1987). However, no significant correlation could be found between the latencies of the P2M and the P100M in the same subject ($r = 0.18$, $p>0.05$; see Chapter 3) which suggests that the responses reflect different aspects of visual processing in the same or closely adjacent neuronal populations.

9. Source localisation results were relatively poor but may suggest that the flash response results from activation of a shallower neural population. However, the system and protocol used was not adequate for accurate source localisation of the P2M and P100M. More precise stimuli should be used ie. half or quarter fields, and the mapping protocol should incorporate mapping in a sphere as close to the head as possible.

10. Varying stimulus parameters may have a greater effect on the

VEMR than the corresponding VEP. Change in latency with check size and intensity appeared to be greater for the VEMR than the VEP. This requires further study in which the EEG and MEG are recorded at the same time. If these results are confirmed, then it suggests that the P100M and P2M may reflect only part of the response seen in the VEP. This increase in sensitivity could be particularly important clinically since it implies that the VEMR may, in some circumstances, be more sensitive to pathology than the VEP.

6.3 PROTOCOL RECOMMENDATIONS

As a result of these studies, the following recommendations as to a protocol for recording the VEMR will be outlined.

1. An introductory talk should be given to the patient for about ten minutes prior to the recording session. The protocol should be carefully explained, as simply and concisely as possible. This procedure relaxed patients in our own study and made the recording of the VEMR considerably easier. Particular care may be needed when a shielded room is used since even normal subjects can feel anxious and claustrophobic in the enclosed space.

2. All jewellery, particularly earrings and hair clips should be removed from the patient. Hearing aids, which produce a large magnetic artifact, should not be removed until after the subject has been fully instructed. It would be advisable to include a statement in the patient appointment letter regarding the wearing of underwired bras' or corsets since these also create considerable artifacts.

3. The subject should be correctly refracted if a small check stimulus is to be used. A non-magnetic trial frame and lenses of appropriate prescription should be used. However, the majority of subjects should not need refracting if a large check or flash stimulus is used. If no response to a large check can be obtained from subjects with relatively high myopia, then correction may be necessary.

4. The subject should be located as comfortably as possible under the magnetometer, regardless of the patient support system. The magnetometer should be situated over the area of scalp found most likely to give a large amplitude response. For a large check, full field pattern reversal P100M and the flash P2M (Intensity 8) this location is 6-9cm above the inion on the midline or 2-3cm to the left. If no response can be recorded at this location then using a higher intensity flash stimulus could be used with the magnetometer located at a more lateral position or slightly lower on the scalp should be attempted. If the patient is co-operative, recording at 9 points widely spaced

over the scalp may be useful in establishing the approximate location of the maxima.

5. The subject should be instructed to fixate a particular point on the stimulus and asked to mentally count the flashes or reversals. Fixation should be carefully monitored during the recording session particularly in the elderly. Deviation from the fixation point and reduced attention can lead to attenuation in the amplitude of the P100M.

6. To obtain an estimate of component latency in an unshielded laboratory to compare with age matched norms or with a future recording in the same patient, an average should be taken of a number of responses.

REFERENCES

Adrian E.D. and Mathews B.H.C. (1934).
The Berger rhythm - potential changes from the occipital lobes of man.
Brain 57 : 355-385.

Aine C.J., Bodis-Wollner I. and George J.S. (1990).
Generation of visually evoked magnetic responses : spatial frequency segregation and evidence for multiple sources.
In : Advances in Neurology : Volume 54 : 141-155.
Eds. : S. Sato. Publisher : Raven Press, New York.

Allison T., Wood C.C. and Goff R. (1983).
Brain stem auditory, pattern reversal visual and short latency somatosensory evoked potentials : latencies in relation to age, sex and brain size.
Electroencephalography and Clinical Neurophysiology 55 : 619-636.

Allison T., Hume A.L., Wood C.C. and Goff R. (1984).
Developmental and aging changes in somatosensory, auditory and visual evoked potentials.
Electroencephalography and Clinical Neurophysiology 58 : 14-24.

Armstrong P. and Wastie M.L. (1987).
Diagnostic Imaging(Second Edition)
Publisher : Blackwell, Oxford and London.

Armstrong R.A., Myers D. and Smith C.U.M. (1989).
Further studies on the patterns of senile plaques of the Alzheimer Type (SDAT) with a hypothesis on the colonisation of the cortex.
Neuroscience Research Communications Vol. 4, No. 1 : 17-24.

Armstrong R.A., Janday B.S., Slaven A. and Harding G.F.A. (1990).
The use of flash and pattern evoked fields in the diagnosis of Alzheimer's Disease.
In : Advances in Biomagnetism : 315-318.
Eds. S.J. Williamson, M. Hoke, G. Stroink and M. Kotani. Publisher : Plenum Press, New York.

Armstrong R.A., Slaven A. and Harding G.F.A. (1991).
The influence of age on the pattern and flash visual evoked magnetic response (VEMR).
Ophthalmic and Physiological Optics 11 : 71-75.

Asselman P., Chadwick D.W. and Marsden C.D. (1975).
Visual evoked responses in the diagnosis and management of patients suspected of multiple sclerosis.
Brain 98 : 261-282.

Bajalan A.A.A., Wright C.E. and Van der Vliet V.J. (1986).
Changes in the human visual evoked potential caused by the anticholinergic agent hyocsine hydrobromide, comparison with results in Alzheimer's Disease.
Journal of Neurology, Neurosurgery and Psychiatry 49 : 175-182.

Balish M. and Sato S. (1989).
Magnetoencephalograph in epilepsy research and its perspectives.
In : Advances in Biomagnetism : 269 272.
Eds. S.J. Williamson, M. Hoke, G. Stroink and M. Kotani. Publisher : Plenum Press, New York.

Barkley G.L., Tepley N., Simkins R., Moran J. and Welch K.M.A. (1990).
Neuromagnetic fields in migraine : preliminary findings.
Cephalgia 10 : 171-176.

Barrett G., Blumhardt L., Halliday A.M., Halliday E. and Kriss A. (1976).
A paradox in the lateralisation of the visual evoked response.
Nature 261 : 253-255.

Barth D.S., Sutherling W., Engel J. and Beatty J. (1982).
Neuromagnetic localisation of epileptiform activity in the human brain.
Science 218 : 891-894.

Barth D.S., Sutherling W., Engel J. and Beatty J. (1984).
Neuromagnetic evidence of spatially distributed sources underlying epileptiform spikes in the human brain.
Science 223 : 293-296.

Barth D.S., Sutherling W., Broffmann J. and Beatty J. (1986).
Magnetic localisation of a dipolar current source implanted in a sphere and a human cranium.
Electroencephalography and Clinical Neurophysiology 63 : 260-273.

Bartl G., Van Lith G.H.M. and Van Marle G.W. (1978).
Cortical potentials evoked by a TV pattern reversal stimulus with varying check sizes and stimulus field.
British Journal of Ophthalmology 62 : 216-219.

Baule G.M. and McFee R. (1965).
Detection of the magnetic field of the heart.
The American Heart Journal 66 : 95-96.

Beck R.W. and Smith C.H. (1988).
Neuro-ophthalmology : a problem oriented approach.
Publisher : Little Brown and Company, Boston and Toronto.

Becker W.J. and Richards I.M. (1984).
Serial pattern shift visual evoked potentials in multiple sclerosis.
Canadian Journal of Neurological Science 11 : 53-59.

Blakemore C.B. and Vital-Durand F. (1981).
Distribution of X and Y cells in the monkey's lateral geniculate nucleus.
Journal of Physiology 320 : 17-18.

Blumhard L.D. and Halliday A.M. (1979).
Hemisphere contributions to the composition of the pattern evoked potential waveform.
Experimental Brain Research 36 : 53-69.

Blumhard L.D., Barrett G., Kriss A. and Halliday M. (1982).
The pattern evoked potential in lesions of the posterior visual pathways.
Annals of the New York Academy of Science 388 : 264-289.

Blumhard L.D. (1987).
The abnormal pattern visual evoked response in neurology.
In : A Textbook of Clinical Neurophysiology : 307-342.
Eds. A.M. Halliday, S.R. Butler and R. Paul. Publisher : John Wiley and Sons, New York and Toronto.

Bobak P., Bodis-Wollner I. and Guillory S.L. (1987).
The effect of blur and contrast on VEP latency : comparison between check and sinusoidal grating patterns.
Electroencephalography and Clinical Neurophysiology 68 : 247-255.

Bodis-Wollner I., Feldman R.G., Guillory S.L. and Mylin L. (1987).
Delayed visual evoked potentials are independent of pattern orientation in macular disease.
Electroencephalography and Clinical Neurophysiology 68 : 172-179.

Bodis-Wollner I., Yahr M., and Thornton J. (1987).
Interocular VEP latency differences and the effect of treatment in Parkinsons Disease.
Electroencephalography and Clinical Neurophysiology 50 : 220P.

Brenner D., Williamson S.J. and Kaufman L. (1975).
Visually evoked magnetic fields of the human brain.
Science 190 : 480.

Brenner D., Okada Y., Maclin E., Williamson S.J. and Kaufman L. (1981).
Evoked magnetic fields reveal different visual areas in human cortex.
In : Biomagnetism : Proceedings of the 3rd International Workshop on Biomagnetism : 431-444.
Eds. S.N. Erne, H-D. Hahlbohm and H. Lubbig. Publisher : Walter de Gruyter, Berlin.

Brindley G.S. (1972).
The variability of the human striate cortex.
Journal of Physiology 225 : 1P-3P.

Cant B.R., Hume A.L. and Shaw N.A. (1978).
Effects of luminance on the pattern visual evoked potential in multiple sclerosis.
Electroencephalography and Clinical Neurophysiology 45 : 496-504.

Carpenter R.H.S. (1984, 1990).
Neurophysiology.
In : Physiological Principles in Medicine Series.
Eds. R.N. Hardy, M. Hobsley and Saunders K.B. Publisher Edward Arnold, London.

Carelli P., Modena I. and Romani G.L. (1983).
Detection coils.
In : Biomagnetism : An Interdisciplinary Approach : 85-100. NATO ASI Series.
Eds. S.J. Williamson, G. Romani, L. Kaufman and I. Modena. Publisher : Plenum Press, New York and London.

Carelli P. and Leoni R. (1986).
Localisation of biological sources with arrays of superconducting gradiometers.
Journal of Applied Physics 59 : 645-650.

Carroll W.M. and Mastaglia F.L. (1979).
Leibers Optic Neuropathy : a clinical and visual evoked potential study of affected and asymptomatic members of a six generation family.
Brain 102 : 559-580.

Carroll W.M., Kriss A., Baraitser M., Barrett G. and Halliday A.M. (1980).
The incidence and nature of visual pathway involvement in Freidrichs Ataxia : a clinical and visual evoked potential study of 22 patients.
Brain 103 : 413-434.

Celesia G.G., Polcyn R.D., Holden J.E., Nickles R.J., Gatley J.S. and Koeppe R.A. (1982).
VEPs' and PET mapping of regional cerebral blood flow and cerebral metabolism : can the neuronal potential generators be visualised.
Electroencephalography and Clinical Neurophysiology 54 : 243-256.

Celesia G.G. and Daly R.F. (1977).
Effects of aging on the visual system.
Archives of Neurology 34 : 403-407.

Celesia G.G., Kaufman D. and Cone S. (1987).
Effects of age and sex on pattern electroretinograms and visual evoked potentials.
Electroencephalography and Clinical Neurophysiology 68 : 161-171.

Ciganek L. (1969).
Variability of the human visual evoked potential : normative data.
Electroencephalography and Clinical Neurophysiology 27 : 35-42.

Cobb W.A. and Dawson G.D. (1960).
The latency and form in man of the occipital potentials evoked by bright flashes.
Journal of Physiology 152 : 108-121.

Cohen D. (1968).
Magnetoencephalography : Evidence of magnetic fields produced by alpha rhythm currents.
Science 161 : 784-786.

Cohen D. (1983).
Steady fields of the body.
In : Biomagnetism : An Interdisciplinary Approach : 328-339. Nato ASI Series.
Eds. S.J. Williamson, G.L. Romani, L. Kaufman and I. Modena.
Publisher : Plenum Press, New York York and London.

Cohen D., Edelsack E.A. and Zimmerman J.P. (1970).
Magnetocardiograms taken inside a shielded room with a superconducting point contact magnetometer.
Applied Physics Letters Vol. 16, No. 7 : 278-280.

Cohen D. and Cuffin B.N. (1983).
Demonstration of useful differences between the magnetoencephalogram and electroencephalogram.
Electroencephalography and Clinical Neurophysiology 56 : 38-51.

Cohn N.B. and Hurley C.W. (1985).
Differential visual evoked cortical responses to direct and peripheral stimulation in man.
Electroencephalography and Clinical Neurophysiology 61 : 157-160.

Cohn N.B., Kircher J., Emmerson R.Y. and Dustman R.E. (1985).
Pattern reversal evoked potentials : age, sex and hemispheric asymmetry.
Electroencephalography and Clinical Neurophysiology 62 : 399-405.

Collins D.W.K., Carroll W.M., Black J.L. and Walsh M. (1978).
Pattern reversal visual evoked potentials.
Journal of Neurological Science 36 : 83-95.

Collins D.W.K., Carroll W.M., Black J.L. and Walsh M. (1979).
Effect of refractive error on the visual evoked response.
British Medical Journal 6158 : 231-232.

Cooper R., Winter A.L., Crow H.J. and Gray Walter W. (1965).
Comparison of subcortical, cortical and scalp activity using chronically indwelling electrodes in man.
Electroencephalography and Clinical Neurophysiology 18 : 217-228.

Cosi V., Vitelli E., Gozzoli L., Corona A., Ceroni M. and Calleico R. (1982).
Visual evoked potentials in aging of the brain.
In : Clinical Application of Evoked Potentials in Neurology : 109-115.
Eds. J. Courjon, F. Maugiere M. Revol. Publisher : Raven Press, New York.

Crum D. (1985).
The design and use of dewars for biomagnetic measurements.
In : Biomagnetism : Applications and Theory : 21-28.
Eds. H. Weinberg, G. Stroink and T. Katila. Publisher : Pergammon Press, New York.

Cuffin B.N. (1985).
Effects of fissures in the brain on electroencephalograms and magnetoencephalograms.
Journal of Applied Physics 57 (1) : 146-153.

Cuffin B.N. (1990).
Effects of head shape on EEGs and MEGs.
IEEE Transactions on Biomedical Engineering 37(1) : 44-52.

Cuffin B.N. and Cohen D. (1979).
Comparison of the magnetoencephalogram and electroencephalogram.
Electroencephalography and Clinical Neurophysiology 47 : 132-146.

Degg C., Armstrong R.A., Slaven A. and Harding G.F.A. (1991).
The visual evoked magnetic response to a pattern onset stimulus.
In : Proceedings of the 8th International Conference on Biomagnetism :
Munster.

Degg C., Slaven A. and Armstrong R.A. (1992).
Chronotopography of the visually evoked magnetic response to a pattern onset stimulus.
Ophthalmic and Physiological Optics (in press).

De Voe R.G., Ripps H. and Vaughan H.G. (1968).
Cortical responses to stimulation of the human fovea.
Vision Research 8 : 135-147.

De Weerde A.W. and Jonkman E.J. (1982).
Changes in visual and short latency somatosensory evoked potentials in patients with multiple sclerosis.
In : Clinical Application of Evoked Potentials in Neurology : 527-534.
Eds. J. Courjon, F. Maugiere and M. Revol. Publisher : Raven Press, New York.

Diener H.C. and Scheibler H. (1980).
Follow up studies of visual potentials in multiple sclerosis evoked by checkerboard and foveal stimulation.
Electroencephalography and Clinical Neurophysiology 49 : 490-496.

Dolman C.L., McCormick A.O. and Drance S.M. (1980).
Aging of the optic nerve.
Archives of Ophthalmology 98 : 2053-2058.

Drasdo N. (1976).
A method of eliciting pattern specific responses and other electrophysiological signals in human subjects.
British Manual of Physiological Optics 31 : 14-22.

Ducati A., Fara E. and Mohl E.D.F. (1988).
Neuronal generators of the visual evoked potential : Intracerebral recording in awake humans.
Electroencephalography and Clinical Neurophysiology 71 : 89-99.

Duret D. and Karp P. (1983).
Instrumentation for Biomagnetism
Il Nuovo Cimento 2(2) : 123-141.

Dustman R.E. and Beck E.C. (1966).
Visually evoked potentials : amplitude changes with age.
Science 151 : 1013-1014.

Dustman R.E., Shearer D.E. and Snyder E.W. (1982).
Age differences in augmenting/reducing of occipital visual evoked potentials.
Electroencephalography and Clinical Neurophysiology 54 : 99-110.

Enroth-Cugell C. and Robson J.G. (1966).
The contrast sensitivity of retinal ganglion cells of the cat.
Journal of Physiology 187 : 517-552.

Erne S.N. (1983).
SQUID sensors.
In : Biomagnetism : An Interdisciplinary Approach : 69-84. Nato ASI Series.
Eds. S.J. Williamson, G. Romani, L. Kaufman and I. Modena. Publisher : Plenum Press, New York.

Erne S.N. and Romani G.L. (1985).
Performance of higher order gradiometers for biomagnetic source localisation.
In : SQUID '85 : Superconducting Quantum Interference Devices and their Applications : 951-961.
Eds. H-D. Hahlbohm and H. Lubbig. Publisher : Walter de Gruyter, Berlin and New York.

Faust U., Heintel H. and Hock R. (1978).
Age dependence of the P2 latency of visually evoked cortical responses to checkerboard pattern-reversal.
EEG and EMG 9 : 219-221.

Fazakas F. (1990).
Neuroimaging of dementia.
Current Opinion in Neurology and Neurosurgery 3 : 103-107.

Ferris S.H. and Leon M.J. (1983).
The PET scan in the study of Alzheimer's disease.
In : Alzheimer's Disease - The Standard Reference : 286-291.
Ed. B. Reisberg. Publisher : MacMillan, London and New York.

Gallop J.C. and Petley B.W. (1976).
SQUIDs and their applications.
Journal of Physics 9 : 417-429.

Gott P.S., Weiss M.H., Apuzzo M.and Van de Meulen J.P. (1979).
Checkerboard visual evoked responses in evaluation and management of pituitary tumours.
Neurosurgery 5(5) : 553-558.

Haimovic I.C and Pedley T.A. (1982).
Hemifield pattern reversal visual evoked potentials : I normal subjects.
Electroencephalography and Clinical Neurophysiology 54 : 111-120.

Halliday A.M., McDonald W.I. and Mushin J. (1972).
Delayed visual evoked response in optic neuritis.
The Lancet May 6th : 982-985.

Halliday A.M., McDonald W.I. and Mushin J. (1973).
Delayed pattern evoked responses in optic neuritis in relation to visual acuity.
Transactions of the Ophthalmological Society UK 93 : 315-324.

Hallpike J.F. (1983).
Clinical aspects of multiple sclerosis.
In : Multiple Sclerosis.
Eds. J.F. Hallpike C.W.M. Adams and W.W. Tourtellote. Publisher : Williams and Wilkins, Baltimore.

Hammond S.R., MacCallum S., Yiannikas C., Walsh J.C. and McLeod J.G. (1987).
Variability on serial testing of pattern reversal visual evoked potential latencies from full field, half field and foveal stimulation in control subjects.
Electroencephalography and Clinical Neurophysiology 66 : 401-408.

Hammond S.R. and Yiannikas C. (1986).
Contribution of pattern reversal foveal and half field stimulation to analysis of VEP abnormalities in multiple sclerosis.
Electroencephalography and Clinical Neurophysiology 64 : 101-118.

Harding G.F.A. (1974).
The visual evoked response.
Advances in Ophthalmology 28 : 2-28.

Harding G.F.A. (1982).
The flash visual evoked response and its use in ocular conditions.
Journal of Electrophysiological Technology 8 : 63-78.

Harding G.F.A. (1988).
Neurophysiology of vision and its clinical applications.
In : Optometry : 44-60.
Eds. K. Edwards and R. Llewellyn. Publisher : Butterworths, London.

Harding G.F.A., Crews S.J. and Good P. (1980).
The VEP as a diagnostic aid in neuro-ophthalmic disease.
In : Evoked Potentials : 235-241.
Ed. C. Barber. Publisher : MTP Press, Lancaster.

Harding G.F.A., Doggett C.E., Orwin A. and Smith E.J. (1981).
Visual evoked potentials in Presenile dementia.
In : Documenta Ophthalmologica Proceedings Series 27 : 193-202.
Eds. H. Spekreijse and P.A. Apkarian. Publisher : Dr. W. Junk, The Hague, Boston and London.

Harding G.F.A., Wright C.E. and Orwin A. (1985).
Primary presenile dementia : the use of the visual evoked potential as a diagnostic indicator.
British Journal of Psychiatry 147 : 533-541.

Harding G.F.A. and Wright C.E. (1986).
Visual evoked potentials.
In : Optic Neuritis : 230-254.
Eds. R.F. Hess and C.T. Plant. Publisher : Cambridge University Press, Cambridge.

Harding G.F.A., Janday B.S. and Armstrong R.A. (1991).
Topographic mapping and source localisation of the pattern reversal visual evoked magnetic response.
Brain Topography 4 : 47-55.

Hari R., Joutsiniemi S.L. and Sarvas J. (1988).
Spatial resolution of neuromagnetic records : theoretical calculations in a spherical model.
Electroencephalography and Clinical Neurophysiology 71 : 64-72.

Hari R., Hamalainen H., Hamalainen M., Kekoni J., Sams M. and Tukonen J. (1990).
Separate finger representations at the human second somatosensory cortex.
Neuroscience 37 : 245-249.

Harter M.R. (1970).
Evoked cortical responses to checkerboard patterns : effect of check size as a function of retinal eccentricity.
Vision Research 10 : 1365-1376.

Harter M.R. and White C.T. (1968).
Effects of contour sharpness and check size on visually evoked cortical potentials.
Vision Research 8 : 701-711.

Harter M.R. and White C.T. (1970).
Evoked cortical responses to checkerboard patterns : effect of check size as a function of visual acuity.
Electroencephalography and Clinical Neurophysiology 28 : 48-54.

Hennerici M., Wenzel D. and Freund H.J. (1977).
The comparison of small size rectangle and checkerboard stimulation for the evaluation of delayed visual evoked responses in patients suspected of multiple sclerosis.
Brain 100 : 119-136.

Hinton D.R. (1986).
Optic nerve degeneration in Alzheimer's Disease.
New England Journal of Medicine 315 : 485-487.

Hobley A. (1988).
An investigation of the primary response of the flash visual evoked response.
PhD Thesis, Aston University.

Hodgkin A.L. (1958).
Ionic movements and electrical activity in giant nerve fibres.
Proceedings of the Royal Society 148 : 1-37.

Hodgkin A.L. and Horowicz P. (1959).
The influence of potassium and chloride ions on the membrane potential of single muscle fibres.
Journal of Physiology 8 : 127-160.

Hoeppner T., Bergen D. and Morrell F. (1980).
Visual evoked potentials after partial occipital lobectomy.
Electroencephalography and Clinical Neurophysiology 50 : 184P.

Hoeppner T. and Lolas F. (1978).
Visual evoked responses and visual symptoms in multiple sclerosis.
Journal of Neurology, Neurosurgery and Psychiatry 41 : 493-498.

Hoke M., Pantev C., Lutkenhoner B. and Lehnertz K. (1989).
Objective evidence of tinnitus in auditory evoked magnetic fields.
Hearing Research 37 : 281-286.

Hoke M., Pantev C., Lutkenhoner B., Lehnertz K. and Surth W. (1989).
Magnetic fields from the auditory cortex of a deaf human individual occuring spontaneously or evoked by stimulation through a cochlear prosthesis.
Audiology 28 : 152-170.

Huang J.C., Nicholson C. and Okada Y. (1990).
Distortion of magnetic evoked fields and surface potentials by conductivity differences at boundaries in brain tissue.
Biophysics Journal 57 : 1155-1166.

Hubel D.H. (1988).
The architecture of the visual cortex.
In : Eye, Brain and Vision : 93-127. Publisher : Scientific American Library, New York.

HughesJ.R., Stone J.L., Fino J.J. and Hart L.A. (1987).
Usefulness of different stimuli in visual evoked potentials.
Neurology 37 : 656-662.

Janday B.S., Swithenby S.J. and Thomas I.M. (1987).
Combined magnetic field and electrical potential investigation of the visual pattern reversal response.
In : Biomagnetism '87 : 6th International Conference on Biomagnetism : 246-249.
Eds. K. Atsumi, M. Kotani, S. Ueno, T. Katila and S. Williamson.

Jansen B.H. and Brandt M.E. (1991).
The effect of the phase of alpha activity on the averaged visual evoked response.
Electroencephalography and Clinical Neurophysiology 80 : 241-250.

Jeffreys D.A. and Axford J.G. (1972).
Source locations of pattern specific components of human visual evoked potentials I : Component of striate cortical origin.
Experimental Brain Research 16 : 1-21.

Jones K.G. and Armington J.C. (1977).
The removal of alpha rhythm from the Visual Evoked Cortical Potential by means of selective averaging.
Vision Research 17 : 949-956.

Jones K.G. and Blume W.T. (1985).
Aberrant waveforms to pattern reversal stimulation : clinical significance and electrographic solutions.
Electroencephalography and Clinical Neurophysiology 61 : 472-481.

Josephson B.D. (1962).
Possible new effects in superconductive tunnelling.
Physics Review Letters 1 : 251.

Kaplan E. and Shapley R.M. (1982).
X and Y cells in the lateral geniculate nucleus of macaque monkeys.
Journal of Physiology 330 : 125-143.

Kaplan E., Lee B. and Shapley R.M. (1991).
New Views of Primate Retinal Function.
In : Progress in Retinal Research : 273-336.
Eds. N. Osborne and J. Cohaden. Publisher : Pergammon Press, Oxford.

Katila T. (1989).
Principles and applications of SQUID sensors.
In : Advances in Biomagnetism : 19-31.
Eds. S.J. Williamson, M. Hoke, G. Stroink and M. Kotani. Publisher : Plenum Press, New York.

Katz B. and Rimmer S. (1989).
Ophthalmologic manifestations of Alzheimer's Disease.
Survey of Ophthalmology 34 : 31-43.

Kaufman L., Okada Y., Tripp J. and Williamson S.J. (1984).
Brain and Information.
Annals of the New York Academy of Science 425 : 722-742.

Kaufman L. and Williamson S.J. (1986).
The neuromagnetic field.
In : Evoked Potentials : 85-98.

Kaufman L., Kaufman J.H. and Wang J.Z. (1991).
On cortical folds and neuromagnetic fields.
Electroencephalography and Clinical Neurophysiology 79 : 211-226.

Kobayashi T, Mukui M., Ii M., Takeuchi F.and Kuriki S. (1991).
Contribution of the volume current for the source localisation of the dipole fields.
Proceedings of the 8th International Conference on Biomagnetism : 73-74. Munster.

Kouijzer W.J.J., Stok C.J., Reits D., Dunajski Z., Lopes da Silva F.H. and Peters M.J. (1985).
Neuromagnetic fields evoked by a patterned on-offset stimulus.
IEEE Transactions on Biomedical Engineering 32(6) : 455-458.

Krauskopf J., Klemic G., Lounasmaa O.V., Travis D., Kaufman L. and Williamson S.J. (1989).
Neuromagnetic measurements of visual responses to chromaticity and luminance.
In : Advances in Biomagnetism : 209-212.
Eds. S.J. Williamson, M. Hoke, G. Stroink and M. Kotani. Publisher : Plenum Press, New York.

Kriss A., Carroll W.M., BlumhardL.D., and Halliday M. (1982).
Pattern and flash evoked potential changes in Toxic (nutritional) optic neuropathy.
In : Clinical Application of Evoked Potentials in Neurology : 11-19.
Eds. J. Courjon, F. Maugiere and M. Revol. Publisher : Raven Press, New York.

Kurita-Tashima S., Tobimatsu S., Nakayama-HiroMatsu M. and Kato M. (1991).
Effect of check size on the pattern reversal visual evoked potential.
Electroencephalography and Clinical Neurophysiology 80 : 161-166.

Kuffler S.W. (1953).
Discharge patterns and functional organisation of mammalian retina.
Journal of Neurophysiology 16 : 37-68.

Lewis G., Blackburn M., Naitoh P. and Metcalfe M. (1985).
Few trial evoked field stability using the dc SQUID.
In : Biomagnetism : Applications and Theory : 21-28.
Eds. H. Weinberg, G. Stroink and T. Katila. Publisher : Pergammon Press, New York.

Lewis G., Trejo L.J., Naitoh P., Blankenship M.H. and Inlow M. (1989).
Temporal variability of the neuromagnetic evoked field : implications for human performance assessment.
In : Advances in Biomagnetism : 217-224.
Eds. S.J. Williamson, M. Hoke, G. Stroink and M. Kotani. Publisher : Plenum Press, New York.

Leuders H., Lesser R.P. and Klem G. (1980).
Pattern evoked potentials.
In : Current Clinical Neurophysiology : 467-525.
Ed. C.E. Henry. Publisher : Elsevier, North Holland.

Livingstone M. and Hubel D. (1988).
Segregation of form, colour, movement and depth : anatomy, physiology and perception.
Science 240 : 740-749.

Lopes da Silva F.H. (1987).
Computerised EEG analysis : A tutorial overview.
In : A Textbook of Clinical Neurophysiology : 61-104.
Eds. A.M. Halliday, S.R. Butler and R. Paul. Publisher : John Wiley and Sons, Chichester, New York, Toronto and Singapore.

Lowitsch K. (1989).
Evoked Potentials : 65-84..
Eds. K. Maurer, K. Lowitsch and M. Stohr. Publisher B.C. Decker Inc., Toronto and Philadelphia.

Lu S.L. and Spafford M.M. (1989).
Pattern visual evoked Potential variability : a nine hour study.
Canadian Journal of Optometry 51(3) : 112-115.

Maclin E., Okada Y., Kaufman L. and Williamson S.J. (1983).
Retinotopic map on the visual cortex for eccentrically placed patterns : first non-invasive measurements.
Il Nuovo Cimento 2D(2) : 410-419.

Mann D.M.A. (1985).
The neuropathology of Alzheimers Disease : a review with pathogenetic, aetiological and therapeutic considerations.
Mechanisms of Aging and Development 31 : 213-255.

Matthews W.B. and Small D.G. (1979).
Serial recording of visual and somatosensory evoked potentials in multiple sclerosis.
Journal of Neurological Science 40 : 11-21.

Maurer K., Lowitsch K. and Stohr M. (1989).
Evoked Potentials : 65-84.
Eds. K. Maurer, K. Lowitsch and M. Stohr. Publisher B.C. Decker Inc., Toronto and Philadelphia.

McGeer D.L. and McGreer P. (1976)
Neurotransmitter metabolism in the aging brain.
In : Neurobiology of Aging : 389-403.
Eds. R.D. Terry and S. Gershon. Publisher : Raven Press, New York.

McGreer E.G., Peppard R.P., McGeer P.L. Tuokko H., Crockett D., Parks R., Calne D.B., Beathe B.L. and Harrop R. (1990).
Fluorodeoxyglucose Positron Emission Tomography studies in presumed Alzheimers cases, including 13 serial scans.
Canadian Journal of Neurological Sciences 17 : 1-11.

Meienberg O., Kutak L., Smolenski C. and Ludin H.P. (1979).
Pattern reversal evoked cortical responses in normals.
Journal of Neurology 222 : 81-93.

Meijs J.W.H., Bosch F.G.C., Peters M.J. and Lopes da Silva F.H. (1987).
On the magnetic field distribution generated by a dipolar current source situated in a realistically shaped compartment model of the head.
Electroencephalography and Clinical Neurophysiology 66 : 286-298.

Melcher M.R. and Cohen D. (1988).
Dependence of the MEG on dipole orientation in the rabbit head.
Electroencephalography and Clinical Neurophysiology 70 : 460-472.

Meredith J.T. and Celesia G.G. (1982).
Pattern reversal visual evoked potentials and retinal eccentricity.
Electroencephalography and Clinical Neurophysiology 53 : 243-253.

Moskowitz A. and Sokol S. (1983).
Developmental changes in the human visual system as reflected by the latency of pattern reversal Visual Evoked Potentials.
Electroencephalography and Clinical Neurophysiology 56 : 1-15.

Muresan L., Nakasato N., Vinet J-F. and Sutherling W. (1991).
Identification of 1 versus 2 dipoles by MEG.
In : Proceedings of the 8th International conference on Biomagnetism : 65-66.
Munster.

Myslobodsky M.S., Glucksohn J., Coppola R. and Weinberger D.R. (1991).
Occipital lobe morphology in normal individuals assessed by Magnetic Resonance Imaging.
Vision Research 31(10) : 1677-1685.

Novak G.P., Wiznitzer M., Kurtzberg D., Giesser B.S. and Vaughan H.G. (1988).
The utility of visual evoked potentials using hemifield stimulation and several check sizes in the evaluation of suspected multiple sclerosis.
Electroencephalography and Clinical Neurophysiology 71 : 1-9.

Nunez P.L. (1986).
The brains magnetic field : some effects of multiple sources on localisation methods.
Electroencephalography and Clinical Neurophysiology 63 : 75-82.

Okada K. (1991).
Eccentricity dependence of neuromagnetic responses to pattern reversal and luminance on-off stimuli.
Proceedings of the 8th International Conference on Biomagnetism : 167-168.
Munster.

Okada Y. (1982).
Visual evoked fields.
In : Biomagnetism : An Interdisciplinary Approach : 443-459. NATO ASI Series.
Eds. S.J. Williamson, G. Romani, L. Kaufman and I. Modena. Publisher : Plenum Press, New York and London.

Okada Y. (1983).
Neurogenesis of evoked magnetic fields.
In : Biomagnetism : An Interdisciplinary Approach : 399-408. NATO ASI Series.
Eds. S.J. Williamson, G. Romani, L. Kaufman and I. Modena. Publisher : Plenum Press, New York and London.

Okada Y., Kaufman L., Brenner D and Williamson S.J. (1982).
Modulation transfer functions of the human visual system revealed by magnetic field measurements.
Vision Research 22 : 319-333.

Okada Y., Kaufman L. and Williamson S.J. (1983).
The hippocampal formation as a source of the slow endogenous potential.
Electroencephalography and Clinical Neurophysiology 55 : 417-426.

Okada Y.C. and Nicholson C. (1988).
Magnetic evoked field associated with transcortical currents in turtle cerebellum.
Biophysics Journal 53 : 723-731.

Oken B.S., Chiappa K.H. and Gill E. (1987).
Normal temporal variability of the P100.
Electroencephalography and Clinical Neurophysiology 68 : 153-156..

Orwin A., Wright C.E., Harding G.F.A., Rowan D.C. and Rolfe E.B. (1986).
Serial visual evoked potential recordings in Alzheimers' Disease.
British Medical Journal 293 : 9-10.

Opfer J.E., Yeo Y.K., Pierce J.M. and Rorden L.H. (1974).
A superconducting second derivative gradiometer.
IEEE Transactions on Magnetism MAG 9 : 536-539.

Padhiar S. and Harding G.F.A. (1991).
Effect of time of day on the flash and pattern reversal visual evoked potential.
Electroencephalography and Clinical Neurophysiology 78 : 87P.

Pantev C., Hoke M., Lehnertz K. and Lutkenhoner B. (1989).
Neuromagnetic evidence of an amplitopic organisation of the human auditory cortex.
Electroencephalography and Clinical Neurophysiology 72 : 225-231.

Parnavelos J.G. and McDonald J.K. (1983).
The cerebral cortex.
In : Chemical Neuroanatomy : 505-549.
Ed. P.C. Emson. Publisher : Raven Press, New York.

Philpot M.P., Amin D. and Levy R. (1990).
Visual evoked potentials in Alzheimers Disease : correlations with age and severity.
Electroencephalography and Clinical Neurophysiology 77 : 323-329.

Plant G.T. and Hess R.F. (1985).
Temporal frequency discrimination in optic neuritis and multiple sclerosis.
Brain 105 : 735-754.

Plant G.T., Zimmern R.L. and Durden K. (1983).
Transient visually evoked potentials to pattern reversal and onset of sinusoidal bar gratings.
Electroencephalography and Clinical Neurophysiology 56 : 147-158.

Plonsey R. (1981).
Generation of magnetic fields by the human body.
In : Biomagnetism : Proceedings of the 3rd International Workshop on Biomagnetism : 177-205.
Eds. S.N. Erne, H-D. Hahlbohm and H. Lubbig. Publisher : Walter de Gruyter, Berlin.

Polyak S. (1957).
In : The Vertebrate Visual System : 102-107.
Publisher : University of Chicago Press, Chicago.

Regan D., Bartol S., Murray T.J. and Beverley K.I. (1982).
Spatial frequency discrimination in normal vision and in patients with multiple sclerosis.
Brain 105 : 735-754.

Ribary U., LLinas R., Kluger A., Suk J. and Ferris S.H. (1989).
Neuropathological dynamics of magnetic auditory steady state responses in Alzheimers disease.
In : Advances in Biomagnetism : 311-314.
Eds. S.J. Williamson, M. Hoke, G. Stroink and M. Kotani. Publisher : Plenum Press, New York.

Richer F., Barth D.S. and Beatty J. (1983).
Neuromagnetic localisation of two components of the transient visual evoked response to pattern stimulation.
Il Nuovo Cimento 2(2) : 420-428.

Ristanovic D. and Hadjukovic R. (1981).
Effects of spatially structured stimulus fields on pattern reversal visual evoked potentials.
Electroencephalography and Clinical Neurophysiology 51 : 599-610.

Rodieck R.W. (1979).
Visual Pathways.
Annual Review of Neurosciences 2 : 193-225.

Romani G.L. (1989).
Fundamentals of neuromagnetism.
In : Advances in Biomagnetism : 33-46.
Eds. S.J. Williamson, M. Hoke, G. Stroink and M. Kotani. Publisher : Plenum Press, New York.

Rose D.F., Smith P.D. and Sato S. (1987).
Magnetoencephalography and epilepsy research.
Science 238 : 329-335.

Rovamo J. and Virsu V. (1979).
An estimation and application of the human cortical magnification factor.
Experimental Brain Research 37 : 495-510.

Rowe M.J. (1982).
The clinical utility of half field pattern reversal visual evoked potential testing.
Electroencephalography and Clinical Neurophysiology 53 : 73-77.

Sabers A., Roenager J., Saermark K., Bak C.K., Lebech J. and Mikkelson K.B. (1989).
Pre- and post-operative magneto encephalography in partial epilepsy : a case story.
In : Advances in Biomagnetism : 295-298.
Eds. S.J. Williamson, M. Hoke, G. Stroink and M. Kotani. Publisher : Plenum Press, New York.

Samuel D., Algeri S., Gershan S., Grimm V.E. and Toffano G. (1983).
In : Aging of the Brain.
Publisher : Raven Press, New York.

Schmidt B. and Blum T. (1984).
Retinotopic examinations with magnetoencephalography.
Developments in Ophthalmology 9 : 46-52.

Shahrohki F., Chiappa K.H. and Young P.R. (1978).
Pattern shift visual evoked responses : Two hundred patients with optic neuritis and/or multiple sclerosis.
Archives of Neurology 35 : 65-71.

Shapley R.M., Kaplan E. and Soodak R. (1981).
Spatial summation and contrast sensitivity of X and Y cells in the lateral geniculate nucleus of the macaque.
Nature 292 : 543-545.

Shearer D.E. and Dustman R.E. (1980).
The pattern reversal evoked potential : the need for laboratory norms.
The American Journal of EEG Technology 20 : 185-200.

Shipley T., Jones R.W. and Fry A. (1966).
Intensity and the evoked occipitogram in man.
Vision Research 6 : 657-667.

Shors T.J., Ary J.P., Eriksen K.J. and Wright K.W. (1986).
P100 amplitude variability of the pattern visual evoked potential.
Electroencephalography and Clinical Neurophysiology 65 : 316-319.

Singer W. (1979).
Central core control of visual cortex functions.
In : The Neurosciences 4th Study Program : 1093-1110.
Eds. F.O. Schmitt and F.G. Worden.

Skuse N.F. and Burke D. (1990).
Power spectrum and optimal filtering for visual evoked potentials to pattern reversal.
Electroencephalography and Clinical Neurophysiology 77 : 199-204.

Snedecor G.W. and Cochran W.G. (1980).
In : Statistical Methods (7th Edition).
Publisher Iowa State Press.

Snyder E.W., Dustman R.E. and Shearer D.E. (1981).
Pattern reversal evoked potential amplitudes : life span changes.
Electroencephalography and Clinical Neurophysiology 52 : 429-434.

Sokol S. and Moskowitz A. (1981).
Effect of retinal blur on peak latency of the pattern evoked potential.
Vision Research 21 : 1279-1286.

Sokol S., Moskowitz A. and Towle V.L. (1981).
Age related changes in the latency of the visual evoked potential : influence of check size.
Electroencephalography and Clinical Neurophysiology 51 : 559-562.

Sokol S., James K. and Nadler D. (1983).
Comparison of the spatial response properties of the human retina and cortex as measured by simultaneously recorded pattern electroretinograms and visual evoked potentials.
Vision Research 23 : 723-727.

Spehlman R. (1981).
In : EEG Primer,
Publisher Elsevier Biomedical Press, Amsterdam, New York and Oxford.

Spehlman R. (1985).
The normal transient VEP to checkerboard pattern reversal.
In : Evoked Potential Primer : 95-115.
Publisher : Butterworth Publishers, London, and Boston.

Spinelli D. and Mecacci L. (1990).
Handedness and hemispheric asymmetry of pattern reversal visual evoked potentials.
Brain and Cognition 13 : 193-210.

Steinmetz H., Furst G. and Meyer B.O. (1989).
Craniocerebral topography within the International 10-20 system.
Electroencephalography and Clinical Neurophysiology 72 : 499-506.

Stensaas S.S., Eddington D.K. and Dobelle W.H. (1974).
The topography and variability of the primary visual cortex in man.
Journal of Neurosurgery 40 : 747-755.

Stockard J.J., Hughes J.F. and Sharbrough F.W. (1979).
Visually evoked potentials to electronic pattern reversal : latency variability with gender, age and technical factors.
American Journal of EEG Technology 19 : 171-204.

Stok C.J. (1986).
The inverse problem in MEG and EEG with application to visual evoked responses.
PhD. Thesis, University of Twente, Netherlands.
Publisher Krisp Repro Meppel, Leiden.

Stolz G., Aschoff J.C., Born J. and Aschoff J. (1988).
VEP, physiological and psychological circadian variation in humans.
Journal of Neurology 235 : 308-313.

Straumanis J.J., Shagass C. and Schwartz M. (1965).
Visually evoked cerebral response changes associated with chronic brain syndromes and aging.
Journal of Gerontology 20 : 498-506.

Sutherling W., Baumgartner C., Darcey T.M. and Barth D.S. (1989).
Comparison of dynamic spatiotemporal field structures of dorsolateral fronto-central seizures and hand sensorimotor cortex.
In : Advances in Biomagnetism : 291-294.
Eds. S.J. Williamson, M. Hoke, G. Stroink and M. Kotani. Publisher : Plenum Press, New York.

Tepas D.I. and Armington J.C. (1962).
Properties of evoked visual potentials.
Vision Research 2 : 449-461.

Tepas D.I., Guiteras V.L. and Klingman D. (1974).
Variability of the human average evoked brain response to visual stimulation : a warning !
Electroencephalography and Clinical Neurophysiology 36 : 533-537.

Teyler T.J., Cuffin B.N. and Cohen D. (1975).
The visual evoked magnetoencephalogram.
Life Sciences 17 : 683-692.

Thorpe-Davis E., Schnider C.M. and Sherman J. (1987).
Normative data and control studies of Flash VEPs' for comparison to a clinical population.
American Journal of Optometry and Physiological Optics Vol. 64, No. 8 : 579-592.

Trimble J.L. and Potts A.M. (1975).
Ongoing occipital rhythms and VER I : stimulation at peaks of alpha rhythm.
Investigations in Ophthalmology and Visual Science 18 : 703-713.

Tripp J.H. (1981).
Biomagnetic fields and cellular current flow.
In : Biomagnetism : Proceedings of the 3rd International Workshop on Biomagnetism : 207-215.
Eds. S.N. Erne, H-D. Hahlbohm and H. Lubbig. Publisher : Walter de Gruyter, Berlin.

Tripp J.H. (1983).
Physical concepts and mathematical models.
Biomagnetism : An Interdisciplinary Approach : 101-138. NATO ASI Series.
Eds. S.J. Williamson, G. Romani, L. Kaufman and I. Modena. Publisher : Plenum Press, New York and London.

Trojaborg W. and Petersen E. (1979).
Visual and somatosensory evoked cortical potentials in multiple sclerosis.
Journal of Neurology, Neurosurgery and Psychiatry 42 : 323-330.

Ueno S., Wakisako H. and Harada K. (1985).
Flux reversal phenomena in spatial distributions of the magnetoencephalogram.
In : Biomagnetism : Applications and Theory : 289-293.
Eds. H. Weinberg, G. Stroink and T. Katila. Publisher : Pergammon Press, New York.

Van der Tweel L.H., Estevez O. and Cavonius C.R. (1979).
Invariance of the contrast evoked potential with changes in retinal illuminance.
Vision Research 19 : 1283-1287.

Van Lith G.H.M., Van Marle G.W. and Van Dok-Mak G.T.M. (1978).
Variation in latency times of visually evoked cortical potentials.
British Journal of Ophthalmology 62 : 220-222.

Varbec F. (1965).
Senile changes in the ganglion cells of the human retina.
British Journal of Ophthalmology 49 : 5061-5072.

Vaughan H.G., Costa L.D. and Gilden L. (1966).
The functional relation of visual evoked response and reaction time to stimulus intensity.
Vision Research 6 : 645-656.

Verma N.P. and Kooi K.A. (1984).
Gender factor in longer P100 latency of elderly persons.
Electroencephalography and Clinical Neurophysiology 59 : 361-365.

Visser S.L., Stam F.C., Van Tilburg W., Op dem Velde W., Blom J.L. and de Rijke W. (1976).
Visual evoked responses in senile and presenile dementia.
Electroencephalography and Clinical Neurophysiology 40 : 385-392..

Walsh J.C., Garrick R. and McLeod R. (1982).
Evoked potential changes in clinically definite Multiple Sclerosis : a two year follow up study.
Journal of Neurology, Neurosurgery and Psychiatry 45 : 494-500.

Wegener W.A. and Alavi A. (1989).
Positron emission tomography in neuropsychiatric disorders.
Current Opinion in Radiology 1 : 475-484.

Weinberg H., Brickett P., Neill R.A., Fenelon B. and Baff M. (1985).
Magnetic fields evoked by random dot stereograms.
In : Biomagnetism : Applications and Theory : 354-358.
Eds. H. Weinberg, G. Stroink and T. Katila. Publisher : Pergammon Press, New York.

Weinberg H., Brickett P., Coolsma F. and Baff M. (1986).
Magnetic localisation of intracranial dipoles : simulation with a physical model.
Electroencephalography and Clinical Neurophysiology 64 : 159-170.

Whittaker S.G. and Seigfried J.B. (1983).
Origin of wavelets in the visual evoked potential.
Electroencephalography and Clinical Neurophysiology 55 : 91-101.

Wikswo J.P. (1983).
Cellular action currents.
In : Biomagnetism : An Interdisciplinary Approach : 173-207. Nato ASI Series.
Eds. S.J. Williamson, G.L. Romani, L. Kaufman and I. Modena. Publisher : Plenum Press, New York York and London.

Wikswo J.P. (1989).
Biomagnetic sources and their models.
In : Advances in Biomagnetism : 1-18.
Eds. S.J. Williamson, M. Hoke, G. Stroink and M. Kotani. Publisher : Plenum Press, New York.

Wikswo J.P. and Roth B.J. (1989).
Magnetic determination of the spatial extent of a single cortical current source : a theoretical analysis.
Electroencephalography and Clinical Neurophysiology 69 : 266-276.

Williamson S.J. and Kaufman L. (1981).
Biomagnetism.
Journal of Magnetism and Magnetic Materials 22 : 129-201.

Williamson S.J., Kaufman L. and Brenner D. (1978).
Latency of the neuromagnetic response of the human visual cortex.
Vision Research 18 : 107-110.

Wilson W.B. (1978).
Visual evoked response differentiationof ischaemic optic neuritis from the neuritis of multiple sclerosis.
American Journal of Ophthalmology 86 : 530-535.

Wood C.C. (1985).
Source identicication using evoked potential measurements.
In : Biomagnetism : Applications and Theory : 191-204.
Eds. H. Weinberg, G. Stroink and T. Katila. Publisher : Pergammon Press, New York.

Wright J.E., Arden G. and Jones B.R. (1973).
Continuous monitoring of the visually evoked response during intra-orbital surgery.
Transactions of the Ophthalmological Society of the United Kingdom Vol. XCIII : 311-314.

Wright C.E., Williams D.E., Drasdo N. and Harding G.F.A. (1985).
The influence of age on the electroretinogram and visual evoked potential.
Documenta Ophthalmologica 59 : 365-384.

Wright C.E., Drasdo N. and Harding G.F.A. (1987).
Pathology of the optic nerve and visual association areas.
Brain 110 : 107-120.

Wright C.E. (1983).
The clinical use of spatial and temporal aspects of vision.
PhD. Thesis, University of Aston in Birmingham.

Yiannikas C. and Walsh J.C. (1982).
The use of visually evoked potentials in the detection of subclinical optic toxicity secondary to ethambutol therapy.
Neurology 32 : A205.

Yiannikas C. and Walsh J.C. (1983).
The variation of the pattern shift visual evoked response with the size of the stimulus field.
Electroencephalography and Clinical Neurophysiology 55 : 427-435.

Zeki S. (1992).
The visual image in mind and brain.
Scientific American 267 ; 69-76.

Zimmerman J.P. (1983).
Cryogenics.
In : Biomagnetism : An Interdisciplinary Approach : 173-207. Nato ASI Series.
Eds. S.J. Williamson, G.L. Romani, L. Kaufman and I. Modena. Publisher : Plenum Press, New York York and London.

Zimmerman J.P. and Frederick N.V. (1971).
Miniture ultrasensitive magnetic gradiometer and its use in cardiography and other applications.
Applied Physics Letters 19 : 16-19.

Zimmerman J.P., Thiene P. and Harding J.T. (1970).
Design and operation of stable rf-biased point contact quantum devices and a note on the operation of perfectly clean metal contacts.
Journal of Applied Physics 41 : 1572-1580.

Zimmerman J.T., Edrich J., Zimmerman J.E. and Reite M.L. (1978).
The human magnetoencephalogram averaged visually evoked field.
Proceedings of the San Diego Biomedical Symposium : 217-221.
Eds. J.T. Martin and E.A. Calvert. Publisher Academic Press, New York.

APPENDIX 1

Normative Data Study - Flash VEMR Component Latencies and Amplitude for the P2M

Subject	Age	P1M (ms)	N1M (ms)	P2M (ms)	P2M (fT)	N2M (ms)
1. SP	15	83	104	135	236	151
2. JP	19	73	94	109	202	130
3. JG	19	64	93	110	-	140
4. JM	21	77	103	139	292	-
5. CJN	22	70	100	120	259	160
6. ER	22	-	82	93	125	144
7. KDM	22	77	113	139	292	185
8. APB	23	67	82	103	292	144
9. TL	23	-	82	103	-	154
10. FO	23	-	85	100	-	140
11. AS	23	68	80	97	169	119
12. RD	23	77	93	128	135	155
13. DC	23	63	76	97	-	110
14. SP	23	77	107	122	349	138
15. MDH	25	67	88	103	225	180
16. JC	25	65	75	90	157	115
17. VVV	26	72	85	114	157	144
18. PG	26	72	93	97	-	-
19. RH	26	68	78	104	225	156
20. JP	26	67	82	113	-	124
21. DJ	26	73	99	114	157	141
22. JG	27	76	-	114	-	140
23. GB	27	60	75	85	146	110
24. BE	27	82	97	117	-	143
25. BJ	28	70	85	105	180	140
26. PD	29	-	82	118	-	180
27. CB	30	82	98	124	-	155
28. HO	31	78	88	114	236	156
29. PF	32	-	93	135	191	-
30. CM	32	-	-	-	214	135
31. AC	35	62	88	130	349	156
32. AP	36	78	91	125	169	203
33. JW	36	73	99	130	146	167
34. SNS	37	68	91	109	247	141
35. RAA	39	65	75	100	326	125
36. KW	39	75	100	110	225	140
37. PA	40	58	83	120	146	161
38. GJC	41	88	99	107	124	135
39. LJ	42	84	110	118	-	144
40. BG	43	68	78	96	191	141
41. MI	45	80	106	139	-	-
42. JH	45	60	878	94	157	114
43. MW	47	-	68	99	146	-
44. AS	47	78	94	104	146	135

APPENDIX 1

Normative Data Study - Flash VEMR Component Latencies and Amplitude for the P2M

Subject	Age	P1M (ms)	N1M (ms)	P2M (ms)	P2M (fT)	N2M (ms)
45. BB	47	62	77	103	135	129
46. HY	48	-	78	94	225	125
47. ADP	49	73	94	104	236	120
48. PL	51	-	72	98	180	113
49. GFAH	51	-	65	104	236	138
50. RL	52	78	114	122	236	135
51. CCT	54	73	86	99	180	130
52. ME	55	73	88	-	-	-
53. CUMS	57	82	92	107	236	148
54. JMS	61	78	104	122	101	146
55. JAB	62	78	101	114	394	127
56. MR B	64	62	70	94	236	130
57. AW	65	88	119	141	135	208
58. MRS S	65	83	99	114	157	130
59. EM	65	-	-	94	146	125
60. MRS M	66	78	104	125	135	146
61. MR S	68	-	-	104	101	-
62. JMS	68	-	88	130	281	208
63. NL	68	-	88	104	292	130
64. JM	69	78	104	-	68	156
65. MRS M	71	83	109	120	483	151
66. MR M	72	73	83	104	247	130
67. MRS EN	72	78	99	130	135	-
68. MRS L	73	78	101	117	225	141
69. MR D	73	-	104	120	225	167
70. MR B	73	78	-	-	68	156
71. MRS B	74	94	114	125	169	146
72. MM	74	-	78	120	281	182
73. MRS C	74	-	112	135	214	172
74. MR EN	74	83	-	109	214	167
75. MRS D	75	78	96	109	68	130
76. MRSH	78	-	91	125	259	151
77. KJM	79	73	99	114	146	161
78. MRS LH	80	91	128	156	124	174
79. MRS H	80	68	83	114	259	146
80. WWF	81	62	83	104	236	167
81. GNH	83	78	114	130	146	-
82. MR H	84	68	99	122	483	156
83. HS	86	78	104	208	169	-

APPENDIX 2

Normative Data Study - Pattern Reversal VEMR Component Latencies and the Amplitude for P100M

Subject	Age	N1M (ms)	P100M (ms)	P100M (fT)	N2M
1. SP	15	83	104	214	120
2. CJR	18	72	113	349	165
3. KJM	18	62	103	326	134
4. JGN	19	-	103	191	129
5. JP	19	91	104	135	161
6. JP	20	52	88	259	134
7. MA	20	77	98	349	113
8. JM	21	57	102	326	149
9. CD	21	88	119	326	161
10. QN	21	62	113	360	-
11. CN	22	100	135	337	161
12. ER	22	-	103	259	-
13. AS	23	75	118	236	150
14. SP	23	91	116	270	133
15. RL	23	88	103	315	129
16. APB	23	97	113	225	134
17. RD	23	99	109	214	146
18. RH	24	83	104	247	161
19. MDH	25	88	125	394	193
20. JC	25	68	99	225	120
21. VVV	26	78	125	157	156
22. DJ	26	68	96	124	114
23. GB	27	-	100	304	-
24. GS	27	103	123	304	175
25. BJ	28	80	110	157	150
26. PD	29	78	104	281	161
27. CB	30	65	95	270	103
28. KR	23	-	99	180	-
29. HO	31	94	120	240	182
30. RH	31	94	120	-	182
31. PF	32	-	100	360	120
32. CM	32	62	112	236	161
33. AC	35	57	104	349	151
34. AP	36	120	143	236	198
35. JW	36	104	119	169	151
36. SNS	37	104	130	146	161
37. RAA	39	75	100	247	140
38. KW	39	90	100	157	150
39. PA	40	65	96	191	117
40. GJC	41	83	114	236	-
41. BG	43	-	114	101	141
J42. H	45	88	109	135	130
43. BB	47	73	101	292	125
44. MW	47	78	94	169	120

APPENDIX 2

Normative Data Study - Pattern Reversal VEMR Component Latencies and the Amplitude for P100M

Subject	Age	N1M (fT)	P100M (ms)	P100M (fT)	N2M (ms)
45. AS	47	73	125	292	156
46. HY	48	78	130	180	161
47. ADP	49	78	104	157	125
48. AR	48	-	120	135	-
49. GFAH	51	73	99	169	122
50. PL	51	82	103	326	129
51. CCT	54	94	120	202	172
52. RL	54	73	109	180	135
53. ME	55	73	99	225	114
54. ND	56	82	118	360	155
55. CUMS	57	90	110	281	135
56. PF	59	82	108	270	134
57. JMS	61	86	104	124	130
58. JAB	62	-	99	202	125
59. MR B	64	88	122	157	146
60.. AW	65	-	119	191	-
61. EM	65	104	135	191	167
62. MRS S	65	94	114	169	-
63. MRS M	66	57	99	135	130
64. NL	68	88	125	225	167
65. MR S	68	84	120	124	140
66. JMS	68	-	115	247	218
67. JM	69	83	104	236	125
68. MRS M	71	-	104	259	172
69. MRS EN	72	94	112	124	125
70. MR M	72	-	141	124	198
71. MRS L	73	68	86	202	114
72. MR D	73	104	135	202	172
73. MR B	73	68	100	124	114
74. MRSB	74	-	99	124	125
75. MRS C	74	-	156	146	190
76. MM	74	78	125	135	130
77. EN	74	-	-	68	-
78. MRSD	75	-	135	169	143
79. MRS H	78	78	112	124	146
80. KJM	79	94	135	146	198
81. MRS LH	80	99	148	112	213
82. MRS H	80	-	-	68	182
83. WWF	81	109	156	157	172
85. GNH	83	104	146	191	182
85. MR H	84	141	156	124	130
86. HS	86	-	-	68	-

APPENDIX 3

Interocular Latency Difference (P100M)

Latency (ms)

SUBJECT	Left Eye	Right Eye	Difference
1. RAA	102	107	5
2. AS	133	135	2
3. CN	117	107	10
4. CUMS	104	96	8
5. BB	141	158	17
6. KR	104	112	8
7. PDG	94	94	0
8. KMW	104	110	6
9. CD	151	146	5
10. SP	146	148	2
11. BJ	135	145	10
12. PF	148	141	7
13. GO	122	130	8
14. SS	148	141	7
15. BE	109	120	11
16. CS	115	130	15
17. MDH	115	127	12
18. RD	104	109	5
19. ON	130	130	0
20. HO	112	120	8
21. FO	122	125	3
22. MH	130	117	13
23. EI	96	94	2
24. DM	99	86	13
25. SF	115	108	7
26. SNS	124	114	10
MEAN±S.D.	120 ± 17.41	121.15 ± 18.84	7.46 ± 4.49

APPENDIX 4

Temporal Variability of the Pattern Reversal P100M Recorded from Subject RAA using Magnetometer A (original system) in an Unshielded Environment

RUN	25/5/90	25/5/90	29/5/90	29/5/90	31/5/90	31/5/90	6/6/90	6/6/90	14/6/90	14/6/90	
	LAT	AMP	LAT	AMP	LAT	AMP	LAT	AMP	LAT	AMP	
1	112.30	125.49	111.30	78.05	118.02	176.22	103.50	183.34	117.20	159.31	
2	111.30	183.34	118.20	167.32	118.20	133.50	112.30	211.82	117.20	25.81	
3	115.20	121.04	117.20	164.65	123.00	142.40	108.40	223.39	121.10	168.21	
4	111.30	161.09	117.20	166.43	116.20	141.51	107.40	88.11	118.20	182.45	
5	118.20	129.94	114.30	142.40	116.20	170.88	109.40	177.11	118.20	205.59	am
6	115.20	135.28	110.40	134.39	114.30	187.79	116.20	168.21	115.20	141.51	
7	118.20	103.24	110.40	98.79	112.30	161.98	106.40	175.33	115.20	165.54	
8	110.30	105.02	111.30	166.43	117.20	183.34	102.50	145.96	115.20	117.48	
9	112.30	157.53	110.40	138.84	121.10	72.09	114.30	179.78	113.30	170.88	
10	114.30	165.54	113.40	140.62	116.20	162.87	120.10	169.10	115.20	161.98	
X	113.90	138.75	113.40	139.79	117.30	153.26	110.10	172.22	116.60	149.88	
S.D.	2.8	26.95	3.3	30.42	3.1	33.89	5.6	36.80	2.23	49.37	
1	127.90	145.96	112.30	194.91	117.20	74.76	112.30	305.27	115.20	229.62	
2	135.37	133.50	116.20	146.85	125.00	166.43	108.40	135.28	107.40	146.85	
3	105.40	145.07	109.40	118.37	120.10	114.81	114.30	306.16	111.30	214.49	
4	113.30	147.74	113.30	73.87	120.10	45.07	106.40	188.68	115.20	185.12	
5	118.20	145.07	118.20	240.30	111.30	145.96	108.40	194.02	115.20	307.94	pm
6	110.30	188.68	125.00	68.71	109.40	146.85	112.30	87.84	110.1	229.62	
7	121.10	116.59	129.90	80.37	116.20	197.58	112.30	163.05	114.3	184.23	
8	113.30	143.29	119.10	103.24	111.30	166.43	112.30	173.55	118.20	195.80	
9	113.30	168.21	114.30	152.19	124.00	126.38	112.30	137.95	112.30	209.15	
10	113.30	130.83	115.80	163.76	131.80	186.01	111.32	78.32	112.30	190.46	
X	117.20	146.49	117.40	134.26	118.60	137.03	111.00	177.01	113.90	209.33	
S.D.	8.9	19.93	6.1	56.11	7.1	48.20	2.45	77.97	3.27	42.47	

KEY :

LAT = Latency (ms)

AMP = Amplitude (fT)

X = Mean

S.D. = Standard Deviation

APPENDIX 5

Temporal Variation of the Pattern Reversal P100M Recorded from Subject CD

RUN	1/11/89 LAT	1/11/89 AMP	16/11/89 LAT	16/11/89 AMP	29/11/89 LAT	29/11/89 AMP	30/11/89 LAT	30/11/89 AMP	18/12/89 LAT	18/12/89 AMP	
1	120.00	162.87	148.40	156.64	110.30	190.46	103.50	151.30	114.30	216.27	
2	116.00	180.67	140.60	163.76	117.20	201.14	110.30	191.35	116.20	143.29	
3	144.00	128.16	142.60	176.22	104.50	266.11	113.30	191.35	106.40	186.01	
4	130.00	147.74	146.50	218.05	114.30	211.82	113.30	153.97	116.20	204.70	
5	146.00	126.38	148.40	125.49	125.90	186.90	124.00	108.58	110.30	192.24	am
6	128.00	142.40	155.30	169.99	124.00	113.92	128.90	150.41	125.00	77.43	
7	125.00	193.13	142.60	157.53	110.40	223.39	153.30	161.09	122.10	127.27	
8	145.00	174.44	135.70	127.27	124.00	161.98	119.10	151.30	110.30	93.45	
9	131.00	185.12	139.70	144.18	124.00	120.15	124.00	163.76	116.20	97.90	
10	136.00	221.61	137.70	161.98	124.00	128.16	135.70	165.54	125.00	67.64	
X	132.10	166.25	143.75	160.11	117.86	181.40	122.54	158.87	116.20	140.62	
S.D.	10.51	30.52	5.91	26.42	7.60	50.36	14.37	23.39	6.32	55.89	
1	143.00	126.38	142.40	114.81	121.10	169.99	109.40	211.82	110.30	87.22	
2	135.00	113.03	137.30	158.42	112.30	198.47	127.90	151.30	110.30	73.87	
3	130.00	108.58	140.20	206.48	126.90	181.56	132.80	266.11	124.20	188.68	
4	127.00	109.47	138.40	196.69	123.00	298.15	119.10	176.22	116.40	154.86	
5	127.00	109.47	127.30	178.00	149.40	190.46	111.30	283.91	119.30	145.07	pm
6	121.00	87.22	142.40	159.31	136.70	87.22	109.40	202.03	127.80	169.10	
7	128.00	111.25	146.40	197.58	136.70	170.88	125.00	178.00	112.20	241.19	
8	116.00	61.41	148.30	166.43	126.00	182.45	148.40	141.51	109.80	127.27	
9	123.00	210.93	150.20	171.77	137.70	228.73	142.60	250.09	110.40	144.18	
10	115.00	154.86	138.30	146.85	133.80	238.52	134.80	181.56	126.00	159.31	
X	126.50	119.26	141.12	169.63	130.36	194.64	126.07	204.26	116.67	149.08	
S.D.	8.46	40.16	6.56	27.31	10.57	54.64	13.83	48.38	7.17	47.83	

KEY :

LAT = Latency (ms)

AMP = Amplitude (fT)

X = Mean

S.D. = Standard Deviation

APPENDIX 6

Temporal Variation of the Pattern Reversal P100M Recorded In a Single Layer Eddy Current Shielded Room and a Two Layer Magnetically Shielded Room

Single Layer Eddy Current Shielded Room

RUN	3/6/91	3/6/91	4/6/91	4/6/91	5/6/91	5/6/91	
	LAT	AMP	LAT	AMP	LAT	AMP	
1	113.28	150.15	125.98	182.17	118.16	137.89	
2	124.02	141.70	125.98	182.51	114.26	55.94	
3	123.05	125.89	123.05	167.77	124.02	104.79	
4	128.91	184.31	119.14	184.32	120.12	93.20	
5	116.21	88.98	115.23	156.85	119.79	88.98	
6	110.35	81.61	114.26	134.00	117.19	54.14	am
7	124.02	143.85	121.09	54.54	124.02	96.35	
8	112.30	78.19	123.05	72.43	120.12	152.96	
9	133.79	162.81	124.02	157.58	123.05	47.10	
10	124.02	70.68	109.38	119.26	117.19	58.76	
X	120.99	122.82	120.12	141.14	119.79	88.98	
S.D.	7.7	40.12	5.5	46.23	3.22	36.18	
1	120.12	148.41	126.95	148.07	113.28	98.83	
2	115.23	129.78	125.00	161.81	125.00	56.28	
3	121.09	71.76	128.91	88.98	137.70	174.07	
4	123.05	122.75	129.88	187.80	137.70	75.24	
5	120.12	37.99	124.02	145.59	123.05	14.74	
6	113.28	65.79	130.86	177.62	123.05	72.43	pm
7	127.93	78.79	127.93	135.07	125.00	74.24	
8	115.23	74.24	125.00	176.88	130.86	39.40	
9	110.35	67.20	126.95	169.84	124.02	164.22	
10	137.70	75.64	121.09	137.15	130.86	56.95	
X	120.41	87.23	126.66	152.89	127.05	82.61	
S.D.	7.95	34.51	2.95	28.88	7.42	50.92	

KEY :

LAT = Latency (ms)

AMP = Amplitude (fT)

X = Mean

S.D. = Standard Deviation

Two Layer Magnetically Shielded Room

RUN	1/10/91	1/10/91	2/10/91	2/10/91	3/10/91	3/10/91	7/10/91	7/10/91	8/10/91	8/10/91	
	LAT	AMP	LAT	AMP	LAT	AMP	LAT	AMP	LAT	AMP	
1	125.00	145.93	130.86	139.96	128.91	151.96	125.98	148.74	121.09	128.04	
2	125.00	115.04	130.86	128.37	121.09	100.97	125.00	152.29	121.09	139.29	
3	117.19	88.31	127.93	116.45	127.93	200.13	120.12	130.11	122.07	153.36	
4	126.95	116.45	125.00	93.20	123.05	152.96	124.02	170.98	128.91	201.54	
5	126.95	184.99	128.91	123.08	128.91	234.57	124.02	164.95	124.02	138.56	am
6	123.05	133.33	127.93	149.94	125.98	136.81	128.91	146.33	133.79	152.69	
7	125.98	137.89	128.91	136.08	126.95	136.81	124.02	122.41	128.91	183.24	
8	125.98	149.48	128.91	155.44	126.95	144.52	128.91	146.99	128.91	193.43	
9	119.14	149.81	125.98	155.77	123.05	140.30	123.05	209.98	125.00	148.74	
10	120.12	150.15	119.14	126.29	121.09	158.25	125.98	171.65	125.98	193.09	
X	123.54	137.15	127.44	132.39	125.39	155.77	125.00	156.44	125.98	163.21	
S.D.	3.51	26.20	3.45	19.30	3.06	36.98	2.64	24.72	4.14	26.87	

1	123.05	129.11	125.00	179.69	125.98	154.03	129.98	116.04	114.26	107.60	
2	120.12	88.64	125.00	160.93	125.98	223.31	129.98	113.23	125.98	161.40	
3	122.07	129.78	125.00	172.66	125.98	150.55	123.05	169.85	118.16	119.60	
4	120.12	109.75	125.00	181.50	127.93	150.55	125.67	140.30	125.00	124.49	
5	120.12	96.35	125.00	155.10	122.07	177.62	122.07	142.71	125.00	188.14	pm
6	123.05	154.77	121.09	109.01	123.05	135.34	125.98	112.56	117.19	126.30	
7	123.05	146.10	125.00	147.33	123.05	184.99	123.05	166.70	117.19	190.28	
8	125.98	135.41	126.95	119.93	121.09	133.33	125.00	163.21	117.19	166.70	
9	119.14	164.15	123.05	135.34	121.09	161.40	125.98	143.85	120.12	178.69	
10	125.00	150.88	123.05	147.73	116.21	143.85	125.98	134.33	115.23	166.03	
X	122.17	130.58	124.40	150.95	123.24	161.47	125.67	140.30	119.53	152.89	
S.D.	2.28	25.33	1.60	24.32	3.41	27.34	2.68	21.71	4.30	30.55	

KEY :

LAT = Latency (ms)

AMP = Amplitude (fT)

X = Mean

S.D. = Standard Deviation

APPENDIX 7

Temporal Variability of the Pattern Reversal P100M Recorded from Subject RAA using Magnetometer B (new system)

RUN	22/6/90	22/6/90	25/6/90	25/6/90	3/7/90	3/7/90	19/7/90	19/7/90	23/7/90	23/7/90	
	LAT	AMP	LAT	AMP	LAT	AMP	LAT	AMP	LAT	AMP	
1	121.10	156.52	126.90	108.29	126.95	168.35	125.00	195.38	125.00	230.23	
2	121.10	188.37	129.90	120.12	133.79	165.62	119.14	192.01	126.95	315.77	
3	121.10	152.88	119.10	164.71	129.88	99.83	121.09	151.06	126.95	217.18	
4	120.10	203.84	128.90	45.50	123.05	219.77	121.09	260.26	125.00	234.78	
5	122.10	74.62	128.90	131.95	127.83	113.75	125.00	208.39	124.02	197.47	am
6	125.00	157.61	124.00	91.91	125.98	172.90	125.98	93.73	124.02	280.28	
7	124.00	177.45	122.10	169.26	125.88	144.69	125.98	77.35	116.21	228.41	
8	123.00	101.92	118.20	139.23	126.95	156.52	123.05	211.12	125.98	265.72	
9	123.00	114.66	125.90	161.07	122.07	175.63	116.21	202.02	131.84	186.55	
10	123.00	163.80	123.10	128.31	126.95	171.08	128.91	174.72	127.93	220.22	
X	122.30	149.17	124.70	126.03	126.90	158.81	123.10	176.60	125.40	237.66	
S.D.	1.52	40.36	4.11	37.72	3.29	33.66	3.78	55.59	3.97	39.16	

1	127.90	163.80	119.14	69.80	119.14	67.34	125.98	180.18	122.07	177.27	
2	125.00	181.09	120.12	152.88	119.14	37.77	123.05	206.57	131.84	182.46	
3	122.10	152.88	124.02	106.47	126.95	148.33	130.86	151.97	128.91	222.59	
4	118.20	101.01	127.93	183.82	126.95	72.62	125.00	263.72	132.81	168.62	
5	118.20	130.13	130.86	139.23	128.91	182.91	125.00	213.03	131.84	82.17	pm
6	128.90	96.46	121.09	170.17	127.93	42.77	123.00	149.51	124.02	292.38	
7	128.90	119.21	122.07	92.82	127.93	78.26	125.00	183.91	118.16	219.94	
8	126.90	123.76	124.02	131.04	129.88	167.44	119.14	190.19	124.02	263.17	
9	130.80	35.49	122.07	209.03	127.93	83.72	119.14	116.57	125.00	220.22	
10	130.80	116.48	128.91	143.78	133.79	128.31	121.10	56.88	125.98	183.91	
X	125.80	122.03	124.00	139.90	126.80	100.95	123.70	171.25	126.46	201.27	
S.D.	4.8	40.66	3.96	42.34	4.5	51.91	3.5	56.82	4.79	57.52	

KEY :

LAT = Latency (ms)

AMP = Amplitude (fT)

X = Mean

S.D. = Standard Deviation

APPENDIX 8

Noise Waveforms

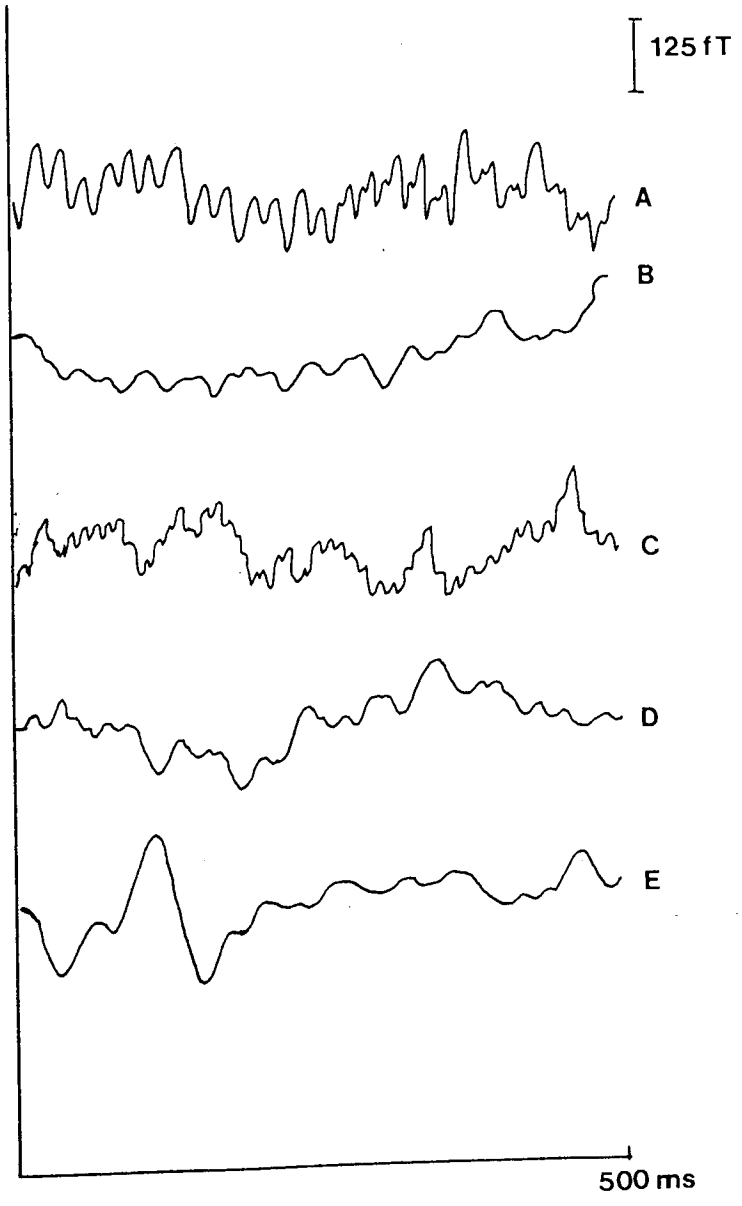

A Magnetic noise recorded on a noisy occasion.

B Magnetic noise recor ded on a quiet occasion.

C Magnetic noise recorded without the 50Hz comb filter.

D Magnetic noise recorded with the 50Hz comb filter in.

E Pattern reversal waveform from subject RAA.

APPENDIX 8

Details of Stimulus Conditions

1. Luminance across pattern reversal screen:- Mean = 1050cd/m^2. Standard Deviation = 94.5 .
2. Distance from subject to screen was 82cm.
3. Mean luminance of room <20cd/m^2.
4. Height of Dewar above scalp 0-1cm.
5. Magnetic noise (peak to peak) quiet time 30-40ft/ Hz.
6. Magnetic noise (peak to peak) noisy time 80-110ft/ Hz.
7. Sampling rate 256Hz.

APPENDIX 9

SUPPORTING PUBLICATIONS

LIST OF SUPPORTING PUBLICATIONS

1. Armstrong,R.A., Harding,G.F.A., Slaven,A., Furlong,P. and Janday,B. (1989). Normative MEG data to flash and pattern reversal stimuli. Electroenceph. clin Neurophysiol., 1P-3P (Abstract). 215

2. Armstrong,R.A., Janday,B., Slaven,A and Armstrong,R.A. (1990a). The use of flash and pattern evoked fields in the diagnosis of Alzheimer's disease. Proceedings of the 7th International Biomagnetism Conference, New York. pp 287-288. 216

3. Slaven,A. and Armstrong,R.A. (1990b). The influence of age on the pattern and flash visual evoked field. Ophthal. Physiol. Opt., 10:414 (Abstract). 220

4. Armstrong,R.A., Degg,C. and Slaven,A. (1991a). Latency and variability of the visual evoked magnetic response: A comparison of two single channel magnetometers. Proceedings of the 8th International Biomagnetism Conference, Munster, pp 163-164. 221

5. Armstrong,R.A., Slaven,A. and Harding,G.F.A. (1991b). Normative data for two visually evoked magnetic components. Proceedings of the 8th International Biomagnetism Conference, Munster, pp 165-166. 223

6. Slaven,A., Degg,C. and Armstrong,R.A. (1991c). Topography of visual evoked magnetic responses to pattern shift, pattern onset and flash stimuli. Opthal. Physiol. Opt.,11:396 (Abstract). 225

7. Armstrong,R.A., Slaven,A. and Harding,G.F.A. (1991d). The influence of age on the pattern and flash visual evoked magnetic response. Opthal. Physiol. Opt., 11:71-75. END POCKET

8. Armstrong,R.A., Slaven,A. and Harding,G.F.A. (1991e). Visual evoked magnetic fields to flash and pattern in 100 normal subjects. Vis. Res., 31:1859-1864. END POCKET

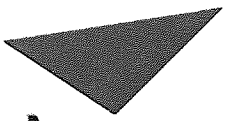

Aston University

Content has been removed for copyright reasons